Cladophora growth in littoral environments of Large Lakes: Spatial complexity and ecological interpretations

by

David C. Depew

A thesis
presented to the University of Waterloo
in fulfillment of the
thesis requirement for the degree of
Doctor of Philosophy
in
Biology

Waterloo, Ontario, Canada, 2009

AUTHOR'S DECLARATION

I hereby declare that I am the sole author of this thesis. This is a true copy of the thesis, including any required final revisions, as accepted by my examiners.

I understand that my thesis may be made electronically available to the public.

Abstract

This thesis brings together a variety of new and evolving technologies in an attempt to characterize spatial variability in highly complex near shore areas of the Laurentian Great Lakes in order to provide methods and mechanisms of answering ecological questions in the presence of dynamic and heterogeneous environmental conditions.

A high frequency echosounder was used to detect and characterize the nuisance macroalgae (*Cladophora*) that currently blooms along many of the lower Great Lakes shorelines. Detection of algal stands that were of high biomass and therefore likely to be considered a nuisance was largely successful and robust. Detection of short stands and those of low biomass were limited by the acoustic resolution of the system. Attempts to use average backscatter strength and integrated scattering volume as predictive metrics to estimate standing crop were largely unsuccessful, likely due to the inability of completely excluding reverberation from the substrate and the presence of invertebrates within the algal mats.

This acoustic system was subsequently used during near shore mobile surveys to map the distrubtion of *Cladophora* at several locations in Lakes Ontario, Erie and Huron. *Cladophora* was detected with the acoustic unit at all sites in Lakes Ontario and Erie, including at offshore shoals, far removed from catchment influence. *Cladophora* was not detected at any of the Lake Huron sites and visual observation combined with underwater camera work confirmed that *Cladophora* did not accumulate to levels that would be detecable with acoustics, or was absent entirely. Nutrient conditions varied surprisingly little among sites, and did not readily explain the differences in *Cladophora* distribution from site to site. In contrast, dreissenid mussel abundance was significantly associated with *Cladophora* biomass, likely due to their effects on water clarity and nutrient regeneration in the benthos.

Despite the strong association between dreissenid abundance and *Cladophora* biomass observed during the multi-lake surveys, urbanized catchments contain a multitude of potential shoreline nutrient sources which may contribute to the current patterns of *Cladophora* growth. No compelling evidence for nutrient supply from shoreline sources or municipal waste water treatment plants was observed, and although some degree of spatial association between *Cladophora* growth and tributaries was observed at one of the study sites, the widespread nature of *Cladophora* growth in

conjunction with a lack of nutrient enrichment evidence argues against shoreline sources as a significant cause.

Although much of the spatial variation of water masses and phytoplankton in the near shore is structured by hydrodynamic processes, some evidence exists that the extensive beds of *Cladophora* may have some ability to affect the overlying water chemistry and water quality. Patterns of dissolved gases in the near shore were largely consistent with the demand for CO_2 and the release of O_2 by *Cladophora* in the summer months when biomass and areal cover were high. Furthermore, changes in phytoplankton photosynthetic efficiency were consistent with changes in nutrient and CO_2 levels, suggesting that perhaps the interplay between benthic algae and pelagic phytoplankton may be important in the shallow waters.

Although *Cladophora* is a major component of the lower Great Lakes benthic community, it does not reach comparable levels in Lake Simcoe despite comparable water clarity, phosphorus concentrations and dreissenid mussel abundance to the lower Great Lakes. The difference in physical size between Lake Simcoe and the Great Lakes may partly explain the relative lack of *Cladophora* growth in Lake Simcoe, perhaps through reduced turbulence or reduced physical disturbance that allows for invertebrate grazers to maintain high abundances relative to the Great Lakes where mussel shells are pulverized to fine grained material that eliminates invertebrate refuge. Differences in water chemistry may also be important; dissolved silica concentrations in Lake Simcoe are comparable to those measured in the upper Great Lakes and do not drop below the threshold for silica limitation of phytoplankton or benthic algae. This may prevent *Cladophora* from outgrowing its epiphyte coating, leaving Cladophora in a state of nearly continuous light limitation.

Although *Cladophora* did not respond in Lake Simcoe as it did in the lower Great Lakes to dreissenid invasion, macrophyte growth has clearly increased. Macrophyte growth covered nearly 100% of Cook's Bay to a depth of 8 m, and macrophytes were observed at depths of up to 10 m. It appears that while historical nutrient loading as provided the nutrient rich sediment in Cook's Bay, dreissenids have supplied the significant increase in water clarity, that has allow for the expansion of macrophytes into deeper water.

Acknowledgements

All students need a bedrock of support. Without a firm footing, there is no foundation to build on, and I am certainly no exception. I would like begin by acknowledging the folks who have admirably served as my bedrock over the past few years. I'd first like to acknowledge my thesis advisors; Bob Hecky and Ralph Smith. Ralph and Bob were instrumental in indentifying key research questions and developing the research programs and approaches that fuelled much of my interest in a broad variety of topics, and were always willing to dispense advice, insight and encouragement. Their exceptional mentoring provided me a unique opportunity to dabble in several areas of biology and ecology and this thesis is a reflection of their efforts.

Committee members Stephanie Guildford, Todd Howell and Lars Rudstam provided a diverse and inter-disciplinary array of ideas, comments and thoughtful questions during committee meetings and other more informal settings. Todd graciously shared *Cladophora* data from Lake Erie, and Lars kindly included me in his fisheries acoustics workshop at the Cornell Biological Field Station.

I would also like to acknowledge the help of many exceptional field assistants. Adam Houben, Emily Hazzard, Andrea Idika were instrumental during the forays to Lakes Erie, Ontario and Huron in 2005. The level of helpfulness and perseverance displayed by these three was directly proportional to the amount of suffering endured and the difficulty of the work I heaped on them. The 2005 surveys could not have been completed without their tireless assistance. Adam Houben (often on one leg) and Tedy Ozersky provided assistance for work in 2006 and 2007 both at Halton and Pickering, as well as at Lake Simcoe in 2006 and 2007. Field assistants Ryan Sorichetti, Yuang Zhang, Zing-Ying Ho and Ann Balasubrumanian were also of great assistance during the Lake Simcoe work.

Laboratory managers Yuri Kozlov and Cindy Wang oversaw much of the sample analsyses for water chemistry data in this thesis, and their efficienct and meticulous laboratory work ensured a quick sample turnaround time and reliable analysis. Undergraduate students Laura Woodworth, Ryan Sorichetti, Yuan Zhang, Shazeen Bandulukawa, and Dusa Vukosavljevic also spent many hours processing samples and running sample analyses.

Scott Higgins and Sairah Malkin both provided responsible and meticulous diving supervision to complete groud-truthing of the acoustic system in Chapter 2. Adam Houben and Ted Ozersky willingly joined me in water that was frequently < 10 degrees due to upwelling, or had questionable material floating in it. Greg Silsbe and Scott Higgins also provided logistical support (navigation and caffeination assistance) for the night time surveys in Chapter 5. Adam Houben chauffered us back to Waterloo after a night on the lake.

Additional logistical assistance was provided by Brian Emo and LOSAAC volunteers who provided a vessel for the spring water quality surveys in 2006. Staff at the MNR Fisheries Assessment Unit at Sibbald Point Provincial Park (Jake LaRose, Brent Metcalfe, Cam Willox, Ron Allen) kindly provided laboratory space and access to a coffee machine, mugs and free coffee during long nights of sample processing on Lake Simcoe.

I would also like to acknowledge the efforts and assistance of Dr. Luis Leon and Greg Silsbe for providing a valuable resource for all problems related to visual basic, Matlab, MS Access and other

various computer programs that needed torturing. Additionally, I am also grateful to my co-author for the paper arising from Chapter 2, Andrew Stevens (USGS) for having the patience to port multiple snippets of code into a working GUI in Matlab. Although driven primarily by his own research objectives, he willingly shared his code and put up with my numerous inquiries and suggestions for code changes. BioSonics Inc. kindly provided the raw data format documentation that allowed construction of the GUI, and technical discussions from technical staff (Assad Ibrahim, Brian Moore and Mike Burger) were always beneficial.

Funding for this work was provided from a number of sources. A National Sicence and Engineering Research Council Co-operative Research and Development Grant provided much of the funding for the work in 2005. Ontario Clean Water Agency funded the Halton region work in 2006, and Ontario Power Generation funded the work at Pickering. A Ministry of Environment Best in Science Grant to Stephanie Guildford provided funding for work on Lake Simcoe. Funding was also provided from an NSERC Postgraduate Scholarship and an Ontario Graduate Scholarship in Science and Technology.

Lastly, a special acknowledgement to the people instrumental to all levels of production: My wife (Barbara) and kids (Alex and Jillian) often had to put up without me for extended durations during field work, most often in the summer months. Yet their acceptance, encouragement and unconditional support provided a strong foundation for me while this work was completed. My parents (Bill and Cathy) and in-laws (Sarah and Partick) were supportive and always willing to help out with the ups and downs experienced by a young family with ambitious parents. Siblings (Tom, Sarah and brother in-law Denis) provided support by maintaining important roles in the kids' lives and at least for Tom and Denis a little academic family competition, though I must concede that their understanding of engineering science far exceeds mine.

Table of Contents

List of Figures

List of Tables

Chapter 1

General Introduction and Overview

In the decades since the initiation of the Great Lakes Water Quality Agreement (GLWQA), the Great Lakes, in particular the lower Great Lakes have experienced ecological destabilization as a consequence of a variety of stressors. For example, much of the land immediately adjacent to the lakes has become increasingly urbanized over the last 10 to 15 years (Wolter et al. 2006) and a nearly continuous stream of exotic species has become established in the Great Lakes (Ricciardi and MacIsaac 2000). The effects of these and other stressors are often manifested in the near shore areas, since this is where the majority of people interact with the lakes. Near shore areas of the Great Lakes have and continue to experience chemical pollution, organic enrichment, physical alterations, degraded beaches, changes in aquatic community structure, and in some areas, increasing frequency of algal blooms (Edsall and Charlton 1997).

There is increasing recognition that the conditions in the near shore zones are maintained by the dynamic interactions among environmental, biological, hydrological features (Mackey and Goforth 2005). Effective management strategies for long term maintenance therefore are dependent not only on understanding these processes, but also characterizing the near shore habitats themselves. Yet, this is not a simple task, as the spatial and temporal scales at which organisms interact with their environment on a day to day basis are typically different than the spatial scales at which environmental change may occur (Mackey and Goforth 2005). For example, near shore substrates may change on a day to day basis in areas where hydrodynamic energy is sufficient to erode and transport sediments across underlying immobile substratum (Mackey and Leibenthal 2005). The rapidly changing nature of the texture and quality of the substratum may have substantial impacts on the use of near shore areas as nursery grounds and habitat for near shore fish communities.

Spatial studies focusing on such environmental and ecological phenomena require a properly and carefully designed strategy for data collection (Stein and Ettema 2003). Data can be logistically difficult or prohibitively expensive to collect, and both the sampling design and the quality of the data may affect the accuracy and precision of the estimates (Cochran 1977). Intensive sampling is expensive but gives a clear picture of spatial variability of a given parameter, while on the other hand sparse sampling may be more economical but miss important spatial features. Field sampling methods such as videography and substrate sampling via benthic grabs are labor intensive and cost prohibitive for highly resolved large scale sampling (Vis et al.

2003). This is particularly true for the Great Lakes near shore areas that are dominated by hard substrate, which are not effectively sampled using a grab device but must be sampled using quadrat or other manual collection methods (e.g., Barton and Hynes 1978). Large scale synoptic methods that are used for terrestrial studies such as remote sensing (Wezernak and Lyzenga 1975) and aerial photography (Fitzgerald et al. 2006, Zhu et al. 2007) can provide a better spatial synopsis of aquatic environments, but are subject to interference from cloud cover, wave action and turbidity that are not readily controllable (Vis et al. 2003). Therefore, the facilitation of inexpensive, robust data collection at high resolution over large spatial scales is advantageous to managers since aquatic communities are influenced by processes operating at small to large scales, and better characteriziation is needed to fully appreciate the complexities of the near shore ecosystems in these large Lakes (Mackey and Goforth 2005).

Since much of the previous scientific programs were focused on offshore regions, near shore areas remain poorly studied. A major difficulty for site–specific management in the near shore at present is to obtain enough information about the site to produce reliable estimates for mapping and visualization. In the following sections, I will introduce some novel and evolving technologies that have been adapted for high resolution spatial surveys in the near shore areas of the Laurentian Great Lakes.

1.1 Acoustics

Acoustic transducers are comprised of multiple piezoelectric elements that function by converting electrical energy into acoustic energy to generate a pressure wave. The piezoelectric elements transmit identical acoustic pulses at a specific frequency (usually in the kHz range) for a specific duration (usually 0.1 to 0.5 milliseconds depending on the object of study). The configuration of the piezoelectric components influences the interaction of the transmitted acoustic pulses, and through constructive and destructive interference, a characteristic beam pattern specific to the transducer is created (Figure 1.1). The acoustic beam is generally conical in shape with the apex angle referred to as the beam angle. The shape of the beam can be altered by controlling the energy to certain elements (Simmonds and MacLennan 2005).

The pressure waves emitted by the transducer are transmitted by the periodic compression and expansion of particles in the transmission medium (Simmonds and MacLennan 2005). For water, sound speed (c; which refers to the movement of the pressure peaks, not the local oscillations of particles) is typically in the range of 1450 to 1550 m sec^{-1}, depending on water temperature, ambient pressure and salinity (Medwin and Clay 1998). The wavelength of the transmitted pulse is also important because it sets the fundamental limit on the resolution of

targets (Simmonds and MacLennan 2005). For a 430 kHz transducer, and a sound speed of 1500 m s^{-1}, the wavelength of the acoustic pulse is on the order of 3.5 mm. As the sound waves travel through the water, some energy is reflected back to the transducer. The reflected energy is received by the same piezoelectric elements, converted back into electrical energy, amplified and recorded (Simmonds and MacLennan 2005).

Reflected acoustic energy (hereafter referred to as echoes) arises from the density contrasts between the transmission media (water) and the target. For example, gas filled swim bladders contribute ~ 90% of the reflected echoes from fish (Simmonds and MacLennan 2005). Some invertebrates also have gas inclusions and reflect acoustic energy quite well (Kubecka et al. 2000). Likewise, submerged aquatic vegetation (e.g., macrophytes) containing gas vacuoles or structural tissues also reflect acoustic energy (Sabol et al. 2002a, Hohausova et al. 2008). For organisms that do not contain such obvious density contrasts within their bodies (e.g., zooplankton, jellyfish, macroalgae) the reflection of acoustic energy derives mostly from the ratio of the sound speed in the scattering body to that in the water, and the ratio of compressibility of the body of the organism to that of the water (Holliday and Pieper 1995).

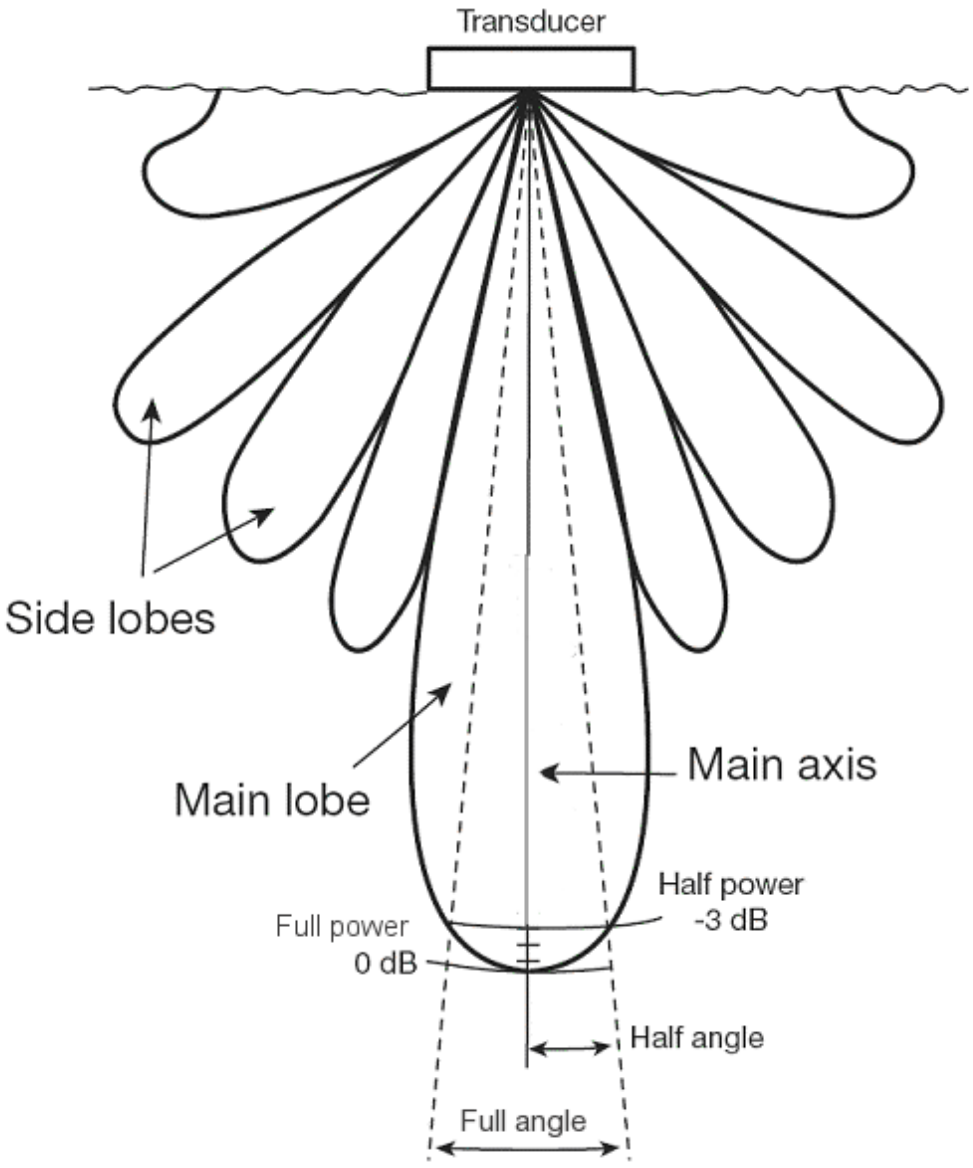

Figure 1.1. Schematic image of a single beam transducer beam pattern (scaled in dB). Image adapted from http://www.acousticsunpacked.org. The full beam angle is the -3 dB beam angle, which is defined as the angle between the lines that represent the half-intensity direction on either side of the main axis.

The transducer beam pattern determines the way the elements receive the echoes and allows for measurements on reflective targets. Acoustic waves are returned in different phases, which vary by the angle of return (Medwin and Clay 1998). The difference in phases can be used to determine angle and direction of the reflected target in specially designed transducers. A single-beam transducer transmits and receives energy in the same area of the transducer, and produces a single echo signal. Range (or distance) can be determined from travel time of the incident transmission to return of the reflected echo. Single-beam transducers, however, cannot be used to determine the direction of the reflected signal, only the distance. Dual beam transducers transmit the signal on the narrow beam and reiceive the echo on both the narrow and wide beams. The ratio between the two echo levels (narrow and wide) can then be used to determine the distance from the target to the center of the beam (Simmonds and MacLennan 2005). Split beam transducers receive the echo in four quadrants. This allows for phase deviations of the returned echo to be compared and these are used to determine the location of the target within the acoustic beam. Split beam transducers also allow for compensation of directivity, calculation of target strength and *in situ* estimation of fish swimming speed (e.g., Arrhenius et al. 2001).

The patterns within the received echoes are used to derive information of interest. For example, in fisheries acoustics, target strengths (TS; echo associated with an individual fish) are used to derive estimates of fish abundance and density (Rudstam et al. 2003). Substrate characteristics can be determined by comparing the shape of the returned echo and its energy to known echo patterns for distinctive substrates (Hamilton 2001), and the acoustic reflectivity of submerged aquatic vegetation (SAV) is used to derive measurements of macrophyte characteristics (e.g., height, percent cover) from acoustic echoes (Sabol et al. 2002a). Acoustic measurements are generally reported in decibel (dB) units rather than the formal SI units for pressure or intensity (Simmonds and MacLennan 2005). The principal reason for this is that the measures can span many orders of magnitude, and the decibel is simply a logarithmic measure of the ratio of two pressures or intensities, the measured pressure (P_0) and reference pressure (P_{ref}) or the measured intensity (I_0) and the reference intensity (I_{ref}), expressed as

$$r_{dB} = 10\log(I_0 / I_{ref})$$
$$or \qquad (1.1)$$
$$r_{dB} = 20\log(P_0 / P_{ref})$$

and a change in acoustic levels covering several orders of magnitude can be expressed as a change in dB (Simmonds and MacLennan 2005). For hydroacoustics, the reference level for pressure is generally 1 μPa (Simmonds and MacLennan 2005).

Compared to single or multiple point sampling techniques such as quadrat or knotted line sampling, acoustic surveys can provide increased data richness and spatial coverage by offering continuous and high resolution observations throughout the water column. Acoustic methods have a distinct advantage in that sound can be transmitted over long distances at high speeds in water (typically 1500 m s^{-1}) (Simmonds and MacLennan 2005). In this way, the entire water column can usually be scanned in less than half a second. During an acoustic survey, the vessel usually navigates along predefined transect lines which cover the survey area in a way that the data collected can be used to provide statistically robust estimates of the obect of interest. Most often, acoustic methods are used to evaluate fish stocks (Simmonds and MacLennan 2005), but increasingly, acoustics have been applied to evaluate substrate characteristics and the distribution of substrate types (Chivers et al. 1990) and the distribution of submerged aquatic vegetation (e.g., Sabol et al. 2002a, Valley et al. 2007). Despite the obvious benefits of acoustic methods, there are some limitations in that one cannot differentiate between species and targets close to the bottom generally cannot be resolved (Ona and Mitson 1996). Therefore hydroacoustics must still be accompanied by more traditional methods of sampling, but ultimately, when properly calibrated and used in an appropriate manner, acoustical techniques can greatly enhance the spatial richness of data collected.

1.2 Fluorimetry

The first measurement of *in vivo* fluorescence was made by Lorenzen (1966) and applied as a proxy for phytoplankton biomass. By the 1970s, commercial instruments were available to measure *in situ* fluorescence, and these have become increasingly common on oceanographic and limnological investigations (Falkowski and Raven 1997). Recent technological advances and progress in understanding *in vivo* fluorescence have provided an array of tools to assess the biomass and physiology of phytoplankton, particularly as it relates to the primary site of photochemistry; photosystem II (PSII) (Falkowski 1992). Located in the thylakoid membrance of plants, algae and cyanobacteria, PSII is the first protein complex in the light dependent reactions of photosynthesis (Hopkins 1999). Electron transport begins with the arrival of excitation energy at the PSII reaction center chlorophyll, P_{680}. The excited form of P_{680}, (P_{680}^{*}) is rapidly photo-oxidized (10^{-12} s) as it passes an electron to pheophytin (Pheo). This initial photochemical act results in the formation of P_{680}^{+} and $Pheo^{-}$, a charge separation. This charge separation effectively stores light energy as redox energy and represents the actual conversion of light energy to chemical energy (Hopkins 1999). The charge separation is subsequently stabilized by the passing of an electron from Pheo to a primary quinine acceptor (Q_A) and then to plastoquinone (PQ) that

binds transiently to the Q_B binding site on the D1 protein. The reduction of PQ to PQH_2 reduces its affinity to the binding site (Q_B). Platoquinol (PQH_2) is subsequently released and replaced by another PQ molecule. The initial charge separation that created P_{680}^+ is stabilized by the extraction of electrons from a molecule of water (H_2O), supplied by the adjacent oxygen evolving complex (OEC). Each excitation of P_{680} is followed by withdrawal of one electron from the OEC. When four successive positive charges have accumulated, two molecules of H_2O are oxidized, resulting in the expulsion of 4 H^+, and evolution of one O_2.

Fast repetition rate fluorometry (FRRF) was developed to measure the above process in phytoplankton and derive photosynthetic parameters, *in situ*, in a rapid and non-destructive manner. The mechanistic model and operational protocols for the FRRF have been developed and discussed in detail in Kolber and Falkowski (1993) and Kolber et al. (1998). While primarily used to estimate phytoplankton photosynthesis, the FRRF provides the ability to measure several physiological parameters that may be useful in determining physiological responses of phytoplankton communities to environmental factors. The ratio of F_v/F_m (where $F_v = F_m - F_0$; F_0 is the minimum level of fluorescence, and F_m is the maximum level of fluorescence) is a measure the maximum quantum efficiency of photosystem II (Kolber et al. 1998). For the purpose of FRRF work, when F_v/F_m is equal to 0.65, it is assumed that 100% of PSII reaction centers are functional (Kolber et al. 1998). Variability in F_v/F_m is associated with the physiological state of the phytoplankton (Olaizola et al. 1994) and has been linked to nitrogen and iron availability in the oceans (Kolber et al. 1990, Greene et al. 1994) and nitrogen, silicate and phosphorus limitation in cultures (Berges et al. 1996, Lippemeier et al. 1999, Beardall et al. 2001). The measurement frequency of the FRRF allows for an estimation of the functional absorption cross section of photosystem II (σ_{PSII}), which is mathematically described as the slope of the fluorescence induction curve F_0 to F_m by fitting an exponential curve to the data (Kolber and Falkowski 1993; Figure 1.2). σ_{PSII} indicates the efficiency with which light is intercepted by the phytoplankton. Higher values of σ_{PSII} are associated with phytoplankton which have been growing at low light intensities, as the phytoplankton increase their photochemical 'target size' to maximize light absorption (Kolber et al. 1988). In contrast, σ_{PSII} has been shown to decrease at higher growth irradiance, which has been linked to an increase in the proportion of pigments that absorb, but do not transfer energy to PSII (Ley and Mauzerall 1982, Kolber et al. 1988). σ_{PSII} has also been shown to increase under both nitrogen (Berges et al.1996, Kolber et al. 1988) and iron starvation (Greene et al. 1991). The increase in σ_{PSII} under nutrient limiting conditions has been linked to a decline in the number of functional reaction centers, causing a more rapid saturation of operational reaction centers from the antenna complex (Falkowski 1992).

The principal advantage of the FRRF is that it provides a high resolution method to characterize vertical, horizontal and temporal scales of variability of photosynthetic processes (Kolber and Falkowski 1993). FRRF can resolve small spatial (on the order of meters) and temporal (on the order of seconds) scales of variability compared to tens of meters and hours to days for more traditional methods of assessing photosynthesis (e.g., C^{14} or $^{18}O_2$) or nutrient stress. When deployed on a towed sensor platform or connected to an online water stream, the FRRF can measure photosynthetic efficiency of phytoplankton continuously. This capability is particularly useful for areas such as estuaries or near tributaries where strong gradients in environmental conditions may exist.

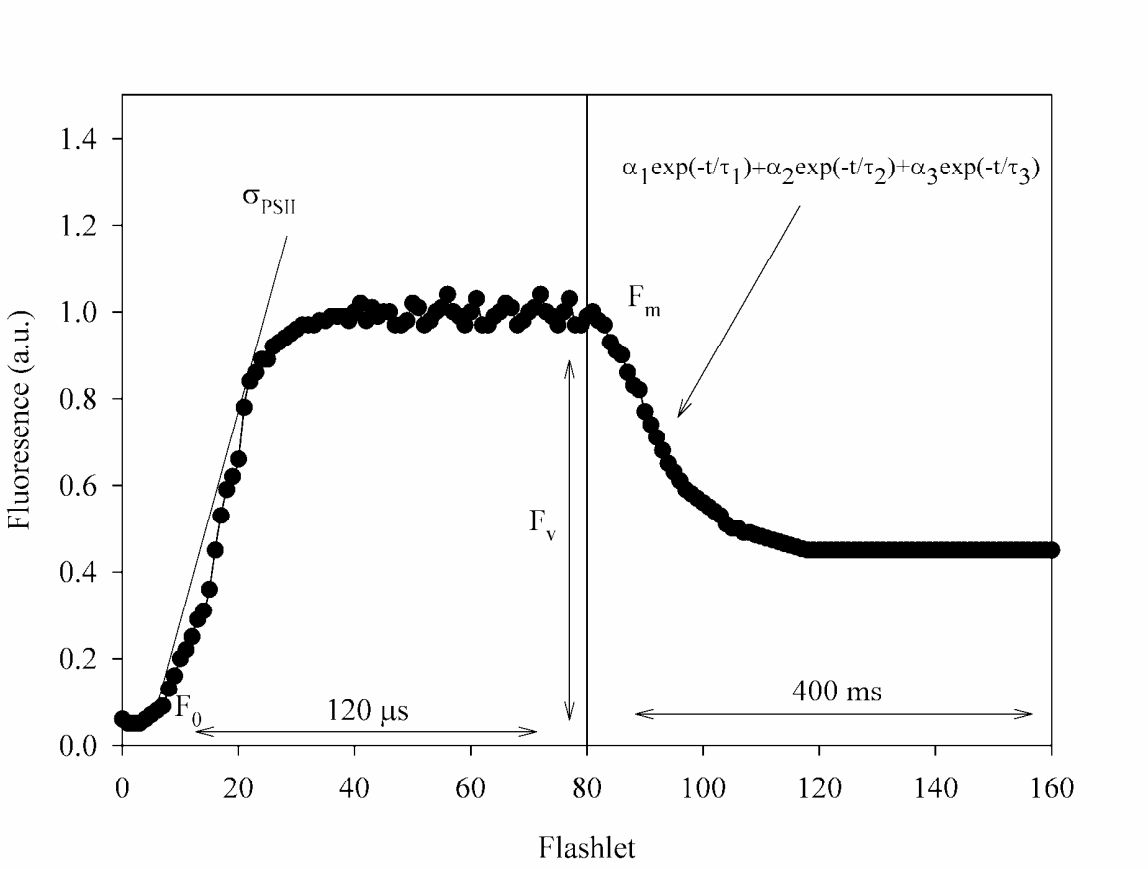

Figure 1.2. Kinetic profile of a single turnover flash as induced and detected by a FRR fluorometer. Parameters of interest to this thesis; F_0, F_m, F_v, σ_{PSII} are noted on the figure. Adapted from Kolber et al. (1998).

1.3 Geostatistics

Geostatistical methods have been a staple of the mining communities for several decades (Journel and Huijbergts 1978), but have been increasingly applied to ecological studies to examine population distributions of fish (Maravelias et al. 1996, Mello and Rose 2005), invertebrates (Rufino et al. 2005), protozoa (Bulit et al. 2003), soft sediment communities (Hewitt et al. 2004), and vegetation (Kendrick et al. 2008). Until recently, the most common factor limiting the application of geostatistical methods to ecological data was simply the relatively low ratio of samples collected to study area size (Rufino et al. 2005). With the advent of GPS technology, it is possible to generate high resolution geo-referenced data which provides a near continuous data stream when combined with certain instrumentation with a high rate of data acquisition (Sabol et al. 2002a). Accordingly, this type of data often exhibits small scale variation that can be modeled (structural analysis and variograms) as spatial correlation. This information can then be incorporated into estimation procedures (kriging) to estimate the variables of interest and create maps of spatial distributions (e.g., Guan et al. 1999, Valley and Drake 2006).

1.3.1 Geostatistical theory

In their basic form, all geo-statistical methods assume some form of stationarity in order to comply with the underlying theory of regionalized variables (Journel and Huijbergts 1978). A regionalized variable is one whose value is dependent on its position. The variation in the regionalized space is generally random, but some regularity (e.g., spatial structure) is imposed on it, reflecting a certain amount of continuity that exists in the spatial distribution of that variable (Matheron 1963). The assumption of stationarity implies that the sample values observed in a 2 or 3 dimensional space are simply different realizations of the same random variable (e.g., the sample values come from the same distribution). Different types of stationarity may be assumed depending on the data in question (for a definition and complete presentation of the theory of regionalized variables and intrinsic random functions see Journel and Huijbergts (1978) and Matheron (1963)). Stationarity is however, a rather ambiguous concept and the presence of stationarity may be dependent on the circumstances of the study itself (e.g., small vs large study area), and may indeed be violated in the presence of any ecologically important gradient in the landscape (Cressie 1986). For example, due to physical forcing by wind and wave action, sediments are likely to be distributed in a gradient in an inshore to offshore direction with coarser, more stable sediments close to shore (such as rocks and pebbles), and smaller, fine-grained sediment in deeper water (such as silt and mud). Langmuir circulation cells can distribute

phytoplankton in elongated patches that are of similar sizes to the Langmuir cells (Checkley 2000), and lake currents and upwelling can distribute zooplankton in heterogeneous patches (e.g., Megard et al. 1997). These examples violate the assumption of stationarity, which implies a spatially constant mean and variance.

Even if stationarity is not clearly violated, spatial autocorrelation may be stronger and extend further in a particular direction. As a result, the variation can be considered anisotropic (e.g., not uniform in all directions). More complicated problems arise when standard distance metrics are not appropriate, for example, in the presence of landscape barriers (e.g., stream networks or embayments; Jensen and Miller 2005). Strictly speaking, the assumption of stationarity concerns the underlying **process** and not the observed **pattern**, thus stationarity cannot be tested directly (Cressie 1986). Nonetheless, checking for possible violations of stationarity is an integral part of performing geostatstical analyses.

1.3.2 Structural Analysis

In order to assess the degree of spatial autocorrelation and evaluate the potential for non-stationary data, the first step is to compute the experimental semivariongram. The semivariogram $\gamma(x,x+\boldsymbol{h})$ or $\gamma(\boldsymbol{h})$, is defined as half the average squared difference between points separated by a distance vector ($\boldsymbol{h}$) (Cressie 1991). The classical empirical semivariogram is described as in equation (1.1);

$$\gamma(h) = \frac{1}{2N(h)} \sum_{i=1}^{N(h)} \{Z(x_i) - Z(x_i + h)\}^2 \qquad (1.1)$$

where $\gamma(\boldsymbol{h})$ is the semivariance at each lag (separation distance), $\boldsymbol{h}$, $N(\boldsymbol{h})$ is the number of point pairs separated by the given lag, and $Z(x_i)$ and $Z(x_i+\boldsymbol{h})$ are data values at locations (x_i) and ($x_i + \boldsymbol{h}$) respectively. By definition, the semivariogram value at zero lag should be zero, but in practice it usually intercepts the y axis at a positive value known as the nugget variance (C_0). The nugget represents measurement error and unexplained or random spatial variation at distances smaller than the shortest sampling interval. The semivariance value where the semivariogram plateaus is called the sill (C), and the lag distance (α), at which the semivariance levels off, is called the range, beyond which there is no longer spatial correlation, and thus, no longer spatial dependence. A finite constant variance will always result in the presence of a sill, whereas continued increase in the semivariance with distance may indicate a spatial trend in the mean, possibly coupled with dependence of the variance on the mean, resulting in a non stationary process (Cressie 1991). The difference between the nugget (C_0) and the sill (C) is called the structural variance, representing the variance accounted for by the spatial dependence.

The classical variogram is the most widely used in geostatistical applications, yet it has many weaknesses (Emery and Ortiz 2007). Perhaps the most critical is that it uses squared increments and is not resistant to the presence of outliers or highly non-normal data distributions (Cressie and Hawkins 1980). Numerous authors have proposed a variety of solutions; Cressie and Hawkins (1980) advocate the use of the "robust" variogram estimator, which is based on the fourth power of the square root of absolute differences as in equation (1.2);

$$\bar{\gamma}(h) = \frac{\left\{ \frac{1}{2 \mid N(h) \mid} \sum_{i=1}^{N(h)} \{Z(x_i) - Z(x_i + h)\}^{1/2} \right\}^4}{0.914 + (0.988 / \mid N(h) \mid)} \qquad (1.2)$$

This particular semivariogram estimator is robust to contamination by outliers, greatly enhances semivariogram continuity and has been successfully used to model spatial distributions of animal densities, which often have data sets characterized by overdispersion and non-normal distributions (Maravelias et al. 1996, Rufino et al. 2005). Other authors advocate transformation of the data (e.g., to normal scores, indicator data, or logarithmic transforms) to solve the problem of outliers and non-normal distributions. However, in applied studies, log transformed or normal score data are difficult to back transform to the original scale of measurement, and can generate unrealistic negative values when back transformed, rendering interpretation difficult (Rufino et al. 2005).

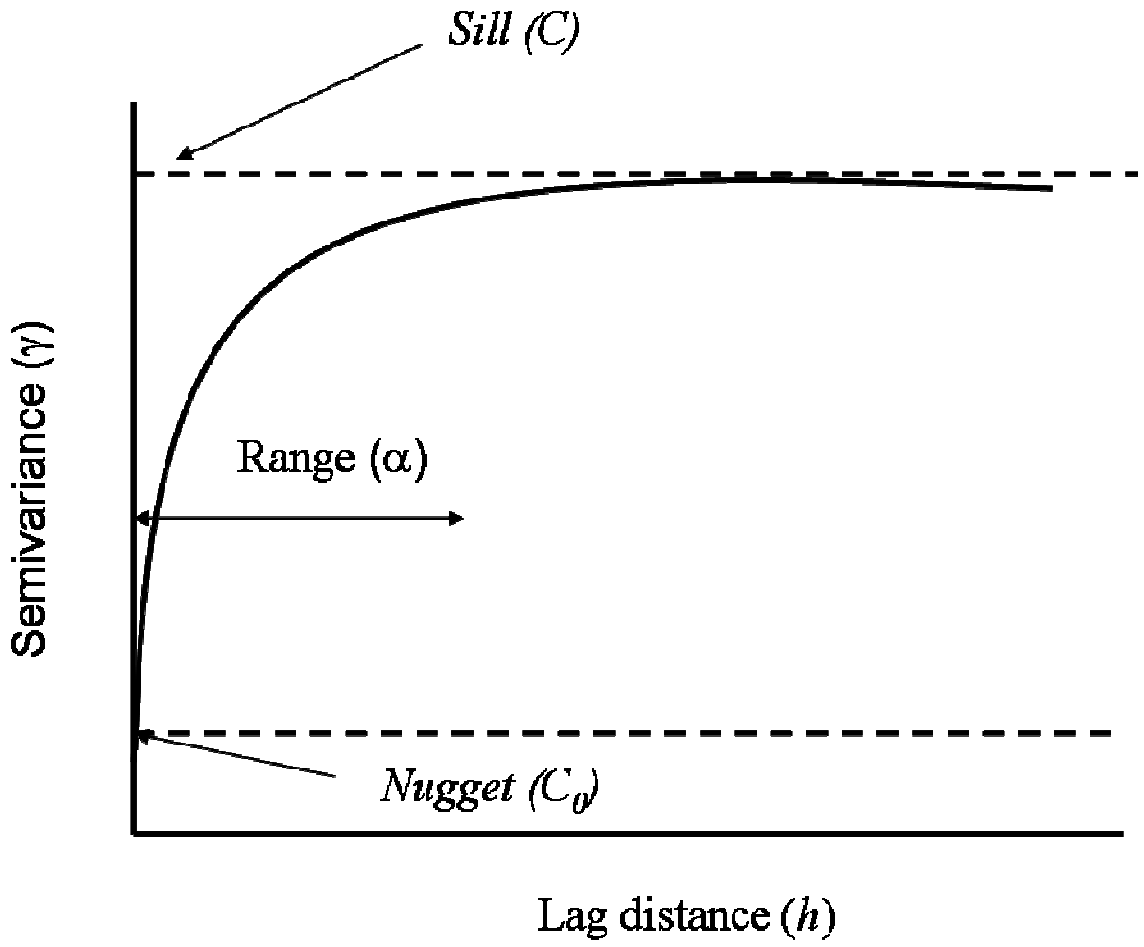

Figure 1.3. Idealized spatial covariance model depicting semivariance (γ) as a function of lag distance (*h*). Nugget (C_0) indicates the nugget effect, the sill (*C*) indicates the maximum semivariance, and (α) indicates the range of autocorrelation. The curved line represents a valid semivariogram model.

1.3.3 Variogram model fitting

Once the experimental semivariogram has been constructed, then next step is to fit a valid model to the experimental data, in order to characterize the semivariance at lag distances that are not covered by the data themselves. There are a number of valid models, and depending on the scope of the work and desired outcome, there are methods by which to test which model is most appropriate (e.g., *n*-fold cross-validation). Two of the three more common models are the spherical and exponential model. These two models in terms of the semivariogram are given in equation (1.3; spherical model) and equation (1.4; exponential model);

$$\gamma(h;\theta) = \begin{Bmatrix} 0, & h = 0 \\ C_0 + C_s\ ((3/2)(\|h\|/\alpha_s) - (1/2)(\|h\|/\alpha_s)^3), & 0 < \|h\| \le \alpha_s \\ C_0 + C_s, & \|h\| \ge \alpha_s \end{Bmatrix} \quad (1.3)$$

$$\gamma(h;\theta) = \begin{pmatrix} 0, & h = 0 \\ C_0 + C_e(1 - \exp(-\|h\|/\alpha_e)), & h \neq 0 \end{pmatrix} \quad (1.4)$$

Here, C is the sill of the semivariogram that represents the maximal variation (C_s for the spherical model and C_e for the exponential model), α is the range of the semivariogram beyond which data are no longer autocorrelated (α_s and α_e as before), and C_0 is the nugget effect. A semivariogram model can also be nested, i.e. it can be a combination of two or more component models such as nugget and exponential. Most semivariograms are nested in this manner, although more complex models (e.g., a double spherical with nugget) are sometimes used. Semivariogram models are generally fit using a weighted least squares (WLS) method of Cressie (1991), though other options are available (Pebesma 2004). The WLS method applies more weight to lags close to the origin and to semivariance estimates that have a large number of point pairs. The WLS procedure thus ensures that a good fit is achieved near the origin, an important precursor to using the semivariogram model for prediction in kriging.

1.3.4 Kriging

Kriging is a generalized least squares regression technique that makes optimal, unbiased predictions at un-sampled locations by accounting for the spatial dependence between observations, relying on a weighting scheme where closer samples have more weight on the final prediction (Webster and Oliver 2001). In kriging, the weights are chosen so that the estimate of the true value of $Z(x)$ is unbiased and the prediction variance $\sigma^2(x_i)$ is minimized. That is;

$$E[\hat{Z}(x_i) - Z(x_i)] = 0 \quad (1.5)$$

and

$$\sigma^2(x_i) = \text{var}[\hat{Z}(x_i) - Z(x_i)] = \min \tag{1.6}$$

The weighting scheme is dictated by the semivariogram, which defines the spatial structure of the data (Cressie 1991). To ensure that the prediction is unbiased, the weights placed on each neighboring point must satisfy

$$\sum_{i=1}^{n} \lambda_i = 1 \tag{1.7}$$

And their unique combination for which the variance $\sigma^2(x_i)$ is minimized can be obtained when

$$\sum_{i=1}^{n} \lambda_i \gamma(x_i - x_j) + \omega = \gamma(x_o - x_j) \qquad \text{for } j=1,2,\ldots,n \tag{1.8}$$

where ω is a Lagrange multiplier. The values $\gamma(x_i-x_j)$ and $\gamma(x_o-x_j)$ are the semivariances between the observation points x_i and x_j and between the point to be interpolated and the jth observation point respectively. The solution of equations 1.6 and 1.7 provide the weights for estimating $Z(x_o)$ from the following equation;

$$\hat{Z}(x_o) = \sum_{i=1}^{n} \lambda_i z(x_i) \tag{1.9}$$

The prediction error variance can be determined by solving

$$\sigma^2(x_0) = \sum_{i=1}^{n} \lambda_i \gamma(x_0 - x_i) + \omega \tag{1.10}$$

The function $\gamma(\mathbf{h})$ (See equations 1.3 and 1.4) from which values are used in equation (1.8) are derived from the fitted semivariogram model (Cressie 1991).

Within the kriging equations, each measurement $Z(x_i)$ is interpreted as a particular realization of a random variable $Z(x)$, or more simply, estimating an unknown value of Z at the un-sampled location x_i as a linear combination of neighboring points (Isaaks and Srivastava 1989). Different kriging variants can be distinguished according to whether the mean component $\mu(x)$ is assumed constant or spatially variable. The simplest kriging method is when the mean is constant and known (Simple kriging; SK, Webster and Oliver 2001). When the mean is constant and unknown, ordinary kriging (OK) is used to estimate the unknown value of x at any location (equation 1.11).

$$Z_{OK}(x) = \sum_{i=1}^{N} \lambda_i Z(x_i) \tag{1.11}$$

Alternatively, the mean component can be modeled as spatially variable by expressing it as a function of auxillary variables (predictors) that vary in space. Universal kriging (UK;

Webster and Oliver 2001), kriging with external drift (KED; Goovaerts 1999), regression kriging (RK; Hengl et al. 2004), and cokriging (CK; Webster and Oliver 2001) are all methods that allow for spatial modeling steps. Universal kriging can be applied when the predictors form a linear relationship with the target variable, though most authors agree that UK should be reserved for the case where the drift is modeled as a function of coordinates only (Hengl et al. 2004). Kriging with external drift refers to the case where the drift is provided by external predictors. Both UK and KED have the same formulation, such that the trend and residuals are modeled and solved concurrently (Minasny and McBratney 2007).

Regression kriging (RK) or "kriging after detrending" is a hybrid technique that involves regression on auxiliary information and then simple kriging (SK) with known mean (0) to interpolate the residuals from the regression model (Odeh et al. 1995, Hengl et al. 2004). RK assumes only that there is a linear relationship between the target variable and the covariate (Hengl et al. 2004). Several studies have shown that these hybrid techniques can give better predictions than single approaches (Bishop and McBratney 2001, Yemefack et al. 2005). Hybrid interpolators have been used to model spatial variability in tropical rainforest soils (Yemefack et al. 2005), abundance of fish in the ocean (Rivoirard 2002) and rainfall erosivity (Goovaerts 1999). The explicit advantage of RK is the ability to extend the method to a broader range of regression techniques, including generalized linear models, and to allow separate interpretation of the two interpolated components (Hengl et al. 2007). Hengl et al. (2004) provide a generic framework for regression kriging, which involves modeling the trend function using ordinary least squares (OLS), and ordinary kriging is performed on the residuals of the trend function. The assumption is that where the trend function and its residuals are uncorrelated, they can be modeled independently (Odeh et al. 1995). Gotway and Stroup (1997) extend this method to Generalized Linear Models (GLM), where the trend can be defined as a generalized linear model. However, this assumption in the method also gives rise to the principal disadvantage of RK and KED; the assumption that the trend function and residuals are independent (Hengl et al. 2004). For unbiased model coefficients, the regression model should be estimated from a generalized least squares (GLS) method that accounts for autocorrelation of the residuals. To do so, however, requires the covariance function of the residuals, which can only be estimated after the model coefficients are defined, thus creating a "chicken or egg" problem. Fortunately, a single iteration using ordinary least squares (OLS) is often satisfactory, provided enough data exists and the sample spacing is somewhat regular (Minasny and McBratney 2007).

UK, KED and RK are essentially equivalent methods, and should yield the same predictions (Hengl et al. 2004). Cokriging (CK) is often used when a more numerous (and

inexpensively sampled) variable is used to aid in predicting the distribution of a second, less numerous (and likely more costly) variable. CK in the presence of exhaustive ancillary data can not only be awkward, but requires heavy computation for large data sets (Minasny and McBratney 2007). UK, KED and RK are less computationally intensive, but require full data coverage.

It is important to note that kriging is normally done at the level of data support (i.e. points). However, there is often a need or a desire to scale up to a specific sized unit (Gotway Crawford and Young 2005). Changing the support of the variable (typically by averaging or aggregation) creates a new variable, related to the original one, but that has different statistical and spatial properties, and methods have been developed to incorporate changes of support since the early 1960s (e.g., Matheron 1963). Most practical applications that use them have data of point support, and the goal is to upscale and predict the average value Z for a specific block size. If the block size is rectangular, integrations can be done quickly and simply (Gotway Crawford and Young 2005).

$$Z_{OK}(B) = \sum_{i=1}^{N} \lambda_i Z(x_i) \qquad (1.12)$$

Here, $Z(B)$ is the prediction of the average value of Z over a discrete block of size D from the n observations of $Z(x_i)$ using the weights λ_i (Webster and Oliver 2001). Importantly, the variability in $Z(B)$ decreases as the size of B increases. Therefore, prediction and estimation procedures must take this into account.

1.4 Organization of the thesis

This thesis is comprised of six data chapters, each written as a discrete study. In Chapter 2, the ability of a high frequency echosounder to detect and characterize the filamentous alga *Cladophora* was evaluated. The principal objective for this chapter was to define a method that could be used to rapidly sample and adequately characterize *Cladophora* growth in the Great Lakes near shore areas to answer research questions posed in subsequent chapters. The contents of this chapter have been published in Limnology and Oceanography Methods.

In Chapter 3, the hydroacoustic methodology was utilized to map the distribution of *Cladophora* along selected shorelines of the Great Lakes. Due to the geographical location of the sites and the time needed to survey a representative segment of shoreline, only two visits per site could be completed, one during the spring, and one during the summer. The objective of this chapter were to contrast the patterns of *Cladophora* growth along shorelines characterized by a range of catchment and coastal land uses, nutrient conditions and dreissenid mussel abundance to

assess the relative importance of these factors to contemporary patterns of *Cladophora* growth in the Great Lakes.

In Chapter 4, similar acoustic surveys were conducted at two highly urbanized shorelines in Lake Ontario. The objective of this chapter was to characterize the spatial patterns of *Cladophora* growth on a finer scale along these highly urbanized shorelines. I hypothesized that, if increased nutrient input from urbanized areas was responsible for driving *Cladophora* growth, consistent and coherent patterns of *Cladophora* growth should present near potential shoreline sources of nutrients such as tributaries and storm sewers. Relationships between *Cladophora* growth and municipal outfalls was also examined given the recent concern over increasing nutrient loading from municipal waste water treatment plants (WWTP) as urban populations increase in size and density. Repeated surveys of these shorelines at a much higher spatial resolution than was used in chapter 3 allowed for a description of seasonal patterns as well.

In Chapter 5, spatial surveys at the Oakville site were undertaken to evaluate spatial patterns of variability in a near shore area of Lake Ontario. Such work has not yet been done for near shore zones, and the methods employed were designed to characterize relevant scales of variation of phytoplankton photosynthetic efficiency, attendant nutrient status and elucidate some potential controls of spatial variation. Additionally, I hypothesized that the seasonal development of *Cladophora* would also impart a characteristic signal on the water column and further structure spatial variability. Tracers for water masses, phytoplankton physiology and composition (FRRF, Floroprobe) and algal metabolism (O_2 and pCO_2), in addition to acoustic measures of *Cladophora* cover and height were used to assess the patterns of spatial variation at two contrasting times of low and high *Cladophora* cover.

In Chapter 6, the acoustic survey methods developed in Chapter 2, 3 and 4 were applied to selected littoral areas of Lake Simcoe. Lake Simcoe was invaded by dreissenid mussels in the mid 1990's and based on the similarities between the nutrient chemistry, dreissenid colonization and subsequent monitoring conducted by the MOE, I hypothesized that *Cladophora* would reach comparable biomass in Lake Simcoe as in the lower Great Lakes as shown in chapters 3 and 4. A finding of excessive *Cladophora* growth at these sites would provide further support for the near shore shunt hypothesis developed for the Great Lakes (Hecky et al. 2004).

In Chapter 7, a further analysis of benthic plant growth in Lake Simcoe was undertaken. Here, two acoustic surveys were conducted in Cook's Bay to assess the response of the macrophyte community to the dreissenid invasion. Previous acoustic surveys were conducted in the 1980s, prior to reductions in nutrient loading and dreissenid invasion. This therefore provided

a unique opportunity to assess changes that could be directly attributed to dreissenid mussels, rather than the additive effects of mussels and nutrient loading.

Chapter 2

Pushing the envelope: detection and characterization of a filamentous alga (*Cladophora* sp.) on rocky substrata using a high frequency echosounder

2.1 Overview

A high frequency echosounder was used to detect and characterize percent cover and stand height of the benthic filamentous green alga *Cladophora* on rocky substratum of the Laurentian Great Lakes. Comparisons between in situ observations and estimates of the algal stand characteristics (percent cover, stand height) derived from the acoustic data show good agreement for algal stands that exceeded the height threshold for detection by acoustics (~ 7.5 cm). Backscatter intensity and volume scattering strength were unable to provide any predictive power for estimating algal biomass. A comparative analysis between the only current commercial software (EcoSAV^{TM}) and an alternate method using a graphical user interface (GUI) written in MATLAB® confirmed previous findings that EcoSAV functions poorly in conditions where the substrate is uneven and bottom depth changes rapidly. The GUI method uses a signal processing algorithm similar to that of EcoSAV but bases bottom depth classification and algal stand height classification on adjustable thresholds that can be visualized by a trained analyst. This study documents the successful characterization of nuisance quantities of filamentous algae on hard substrate using an acoustic system demonstrates the potential to significantly increase the efficiency of collecting information on the distribution of nuisance macroalgae. This study also highlights the need for further development of more flexible classification algorithms that can be used in a variety of aquatic ecosystems.

2.2 Introduction

The attached filamentous green macroalga *Cladophora* is a well-known indicator species of cultural eutrophication in the Laurentian Great Lakes (Shear and Konasewich 1975). During the 1950s through 1970s, *Cladophora* growth in the rocky littoral areas and other submerged hard surfaces in the lower lakes (Michigan, Erie, and Ontario) was prolific and supported mainly by elevated lake-wide nutrient concentrations. In the upper lakes (Huron and Superior) ambient nutrient concentrations were not sufficient to support extensive growth, and *Cladophora* was principally associated with point source discharges of nutrients (e.g., sewage treatment plants, tributaries; Auer et al. 1982). Extensive research into the controlling factors of *Cladophora* growth (Auer et al. 1982) and subsequent phosphorus control legislation introduced in the late 1970s was largely successful at reducing the growth of *Cladophora* to levels that were no longer considered a nuisance (Higgins et al. 2008). In recent years, however, Lakes Erie (Higgins et al. 2005a), Ontario (DeJong 2000, Malkin et al. 2008) and Michigan (Olapade et al. 2006) have all experienced an increase in shoreline fouling by *Cladophora* and recent studies have found that biomass in many areas can exceed 100 g m^{-2} of dry mass (Higgins et al. 2005a, Malkin et al. 2008).

The many problems associated with nuisance *Cladophora* growth and the desire for effective management, have triggered renewed interest into the ecology of *Cladophora* in the Great Lakes (Higgins et al. 2008). In particular, little is known about the spatial distribution of nuisance crops of *Cladophora* in the littoral zones of the Great Lakes except that which is collected by SCUBA diving or shoreline sampling to wading depths. Although quadrat sampling by SCUBA tends to be more accurate than other quantitative methods, it remains a costly and time consuming effort (Duarte 1987) and does not provide enough data for large scale synoptic assessments of spatial patterns, especially in large systems (Wezernak and Lyzenga 1975). Remote sensing and other optical methods such as aerial photo interpretation (Zhu et al. 2007) can provide a more spatially extensive assessment, but image interpretation and the accuracy of spatial characterization depend heavily on uncontrollable factors such as water clarity, surface roughness and cloud cover (Vis et al. 2003). In the Great Lakes, the invasion by dreissenid mussels in the mid 1980s to 1990s has been credited with greatly increasing water clarity (e.g., Binding et al. 2007), and shell material from both live and dead mussels has created additional hard substrate for *Cladophora* attachment (Hecky et al. 2004). The net effect of these changes has been to dramatically increase the potential depth range and areal coverage for *Cladophora* to colonize and grow (Higgins et al. 2005a, Malkin et al. 2008). Furthermore, since

Cladophora growth mostly occurs in high energy, exposed near shore areas, excessive surface roughness and the presence of tributary plumes and sediment resuspension renders the use of remote sensing technology difficult (Budd et al. 2001).

One method that is not encumbered by limitations inherent to the time-consuming, laborious manualt methods or limitations and incertainty imposed by environmental conditions is the use of hydroacoustics to measure the amount of acoustic energy scattered by vegetation (Sabol et al. 2002a). Coupled with recent advances in GPS technology and acoustic signal processing, hydroacoustics provide a rapid and efficient means to collect data over large areas with significant spatial resolution (Sabol et al. 2002a). Such information would be of considerable value for delineating the spatial distribution of *Cladophora* or other unwanted vegetation, particularly for evaluating growth patterns as they relate to potential nutrient sources, or important infrastructure such as water intakes or public beaches.

Proper interpretation of acoustic data requires an understanding of the scattering processes occurring within the water column and at the lake bottom. In addition to vegetation, other scattering sources are often present in the water: fish (Rudstam et al. 2003), zooplankton (Gal et al. 1999), bubbles (Ostrovsky 2003), currents (Pawlowicz 2002), and gradients of salinity or temperature (Medwin and Clay 1998). The reflection of acoustic energy by vegetation arises from the density and speed of sound contrasts as the acoustic wave crosses the medium. For example, many species of vascular macrophytes (e.g., *Myriophyllum spicatum*), marine macroalgae (e.g., *Laminaria* sp.) and seagrasses (e.g., *Zostera* sp.,) contain gas vacuoles or inclusions within the tissues that strongly scatter acoustic energy (Hohausova et al. 2008). Consenquently, this has been exploited in freshwater (Duarte 1987, Thomas et al. 1990) and marine (Sabol and Burczynski 1998, Warren and Peterson 2007) systems. Considerably less information exists about the scattering properties of vegetation that do not contain gas inclusions (e.g., filamentous macroalgae such as *Cladophora*), yet their presence has been recorded in acoustic surveys (Riegl et al. 2005).

For vegetation that does not contain such sharp density contrasts within their tissues, the critical acoustical properties likely depend on the density and elasticity contrasts between the organism and the medium, similar to zooplankton (Holliday and Pieper 1995). Formation of oxygen bubbles during photosynthesis will also greatly influence the scattering of sound (Hermand 2006). So far, only one controlled laboratory study (Carbó et al. 1997) has empirically examined the acoustical properties of a macroalga. This study confirmed that while the density (g mL^{-1}) of the sesquipedale seaweed

Gelidium is only marginally greater than that of water, stands of *Gelidium* scattered acoustic energy in proportion to the stand thickness, allowing for detection at frequencies exceeding 200 kHz.

The objectives of this study are twofold. First, I sought to evaluate the ability of a high-frequency echo sounder to detect nuisance stands of *Cladophora* commonly found growing on rocky substratum in the lower Great Lakes. Second, I sought to evaluate the performance of the only commercially available software (EcoSAV; BioSonics) and an alternate method of acoustic data analysis and classification via a graphical user interface (GUI) written in MATLAB, based on the processing algorithm of EcoSAV (e.g., Stevens et al. 2008) for generating estimates of percent cover and algal stand height. Processed acoustic data are compared with corresponding ground truth data collected by SCUBA or snorkeling from selected locations in Lake Ontario. The system and data processing steps are discussed and accuracy and performance examined by comparison with the physical data.

2.3 Materials and Procedures

2.3.1 Study sites

Surveys to assess algal abundance were conducted at two sites in western Lake Ontario in water depths ranging from 1 to 10 m during the summer months of 2007 and 2008 (Figure 2.1). The substratum at the Oakville site was primarily rock, but varied in composition and size from flat bedrock expanses to boulders and small cobble/gravel mixtures. The Pickering site was characterized by a more diverse substrate assemblage that included fine grained sand and consolidated clay in depositional areas near tributary mouths and embayments. At Pickering, acoustic data collection was restricted to areas with rocky substratum, as *Cladophora* is rarely found growing attached to soft substrate (Whitton 1970).

2.3.2 Acoustic data collection

Acoustic data were collected during daytime hours (0900 - 1800) using a downward looking BioSonics single beam echosounder mounted on a 2-m adjustable aluminum sliding mount affixed to the side of the vessel by a series of clamps and bolts. The transducer was positioned 0.2 – 0.25 m below the surface of the water. The transducer had a beam angle of 10.2˚ (full beam angle) and a working frequency of 430 kHz (Source Level = 213 dB re 1 µPa at 1 m). A BioSonics DTX system running Visual Acquisition 5.1 was used to control the echosounder with a pulse width of 0.1 ms, and

a ping rate between 5 and 8 Hz at full power transmission. The ping rate was increased to allow characterization of the bottom roughness. Full power transmission was required for depths beyond 7-8 m, as the decline in the signal-to-noise ratio caused background noise to approach the desired threshold for analysis. Due to the use of full power transmission, some saturation of the acoustic signal in shallow depths (< 2 m) was noted, but this was not severe enough to interfere with characterization of the SAV signal. Acoustic data were recorded from 0.4 to 0.5 m from the transducer face (e.g., outside the transducer nearfield) to 50 % beyond the bottom depth as determined by an on board depth sounder (Garmin Fishfinder 90). Positional data were provided by a JRC 212 DGPS with positional accuracy of better than 5 m and a fix update interval of 1 s. Both the acoustic and GPS data were stored on a laptop PC. Algal canopy height and percent cover were quantified during post processing using two signal processing techniques described in the next section. The acoustic transducer was calibrated prior to this study with the use of a 17 mm tungsten carbide sphere with a target strength (TS) of -46.2 dB with a sound velocity in water of 1440 m s^{-1}.

Figure 2.1. Map of Lake Ontario showing the sites of acoustic ground truthing. Inset panel A: Oakville, Inset Panel B: Pickering. Hatched boxes indicate approximate locations of ground truth stations and transects.

2.3.3 Ground truthing sample collection

Direct measurements of algal canopy height, percent cover, and biomass were made by divers, sampling quadrats for stand cover, height and biomass at select locations for comparison with acoustic estimates (these were also collected during daylight hours). The first approach was similar to methods described in Sabol et al. (2002a) and Valley and Drake (2006). Acoustic methods are not immune to environmental conditions affecting the quality of data collected. In large systems, a common source of acoustic interference is entrained air (Kubecka 1996). Bubble induced acoustic noise can mask the presence of submerged vegetation by raising the ambient noise level to that used to characterize the canopy tops (Sabol et al. 2002b). Because the near shore areas of the Laurentian Great Lakes are high energy environments, excessive water column noise is a potential concern. To minimize this, acoustic data were collected on days when wind speed and/or direction were favorable for quiescent conditions.

Acoustic data were collected while the transducer (and vessel) remained at anchor over a fixed position. A distinct area of the bottom was ensonified for ~ 100 - 200 pings while slowly sweeping the transducer back and forth and holding the transducer at a horizontal level. After ensonification was complete, divers placed a 0.25 m^2 or a 0.0625 m^2 quadrat over the centroid of the ensonified area, measured the height of the algal mat at three random locations (to the nearest 0.01 m), visually estimated the percent cover to the nearest 10%, and harvested all the biomass from within the quadrat using an airlift suction device (Barton and Hynes 1978) or by hand. These quantitative quadrat methods have been employed in the Great Lakes for numerous studies (e.g., Higgins et al. 2005a).

Acoustic data for estimating vegetation abundance are typically collected over continuous distances with the vessel underway. Therefore, a second approach incorporating vessel motion was adopted to complement the data collected while the vessel was at anchor. Several short randomly selected transects (50 – 200 m) were surveyed acoustically at a low speed (~ 1-3 m s^{-1}), and weighted buoys were dropped at 3 – 4 locations along the transect. The weights were dropped as close to the transducer beam path as possible without interfering with the data collection, and the approximate ping window (± 50 pings) where the buoy was dropped was recorded. Upon completion of the transect, divers measured algal bed characteristics and harvested algal biomass at each buoy location as outlined above. Upon return to the laboratory, algal material was washed in a mesh sieve (pore size ~ 500 µm) to remove debris and invertebrates and dried in a drying oven at 65 °C for one week. Dried algal material was weighed to the nearest 0.01 g and the biomass per unit area in each quadrat was calculated as g m^{-2}. All of the ground truth data were

compiled into a single database for comparison against acoustic data regardless of the method of collection.

2.3.4 Acoustic Data Analysis

A single-beam echosounder functions by emitting a short burst of sound (ping) and recording the sound that is reflected back to the receiver (echoes). The intensity of the reflected sound (backscatter intensity) is recorded at a series of time intervals, resulting in a profile of acoustic backscatter intensity versus time. The distance between the transducer and the objects in the water (range) is calculated based on the elapsed time and the speed of sound in water. As the vessel navigates along survey lines, data from successive pings are recorded, resulting in a two-dimensional (ping number, or distance along transect, and range, or depth below the echosounder) record of backscatter intensity (Figure 2.2).

Detection of vegetation in echosounder data relies on distinct differences in the acoustic signal between vegetated and unvegetated surfaces. Vegetation in single-beam acoustic data is generally visible as a contiguous vertical echo return immediately above the bottom, which is characterized by backscatter intensity weaker than the backscatter from the substrate but stronger than the backscatter of the water column. The basic algorithm is straightforward. For each ping, the range (depth) of the first strong return is determined using a user-specified threshold. Next, the algorithm finds the bottom depth, which is typically the strongest return in the backscatter profile. The region between the first strong return and the bottom is considered the bottom envelope. A ping is classified as “vegetated” or “bare” based on the thickness of the bottom envelope. If the bottom envelope for a given ping is wider than a user-specified minimum plant height, the ping is classified as “vegetated”, otherwise the bottom is considered “bare”. This process is repeated for a series of pings that are bounded by GPS records. Once complete, summary statistics are computed for the cycle of pings, percent cover is determined by the number of vegetated pings divided by the total pings in the cycle, and the average height of the canopy estimated from those positively classified pings is computed. This process is repeated until the end of the file is reached.

2.3.5 Estimation of percent cover and canopy height

The presence and height of vegetation at the two study sites were quantified from the acoustic data using a pre-release version of the commercial software EcoSAV v2.0 (BioSonics Inc. 2004a), and a graphical user interface (GUI) created in Matlab (Stevens et al. 2008). The pre-release version of EcoSAV was necessary because the first version (v1.0) does not allow

thresholds for vegetation detection to be set lower than -80 dB (BioSonics Inc. 2001, see below). Unfortunately, the pre-release version of EcoSAV v2.0 is not yet configured to process data from multiplexed transducers, thus the performance between the two systems when only one transducer was connected (19 July 2007; Oakville site only) could be used to compare output from both software. The EcoSAV v2.0 algorithm classifies acoustic data that are corrected for one-way transmission loss (20 log R) time varied gain (TVG) to the raw acoustic data before analysis. The GUI was configured to allow for analysis of both raw data or TVG corrected data (20 log R or 40 log R) as specified in BioSonics Inc. (2004b). For comparisons with EcoSAV, all analyses were conducted using 20 log R TVG, and hereafter, backscatter intensity shall refer to 20 log R corrected backscatter intensity unless otherwise explicitly stated.

The quantification of plant abundance and height in both algorithms is controlled largely by two adjustable parameters: the classification threshold (noise level above ambient where plant canopy is detected) and the minimum plant height. A classification threshold for *Cladophora* canopy between -86 to -88 dB was selected for three reasons. First and principally, this value was selected based on visual inspection of echograms which suggested a value in this range would be appropriate to identify the algal canopy without substantial interference from water column noise (~ -100 to -120 dB). Second, due to the absence of gas inclusions in *Cladophora* tissue, it was hypothesized that the acoustic backscatter associated with stands of *Cladophora* would be of lower energy than that associated with vascular macrophytes, for which a value of -65 dB has been successfully applied (Sabol et al. 2002a, Valley and Drake 2006; Istvanovics et al. 2008). Third, a controlled laboratory experiment with the sesquipedale seaweed *Gelidium* estimated the target strength of a single plant at -70 dB re 1 m^2 (Carbó and Molero 1997). Mats of *Gelidium* are morphologically similar to mats of *Cladophora* on a macroscopic level, averaging 20 cm in height (Carbó and Molero 1997), although the filament diameter of *Gelidium* (~2 mm; Carbó and Molero 1997) is at least an order of magnitude larger than that reported for *Cladophora* (~ 0.04 – 0.1 mm; Johnson et al. 1996).

The minimum plant height was selected based on acoustic resolution of single targets (for example, two separate fish, or a fish and the bottom), determined according to $R = c\tau/2$ (i.e. speed of sound in medium, c, [~1500 m s^{-1}] x pulse length, τ, [0.1ms] / 2 = 0.075 m; Simmonds and MacLennan 2005). Mitson (1983) termed this distance R the "acoustic dead zone" based on the difficulty of discriminating fish echoes from bottom echoes (Ona and Mitson 1996). How suitable this method is for interpreting echoes from vegetation is unclear, as plants tend to occupy the entire area from the canopy top right to the substrate and thus are not spatially separated from the bottom as a fish would be. The EcoSAV algorithm does, by default, utilize the separation distance

rule when setting the minimum height that must be met before the signal is classified as "plant". However, the primary purpose of this is to minimize the rate of false detections as EcoSAV is intended to be used in an un-supervised mode (B.M. Sabol, Environmental Laboratory (EE-C), U.S. Army Engineer Research and Development Center, 3909 Halls Ferry Rd., Vicksburg, MS 39180, pers. comm.). Lacking sufficient precedent and evidence that signals from vegetation shorter than ~ 7.5 cm could be detected, the same level of caution was incorporated into the analysis of acoustic data with the GUI. Other adjustable parameters are available to control the extraction of vegetation information in both EcoSAV and the GUI, but their importance is not crucial to the results described herein. Summary output data from the GUI are identical to those provided by EcoSAV and consist of a record combining georeferenced location information, mid-ping number of the cycle sequence, and the average stand height and percent cover (e.g., the number of plant pings in a cycle) from classified pings. The reader is referred to the previously mentioned literature for more details.

2.3.6 Prediction of biomass

To evaluate the ability of acoustic data to predict the biomass of attached *Cladophora*, average backscatter intensity and the volume backscatter (Sv; dB) within the plant canopy for each classified ping was computed following BioSonics (2004b). Both measures were then compared against the dry biomass harvested from each quadrat.

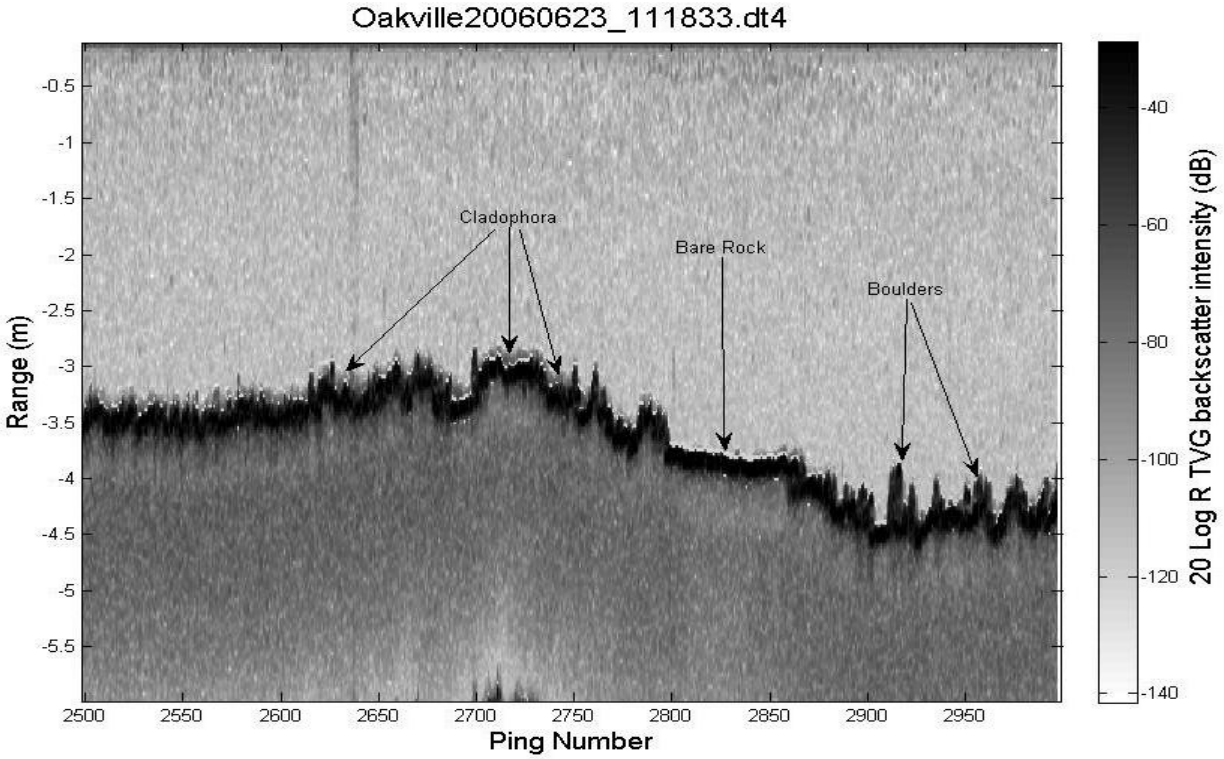

Figure 2.2. Sample echogram from the Oakville site in Lake Ontario showing 20 Log R corrected backscatter as a function of range across a 500 ping segment of a data file. Range here is equivalent to depth (in m), and ping number represents sequential ping numbers in a file, or simply, distance along a transect. 500 pings is equivalent to a distance of ~ 250 m. The lake bottom is the darkest feature on the echogram. Note the structural differences between flat rock bottom, and areas with boulders. Algal stands are represented by a weaker (lighter grey) scattering layer immediately above the lake bottom, but still stronger than background scattering (water column noise).

2.4 Results

A typical echogram collected in mid summer in Lake Ontario is displayed in Figure 2.2. Distinct differences in the acoustic signal from the substrate can be observed. Generally, the acoustic signal from rocky substrate ranged from moderately smooth to rough, randomly changing the "thickness" of the echo envelope for the bottom signal (Figure 2.2; pings 2500 to 2800). Large expanses of bedrock sheets were also encountered, and generated a very strong return characterized by a very smooth, along-track bottom signal (Figure 2.2; pings 2800 to 2850). More structurally complex substratum usually consisted of larger rocks or boulders sitting on top of cobble or bedrock expanses (Figure 2.2; pings 2900 to 2950), and these produce highly variable shaped echo envelopes. Acoustic backscatter profiles from this area (Figure 2.3) revealed that the strongest acoustic return always occurred at the substratum-water interface. For pings classified as "bare", minimal backscatter occurred in the water column and the bottom appears as a distinct peak in the backscatter profile (Figure 2.3a). For pings that were classified as "plant", a distinct backscatter peak was evident above the bottom ranging in height from ~ 8 to 25 cm (Figure 2.3b). Comparing 'bare' to 'plant' profiles shows that the plant material along this transect was characterized by elevated backscatter relative to ambient backscatter in the water column (Figure 2.3c).

Thirty eight ground truth samples and associated echogram files were collected between 2007 and 2008. In 12 of the 38 cases, *in situ* estimates of bed height were < 7.5 cm; these cases were not included in subsequent analyses because the minimum allowable detection height was set to ~ 7.5 cm (see Materials and Methods). For the remainder of the data set, close agreement is evident between diver measured stand height and stand heights estimated using acoustic data and GUI processing (Figure 2.4a). The GUI under-estimated diver-measured bed heights by an average of 0.2 ± 3.9 cm (mean ± SD), but they were not significantly different from *in situ* measured heights (paired *t*-test, $t=0.323$, $p>0.5$, df = 25). Conversely, based on the limited number of comparisons with EcoSAV, EcoSAV significantly overestimated algal bed heights by an average of 12.5 ± 7.0 cm (paired *t*-test, t= -7.03, $p<0.01$, df=12). For EcoSAV, height overestimation increased significantly as bottom depth increased (Figure 2.4b).

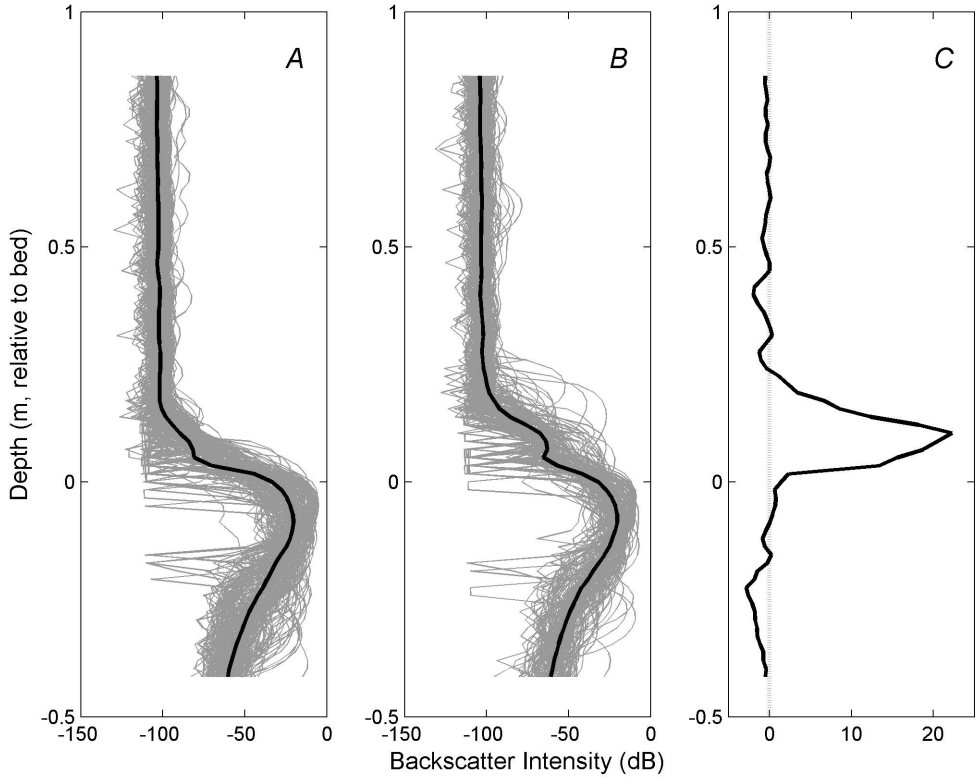

Figure 2.3. Profiles of acoustic backscatter intensity from the data displayed in Figure 2 showing A, profiles classified as bare rock, B, profiles classified as containing *Cladophora*, and C, the average difference between the backscatter profile of bare and vegetated bottom signals (all units in dB). For both A and B, the mean profile is given by the solid line.

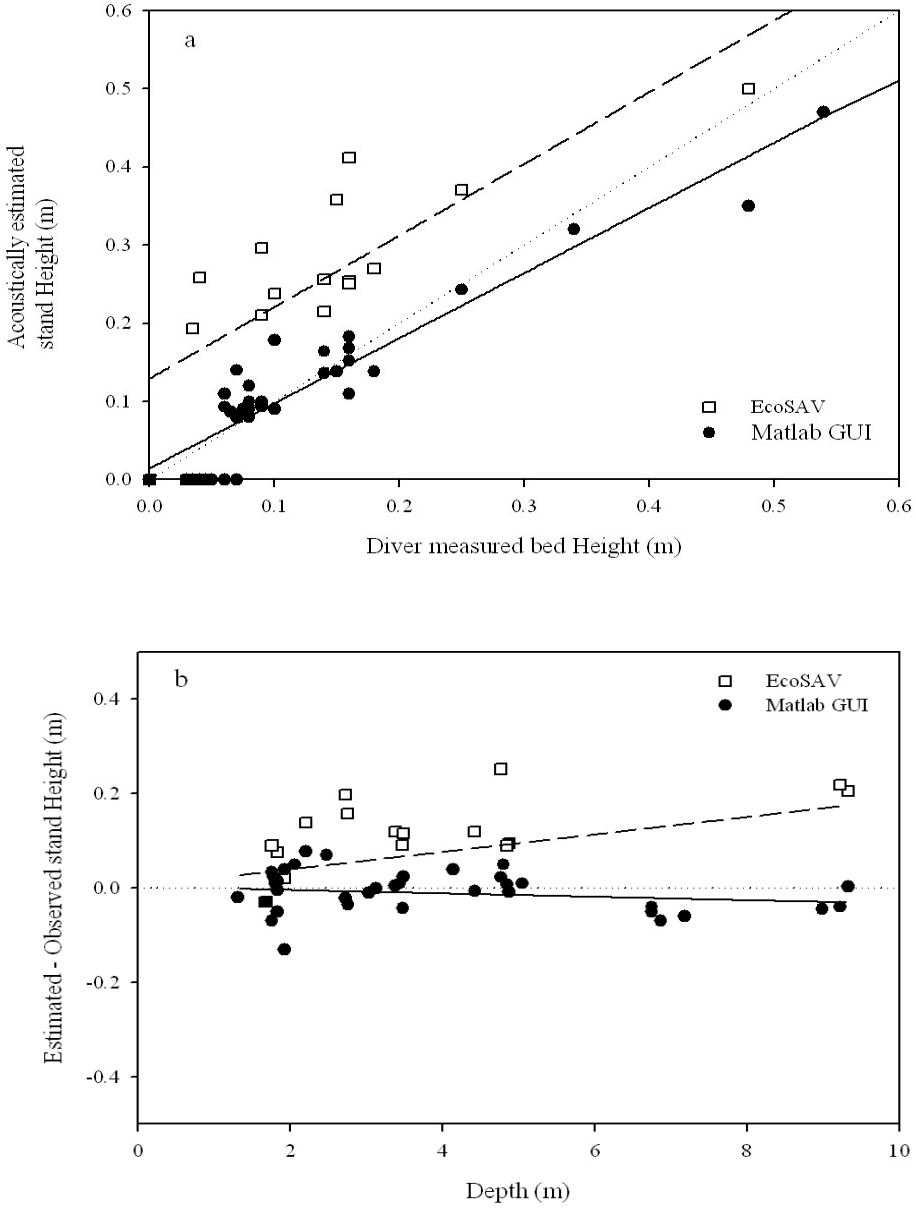

Figure 2.4 a) Relationship between algal stand height estimated from acoustic data and diver measured stand height from the corresponding ground truth samples. Note: data recorded as zero acoustic height along the x-axis indicate measurable bed height *in situ*, but were not detected by EcoSAVor the GUI because they failed to meet the minimum height requirement. Dotted line represents 1:1 line, regression line (solid line) is $StandHeight_{GUI}=0.014 \pm 0.009 + 0.83 \pm 0.056[StandHeight_{Diver}]$, $r^2= 0.87$, $p < 0.0001$. Regression line (dashed line) is $StandHeight_{EcoSAV}=0.13 \pm 0.02 + 0.92 \pm 0.11[StandHeight_{Diver}]$, $r^2=0.75$, $p<0.0001$. Note that stand heights below detection limit were excluded from regression. b) Plot of residuals of acoustic vs ground truth stand heights as a function of site depth. Dashed line is regression for EcoSAV® generated residuals ($y=0.05 \pm 0.019 + 0.018 \pm 0.01[Depth]$, $r^2=0.37$, $p<0.05$), solid line is regression for GUI residuals ($y=0.012 \pm 0.014 – 0.005 \pm 0.003[Depth]$, $r^2=0.04$, $p = 0.12$) Note: The depth values (x axis) are taken as the reported depth from the GUI output.

Correlations between percent algal cover from quadrats were poor when compared to percent algal cover estimated from the acoustic methods (Pearson r = 0.51 for EcoSAV and r = 0.49 for GUI). This is likely due to the preponderance of high algal coverage in the quadrat data (mean algal cover 84%).

The minimum biomass detection limit was estimated to be 31 ± 18 g m^{-2} (Figure 2.5a). The largest biomass value that went undetected was 28 g m^{-2} (Figure 2.5a). This sample had a mean bed height of 6 cm, below the threshold allowed for detection. The minimum biomass value that was detected was 41 g m^{-2}, on a relatively flat bottom with an average stand height of 7.5 cm. Detection rates increased rapidly for higher biomass stands. Success of detection also was influenced by stand height, but this may be due to the strong correlation (Pearson r = 0.86, p <0.01) between stand height and biomass (Figure 2.5b).

To examine the ability of the classified data to predict algal biomass, diver-estimated biomass with the average and integrated backscatter intensity from the plant canopy for each ping in the successful classifications were compared (Figure 2.6a). A positive relationship does appear to exist between biomass and 20 Log R backscatter intensity, but its predictive power is poor due to the large standard deviation between pings in the cycle sequence (Figure 2.6a). Integration of the acoustic signal (volume backscatter; Sv) between the canopy top and the declared bottom is considerably worse, showing differences only for the two highest biomass samples (Figure 2.6b). Sub-setting the data into classes of biomass (low <100 g m^{-2}, medium 100-300 g m^{-2}, moderate 300-500 g m^{-2}, and high >500 g m^{-2}) did not yield much improvement, as significant differences in average backscatter intensity were observed only for the "high" bin when compared to the other bins (ANOVA, $F_{3,22}$=8.413, p <0.05; Tukey-Kraemer post hoc test p<0.05).

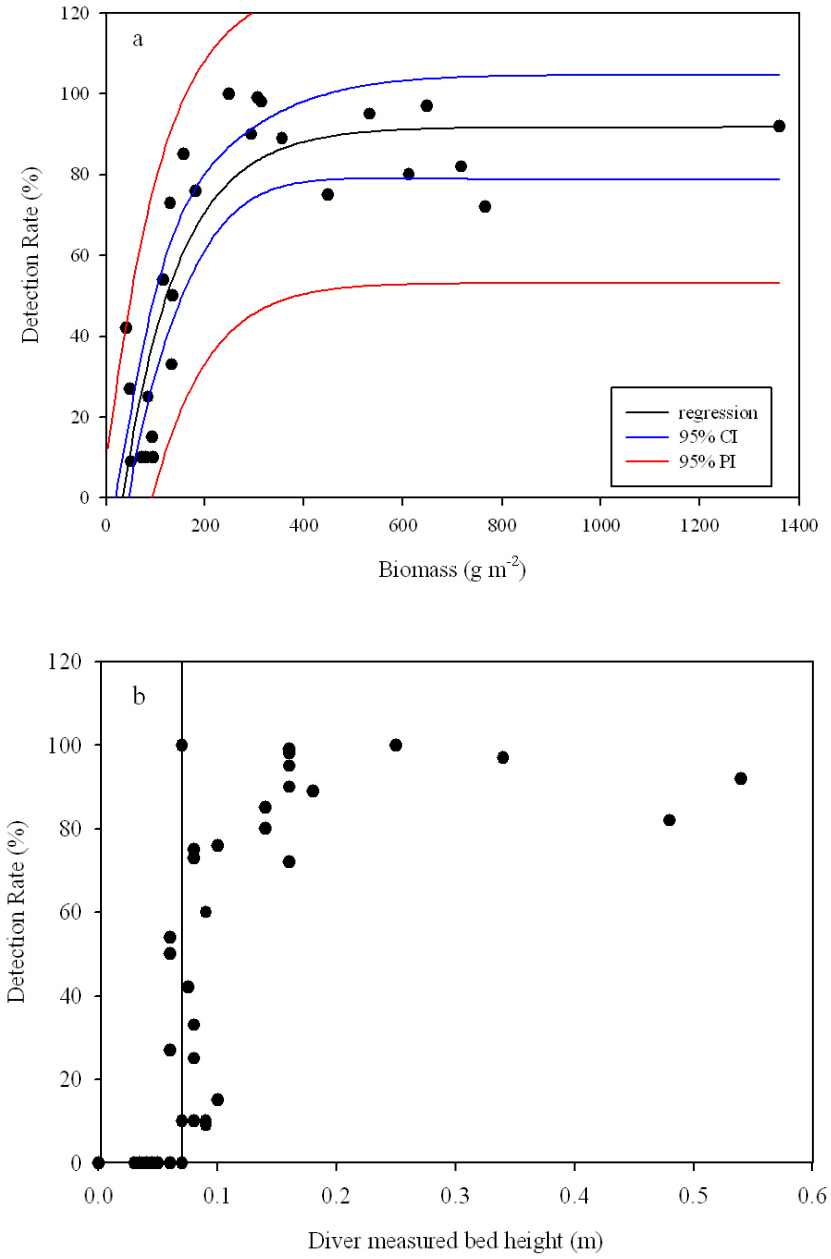

Figure 2.5 a) Detection rate (# of positive pings in a cycle sequence) vs dry biomass of *Cladophora* sp. Regression line (Equation; DetectionRate = -31.88 ± 18.6 + 123.55 ± 10.15(1-$e^{(-0.0089 \pm 0.001 \text{ x Biomass})}$), r^2=0.72, p< 0.0001) and 95% confidence intervals and 95% prediction intervals are also shown and (b) Detection rate vs *in situ* bed height as measured by divers. The solid line denotes the GUI classification threshold of 7.5 cm.

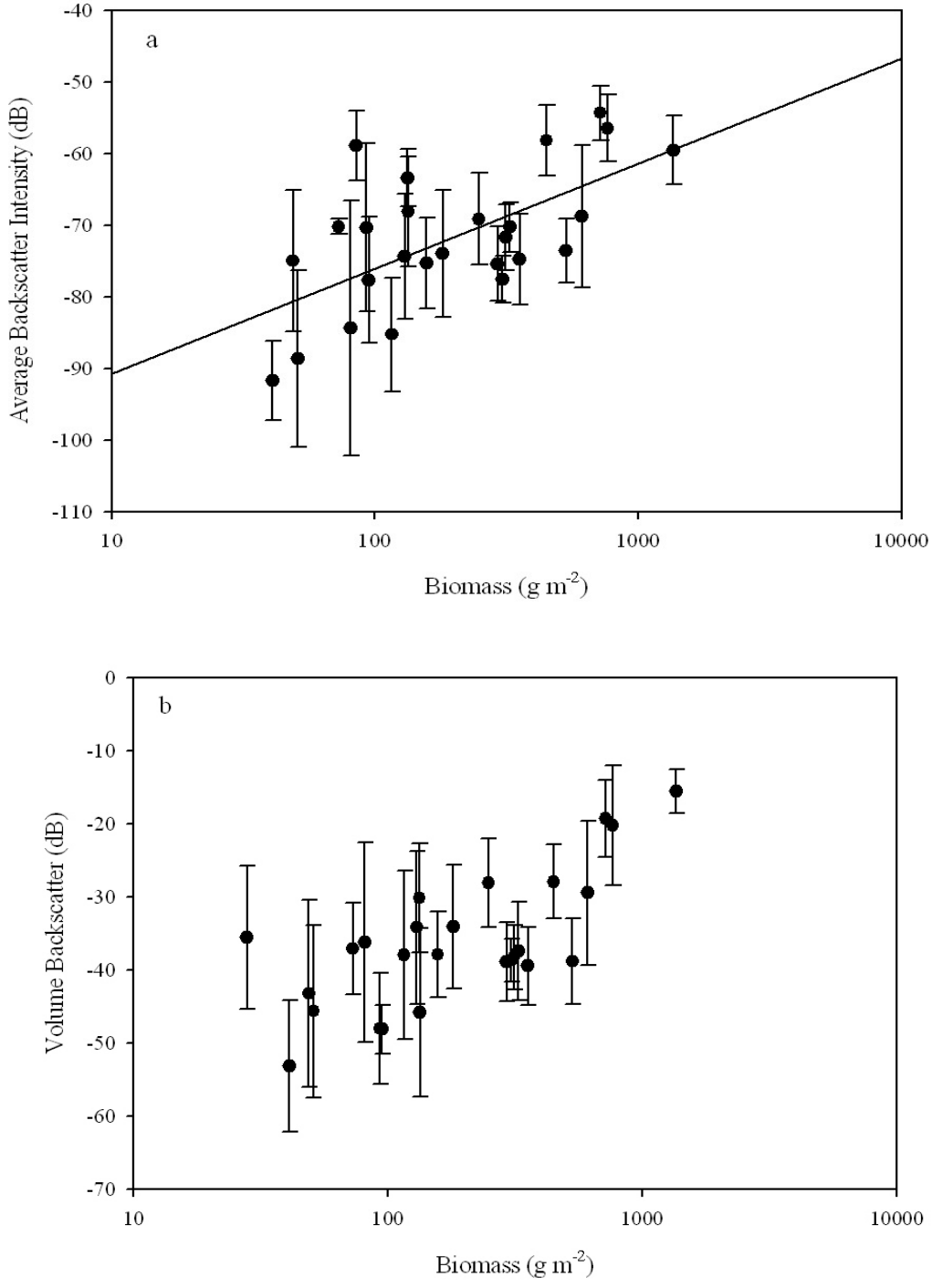

Figure 2.6. a) Mean 20 log R TVG backscatter intensity (dB) within the algal canopy, and b) volume backscatter (Sv; dB) computed for the echo envelope form the top of the algal canopy to the declared bottom depth vs Dry Biomass of *Cladophora*. Average values and standard deviations for backscatter intensity in a) and volume backscatter in b) were computed by taking the antilog of the 20log R TVG corrected data, averaging and then expressing as dB.

2.5 Discussion

2.5.1 Detection of algal presence

Acoustic detection of *Cladophora* at the two study sites was especially challenging because the areas are characterized by uneven rocky and boulder bottoms. For example, during early spring surveys at the Oakville location, *Cladophora* growth was confirmed with the use of an underwater drop video camera to be either absent or growing only in very short (< 5 cm) tufts. When the echograms were inspected, a short, weak echo directly above the stronger bottom return in the range of -50 to -60 dB was observed when passing over moderately rough cobble (pings 2850-2900; Figure 2.2). This feature is not observed over flat rocky bottoms (pings 2800-2850; Figure 2.2) or over softer depositional substrata (e.g. sand or silts – data not shown). This moderate backscatter intensity may be related to the varying perturbations of the echo associated with the highly variable surface orientation common on rocky bottoms (Hamilton 2001). Additional problems were encountered with reflection of sidelobe energy. Boulders and other vertically distinct substrata not directly in the transducer beam path often returned an echo characterized by backscatter intensity similar to that of algae, causing the unsupervised EcoSAV algorithm to falsely classify these areas as "vegetated". During supervised classification with the GUI, the rocky areas were easily distinguished by a trained analyst from the algal signal based on their curved shape and obvious height difference compared to the algal canopy and/or bottom.

2.5.2 Estimation of algal stand height

Estimation of algal stand height was significantly better with the use of the GUI when compared to estimated stand heights from EcoSAV. While the GUI underestimated stand heights by and average of 0.2 ± 3.9 cm, EcoSAV overestimated stand height by an average of 12.5 ± 7.0 cm. This is far greater than the overestimation reported by Sabol et al. (2002a) of 1 ± 4.8 cm for vascular submerged aquatic vegetation. Other studies have found larger and more variable disagreements between acoustically estimated and *in situ* plant heights, but these discrepancies are likely the result of different methods of comparison between ground truth data and acoustic data (Valley and Drake 2006).

The overestimation of stand height reported by EcoSAV is almost entirely due to the differences in algorithm logic in defining the bottom depth. Although the signal processing algorithms used in EcoSAV and the GUI are based on the rationale described in Sabol et al. (2002a), EcoSAV was primarily built to work in shallow, soft bottom estuaries and systems that would be conducive for the growth of seagrasses and macrophytes Sabol et al. (2002a). In

systems with soft substrate and strongly scattering vascular vegetation, the strongest scattering may occur in the plant canopy rather than at the substrate – water column interface (Sabol et al. 2002a). Therefore, to correctly track the bottom, a two feature bottom tracking algorithm was implemented in EcoSAV so that the declared bottom depth did not occur in the plant canopy (Sabol et al. 2002a,b). Simply speaking, the EcoSAV algorithm associates the sharpest rise in acoustic backscatter with the bottom unless the sharpest rise occurs well above the trailing edge of the bottom echo envelope. In the latter case, EcoSAV assumes that the sharpest rise occurs within the plant canopy, and not at the water column – substrate interface, and implements a depth adjustment to place the bottom depth deeper in the water column (BioSonics 2004a).

In contrast to EcoSAV, the GUI was configured to place the bottom at a user specified backscatter intensity threshold. This configuration was chose for two reasons. First, because all data were collected over rocky substrate with an overlying canopy of weakly scattering algal stands, the strongest backscatter always occurred at the water column – substrate interface. Second, the presence of rocks and uneven substrate may generate wide echo envelopes that exceed the threshold for positive classification, even if there is no growth of algae on the substratum, and in an unsupervised mode, generates a false positive. To illustrate this, two echograms and associated classification results are provided in Figure 2.7 and Figure 2.8. The MATLAB GUI classification of the two echograms is provided in Figure 2.7a and Figure 2.8a. The first case, moving slowly over a relatively shallow area (depth ~ 2 m), extreme variability in algal stand height is observed in addition to large variations in the GUI declared bottom depths, primarily due to the presence of rocks. Both EcoSAV and the GUI track the bottom reasonably well (Figure 2.7b) but EcoSAV® appears to always place the bottom depth deeper than the GUI. This is likely caused by the two point bottom tracking feature (see above). While the depth of the algal canopy is generally close between the two (Figure 2.7c; but note that EcoSAV appears to classify excessive surface noise as plant canopy, pings 1850-2100), the deeper placement of the bottom depth (mean 0.08 ± 0.06 m) results in the subsequent overestimation of algal canopy height by EcoSAV because canopy height is computed as top of plant canopy minus the declared bottom depth (BioSonics 2001). This deeper bottom depth placement by EcoSAV appears to increase as the acoustic range (or bottom depth) increases, so while the classifications in Figure 2.7 are reasonably close (~ 2 m depth) those generated for Figure 2.8 indicate that the bottom depth declared by EcoSAV is nearly double that in Figure 2.7 (0.16 ± 0.05 m) (Figure 2.8b). The depth of the algal canopy identified by both platforms, however, appears to be reasonably close (Figure 2.8c), but the corresponding estimates of algal stand height here were ~ 0.16 m greater than those produced by the GUI.

The tendency for EcoSAV to increase the overestimation of algal stand height as depth increases likely results from the use of non-normalized echo envelopes. The time to ensonify to a given angle increases with depth, causing a lengthening of the echo signal (Hamilton 2001). This phenomenon has been observed to influence substrate classification accuracy (Hamilton 2001, Dommise et al. 2005), and is most simply described as a "thickening" of the echo envelope as depth increases. The width of the echo envelope associated with the bottom is a function of pulse length, spreading time of the wave front, and the travel time in the substrate. On hard substrate at the working frequency, there should be negligible penetration of the acoustic wave into the substrate (Hamilton 2001). Since the pulse length is constant (0.1 ms), the spreading time of the wave front is the only quantity that can influence the width of the returned echo. Because the BioSonics system samples the returned echo at a constant rate (41.67 kHz; BioSonics 2004b), the width of the returned echo envelope from a ping in deep water will appear "thicker" than the width of the echo envelope from a ping in shallow water. Although newer bottom classification software (e.g., QTCView®) can correct this by normalizing the echoes to a reference depth, this feature is not implemented in EcoSAV, perhaps because it is not useful when surveying shallow estuaries for submerged vegetation.

Based on the processing algorithm in EcoSAV, such errors will increase on structurally complex bottoms where large boulders or other debris are present, as the trailing edge of the echo envelope will determine the placement of the bottom rather than the sharpest rise feature. This will lead to increasingly worse performance over very rocky bottoms, or those that produce "thick" echo envelopes (e.g., very soft silt; Valley and Drake 2006). Although the distance from the transducer to the lake bottom was not routinely measured in this study, and cannot comment on the agreement between depths predicted by EcoSAV or the GUI in relation to the true bottom depth, the deeper depth placement is the most likely cause for the disagreement between the two platforms when determining the height of the algal canopy.

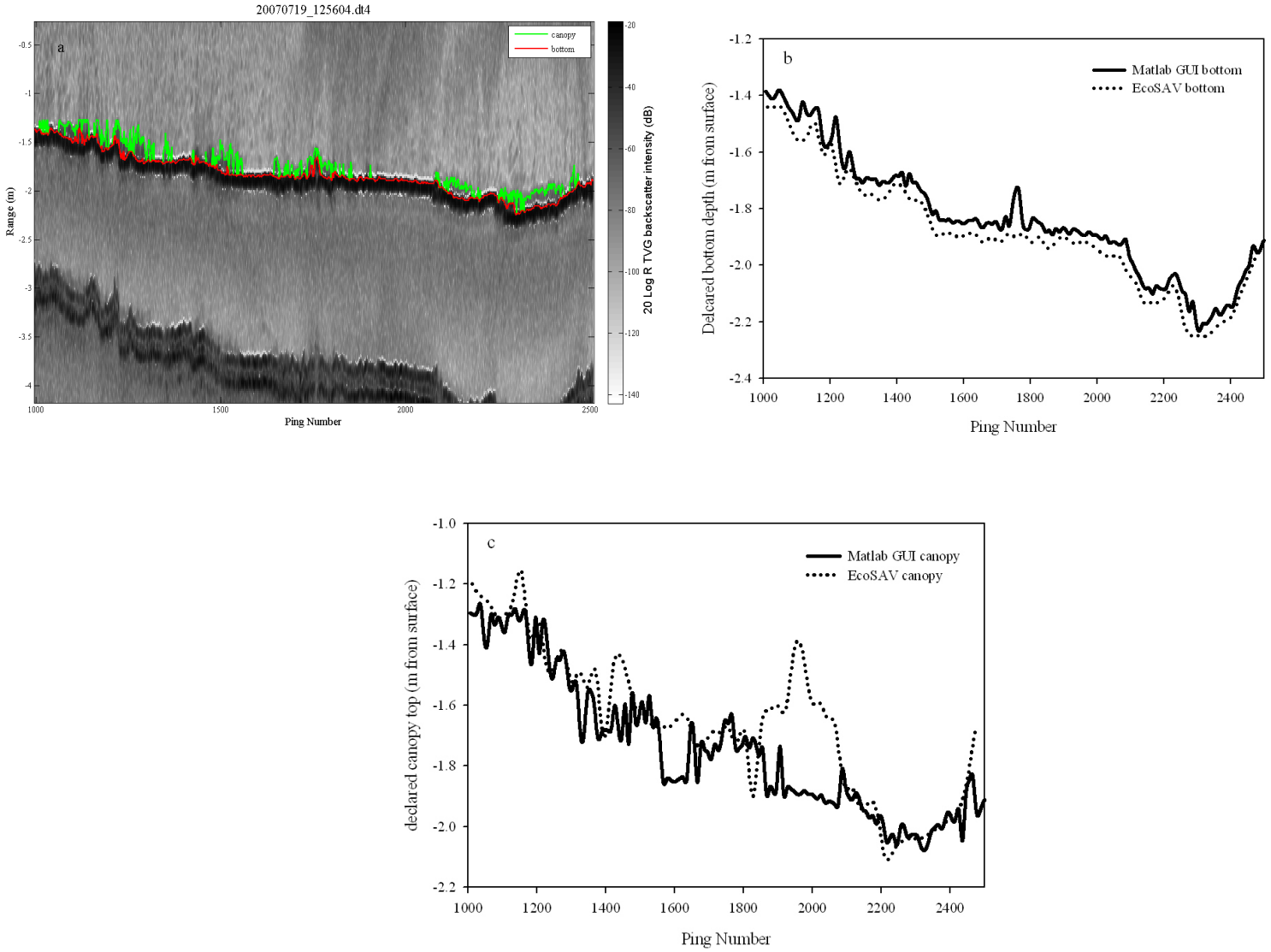

Figure 2.7. Sample echogram showing a) classification as done in Matlab GUI, b)declared bottom depths from Matlab Classification in (a) and EcoSAV® v2.0, c) estimated canopy height from Matlab GUI classification in (a) and EcoSAV® v2.0. The depth of the algal canopy was computed by adding the estimated algal canopy height to the declared bottom depth.

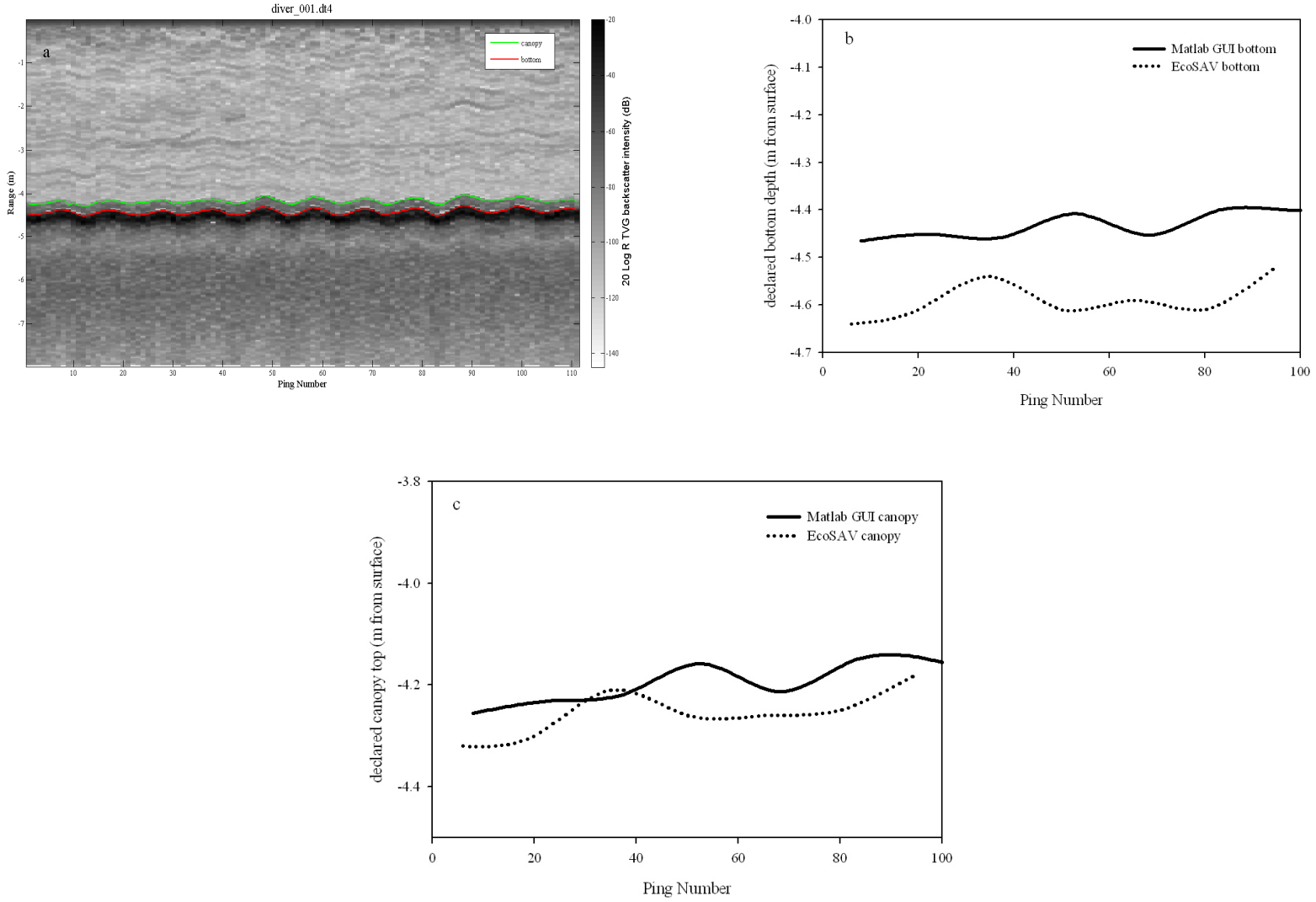

Figure 2.8. Sample echogram showing a) Matlab GUI classification, b) Matlab GUI and EcoSAV® v2.0. declared bottom depth from classified data in a), c) Matlab GUI and EcoSAV® v2.0. classified canopy top from data in a). The depth of the algal canopy was computed by adding the estimated algal canopy height to the declared bottom depth.

2.5.3 Estimation of percent cover

I observed poor correlations between percent cover estimated by acoustic methods and percent cover estimated by divers in the quadrats. Percent cover as computed by the algorithms is based on the number of plant pings divded by the total number of pings in the summary cycle. This is obviously a different quantity than percent of a quadrat covered by *Cladophora*. Furthermore, the range of percent cover values in the ground truth data set (80% to 100%; typical conditions in the study areas) were not likely of sufficient range to rigorously evaluate the ability of the acoustic method to assess percent cover. Prior work with EcoSAV using towed underwater geo-referenced video has indicated that EcoSAV reliably estimated percent cover when compared over short distances (Sabol et al 2002a, Stevens et al. 2008) or longer transects (Winfield et al. 2007) across a range of acoustic frequencies (e.g., 200 kHz – 420 kHz). Lacking access to a video system comparable to those used in previous studies, and because the nature of the ground truth data set (80% to 100% cover) makes comparisions against previous studies difficult, future work should incorporate a similar means of assessing percent cover that better relates to the nature of the percent cover as computed by the algorithms. Nevertheless, the GUI proved to be robust at characterizing the algal stand height on rocky substratum, and by extension, the estimation of percent cover should achieve a similar level of sensitivity, since a ping must be classified as plant before the stand height is computed.

2.5.4 Estimation of Biomass

Estimation of biomass or standing crop is a frequently desired endpoint in many surveys and management programs (Vis et al. 2003). Previous studies have found a linear relationship between backscatter strength and biomass (Sabol et al. 2002a), but the predictive capacity tends to be poor due to high variability of lacunae in difference species of vascular plants and the presence of epiphytic algae and/or organisms (Sabol et al. 2002a). Summation of backscatter has also been examined, but appears to suffer from a saturation effect at high biomass values (Haga et al. 2007). It is probable that for high densities of strongly scattering vegetation, acoustic shadowing becomes a factor, making the accurate determination of biomass a difficult task (Simmonds and MacLennan 2005).

The comparison of the average backscatter and biomass (Figure 2.6a) and volume backscatter and biomass (Figure 2.6b) in this study yielded poor relationships. Variability is particularly high at the low to moderate biomass levels, which are most commonly observed in the Great Lakes (e.g., Higgins et al. 2005a); thus such relationships are not likely to be of any practical value. The high variability in both the average backscatter and volume backscatter may

be due to several factors; first, although much care was taken to exclude backscatter from the substrate, the high degree of bottom roughness and the vertical resolution of the sampled echo (~ 1.8 cm) may have nonetheless included some contribution from the substratum (Ona and Mitson 1996). Second, stands of *Cladophora* are often inhabited by benthic invertebrates such as the amphipods *Echinogammarus ischnus*, *Gammarus fasciatus* and midge larvae (Chironomidae) (Barton et al. 2005, Malkin 2007). These invertebrates are characterized by target strengths (TS) that are strong enough to produce backscatter within the range used to classify *Cladophora* (-76 to -65 dB TS for chironomids [Kubecka et al. 2000] and -76 dB TS for a single amphipod [Wiebe, et al 1990]). Furthermore, the area abundances of these organisms in stands of *Cladophora* is extremely variable and can be appreicable (*E. ischnus* at up to 2,900 m^{-2} [Dermott et al. 1998 and *G. fasciatus* up to 680 m^{-2} [Haynes et al. 2005] and chironomids from 2 to 12,000 m^{-2} [Barton et al. 2005]). Because I did not attempt to quantify the numbers or types of invertebrates in the ground truth samples, the possible contribution (if any) of these animals to the backscatter measured from *Cladophora* is not known. Third, *Cladophora* growing in the lower Great Lakes is commonly encrusted with epiphytic diatoms (Stevenson and Stoermer 1982, Malkin et al. 2009). Because the density of diatom silica is ~ 2.6 g cm^{-3} (Blanc et al. 2000), it is likely that the epiphytic coating acts to increase the acoustic impedence of *Cladophora* filaments, leading to an increase in measured acoustic backscatter. The degree to which this may have affected the measures of acoustic backscatter is not easily assessed since the ground-truth data was collected during the growing season (June – August), and the abundance of epiphytic diatoms in the ground-truth samples was not determined. Last, as mentioned in the introduction, production of oxygen bubbles during photosynthesis (Hermand 2006) may significantly affect the measured backscatter, particularly at depths where light saturation is sufficient.

2.5.5 Conclusion

Acoustic methods have proven to be effective tools for estimating the abundance and cover of submerged aquatic vegetation in various habitats (Sabol et al. 2002a, Valley and Drake 2006, Warren and Peterson 2007, Winfield et al. 2007, Zhu et al. 2007) using frequencies ranging from 70 kHz (Zhu et al. 2007) to 600 kHz (Warren and Peterson 2007). Here, I show that detection and estimation of nuisance filamentous algal stand height was successful for algal stands that exceeded 7.5 cm in height, suggesting that this approach could be useful in environments previously thought to be incompatible with acoustic surveys (Sabol et al. 2002b). There are, however, some shortcomings of the acoustic method that must be noted. First, in areas where *Cladophora* is present, but at low biomass or insufficient stand height, acoustic methods will fail because of the inability to detect algal stands shorter than 7.5 cm. While this would undoubtedly be problematic for surveys designed to examine absolute presence or absence of *Cladophora*, it is

far less of a problem for those designed to characterize the distribution of nuisance growths where stand heights often exceed 7.5 cm. In the Laurentian Great Lakes, the majority of the algal fouling problems occur when algal biomass accrues to nuisance levels (e.g., Higgins et al. 2005a). A tool, therefore, that has the ability to characterize *Cladophora* (or other macroalgal) stands would be of great value for monitoring programs. Second, the nature of the algorithm in the GUI is based on interpretation of vegetated and unvegetated surfaces, and therefore requires a trained operator to interpret the collected echograms and supervise the classification procedure. Although this may seem an onerous task, the visualization of the acoustic data and classification in the GUI provides a functionality not yet available in commercial software. The analyst can observe the classification and adjust relevant parameters to achieve the best possible classification. The GUI additionally contains the ability to manually remove improperly classified data (for example, schools of fish, large boulders, logs, or steep bottom slopes) much in the same manner as other acoustic analysis programs (e.g. EchoView®) can do for data collected during fisheries surveys.

Despite the challenges of acoustic detection of *Cladophora*, I believe that this method can be a valuable addition to current research and monitoring programs. The combination of robustly characterized acoustic signals and geo-referenced position data allows for rapid mapping of the spatial distribution of nuisance algal growth; information that is important for designing and assessing effective management strategies. Although *in situ* sampling is still needed for species identification and ground truthing, acoustic survey data provide much better spatial resolution than can be obtained from more laborious manual methods. The combination of acoustic and *in situ* methods will ultimately provide a much better tool for characterizing benthic algal growth in shallow water environments than has been available previously.

Chapter 3

The distribution of nuisance *Cladophora* in the Laurentian Great Lakes; Influence of land use, water quality and dreissenid mussels

3.1 Overview

Selected shorelines in Lakes Erie, Huron and Ontario in addition to two offshore shoals (Lake Erie and Lake Ontario) were surveyed with a high frequency hydroacoustic system to assess how current spatial patterns of nuisance benthic filamentous algal (e.g., *Cladophora*) growth and biomass relate to current distributional patterns of water quality, land use and dreissenid abundance. Results from these surveys indicate that *Cladophora* grows to nuisance amounts in Lakes Erie and Ontario where suitable substrate exists, but does not accumulate to similar biomass in Lake Huron or Georgian Bay. Remarkable similarity between lakes and study sites with respect to nutrient concentrations suggest that the present day distribution of nuisance *Cladophora* growth is not simply determined by measures of near shore phosphorus. In contrast to differences in coastal land use and near shore nutrient regimes, abundances of dreissenid mussels appear to be key determinants governing the contemporary distribution of nuisance *Cladophora* in the Great Lakes.

3.2 Introduction

In the 1960s and 1970s, many areas in the Great Lakes, including most of Lakes Erie and Ontario supported excessive production of both planktonic and benthic algae as a result of decades of eutrophication (Glooshenko et al. 1974, Shear and Konasewich 1975). Luxuriant growths of benthic algae (dominated by the filamentous green alga *Cladophora*) were commonly observed in the rocky littoral areas (Neil and Owen 1964, Herbst 1969) and in close proximity to tributary mouths or waste water treatment plant outfalls (Auer et al. 1982, Ontario Ministry of the Environment 1982). These excessive growths of benthic algae tended to detach in mid-summer, frequently fouling municipal and industrial water intakes and generally interfering with recreational use of nearshore areas of the lakes, mainly through the deposition of vast accumulations of rotting algal material (Higgins et al. 2008a). These nuisance blooms of *Cladophora* were a key driver for the Great Lakes Water Quality Agreement (GLWQA) first signed in 1972. Phosphorus abatement programs were implemented to reduce the phosphorus emitted from point sources such as sewage treatment plants. These strategies were effective at reducing both near shore (Nicholls et al. 2001) and open lake phosphorus concentrations (Lean et al. 1990), and there is evidence that the phosphorus control strategies contributed to the decline in nuisance *Cladophora* growth in the Great Lakes (Auer et al. 1982, Painter and Kamaitis 1987).

Beginning in 1995, reports of shoreline fouling in Lake Erie were increasing (Higgins et al. 2008), and in subsequent years (1999 to 2004), areas in Lake Erie (Higgins et al. 2005a), Ontario (DeJong 2000, Malkin et al. 2008) and Michigan (Bootsma et al. 2005) were all experiencing a resurgence of fouling by filamentous algae, again dominated by *Cladophora*. The proximal causes of increased benthic algal fouling were not immediately clear. Between 1981 and the mid 1990s, total phosphorus loading to Lakes Superior, Michigan and Huron were at or below targets as were the offshore total phosphorus concentrations (Neilson et al. 1995). In Lakes Erie and Ontario, total loads and open lake concentrations were also generally at levels set by the International Joint Commission (Neilson et al. 1995). Although diffuse non-point sources of P remain difficult to characterize and accurately estimate (Dolan and McGunagle 2005), the apparent stability of measured P loads coupled with the continued maintenance of near or below target TP concentrations in offshore waters (e.g. Kelly 2009, Malkin et al. submitted), the symptoms of eutrophication in the near shore were rather contradictory, and have led to questions whether the renewed frequency of shoreline fouling by *Cladophora* in the Great Lakes are driven by changes to the lake ecosystems or by an increased nutrient load from poorly characterized catchments and municipal sources that are closely coupled to the near shore waters.

During the last 15 years, the arrival and establishment of a number of exotic species have impacted the ecology of the Great Lakes. Dreissenid mussels (e.g., *Dreissena polymorpha* and *D. bugensis*) are arguably the species that have affected the greatest changes, especially in the rocky near shore regions which are conducive to heavy colonization (Vanderploeg et al. 2002). Even in areas with soft substrate, mussels are able to colonize and form druses (Haltuch et al. 2000) and shell material from expired mussels can also expand the habitat for colonization (Hecky et al. 2004). As sessile benthic filter feeders, mussels feed primarily on phytoplankton and suspended detritus and expell fully and partially digested material as feces and pseudofeces (Vanderploeg et al. 2002) in addition to soluble PO_4 and NH_4^+ released through excretion (e.g., Arnott and Vanni 1996, Conroy et al. 2005). The filtration of suspended matter from the water column not only increases water clarity (Howell et al. 1996), but re-locates particulate nutrients from the pelagic environment to the benthos (Hecky et al. 2004) where they may be remobilized and are available for use by benthic organisms such as detritivores (Stewart et al. 1998a). Due to their high biomass and resultant filtration capacity, mussels have been implicated as key agents altering near shore nutrient dynamics in the Great Lakes, such that while total nutrient loads may not have changed, the distribution of the nutrients within the system may have (Hecky et al. 2004).

Changes to the ecology of near shore environments as a result of exotic species invasions are not the only stressors acting on the coastal areas. Much of the land immediately adjacent to the lower lakes has experienced drastic changes in recent years, to the point where the pace of land use – land cover change in these areas has exceeded that predicted on the basis of population growth alone (Wolter et al. 2006). In particular, conversion of un-developed land to urbanized, impervious developed land within a relatively narrow band (10 km) of the lake shores has increased between 1992 and 2001 (Wolter et al. 2006). Because the GLWQA mainly addressed the P loading issue by regulating P concentrations at point sources rather than non-point sources, increases in the impervious surface area adjacent to the waterways and lakes have the potential to increase the non-point source load from increasingly urbanized watersheds to the nearshore areas of the lakes. Moreover, the increasing population in expanding urban areas generates increased waste loads. Waste water treatment plants must manage this increased load to keep effluent concentrations at mandated levels. But mandated levels are based on concentrations and not total loads. Consequently, the total load may increase unless treatment efficiencies are imposed by the plants. Urban areas also must deal with problems of combined sewer overflows (CSOs) as a result of increased discharge volumes from impervious landscapes (Marsalek and Rochfort 2004). This has led to concern that increased urbanization especially in coastal areas may be causing

increased point and non-point loadings from these urban areas which may be fueling a resurgence of *Cladophora* and nuisance algal growth.

To date, much of the success of P control programs has been evaluated through the monitoring of offshore concentrations and the response of the phytoplankton community. In contrast, there is a relative dearth of data on benthic algal growth in the nearshore zone despite its proximity to human uses. At least part of this paucity of information is related to the inherent spatial variability of the near shore benthic environment which requires sampling of extensive areas to ensure that results are meaningful and representative of different shoreline types, but the primary reason for the disparate levels of information is due to the direction of monitoring objectives implemented with the GLWQA which directed the research foci to offshore processes and effects of eutrophication on fisheries.

Chapter 2 reports the development of a hydroacoustic method that enables rapid sampling and mapping of *Cladophora* distributions over large areas that overcome the uncertainties that arise from undersampling with point sampling methods. The objectives of this chapter were to utilize the hydroacoustic methodology presented in Chapter 2 to assess the current state of benthic algal growth in the near shore zones of the Great Lakes and generate accurate maps to describe the spatial patterns of benthic algal (mainly *Cladophora*) cover and bed height along selected shorelines in the Lower Great Lakes. Shorelines in Lakes Ontario, Erie and Huron were chosen to allow evaluation of *Cladophora* growth along contrasting shorelines with differing land use types (urban and rural/agricultural). Two offshore shoals that should represent open lake nutrient and light conditions were also surveyed.

3.3 Materials and Methods

3.3.1 Site Selection and Descriptions

This study examines spatial patterns in nuisance benthic algal (*Cladophora*) cover and bed height, associated water quality parameters and dreissenid mussel abundance in the lower Great Lakes (Erie, Ontario and Huron) during 2005 along shorelines that provided contrasting coastal land use types (Figure 3.1, Figure 3.2, Figure 3.3 and Table 3.1). Two offshore shoal sites (Nanticoke Shoal in Lake Erie and Dobb's Bank in Lake Ontario) were selected to represent open lake nutrient conditions while retaining enough area with suitable light and substrate for *Cladophora* growth. Sites were chosen on the basis of having a dominant underlying substratum primarily composed of rock, and where possible, had been previously sampled for *Cladophora* and/or dreissenid mussels.

Coastal land use was characterized using NRVIS (Natural Resources and Values Information System) data from SOLRIS (Southern Ontario Land Resource Inventory System v.1.2; Ministry of Natural Resources 2002) land use / land cover inventory. SOLRIS provides a comprehensive, landscape level inventory of natural, rural and urban areas in Southern Ontario following the standardized ecological land classification for southern Ontario for the years 2000-2002 on a 25 m^2 raster format for most of Southern Ontario (Lee et al. 1998). Land use / land cover of the coastal areas immediately adjacent to the surveyed shorelines was characterized by creating a polygon that extended up to five kilometers inland along the length of the shoreline surveyed. Land use / land cover of the watershed draining into the lake at the study areas was characterized by clipping with the watershed boundaries for the respective study sites. This information is summarized in Table 3.1.

Provincial Water Quality Monitoring Network (PWQMN; Ontario Ministry of the Environment; Figure 3.4) data were used to assess trends in TP, NO_3^- and Cl^- concentrations in the closest monitored major tributaries to the study sites (Figure 3.4). Loadings were not computed as discharge data was not available for all stations and years, however, trends in tributary concentrations may provide a proxy for increases in loading from the respective catchments. Temporal trends in annual median concentrations (TP, NO_3^-, Cl^-) between 1964 and 1984 (pre-P control to post-P control) and between 1985 and 2008 (post-P control) were assessed using a Mann-Kendall trend test.

Table 3.1. Summary of the survey sites visited in 2005 with land cover characteristics. Site names as in Figures 3.1 to 3.3. Survey dates; date of acoustic survey, WQ date; date of water quality sampling, Coastal Land Use indicates the % of land use type within 5 km of the shoreline adjacent to the survey area, Watershed Land Use indicates the % land use of the quaternary watershed for the surveyed shoreline extent. Land Use types are denoted as; AG: Agricultural/Rural, CF; Coniferous Forest, DF: Deciduous forest, M: Marsh, MF: Mixed forest, UR: Urban/developed, SW: Swamp.

Site	*Lake*	*Survey Dates*	*WQ Dates*	*Coastal Land Use**	*Watershed Land Use***
Peacock Pt	Erie	May 25 July 19	April 29, July 12	AG (76.2%), SW (7.1%), UR (6.7%)	AG (84.5%), SW (4.8%), DF (2.7%)
Grand River	Erie	May 21 July 14	May 11, July 15	AG (66.4%), SW (10.4%), UR (9.9%)	AG (66.2%), UR (11.1%), SW (9.3%)
Nanticoke Shoal	Erie	May 26, July 12	May 5, July 12	None	None
Oakville	Ontario	May 30, July 25	June 1, July 25	UR (83.5%), AG (7.7%), DF (2.7%)	AG (50.9%), UR (23.7%), DF (10.8%)
Port Credit	Ontario	May 31, July 21	June 2, July 21	UR (89.6%), AG (2.9%), CF (1.9%)	UR (50.3%), AG (33.1%), DF (4.4%)
Presqu'ile Prov Pk.	Ontario	June 7, July 27	June 8, July 27	SW (32%), UR (21.6%), M (8.9%)	AG (52.7%), SW (15.7%), DF (6.7%)
Dobbs Bank	Ontario	June 7, July 27	June 8, July 27	None	None
Southampton	Huron	August 4	August 4	AG (46.9%), SW (30.4%), MF (7.5%)	AG (61.6%), SW (17.5%), DF (6.5%)
Pike Bay	Huron	June 13	June 13	CF (77.3%), AG (19.0%), MF (9.3%)	CF (40.5%), AG (14.9%), DF (14.6%)
Cape Chin	Georgian Bay	June 15, August 8	June 15, August 8	CF (34.7%), DF (24.1%), AG (11.9%)	CF (42.4%), DF (15.8%), AG (15.4%)

*Coastal Land Use data was summarized using SOLRIS data (25m grid raster) and digitizing a polygon the length of the survey area extending 5 km inland.**Watershed land use was computed using SOLRIS data and quaternary watershed boundaries that drained into the study area.

The Georgian Bay site (Cape Chin – Dyers Bay; Figure 3.1) was located on the submerged portion of the Niagara escarpment, approximately 40 km south of the tip of the Bruce Peninsula. The shoreline here is characterized by the limestone cliffs of the Niagara Escarpment, and is predominantly forested with minimal development (Table 3.1). The steeply sloping boulders and rocks continue underwater to a depth of 20 m before changing to softer depositional silt (Duthie and Jones 1990).

The first of two Lake Huron sites (Pike Bay) was located on the west coast of the Bruce Peninsula (Figure 3.1b). The shoreline at this site is characterized by mostly forest cover (Table 3.1). The second site (Southampton; Figure 3.1c) was split into two parts; the first was located at MacGregor Point, and the second adjacent to the mouth of the Saugeen River (Figure 3.1c). Land use along this section of shoreline is mostly agricultural, and the Saugeen River drains a large, agriculturally intensive watershed. Urban development is relatively low on this portion of Lake Huron shoreline, with the towns of Southampton and Port Elgin the most obvious developed areas. The substratum at both these sites is predominantly glacial till and bedrock in the littoral, changing to glaciolacustrine clay and mud in deeper profundal waters (Thomas et al. 1973). The bottom topography at Pike Bay is more complex with many shallow shoals and ridges (Figure 3.1b).

The three sites in Lake Erie were situated in the East Basin. The northern shoreline of the East Basin of Lake Erie is dominated by bedrock, with smaller areas of glacial till and sand (Rukavina 1976). Nanticoke shoal (42 44.4° N, 80 04.2° W) is located ~ 6.1 km offshore (Figure 3.2a), and provides a site with suitable substrate and light conditions, but nutrient conditions that are primarily driven by open lake processes. The first of two shoreline sites extended from Peacock Point to Hoover Point (Figure 3.2b), while the second was located where the Grand River enters the lake (Figure 3.2c). Both the Peacock Point and Grand River sites are characterized by land use dominated by agriculture (Table 3.1).

The western end of Lake Ontario is highly urbanized forming a near continuous urban landscape from Oshawa, east of Toronto westward to St. Catharines near the Niagara River. Home to over 4 million residents (Rao et al. 2003), municipal water intakes and discharges are situated in a narrow band of the lake, extending at most, a few kilometers offshore (Rao et al. 2003). The shoreline contains numerous tributaries, creeks and storm sewers that discharge a mixture of both urban and agricultural runoff to the nearshore waters. The first site in lake Ontario, adjacent to the town of Oakville (Figure 3.3a) features moderately steep bathymetry with a substratum composed of bedrock and cobble. Within the study site there were two active waste water treatment plant (WWTP) outfalls (Southeast WWTP; situated 300 m from shore at a depth

of 4 m and Clarkson WWTP; situated ~ 1 km from shore at a depth of 16.5 m) and 20 storm sewers discharging at the lake shore (Figure 3.3a). An additional 49 storm sewers discharged into a tributary or creek that eventually discharged into the near shore waters (Figure 3.3a). The main tributary for this segment of shoreline (16 Mile Creek) discharges at the approximate middle of the survey area.

The second heavily urbanized site in Lake Ontario was located north east of Oakville at the town of Port Credit (Figure 3.3b). Similar to the Oakville site, substratum here is characterized by bedrock and cobble, but softer substrate such as sand and compact clay comprise appreciable portions of the bay at the northeast end of the survey area. While the numbers of storm sewers and municipal water outfalls appears similar to that at the Oakville site, the largest concentration of storm sewers was at the easternmost end of the survey area, and only one WWTP was operational (Lakeview WWTP) during the time of the survey. The Credit River is the largest tributary within the study site and drains a heavily urbanized watershed (Table 3.1).

The remaining two sites in Lake Ontario were located toward the east end of the lake. Presqu'ile peninsula is a Provincial Park and has minimal urban development (Figure 3.3c). This peninsula is a tombolo (depositional landform) that grows approximately 2 m each year as eroded material from the bluffs along the northern Lake Ontario shoreline is deposited in Popham Bay (Martini and Kwong 1985). The substrate on the lakeward side of the Presqu'ile peninsula is mostly comprised of bedrock and glacial till, but areas of sand and softer substrate are present in the lee of High Bluff and Gull Island (Rukavina 1970). The last site was located approximately 7 km southeast of Presqu'ile peninsula, on a long, southwesterly trending bedrock ridge (Figure 3.3d). There are a number of these forms in Presqu'ile – Wellington Bay that protrude onto the shelf as shoals and islets, intersecting the softer, sandy deposits in the bay (Martini and Kwong 1985). Similar to Nanticoke shoal, this site provided a suitable substrate and light environment, but nutrient conditions more similar to open lake conditions.

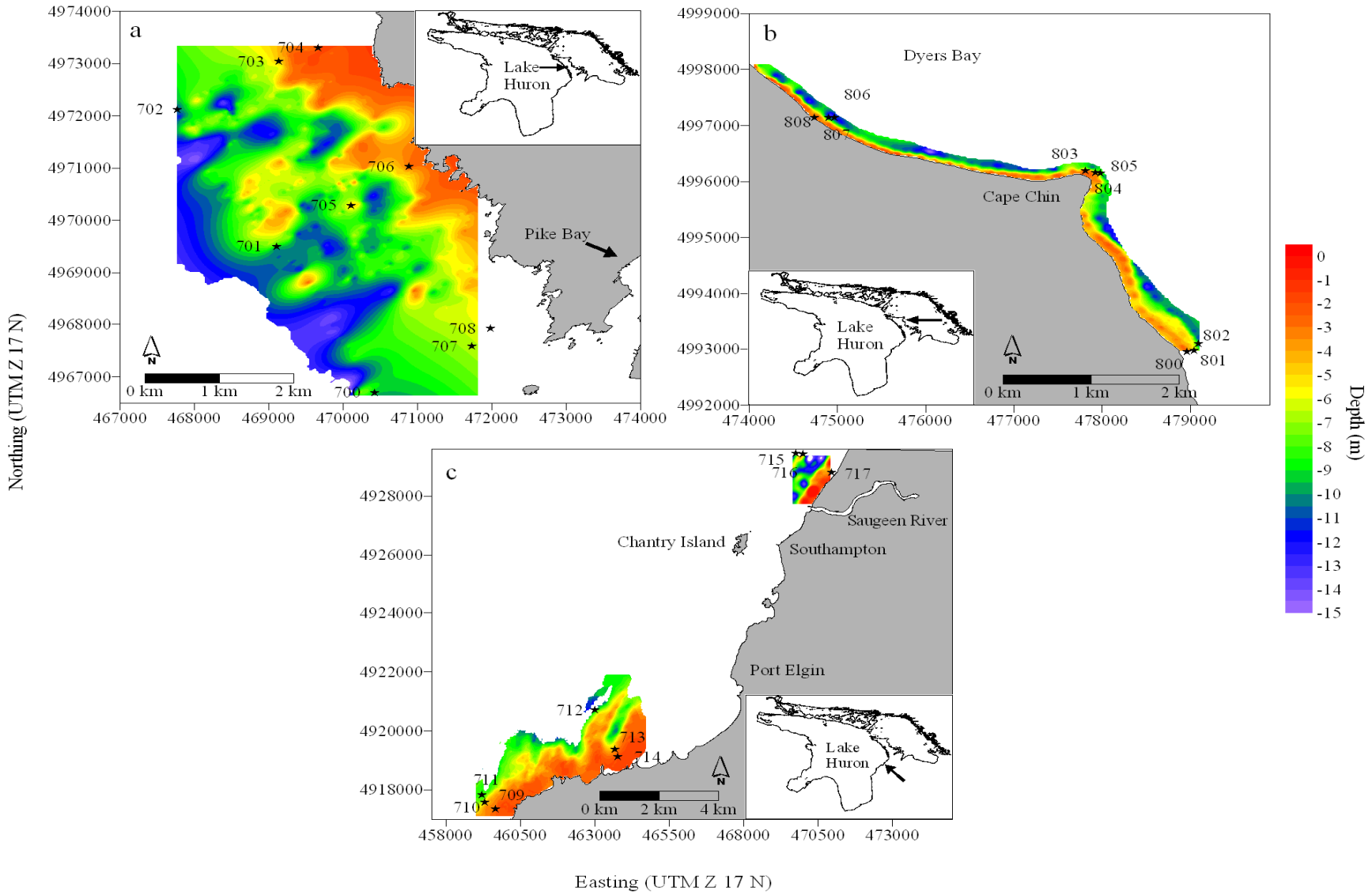

Figure 3.1. Map of the Pike Bay (a), Cape Chin – Dyers Bay (b) and Southampton (c) study sites showing locations of water quality and underwater camera sampling stations and associated bathymetry where acoustic surveys were conducted. Inset panel denotes location of the study site in Georgian Bay or Lake Huron. Water quality and underwater camera stations denoted by (★). Station labels are noted on figures.

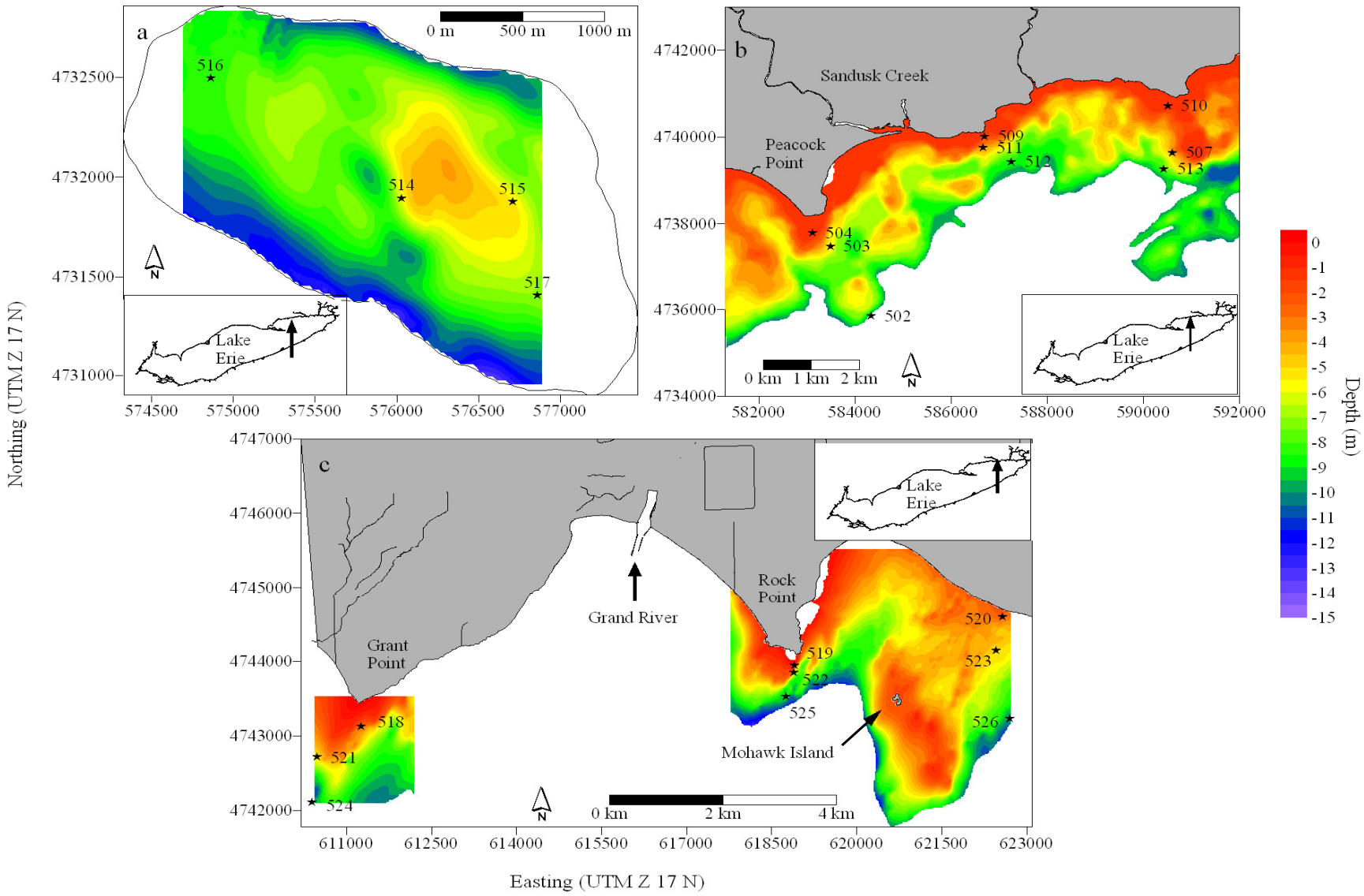

Figure 3.2. Map of Nanticoke shoal (a), Peacock Point (b) and Grand River (c) study sites showing locations of water quality and underwater camera sampling stations and associated bathymetry where acoustic surveys were conducted. Inset panel denotes the location of the study site (arrow) within Lake Erie. Water quality and underwater camera stations denoted by (★). Station labels are noted on figures.

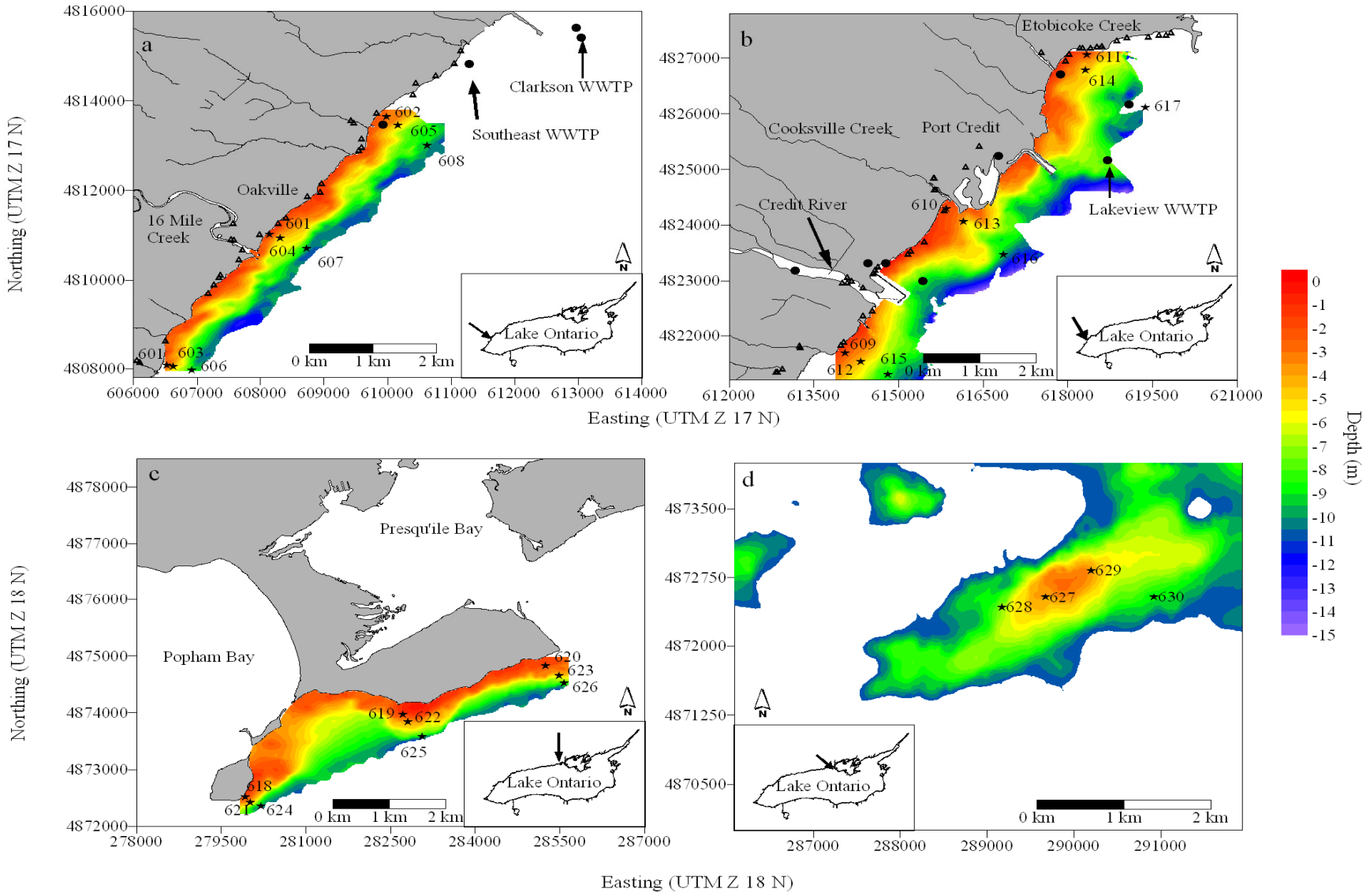

Figure 3.3. Maps of Oakville (a), Port Credit (b), Presqu'ile Provincial Park (c) and Dobb's Bank (d) study sites showing locations of water quality and underwater camera sampling stations (★) and bathymetry where acoustic surveys were conducted. Inset panel denotes the location of the study site (arrow) within Lake Ontario. Storm sewers discharging to tributaries or directly to the lake are denoted by (△), industrial and municipal outfalls with (●).Locations for storm sewers and outfall locations from Griffiths (1990). Note that UTM zone differs between upper and lower panels.

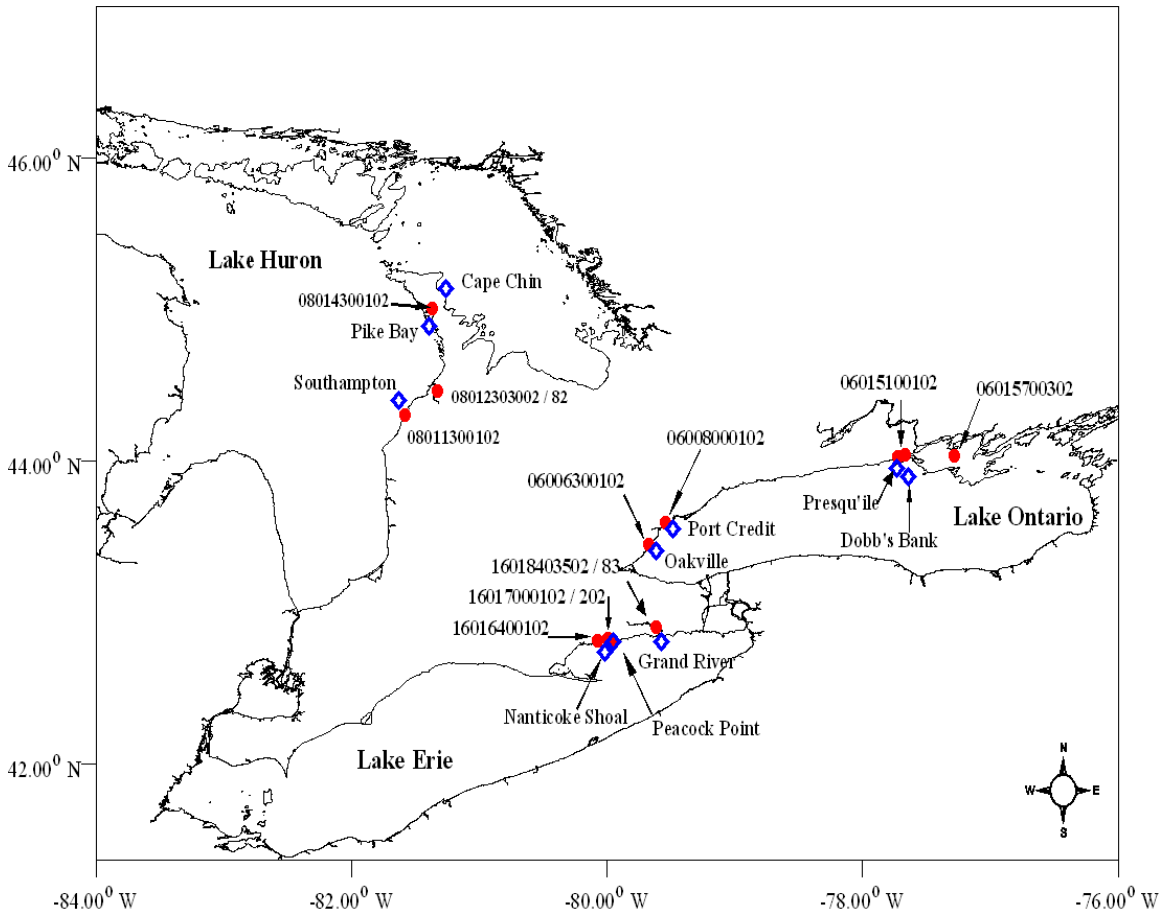

Figure 3.4. Map of Lake Huron, Lake Erie and Lake Ontario showing the approximate locations of the acoustic and water quality surveys and the locations of provincial water quality monitoring network (PWQMN) stations nearby the acoustic survey sites. Locations of acoustic and water quality surveys are denoted by (◇) and locations of PWQMN sites are denoted by (●). PWQMN Station IDs as in Table 3.5.

3.3.2 Physical and Chemical Measurements

At each survey location, three transects consisting of three stations on each transect were placed at approximately the middle and end of the survey grids (see Figure 3.1 to Figure 3.3), giving an inter-transect spacing of ~ 3 km. Stations were located at the 2, 5 and 10 m depth contours. At each station, CTD profiles were taken using aYSI-6600 profiler or an RBR CTD. Photosynthetically active radiation (PAR) profiles were measured with a LI-COR quantum sensor at 0.5 m to 1 m intervals from the surface to the lake bottom. Water samples to characterize nutrient conditions were collected at pre-selected stations (see Figure 3.1 to Figure 3.3) during the days of the acoustic surveys (Lake Huron, Lake Ontario) or within 1-2 days of the acoustic surveys (Lake Erie, Nanticoke Shoal excepted; see Table 3.1). A 6 L Niskin bottle was used to collect ~ 15 L of water at a depth equal to 50% of the mixed layer depth (determined from CTD cast). Water was transferred to covered carboys and stored in coolers until transported to the laboratory (Univ. Waterloo). Samples for total dissolved P (TDP) and soluble reactive P (SRP) were filtered through a 0.2 µm polycarbonate filter, particulate P (Part P) by filtering 500 mL of lake water onto acid soaked (5% HCl ~ 4 hr) Whatman GF/F filters (nominal pore size ~ 0.8 µm). Total P (TP) and all composite fractions (TDP, SRP, Part P) were determined according to Stainton et al. (1977). Samples for other particulate nutrients (carbon – Part C, nitrogen – Part N) were determined by filtering 500 mL of lake water onto pre-combusted (500 C ~ 4hr) GF/F filters and assayed using a CEC-440 Elemental Analyzer (Exeter Analytical, MA). Phytoplankton chlorophyll *a* was measured in triplicate on extracts of GF/F filters (22 hr in 90% acetone @ -20 °C) after filtration of 500 mL of lake water using a Turner Designs 10-AU fluorometer (Smith et al. 1999). Additional ions (NO_3^-, Cl^-, SO_4^-) were determined using ion chromatography (Dionex DX 500, Dionex AS17 and AG17 guard column). Ammonium was determined following the method of Holmes et al. (1999) on a Turner Designs TD-700 fluorometer. Total suspended solids (TSS) were determined by filtering 2 to 5 L of lake water onto pre-combusted (500 °C for 4 hr) pre-weighed GF/F filters, drying at 65 °C to a constant weight and re-weighing. AFDW was determined after combustion at 500 °C for 4 hrs.

3.3.3 Dreissenid Mussel abundance

A drop video camera (SplashCam) fitted in an aluminum frame was used to estimate dreissenid abundance and qualitative information on substrate at all sites where water chemistry and physical measurements were made. This system and methodology is described in detail in Ozersky et al. (2009). At each site, the camera frame was allowed to rest at 8 to 10 randomly

selected areas. After the video was complete, screen captures of the 8 to 10 areas of the bottom were extracted and processed using Adobe Photoshop 5.0. Dreissenids were enumerated by counting mussel valves as outlined in Ozersky et al. (2009). Unfortunately, the spring sampling period did not allow us to capture unobstructed views of the bottom and dreissenid community in Lakes Erie and Ontario as *Cladophora* growth obscured the bottom. Consequently, dreissenid abundances for Lake Erie site from Patterson et al. (2005) and Lake Ontario sites from Wilson et al. (2006) and Ozersky et al. (2009) have been substituted. Abundances at Peacock Point, and the Grand River site were determined by averaging data from 2, 5 and 10 m depths from Patterson et al. (2005). Abundances for Nanticoke shoal were determined by averaging data from 5 and 10 m depths from Patterson et al. (2005). Dreissenid abundance reported for Oakville was the mean abundance reported by Ozersky et al. (2009) for depths between 2 and 15 m. Abundances for Port Credit, and Presqu'ile and Dobb's Bank were estimated by averaging abundances from 5 and 20 m depths from Wilson et al. (2006).

3.3.4 Acoustic Surveys

Acoustic surveys to assess the spatial patterns of *Cladophora* abundance were conducted using a BioSonics® DTX system connected to two single beam transducers. Both transducers were mounted on 2 m adjustable aluminum sliding mounts attached to the side of a 21 ft vessel with a series of clamps and bolts. The first transducer was used to characterize the algal canopy (430 kHz, 10.2° full beam angle, source level 213 dB re 1 µPa at 1 m) while the second transducer (120 kHz, 7° full beam angle, source level 216 dB re 1 µPa at 1 m) was used to characterize substrate. Both transducers were set to ping at 5 Hz, with pulse lengths of 0.1 ms (430 kHz) and 0.4 ms (120 kHz) using the software Visual Acquisition 5.0 (BioSonics Inc, Seattle, WA).

Acoustic surveys were conducted on hydroacoustic line transects that ran perpendicular to shore, from the 1.5 m depth contour to the 10 m depth contour, with an inter-transect spacing of ~ 50 - 90 m. At a cruising speed of 1.8 to 2.3 m s^{-1} between 10 and 15 hours were needed to survey ~ 6 km of shoreline with the transect spacing employed. Saturation of the acoustic signal was observed for all data collected with the 120 kHz transducer at depths < 6 m making accurate separation of bottom substrate classes using standard classification methods (i.e. RoxAnn) nearly impossible, therefore these data are not reported here nor discussed further. Analysis of the acoustic data to determine percent cover and bed height of *Cladophora* was conducted using a graphical user interface (GUI) written in MATLAB v7.2 (see Chapter 2).

3.3.5 Geostatistical Methods

The fundamentals of geostatistical analysis, with emphasis on the assumptions and methodology involved are thoroughly explained in several publications (e.g., Isaaks and Srivastava 1989, Cressie 1991, Webster and Oliver 2001) and summarized in Chapter 1, so only a brief summary will be provided here. In this study, a spatial correlation function called the "semivariogram" (Cressie 1991) was employed to characterize the spatial autocorrelation of the data collected. The semivariogram is derived from the experimental data, taking into account the spatial position of the samples by the following equation;

$$\gamma(h) = \frac{1}{2N(h)} \sum_{i=1}^{N(h)} \{Z(x_i) - Z(x_i + h)\}^2 \tag{3.1}$$

where $Z(x_i)$ is the value of the variable Z at location x_i, h is a lag distance over which the local average is taken and $N(h)$ is the number of point pairs at the lag distance (h) (Cressie 1991). The semivariogram is the average of the Euclidean distance between pairs of samples (h) plotted against average variance at distance h.

For prediction, a function (the spatial covariance function or semivariogram model) is fit to the empirical semivariogram through an automated fitting procedure. The weighted least squares method (WLS) of fitting the semivariogram model was used as it typically defines the behavior of the semivariogram model at the origin most clearly, which is essential for prediction (Cressie 1991). Either spherical or exponential semivariograms were fit to the data as given by the following equations;

$$\gamma(h;\theta) = \begin{Bmatrix} 0, & h = 0 \\ C_0 + C_s\ ((3/2)(\|h\|/\alpha_s) - (1/2)(\|h\|/\alpha_s)^3), & 0 < \|h\| \le \alpha_s \\ C_0 + C_s, & \|h\| \ge \alpha_s \end{Bmatrix} \tag{3.3}$$

$$\gamma(h;\theta) = \begin{pmatrix} 0, & h = 0 \\ C_0 + C_e(1 - \exp(-\|h\|/\alpha_e)), & h \neq 0 \end{pmatrix} \tag{3.4}$$

These spatial covariance models are defined by three essential parameters: the nugget (C_0) (indicating the variance not explained by the spatial model), the sill C_s (indicating the variance explained by the spatial model) and the range α (distance beyond which spatial autocorrelation is no longer significant). After computation of the semivariogram models for each of the respective variables, block kriging was used to predict the value of algal cover and stand heights for grid cells of size 25 m by 25 m.

Exploratory data analysis was conducted on the acoustic data prior to spatial modeling using scatter plots, histograms and correlations to assess the presence of possible predictive

trends. With a sampling frequency of 5 Hz, a summary cycle output every 10 pings, and an average survey area size of 5 km^2, a full day of surveying (0600 to ~ 2000 hrs) yielded an average of 8,000 to 10,000 individual geo-referenced datum reports. The frequency distributions of the percent cover and stand height variables derived by acoustic analysis displayed some tendency for overdispersion, but it was generally not severe. Relationships between depth and percent cover were strong and generally linear in nature (r^2=0.31 to 0.74). Strong correlations were evident between percent cover and height ($r^2 > 0.7$) when coverage was moderate or high. To account for these potentially non-stationary processes, block regression kriging (RK; see Hengl et al. 2004) was performed for the percent cover data using a Generalized Linear Model (e.g., Gotway and Stroup 1997) to model the relationship with depth. Briefly, a quasi-Poisson family of probability distributions was used with a log-link function to account for the overdispersion in the data distributions. The model trend was subtracted from the percent cover data and SK was performed on the residuals (i.e. the mean of the residuals should be "0"). The trend was then added back to the kriged residuals to generate the predicted surface maps. Algal stand height was interpolated using KED, with percent cover as a predictor. While both percent cover and height variables are characterized by skewed distributions, the residuals from the relationship were not. Bathymetric grids for each survey site were generated using universal kriging of acoustically determined bottom depths from the individual surveys (Peacock Point and Dobb's Bank excepted; spatial re-sampling of NOAA bathymetric data was used). All bathymetric survey grids were clipped using the lake shorelines and the 10 m depth contour for each lake as downloaded from the National Geophysical Data Center Great Lakes Bathymetry ArcIMS web server (http://map.ngdc.noaa.gov/website/mgg/greatlakesbathy/viewer.htm).

Experimental residual semivariograms were computed for interpolation onto 25 m by 25 m grids. Directional semivariograms were computed by limiting all point pairs within a directional tolerance (0° to 135°, 45° ± 22.5° step tolerance) in addition to the omni-directional semivariogram to assess the degree of anisotropy. All exploratory data analysis, regression and variogram modeling, and subsequent kriging computations were performed using the statistical software R (R Core Development Team 2007) and the R package *gstat* (Pebesma 2004).

3.3.6 Estimation of *Cladophora* biomass

Estimation of standing crop is a frequently desired endpoint in many surveys of benthic vegetation (Vis et al. 2003). Previous attempts with acoustic methods to use echo integration (Sabol et al. 2002a) or summing of acoustic backscatter (Haga et al. 2007) have shown limited success due to mixed species assemblages and high variability due to variations in gas vacuoles

and epiphytic organisms. While better success with these methods might be envisioned for a monospecific assemblage of *Cladophora*, attempts to estimate *Cladophora* biomass from integrated signal voltage or volume backscatter were largely unsuccessful (Chapter 2). A strategy similar to that described by Duarte (1987) was therefore employed, using the height of the algal canopy as a predictor of biomass. Quantitative data from recent studies in Lakes Erie and Ontario where measurements of algal stand height were also recorded were compiled and dry biomass as a function of algal stand height was plotted. Since most of the quantitative data was derived from mid summer maximal biomass measured on quadrats with >80% algal cover, I was unable to derive relationships for non-maximal biomass time periods. A linear model of sqrt (DryMass) as a function of canopy height produced apparent linear relationships across the range of canopy heights encountered in the quadrat data set (Figure 3.5). Although a linear model with an intercept term initially yielded a non zero intercept (4.41 ± 0.62, t=7.01, p <0.001) I used a linear model that forces the regression through the origin. The reasoning for this was that biomass should not be present when bed height is zero. The non-zero intercept was likely due to inflation by the inclusion of quadrat data from very shallow depths (< 1.5 m), some which were characterized by very high biomass (> 200 g m^{-2}). The high biomass relative to bed height at these wave zone sites may be due to compression of biomass by wave action, thus inflating the estimated intercept. The resulting model ($\sqrt{}$Biomass = 0.877 ± 0.034 x BedHeight(cm), r^2=0.73, df=234, p<0.0001) was used to estimate the biomass in each grid cell from the kriged surfaces of canopy height. These "biomass" cells were then multiplied by the percent cover surfaces to account for the fact that the biomass vs stand height relationship was derived from quadrats that were primarily > 80% cover. In addition to *Cladophora*, macrophytes were also present at several sites (Peacock Point, Rock Point (Grand River), Presqu'ile and Dobb's Bank). Because the macrophytes rarely occurred in extensive mono-specific stands, but rather as isolated groups of plants growing with *Cladophora*, I assigned a single biomass value of 100 g m^{-2} DW for macrophyte dominated cells to represent a compromise between low areal biomass of macrophytes found in the nearshore areas of the Great Lakes (< 50 g m^{-2}; Makarewicz and Dilcher 1988) and the much higher areal biomass of *Cladophora*. Macrophyte dominated cells were identified as those that exceeded 0.35 m in height based on comparisons of echograms where macrophytes were clearly present.

Approximate standard errors for percent cover and canopy height were computed by adding the kriging standard errors (residual standard errors) to the trend standard errors. Propagation of error through the equations used to estimated biomass was estimated following the

procedures outlined in Heuvelink (2002) to estimate approximate standard errors for the predicted biomass.

3.3.7 Statistical analysis

Testing for differences in water chemistry among sites and within lakes is complicated by the unbalanced nature of the study. For example, offshore shoals were only accessible in Lake Erie and Ontario, not in Lake Huron or Georgian Bay, and neither shoal reached depths shallower than ~ 3.5 m, thus the shoal sites lacked a 2 m isobath equivalent sampling sites that were available along shorelines. Furthermore, sampling at Pike Bay and Southampton was limited to one site visit each (spring and summer respectively), this results in further losses of degrees of freedom in standard parametric analyses. Initial two-way ANOVA ($\log_{10}$ transformed variables, season and depth as factors) did not show significant differences among depth for any of the variables sampled except kPAR, which was significantly higher at 2 and 5 m depths at Peacock Point (Lake Erie) during the summer and Pike Bay (Lake Huron) during the spring ($p<0.05$). Therefore, for comparisons among sites and lakes, water chemistry and physical data were aggregated and simple correlation analysis was performed using the site means within both the spring and summer periods. Correlations among water chemistry and physical parameters, dreissenid mussel abundance, land use percentages (Table 3.1) and data from the hydroacoustic surveys were assessed using a non parametric correlation coefficient (Spearman's ρ).

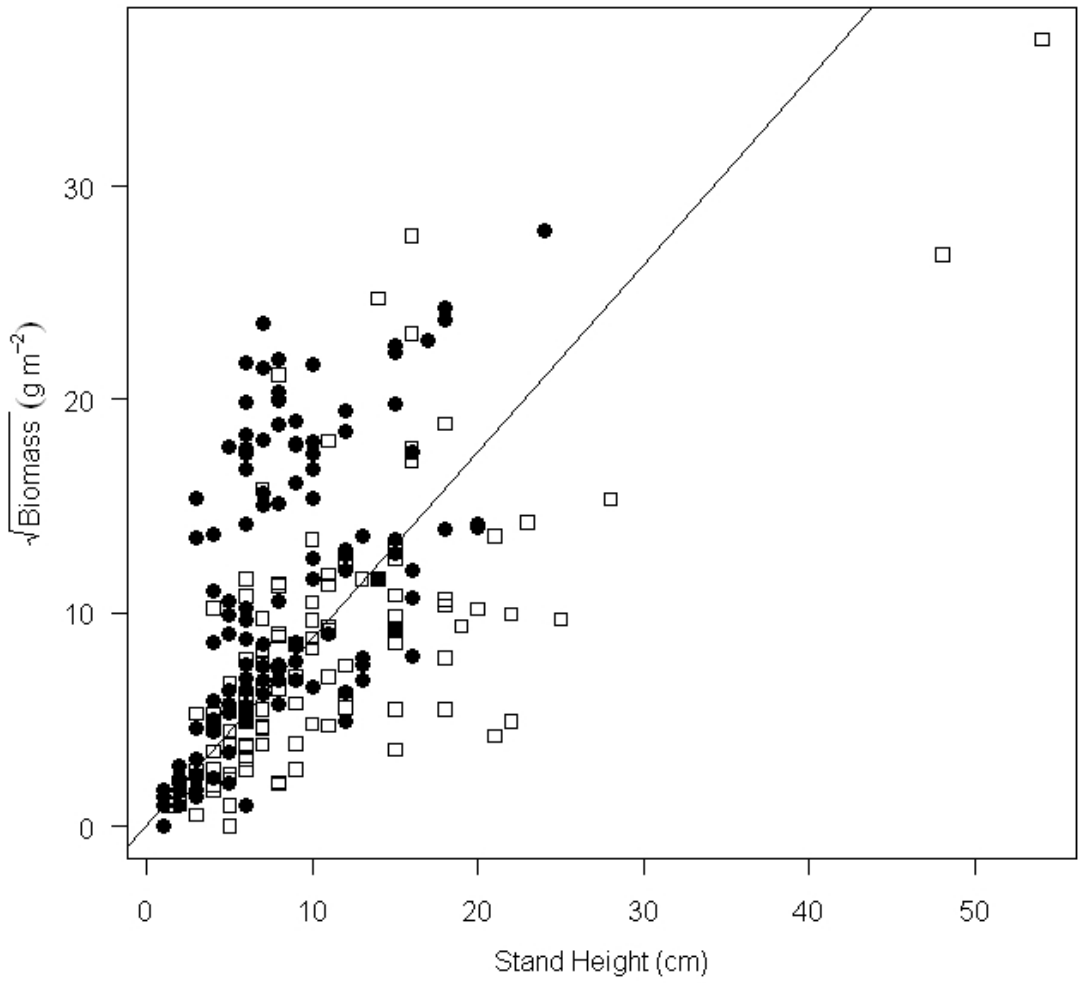

Figure 3.5. Relationship between quadrat biomass (g DM m^{-2}) and algal canopy height (cm). Data sources include East Basin Lake Erie (•;Higgins 2005, T. Howell; unpubl. data) and Lake Ontario (□; S. Malkin 2007, Malkin et al. 2008, D.Depew, upubl.data). Equation of the linear model is √Biomass (g m^{-2}) = 0.877±0.034 x BedHeight(cm); r^2=0.73, df=234.

3.4 Results

3.4.1 Dreissenid abundances

Logistical problems delayed the spring acoustic surveys in 2005 until the latter part of May, and water quality sampling at some sites was pushed into June (Table 3.1). As a result, underwater video from Lakes Erie and Ontario was not suitable for analysis for mussel abundances as outlined in the methods section, because the majority of the bottom was already covered by *Cladophora* and other filamentous algae (*Spirogyra* and *Ulothrix*). Although the underwater camera method was not suitable to estimate dreissenid abundance at the sites in Lake Erie and Ontario due to overlying algal cover, qualitative observations mostly confirm the results of other studies (e.g., Patterson et al. 2005; Lake Erie, Wilson et al. 2006; Lake Ontario, Ozersky et al. 2009; western Lake Ontario), that mussel densities on hard substrates in the lower lakes remain high (Table 3.2). In contrast, the sites in Lake Huron and Georgian Bay afforded an unobstructed view of the substratum therefore estimates of dreissenid abundance using the underwater video camera system were feasible. Dreissenid abundance in Lake Huron and Georgian Bay is much lower than abundances reported for Lakes Erie or Ontario. Mean abundance at Lake Huron sites was lowest at 2 m and increased at depths of 5 m and 10 m. Mussels were distributed in clumps mostly between rocks and along the sides of larger boulders, with very few attached to the upper surface of rocks. In Georgian Bay, the transect at the south end of the survey area had the highest number of mussels, and average abundances were similar across the range of depths sampled (Table 3.2). The patchy distribution was similar to that observed in Lake Huron sites, with mussels often colonizing sides and indentations in large rocks and boulders rather than flat surfaces. As the substrate changed from large rocks to smaller cobble toward Dyer's Bay, mussels became less abundant.

Table 3.2. Table of dreissenid abundances used in this study. Year represents year data collected, site indicates site where abundances assigned. Dreissenid abundance indicates mean abundance (± standard deviation) if specified. Source denotes data source.

Year	*Site*	*Depth*	*Dreissenid abundance (# m^{-2})*	*Source*
2002	Lake Erie (mean of all transects)	2	14,401 ± 10,158	Patterson et al. 2005[1]
		5	9,311 ± 6,042	
		10	8,228 ± 7,059	
2006	Lake Ontario (Oakville)	2	95 ± 93	Ozersky et al. 2009[2]
		5	4,580 ± 2,788	
		10	4,585 ± 930	
		15	3,918 ± 920	
2003	Lake Ontario (Port Credit)	5	2,124	Wilson et al. 2006[3]
		5	268	
		20	8,445	
2003	Lake Ontario (Presquile)	5	24,271	Wilson et al. 2006[3]
		20	13,466	
2003	Lake Ontario (Wellington Bay)	5	7,655	Wilson et al. 2006[3]
		20	3,862	
2005	Lake Huron (Southampton)	2	42 ±47	This study[4]
		5	449 ± 549	
		10	340 ±186	
2005	Georgian Bay (Cape Chin)	2	381 ± 255	This study[4]
		5	357 ± 277	
		10	229 ± 391	

Note [1]Mean abundances of triplicate quadrats sampled at depths of 2, 5 and 10 m at 3 transects within the East basin of Lake Erie, [2]Mean abundances from 3 – 10 camera frames sampled at 17 sites at 2, 5, 10 and 15 m, [3]Mean abundance of triplicate quadrats (0.15 m^2) sampled at 5 and 20 m.[4]Mean of 8 to 10 camera frames sampled at each of 2, 5 and 10 m depths at 3 transects.

3.4.2 Near shore physical and chemical conditions

The staggered water quality sampling makes comparisons among all lakes somewhat ambiguous, but several trends were evident in the water quality data. During the early season sampling (April to early June), concentrations of most parameters were far more variable at shoreline sites in Lake Erie and Ontario than at the shoal sites in those lakes or the shoreline sites in Lake Huron and Georgian Bay (Table 3.3 and Table 3.4). Conductivity was highest and most variable at the Grand River site in Lake Erie (Table 3.3). Lake Erie sites (both shoreline and shoal) had relatively higher phosphorus concentrations (TP, TDP and SRP) compared to other sites, but these rarely exceeded 10 $\mu g\ L^{-1}$ (Table 3.3). NO_3^- concentrations were high and far more variable in Lakes Erie and Lake Ontario compared to Lake Huron and Georgian Bay (Table 3.3). In contrast to Lakes Erie and Ontario, light attenuation (kPAR) was quite low in Lake Huron and Georgian Bay, consistent with the low concentrations of suspended solids and chlorophyll a (Table 3.3). Regrettably, the NH_4^+ samples collected after June appeared to have suffered contamination likely due to atmospheric invasion, thus the data are not reported here as average concentrations were 10 fold higher than those reported in prior years (see North 2008).

In the summer sampling, variability in many parameters was reduced, except at sites that had major tributaries. For example, although conductivity had dropped from spring levels, variability in conductivity was highest at the Grand River, Port Credit and Southampton sites, each of which are in close proximity to a major tributary (Table 3.4). Only sites near urban centers had increased variability in Cl^- during the summer (Table 3.4). Concentrations of P were again remarkably low during the summer sampling, with the highest concentration occurring at the Southampton site just above 10 $\mu g\ L^{-1}$. SRP concentrations were not detectable in Lake Erie at this time, but were detectable in Lake Ontario and Lake Huron though concentrations generally remained between 1.5 and 3 $\mu g\ L^{-1}$ (Table 3.4). NO_3^- concentrations also appeared to have declined from spring concentrations, but concentrations in Lake Ontario remained near those measured in Lake Huron and Georgian Bay (Table 3.4). Despite considerable variability in chlorophyll a concentrations, total suspended solids rarely exceeded 1 $mg\ L^{-1}$, and corresponding measures of light attenuation indicated water clarity in the near shore sites was comparable to that observed in the offshore (shoals) unless in proximity to a major tributary (e.g., Grand River, Oakville, Port Credit) (Table 3.4).

Significant correlations among average water quality parameters and % land use were rare at the coastal level (e.g., ~ 5 km inland from the lake; Table 3.5). Only spring Cl^- concentrations were significantly associated with % coastal agricultural land use (Table 3.5).

Coastal urban land use was significantly associated with higher spring NO_3^-, and higher light attenuation in the summer (e.g., kPAR, TSS). At the watershed scale, % agriculture was associated with high spring NO_3^-, and % urban land use was again associated with increased summer light attenuation, spring NO_3 and spring chlorophyll a (Table 3.5). No significant associations were found among land use percentages for TP or SRP.

Table 3.3. Summary of relevant physical and water chemistry data for the study sites during the early season sampling (April 29 – June 13). Mean values are bolded, standard deviations in brackets, *n* denotes number of samples. Surface temperature (Temp; °C) and conductivity (Cond; µS cm^{-1}) are taken from 1 m below surface from the CTD casts. Light attenuation coefficient (kPAR; m^{-1}), phytoplankton chlorophyll a (chl a; µg L^{-1}), total suspended solids (TSS; mg L^{-1}), total phosphorus (TP; µg L^{-1}), total dissolved phosphorus (TDP µg L^{-1}), soluble reactive phosphorus (SRP; µg L^{-1}), dissolved silica (SiO_2; µg L^{-1}), nitrate (NO_3^-; µg L^{-1}) and chloride ion (Cl^-; mg L^{-1}).

Season	*Lake*	*Site*	*Temp*	*Cond*	*kPAR*	*Chl a*	*TSS*	*TP*	*TDP*	*SRP*	*SiO_2*	*NO_3^-*	*Cl^-*
Spring	Erie	Peacock Point	**8.16**	**309**	**0.57**	**1.84**	**2.56**	**12.11**	**7.44**	**3.67**	**223**	**516**	**29.7**
	n=9		(0.67)	(16)	(0.38)	(0.29)	(2.06)	(6.81)	(4.39)	(2.23)	(114)	(294)	(7.9)
	Erie	Grand River	**11.82**	**357**	**0.46**	**4.09**	**2.04**	**8.74**	**4.93**	**3.95**	**144**	**759**	**24.9***
	n=9		(1.04)	(80)	(0.24)	(4.68)	(2.24)	(3.30)	(1.30)	(1.84)	(52)	(545)	nd
	Erie	Nanticoke Shoal	**4.50**	**280**	**0.21**	**1.64**	**1.00**	**7.06**	**3.25**	**3.52**	**362**	**168**	**16.1**
	n=4		(0.77)	(1)	(0.03)	(0.31)	(0.40)	(0.74)	(0.42)	(0.68)	(60)	(67)	(1.2)
	Ontario	Oakville	**11.26**	**301**	**0.31**	**1.64**	**0.75**	**6.28**	**3.31**	**0.54**	**234**	**647**	**22.2**
	n=9		(0.59)	(12)	(0.06)	(0.54)	(0.09)	(1.58)	(0.45)	(0.39)	(42)	(265)	(4.3)
	Ontario	Port Credit	**14.98**	**nd**	**0.34**	**1.97**	**0.98**	**6.85**	**3.41**	**0.66**	**278**	**552**	**25.0**
	n=9		(0.92)	nd	(0.06)	(0.21)	(0.39)	(1.41)	(0.82)	(0.49)	(118)	(119)	(7.6)
	Ontario	Presqu'ile	**12.57**	**275**	**0.37**	**3.20**	**0.89**	**6.89**	**3.99**	**1.18**	**253**	**360**	**13.6**
	n=9		(1.67)	(13)	(0.10)	(0.86)	(0.35)	(1.52)	(1.09)	(0.76)	(23)	(23)	(2.05)
	Ontario	Dobb's Bank	**16.39**	**295**	**0.46**	**1.98**	**0.46**	**6.43**	**3.72**	**0.76**	**261**	**344**	**19.5**
	n=4		(0.66)	(15)	(0.08)	(0.18)	(0.20)	(2.48)	(1.29)	(0.11)	(24)	(59)	(1.2)
	Huron	Pike Bay	**21.05**	**253**	**0.17**	**0.94**	**0.50**	**3.16**	**1.48**	**<0.35**	**1004**	**342**	**nd**
	n=9		(1.38)	(20)	(0.09)	(0.18)	(0.20)	(0.80)	(0.54)	0	(94)	(55)	nd
	Huron	Cape Chin	**14.94**	**124**	**0.14**	**0.47**	**0.41**	**4.02**	**1.81**	**1.09**	**1144**	**376**	**nd**
	n=9		(0.55)	(43)	(0.09)	(0.10)	(0.12)	(2.05)	(0.56)	(0.39)	(57)	(29)	nd

Note: nd indicated no data available, *only one measurement available.

Table 3.4. Summary of relevant physical and water chemistry data for the study sites during the summer season sampling (July 12 – August 8). Mean values are bolded, standard deviations in brackets, n denotes number of samples. Surface temperature (Temp; °C) and conductivity (Cond; µS cm^{-1}) are taken from 1 m below surface from the CTD casts. Light attenuation coefficient (kPAR; m^{-1}), phytoplankton chlorophyll a (chl a; µg L^{-1}), total suspended solids (TSS; mg L^{-1}), total phosphorus (TP; µg L^{-1}), total dissolved phosphorus (TDP µg L^{-1}), soluble reactive phosphorus (SRP; µg L^{-1}), dissolved silica (SiO_2; µg L^{-1}), nitrate (NO_3^-; µg L^{-1}) and chloride ion (Cl^-; mg L^{-1}).

Season	*Lake*	*Site*	*Temp*	*Cond*	*kPAR*	*Chl a*	*TSS*	*TP*	*TDP*	*SRP*	*SiO_2*	*NO_3^-*	*Cl^-*
Summer	Erie	Peacock Point	**23.20**	**nd**	**0.29**	**1.10**	**1.11**	**5.62**	**2.08**	**<0.35**	**83**	**250**	**14.6**
	n=9		(0.46)	nd	(0.06)	(0.48)	(0.19)	(0.94)	(0.82)	0	(37)	(120)	(2.0)
	Erie	Grand River	**24.65**	**279**	**0.40**	**2.68**	**1.15**	**3.74**	**0.88**	**<0.35**	**160**	**204**	**16.3**
	n=9		(0.55)	(49)	(0.17)	(1.21)	(0.72)	(2.24)	(0.92)	0	(115)	(74)	(3.5)
	Erie	Nanticoke Shoal	**24.25**	**nd**	**0.27**	**1.84**	**0.73**	**5.37**	**1.95**	**<0.35**	**113**	**262**	**13.5**
	n=4		(1.63)	nd	(0.09)	(1.27)	(0.34)	(1.57)	(1.01)	0	(52)	(124)	(2.5)
	Ontario	Oakville	**16.37**	**302**	**0.50**	**2.16**	**1.04**	**7.24**	**3.03**	**0.77**	**76**	**392**	**21.3**
	n=9		(1.59)	(4)	(0.23)	(0.58)	(0.16)	(1.70)	(0.89)	(0.29)	(43)	(140)	(1.56)
	Ontario	Port Credit	**22.93**	**308**	**0.46**	**1.01**	**1.15**	**7.49**	**2.69**	**0.71**	**108**	**371**	**24.6**
	n=9		(1.66)	(8)	(0.07)	(0.22)	(0.76)	(1.40)	(0.63)	(0.28)	(52)	(111)	(11.3)
	Ontario	Presquile	**19.42**	**302**	**0.35**	**1.30**	**1.05**	**5.08**	**2.33**	**1.54**	**111**	**318**	**18.5**
	n=8		(1.19)	(4)	(0.04)	(0.30)	(0.28)	(0.67)	(0.86)	(0.45)	(33)	(78)	(1.7)
	Ontario	Dobbs Bank	**18.31**	**301**	**0.26**	**1.38**	**0.47**	**5.21**	**2.61**	**1.57**	**96**	**303**	**23.2**
	n=4		(0.18)	(1)	(0.04)	(0.11)	(0.26)	(0.61)	(1.03)	(0.23)	(19)	(64)	(2.1)
	Huron	Southampton	**24.32**	**245**	**0.23**	**0.51**	**0.52**	**10.38**	**3.43**	**1.26**	**1293**	**335**	**4.81**
	n=9		(0.81)	(87)	(0.07)	(0.19)	(0.15)	(1.61)	(0.92)	(0.26)	(555)	(61)	(1.55)
	Huron	Cape Chin	**18.59**	**nd**	**(0.27)**	**0.46**	**0.39**	**8.09**	**4.17**	**1.37**	**754**	**311**	**4.40**
	n=9		(3.32)	nd	(0.10)	(0.07)	(0.17)	(3.79)	(1.56)	(0.27)	(125)	(38)	(0.36)

Note: nd indicates no data available. SRP concentrations below 0.35 µg L^{-1} are below the analytical detection limit.

Table 3.5. Spearman correlation coefficients (ρ) for mean water chemistry parameters and % land use at the coastal margin (~5 km inland) and the watershed scale. Bolded values are significant at the $p<0.05$ level.

Variable	Coastal % Agricultural	Coastal % Urban	Watershed %Agricultural	Watershed % Urban
Spring TSS	0.27	0.37	0.59	0.43
Summer TSS	0.32	**0.77**	0.57	**0.75**
Spring kPAR	0.14	0.31	0.56	0.34
Summer kPAR	0.13	**0.83**	0.25	**0.81**
Spring TP	0.13	0.24	0.54	0.27
Summer TP	0.25	-0.05	-0.07	0
Spring SRP	0.20	-0.06	0.46	0
Summer SRP	-0.48	-0.19	-0.38	-0.22
Spring NO_3	0.49	**0.73**	**0.73**	**0.81**
Summer NO_3	-0.29	0.49	-0.19	0.49
Spring Cl^-	**0.85**	0.27	0.48	0.41
Summer Cl^-	-0.41	0.61	-0.14	0.55
Spring Chl a	0.48	0.56	0.56	0.67
Summer Chl a	-0.15	0.19	0.02	0.22

.

3.4.3 Trends in tributary concentrations

Significant increases in Cl^- concentration are seen in tributaries that drain urbanized watersheds (Table 3.6; Figure 3.6). Increases in Cl^- concentrations are also apparent in more agricultural areas, but these are generally of lower magnitude, and may reflect the urban expansion into agricultural areas. Increases in NO_3^- concentrations are seen for the period 1964 to 1984 for some tributaries, but the lack of data makes broad generalizations difficult. In contrast to NO_3^- and Cl^-, large declines in annual median TP concentrations occurred in the 1964 to 1984 period for all the tributaries in Lake Ontario, but not for Lake Erie. Annual median TP concentrations appeared to increase in Lake Huron tributaries before declining in the 1985 to 2008 period. Further declines of TP in the 1985 to 2008 period are also observed in Lake Ontario tributaries, but not in Lake Erie tributaries (Figure 3.6, Table 3.6). Concentrations in recent years still frequently exceed the PWQMN target of 0.030 mg L^{-1}, particularly in Lake Erie and some Lake Ontario tributaries (Figure 3.6).

Table 3.6. Mann-Kendall trend tests for annual median TP, NO_3, Cl^- concentrations in selected tributaries. τ denotes the strength and direction of the trend. Significant trends are bolded. ND* denotes not enough data to compute a trend. PWQMN station id's are noted below the tributary name and correspond to figure 3.4. Number in brackets beside the variable denotes the numbers of years included in the analysis.

Location	*Station*	*Variable*	*τ (1964 – 1983)*	*P*	*Variable*	*τ (1984 – 2009)*	*P*
Pike Bay (Huron)	Stokes River	TP (9)	0.048	0.99	TP (12)	**-0.487**	**<0.05**
	08014300102	NO_3 (9)	0.724	0.06	NO_3 (12)	**0.493**	**<0.05**
		Cl^- (9)	0.238	0.55	Cl^- (12)	.405	0.06
Southampton (Huron)	Saugeen River	TP (9)	**0.592**	**<0.05**	TP (25)	**-0.579**	**<0.01**
	08012303002	NO_3 (5)	0.40	0.46	NO_3 (1)	ND	
	08012303082	Cl^- (0)	ND		Cl^- (20)	**0.56**	**<0.01**
Southampton (Huron)	Little Sauble	TP (7)	0.611	<0.05	TP (13)	**-0.565**	**<0.05**
	08012303002	NO_3 (7)	0.500	0.07	NO_3 (13)	-0.364	0.11
		Cl^- (7)	0.370	0.21	Cl^- (13)	0.204	0.43
Peacock Point (Erie)	Nanticoke	TP (20)	0.138	0.416	TP (19)	-0.07	0.699
	16016400102	NO_3 (20)	**0.61**	**<0.01**	NO_3 (1)	ND	
		Cl^- (20)	0.11	0.53	Cl^- (19)	**0.563**	**<0.01**
Peacock Point (Erie)	Sandusk	TP (11)	0.273	0.243	TP (2)	ND	
	16017000102	NO_3 (11)	0.164	0.53	NO_3 (0)	ND	
	16017000202	Cl^- (11)	-0.154	0.53	Cl^- (2)	ND	
Grand River (Erie)	Grand River	TP (4)	-0.333	0.73	TP (25)	-0.152	0.289
	16018403502	NO_3 (4)	ND		NO_3 (0)	ND	
	16018403583	Cl^- (3)	-0.333	0.99	Cl^- (25)	**0.586**	**<0.01**
Oakville (Ontario)	16 Mile Creek	TP (20)	**-0.565**	**<0.01**	TP (23)	0.018	0.92
	06006300102	NO_3 (20)	**0.681**	**<0.01**	NO_3 (1)	ND	
		Cl^- (19)	**0.645**	**<0.01**	Cl^- (23)	**0.703**	**<0.01**
Port Credit (Ontario)	Etobicoke Creek	TP (20)	**-0.744**	**<0.01**	TP (13)	**-0.462**	**<0.05**
	06008000102	NO_3 (19)	-0.263	0.12	NO_3 (1)	ND	
		Cl^- (17)	0.17	0.36	Cl^- (13)	**0.538**	**<0.05**
Presquile (Ontario)	Proctor Creek	TP (20)	**-0.649**	**<0.01**	TP (12)	-0.255	0.263
	06015100102	NO_3 (20)	**0.828**	**<0.01**	NO_3 (1)	ND	
		Cl^- (19)	**0.582**	**<0.01**	Cl^- (12)	-0.103	0.669
Presquile (Ontario)	Consecon Creek	TP (9)	**0.686**	**<0.05**	TP (20)	-0.06	0.715
	06015700302	NO_3 (6)	0.552	0.181	NO_3 (0)	ND	
		Cl^- (6)	**0.61**	**<0.01**	Cl^- (17)	0.429	0.229

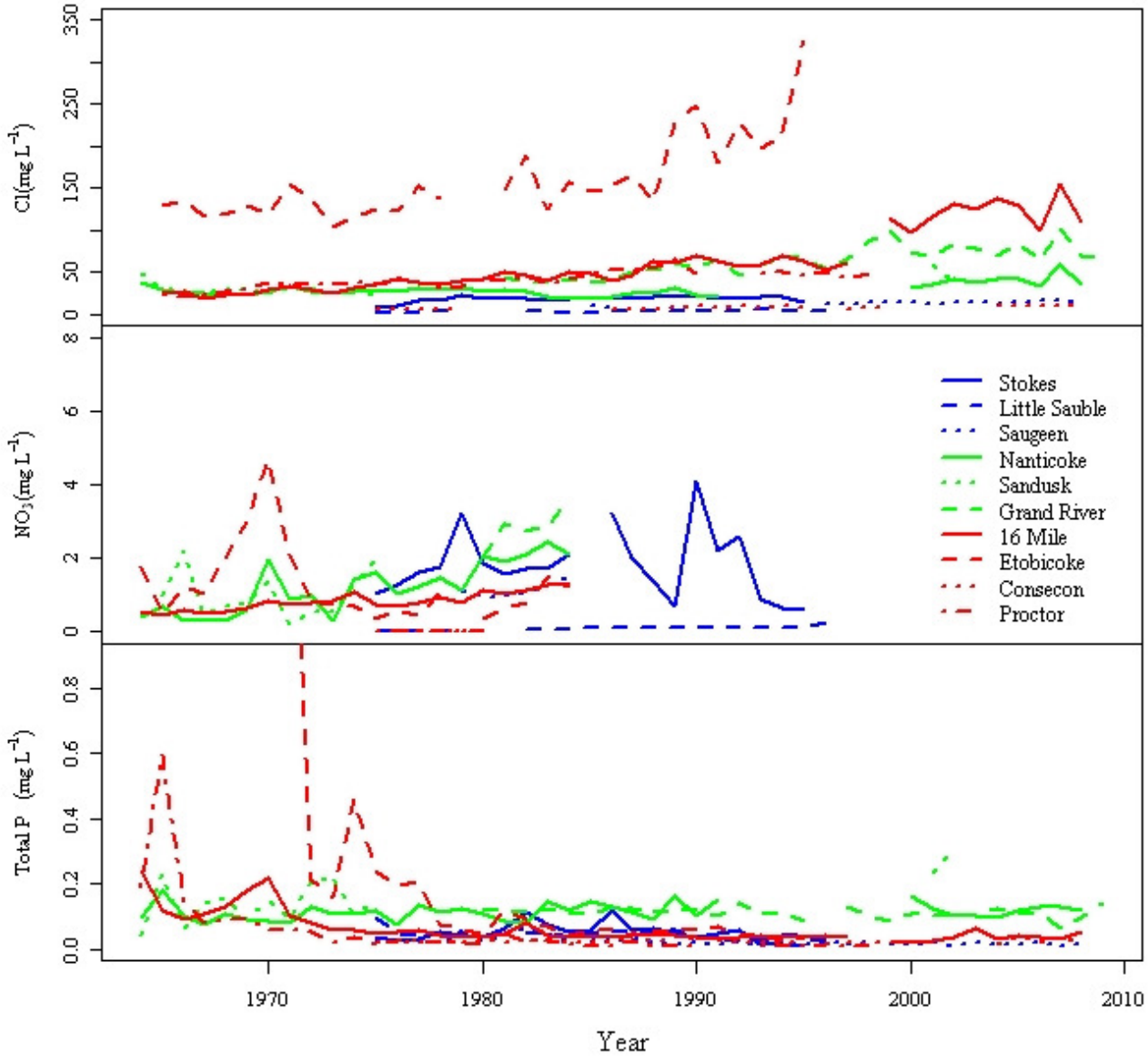

Figure 3.6. Plots of annual median Cl^- concentration (mg L^{-1}) (top panel), NO_3 concentration (mg L^{-1}) (middle panel), and TP concentration (mg L^{-1}) (bottom panel) for PWQMN stations nearest the study sites. Blue lines represent Lake Huron sites, green for Lake Erie, and red for Lake Ontario.

3.4.4 Distribution of nuisance *Cladophora*

Example semi-variograms for percent algal cover and stand height determined by the acoustic surveys are shown in Figure 3.7 and summarized in Table 3.7. The degree of spatial dependency for semivariogram models ($1 - C_0 / C_0 + C$) was generally high for percent cover residuals, being > 50 % for most sites. This indicates the presence of a moderately strong spatial structure even after accounting for the trend with depth. Spatial dependency of the height residuals was generally weaker than that observed for percent cover, owing primarily to the fact that most of the variance in stand height appears to be accounted for by percent cover rather than spatial variation.

Kriged maps of percent algal cover, stand heights and estimated biomass for Lake Erie and Lake Ontario sites are presented in Figure 3.8 to Figure 3.14. Maps for Lake Huron and the Georgian Bay site are not shown, since *Cladophora* was not detected using acoustic methods at these sites. Underwater video did reveal sparse, short (< 5 cm) tufts at the Southampton site at most stations and at one station in Georgian Bay (station 800) where dreissenid mussels were relatively abundant compared to other Lake Huron sites. Weather conditions prevented any sampling of the Southampton site during the "spring" surveys and the Pike Bay site during the "summer" surveys. In addition, acoustic data from the Pike Bay spring survey were contaminated with excessive water column noise as a result of heavy rainfall. Acoustic noise extended down ~ 6 m in the water column, making separation of ambient noise from potential algal signal difficult, and nearly impossible in shallow waters. Visual observations of the substratum in shallow waters (< 5 m) and underwater video revealed that the substrate was mostly devoid of any filamentous algae.

In contrast to the sites in Lake Huron and Georgian Bay, nuisance *Cladophora* growth was observed at all shoreline sites in Lake Erie and Lake Ontario. In general, moderate to strong anisotropy (direction of strongest autocorrelation) existed in these data sets, and appeared to be primarily driven by the orientation of the shoreline. West to east oriented shorelines (e.g., Presqu'ile Provincial Park, Grand River; Rock Point portion) typically had directions of maximal correlation in the west to east direction (i.e. 90°) and southwest to northeast oriented shorelines (e.g., Port Credit, Oakville, Grand River; Grant Point portion) had a direction of maximal correlation in the same direction (e.g., 45°), presumably because of the strong effect of depth on light availability. No obvious anisotropy was present at either of the shoal sites, likely because these were relatively smaller areas with a limited amount of area at shallow depths.

Because shoreline sites typically have greater areas at shallow depths compared to the offshore shoals, larger average patch sizes might be expected to occur along shoreline sites. However, the data here do not suggest this is that case (e.g., range (α); Table 3.7). The large variation in range (α) is likely due to a combination of factors. For example, the large range in percent cover at the Rock Point portion of the Grand River site is primarily due to the large shallow shoal that extends southeastward from Mohawk Island (Figure 3.10). In contrast, the large range at Presqu'ile is due to the large area of heavy cover in the lee of Big Bluff and Gull Island, which act to shelter the adjacent embayment area from wind and wave action (Figure 3.13). Smaller ranges were observed at exposed shorelines (e.g. Peacock Point, Grant Point, Oakville, and Port Credit) where large sheltered areas are not present (Figure 3.9, Figure 3.10, Figure 3.11, Figure 3.12).

In general, sites with a low sill (*C*) value for percent cover, had relatively low variability in *Cladophora* sp. cover, and sites with a low sill (*C*) for height had low variability in observed canopy heights. The putative cause of the low variability in cover likely varies from site to site. For example, the low sill at Nanticoke shoal is due to the depth range (3.5 m to 11 m depth) being deeper than those encountered at the shoreline sites. As a consequence, algal biomass likely does not reach comparable levels that might occur in shallower water along the shoreline sites where light is not limiting. In addition, lower exposure to physical disturbance probably leads to large areas of moderate growth over areas which are exposed to frequent wave action. In contrast, the low sill at Peacock Point is partly due to the smaller area surveyed, but also to a major detachment event that was observed to occur on the 12th of July (personal observation) in the vicinity of Peacock Point. Since much of the algal biomass appeared to have detached from the bottom, there were very few areas of heavy cover remaining at the time of the survey, and the resultant large areas with little to no cover contributed to the low sill.

Large sill values tended to occur at the larger shoreline sites (e.g., Oakville, Port Credit, Presqu'ile) and displayed a high degree of patchiness (e.g., varying degrees of shoreline exposure), although the high sill observed at Grant Point and Dobb's Bank may have been due to a combination of a) a small survey area (< 2km^2) and b) appreciable variation in cover, although at Dobb's Bank, much of this was imparted by stands of macrophytes that showed heavy cover at deeper depths compared to *Cladophora*. Isolated stands of macrophytes were also observed at the Rock point portion of the Grand River site, but these were mostly restricted to the north side of Mohawk Island, and toward the east where the substrate changed from rock to sand and gravel (Figure 3.10). The large heavily covered shallow shoal (near Mohawk Island) may have helped to moderate the sill at this site.

The principal cause for a high sill (C) in canopy height was the presence of a) macrophytes in the survey area (e.g. Peacock Point, Rock Point, Presqu'ile and Dobb's Bank) or b) considerable variation in observed canopy heights of *Cladophora* (Rock Point and Grant Point). Trends in the nugget variance (C_0) also reflect this, though the variable sizes of the survey areas may obscure such relationships (see for example, Chapter 4).

In order to estimate the approximate depth detection limit at each site, average estimated biomass values were binned according to depth strata (1 m depth bins) and averaged. The resultant profiles (Figure 3.15 and Figure 3.16) were then examined to see at what depth the estimated biomass fell below the apparent detection limit for the acoustic system (31 ± 18 g m^{-2}; Chapter 2). The depth distribution of estimated biomass in Lake Erie suggested that detectable (and therefore biomass approaching nuisance levels occurred to depths of 5-6 m at the shoreline sites, and to ~ 7 m at Nanticoke Shoal (Figure 3.15). In the western basin of Lake Ontario, the depth range was slightly deeper, extending to 7 m for west basin sites, but appeared to extend to ~ 9 m at Presqu'ile and at Dobb's Bank (Figure 3.16).

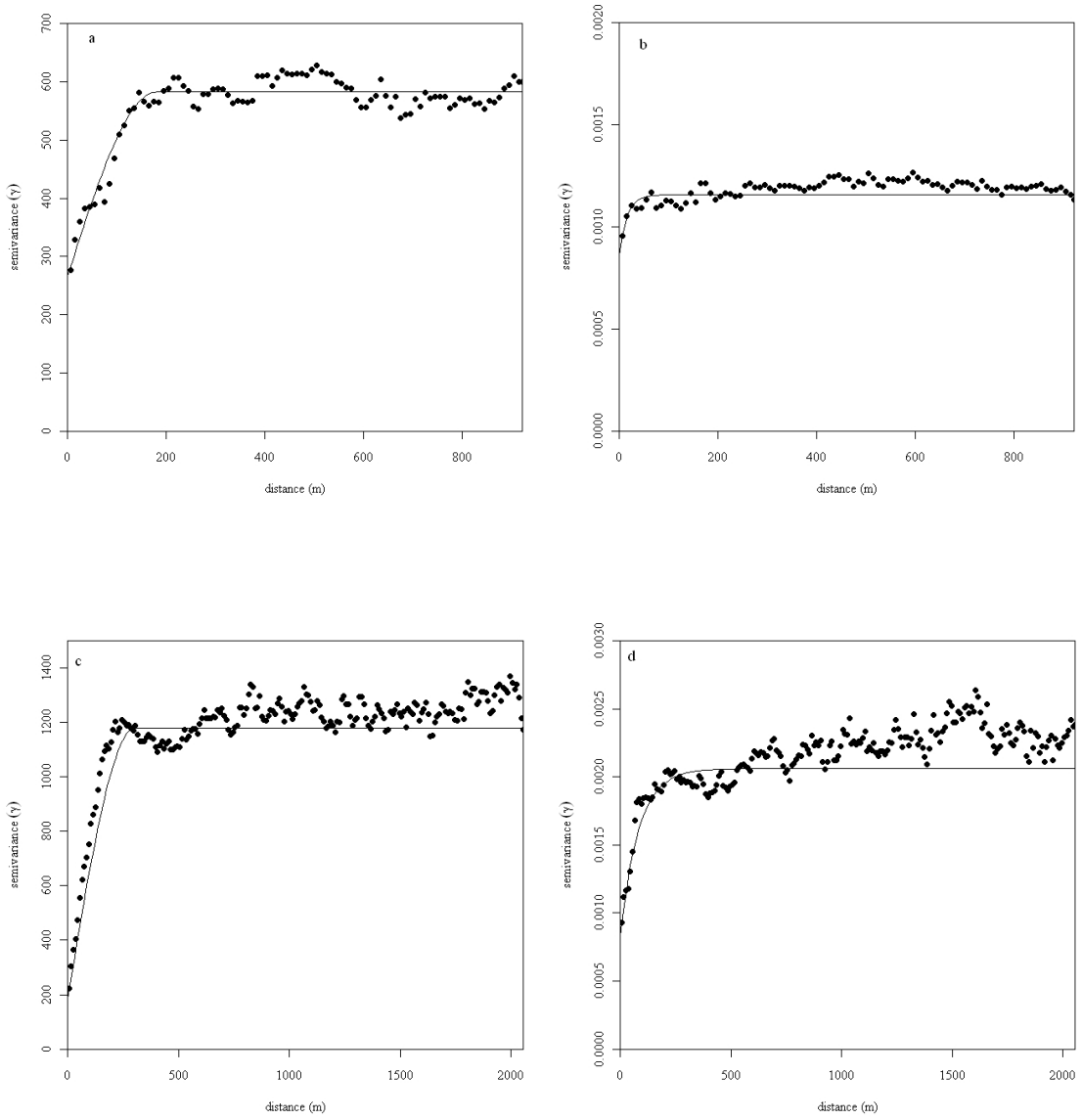

Figure 3.7. Residual semivariograms for a) percent cover at Nanticoke Shoal (July 12 2005), b) algal stand height at Nanticoke Shoal (July 12 2005), c) percent cover at Presqu'ile Provincial Park (July 27 2005), and d) algal stand height at Presqu'ile Provincial Park (July 27 2005). Note the differences total semivariance for panels a) (offshore shoal site) and c) (nearshore site high exposure) and the difference in the sill between panels b) (no macrophytes present) and d) (macrophytes present).

Table 3.7. Semivariogram parameters and kriging cross validation results for 2005 surveys. Date and site give the location of the acoustic surveys. C_0 denotes the nugget variance, C denotes the sill, and α the range (m). Sp% is the degree of spatial dependence described by the fitted semivariogram model. Model Type indicates the form of model fitted to the experimental semivariogram."Exp" denotes exponential model, and "Sph" denotes spherical model.

Date	*Site*	*Variable*	C_0	C	α	*Sp%*	*Model Type*	*Anisotropy*
July 12	Nanticoke	% Cover	266.96	314.70	177.16	54 %	Exp	None
July 12	Nanticoke	Height	8.5×10^{-4}	3.0×10^{-4}	16.6	30 %	Exp	None
July 14/15	Rock Pt	%Cover	323.15	390.53	205.14	54 %	Exp	90°
July 14/15	Rock Pt	Height	1.0×10^{-3}	9.6×10^{-4}	47.07	48 %	Exp	90°
July 15	Grant Pt	%Cover	377.84	522.89	58.93	58 %	Exp	45°
July 15	Grant Pt	Height	9.0×10^{-4}	3.5×10^{-4}	84.93	26 %	Exp	45°
July 19	Peacock Pt	% Cover	228.04	308.06	91.64	58 %	Exp	45°
July 19	Peacock Pt	Height	5.3×10^{-3}	4.6×10^{-3}	1127.55	46 %	Sph	45°
July 21	Oakville	%Cover	272.86	553.53	48.99	66 %	Exp	45°
July 21	Oakville	Height	1.7×10^{-3}	7.1×10^{-4}	171.13	29 %	Exp	45°
July 25	Port Credit	%Cover	399.45	573.64	65.28	59 %	Exp	45°
July 25	Port Credit	Height	1.2×10^{-3}	3.5×10^{-4}	57.5	63 %	Exp	45°
July 27	Presqu'ile	%Cover	392.58	734.65	245.7	65 %	Exp	90°
July 27	Presqu'ile	Height	8.2×10^{-4}	1.2×10^{-3}	81.10	27 %	Exp	90°
July 27	Dobb's Bank	% Cover	407.47	537.66	68.93	57 %	Exp	None
July 27	Dobb's Bank	Height	2.2×10^{-3}	4.2×10^{-3}	269.61	66 %	Sph	None

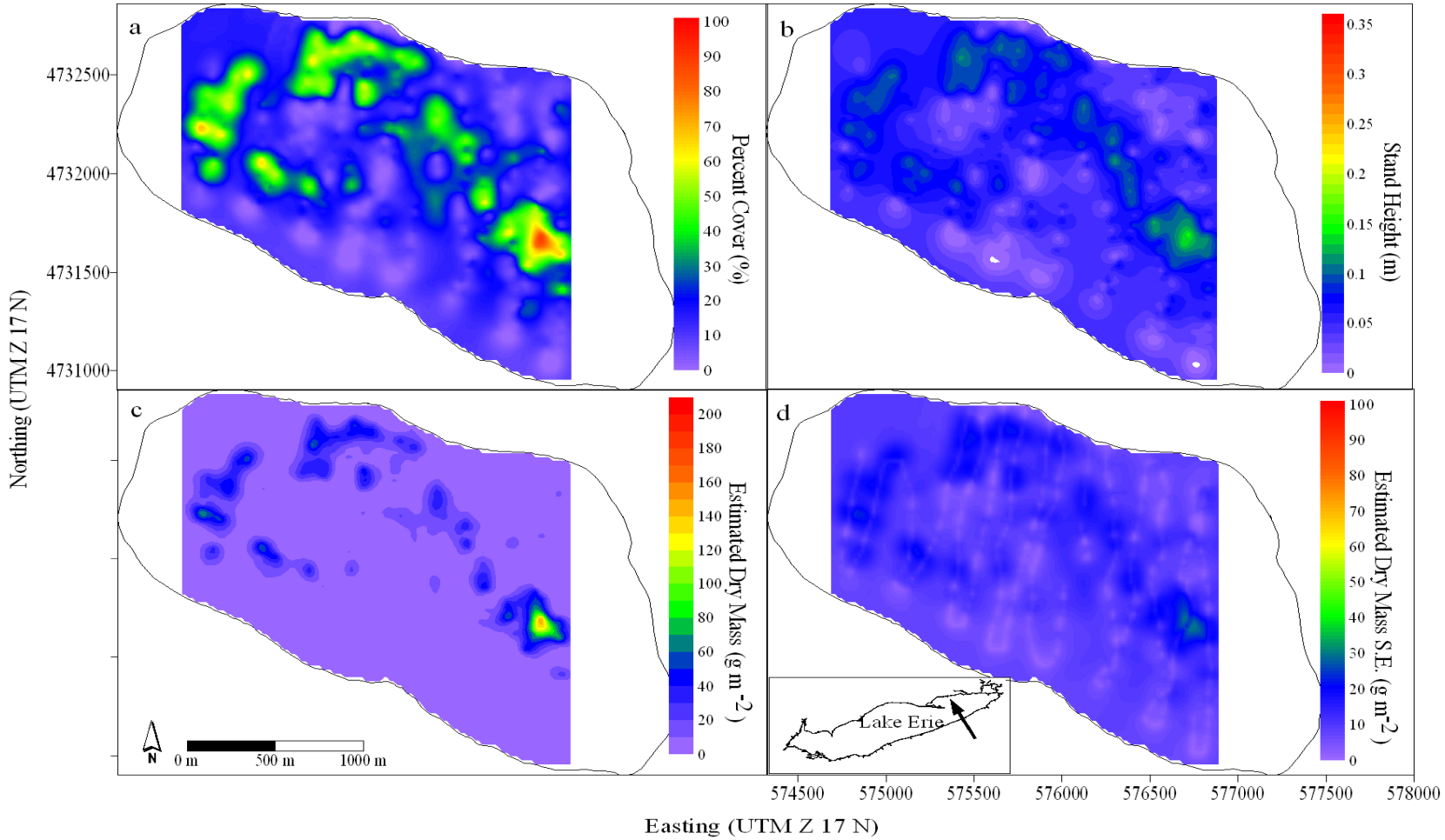

Figure 3.8. Kriged maps showing a) percent cover, b) stand height, c) estimated dry biomass and d) estimated biomass standard error for Nanticoke shoal, July 12, 2005. The black line denotes the outline of the 11 m depth contour of the shoal. Arrow denotes approximate location of Nanticoke Shoal in Lake Erie (inset box in panel d). Note that the scale for stand height (panel b) and estimated biomass (panel c) are of different range than following figures.

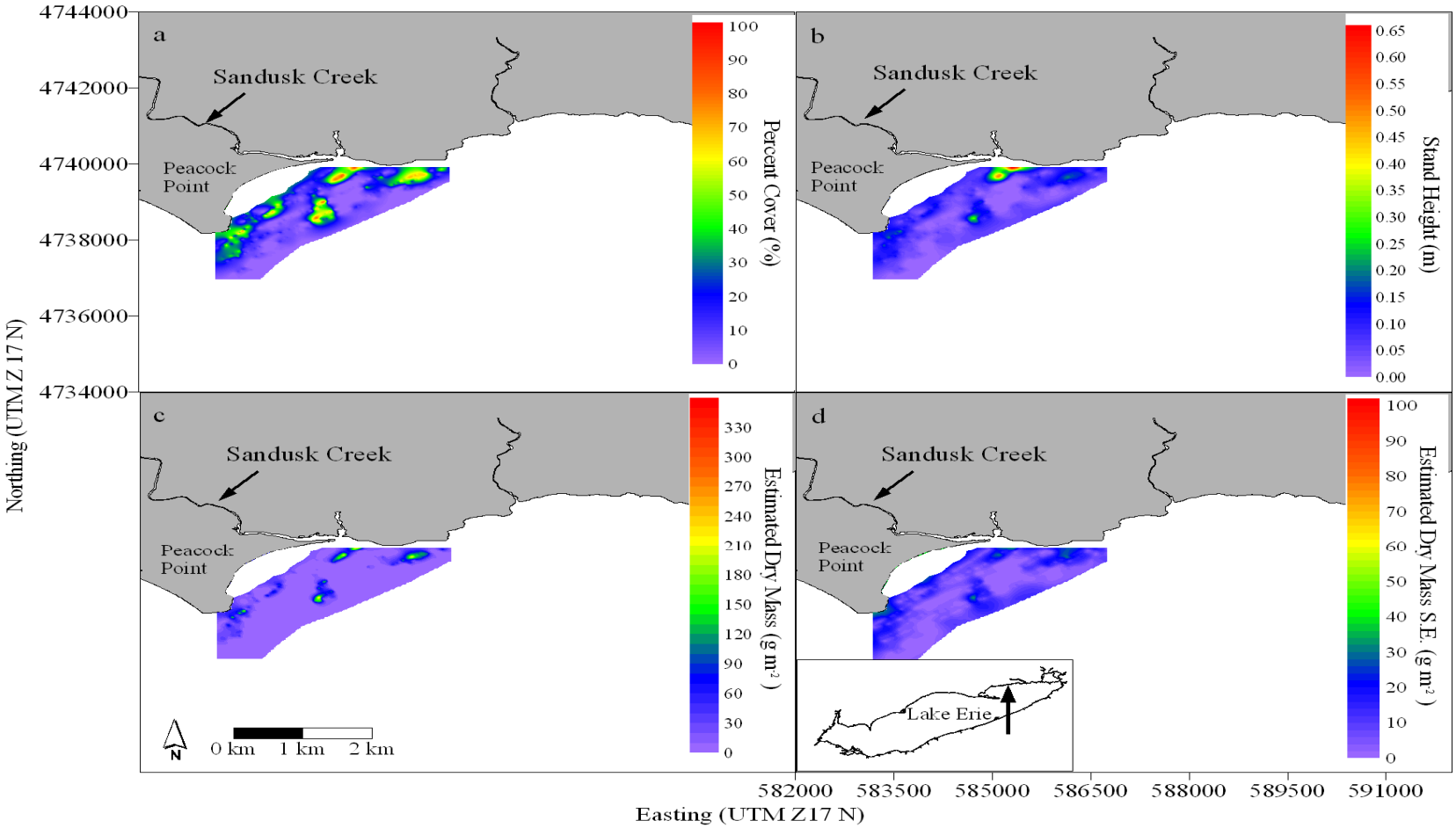

Figure 3.9. Kriged maps showing a) percent cover, b) algal stand height, c) estimated dry biomass and d) estimated biomass standard error for Peacock Point, July 19, 2005. Arrow denotes approximate location of Peacock Point in Lake Erie (inset box in panel d). Note that the scale for stand height (panel b) and estimated biomass (panel c) are of different range than following figures.

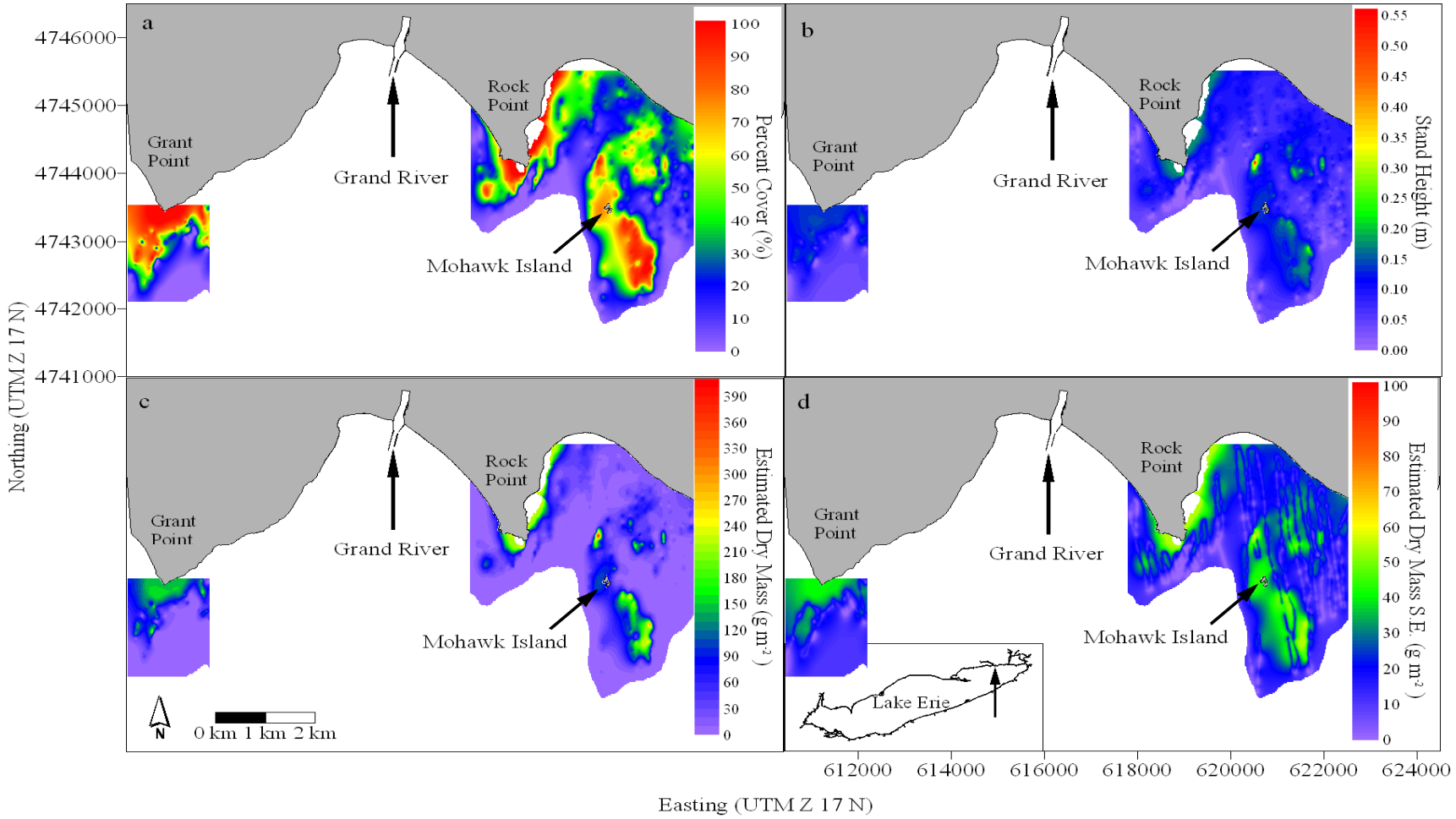

Figure 3.10. Kriged maps showing a) percent cover, b) stand height, c) estimated biomass and d) approximate standard errors for biomass estimates for the Grand River sites July 14-15, 2005. Note that the scale for stand height (panel b) and estimated biomass (panel c) are of different range than following figures.

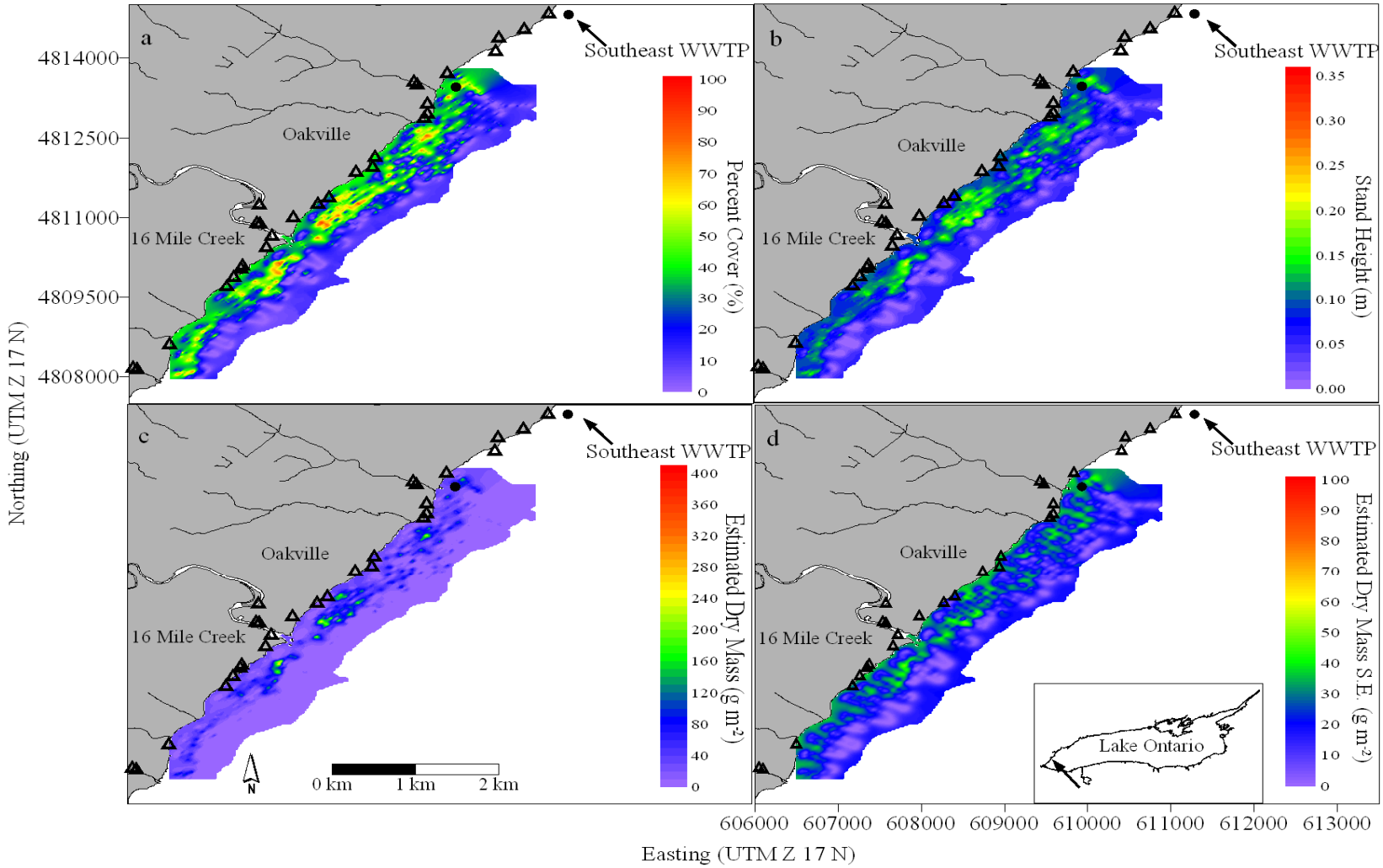

Figure 3.11. Kriged maps showing a) percent cover, b) stand height, c) estimated biomass and d) approximate standard errors for biomass estimates for Oakville, July 25 2005.

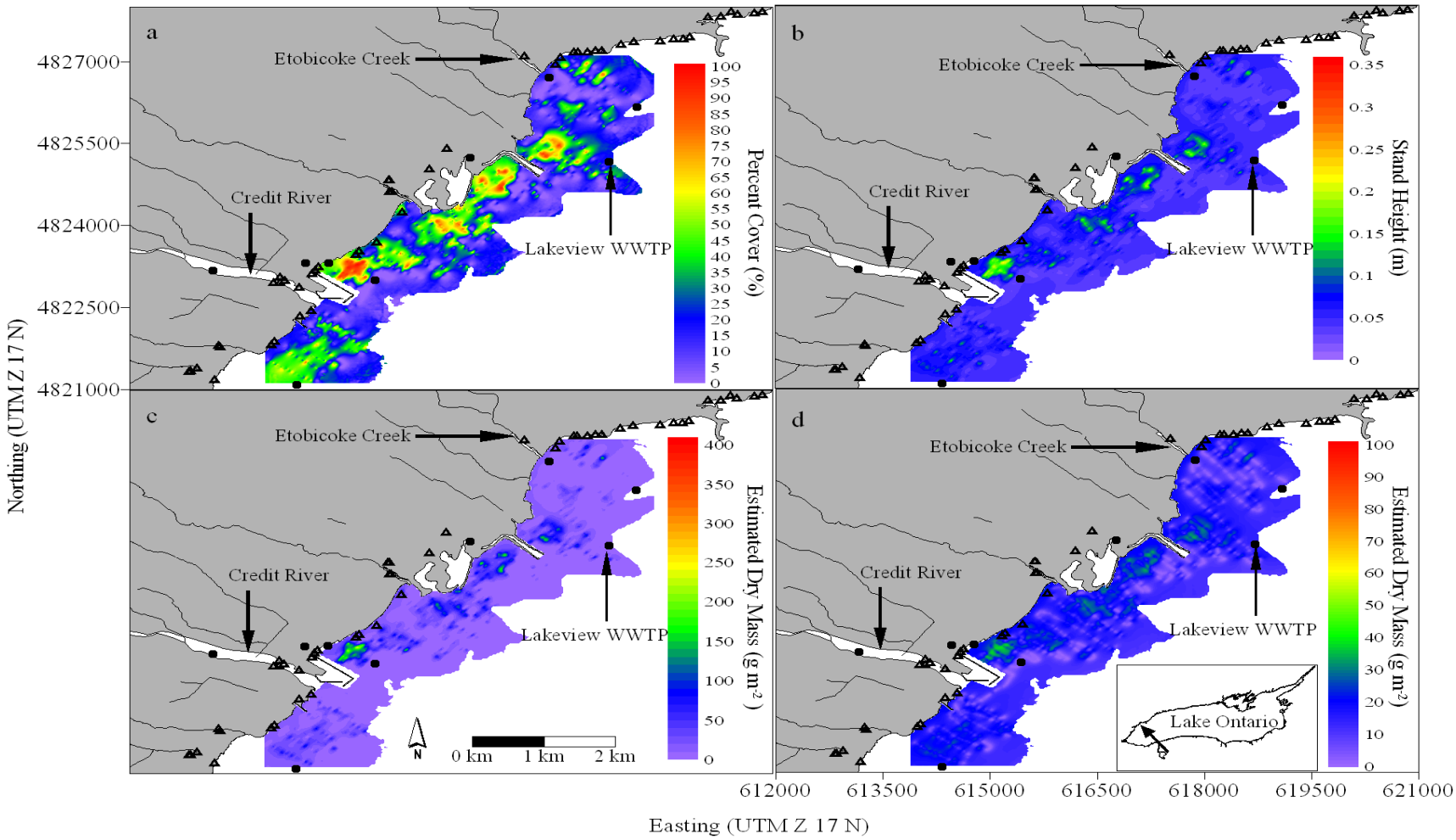

Figure 3.12. Kriged maps showing a) percent cover, b) stand height, c) estimated biomass and d) approximate standard errors for biomass estimates for Port Credit, July 21 2005. Note that the scale for stand height (panel b) and estimated biomass (panel c) are of different range than following figures.

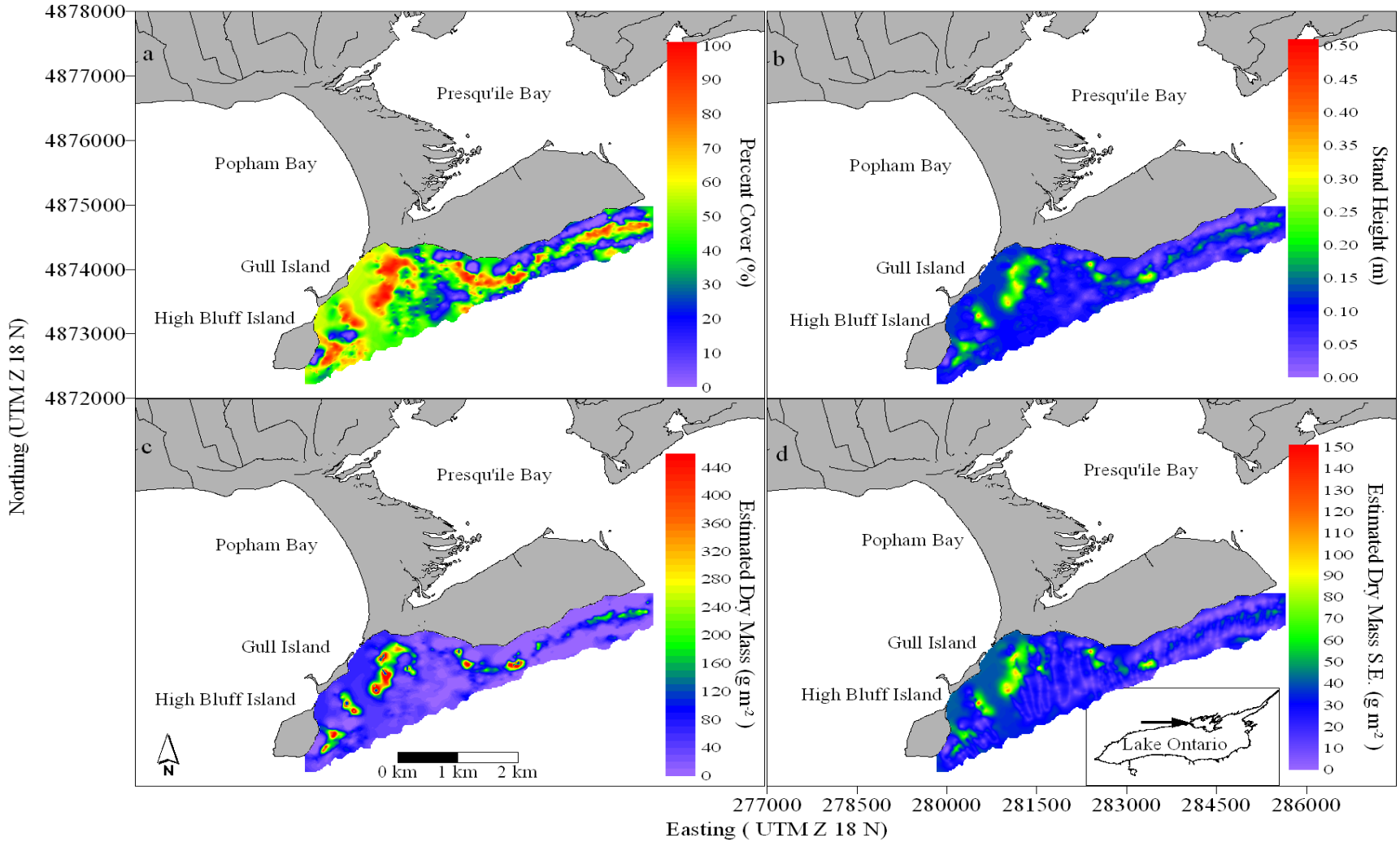

Figure 3.13. Kriged maps showing a) percent cover, b) stand height, c) estimated biomass and d) approximate standard errors for biomass estimates for Presqu'ile Provincial Park, July 27 2005.

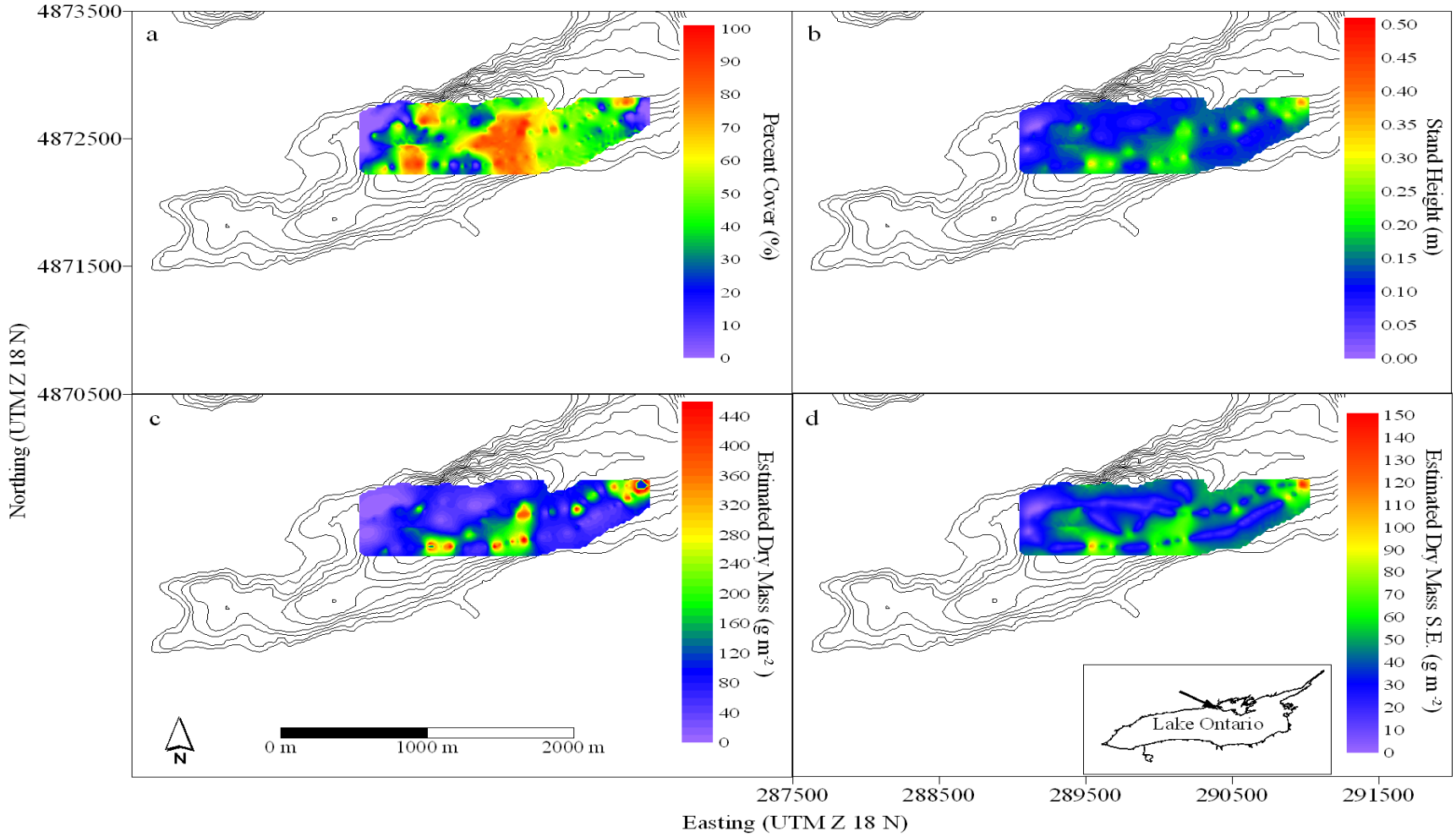

Figure 3.14. Kriged maps showing a) percent cover, b) stand height, c) estimated biomass and d) approximate standard errors for biomass estimates for Dobb's Bank July 27 2005.

3.4.5 Relationships of *Cladophora* biomass to land use, water quality and dreissenid mussel abundance

For comparative purposes, mean biomass as estimated from acoustic methods was chosen to compare individual sites among land uses, average water chemistry and dreissenid abundance. Grid cells with an estimated biomass value exceeding 50 g m^{-2} (above the apparent detection limit of the acoustic unit) were selected. Using only cells that exceed the threshold of estimated biomass allows for site specific trends to be expressed more clearly, since averaging over large and variably sized survey areas (particularly where an over abundance of zeros is present) will obscure differences that are imparted by differences in bathymetry, substrate types and light climate. In addition, since a common value of 100 g m^{-2} was assigned to all macrophyte stands (e.g., bed height > 0.30 m), inclusion of areas with macrophytes would artificially inflate the estimated mean biomass, therefore, to eliminate the effects of the presence of macrophytes, cells with an estimated stand height > 30 cm were discarded.

No correlations were observed with spring water chemistry variables (Figure 3.17). A strong negative correlation was observed between summer TP and mean biomass (Spearman's ρ=-0.83, $p<0.01$). No significant relationships were observed between mean biomass and spring or summer SRP (Spearman's ρ=0.36, $p>0.3$ and Spearman's ρ=-0.04, $p>0.9$) or spring or summer NO_3 (Spearman's ρ=0.47 and -0.20, $p>0.2$ respectively). Mean biomass did not show a significant correlation with % coastal agricultural land use or % coastal urban land use, though the relationship with % coastal urban land use was only marginally non significant (Spearman's ρ=0.55, $p=0.10$). In contrast, a strong positive correlation was observed with dreissenid mussel abundance (Spearman's ρ=0.76, $p<0.05$).

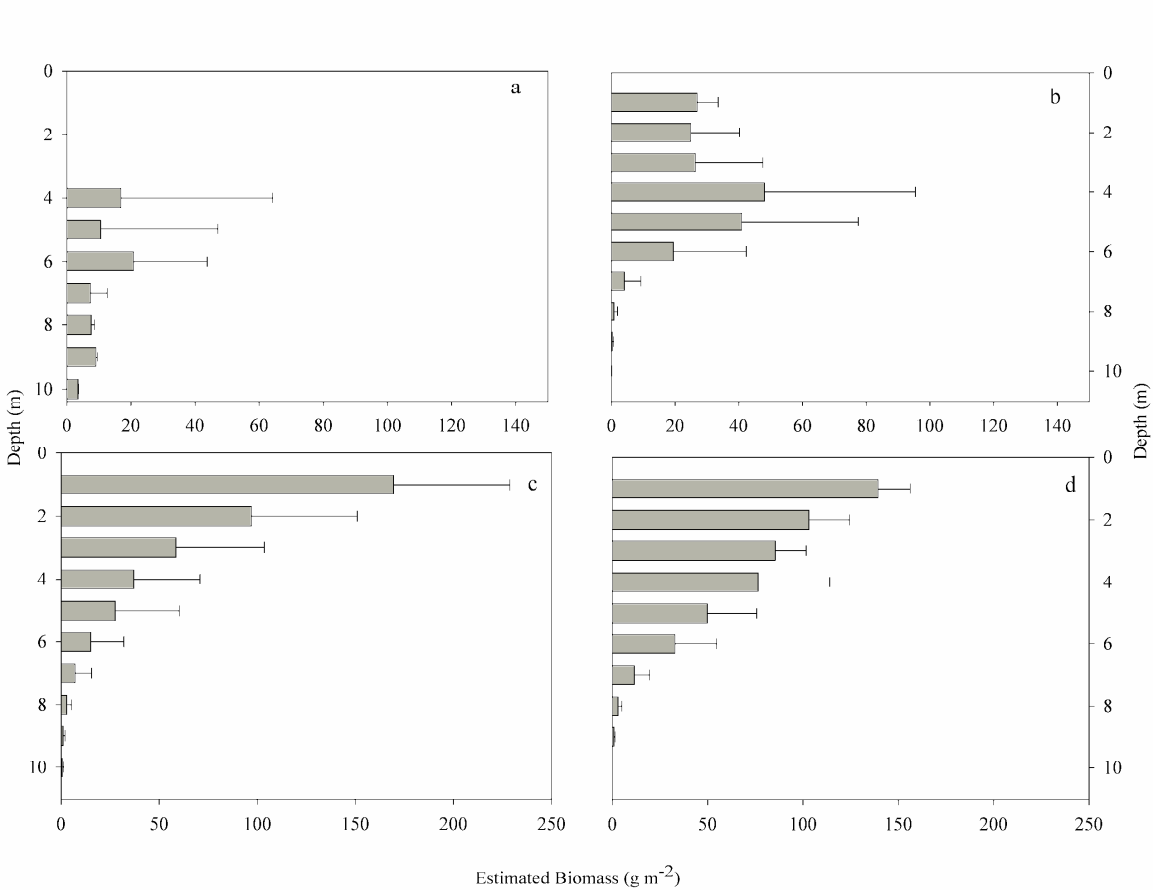

Figure 3.15. Depth profiles of average estimated biomass from acoustic methods for a) Nanticoke Shoal, b) Peacock Point, c) Rock Point (Grand River) and d) Grant Point (Grand River). Error bars are one standard deviation. Note x axis scale is different for panels a and b.

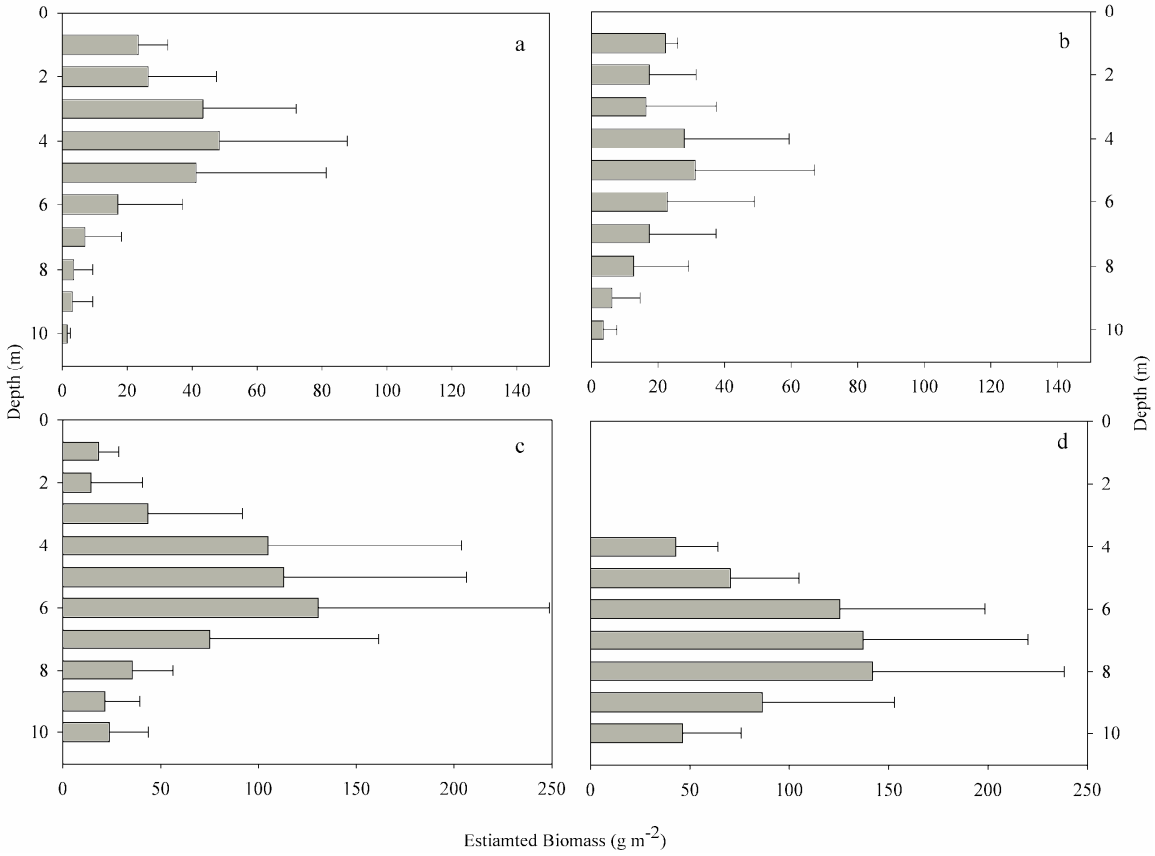

Figure 3.16. Depth profiles of average estimated biomass from acoustic methods for a) Oakville, b) Port Credit, c) Presqu'ile and d) Dobb's Bank. Error bars are one standard deviation. Note x-axis scale in panels a and b is different.

3.5 Discussion

This study describes the application of a non-invasive hydroacoustic system to rapidly sample large areas and map the distribution of nuisance *Cladophora* biomass. Operationally, the definition of nuisance *Cladophora* biomass is largely dependent on the objective of the study, and the biases of the observer; what is a nuisance in one case may not be considered a nuisance in another case. In this study, nuisance biomass is defined as that which exceeds 50 g m^2 DW. This value is well above the estimated detection limit of the hydroacoustic system as determined in Chapter 2, and close to the level observed by Canale and Auer (1982) when SRP concentrations declined < 2 μg L^{-1}. Like any remote sampling method, there are inherent limitations. First and foremost, the detection of algae or macrophytes on the lake bottom is limited by both biomass and height of the canopy (Chapter 2; Sabol et al. 2002a). In this study, a minimum detection height of 7.5 cm was used to characterize the algal canopy. This distance corresponds to one half the pulse width which is considered the minimum distance between two targets for reliable separation (Simmonds and MacLennan 2005), and is used in this purpose to limit the rate of false positive detections. Clearly algal stands with canopy heights less than this threshold will not be adequately characterized and corresponding estimates of percent cover, stand height and biomass are likely conservative. Moreover, the distribution of nuisance *Cladophora* biomass is more likely to be of interest to managers and shoreline residents. Additional limitations to successful detection of algal mats are imposed by environmental factors such as wind and waves which act to entrain air in the form of bubbles that strongly scatter acoustic energy (Kubecka 1996). These bubbles can obscure the presence of an algal signal on the bottom, particularly if bubbles are well distributed in the water column. Such interference was minimized by conducting the acoustic surveys on calm days when environmental conditions (e.g., wind and waves) were not conducive to bubble formation or excessive vessel pitch and roll.

The use of kriging as applied in this study was to build a reliable representation of the spatial structure of nuisance *Cladophora* distribution along sections of the Great Lakes shorelines. The ultimate result of this process is a smoothing of more ragged sample dataset. Acoustically generated data corresponding to *Cladophora* cover and height proved to be suitable for kriging provided appropriate caution is exercised. In particular, the results illustrate the importance of checking the assumptions of stationarity, as significant, although variable trends with depth were found for percent cover, and strong relationships between stand height and percent cover existed for all datasets where *Cladophora* was detected with the acoustic system. The choice of semivariogram models and fitting methods with “messy” biological data (c.f.

Rufino et al. 2005) continues to be a topic of considerable discussion in the literature (Rufino et al. 2005, Sullivan 1991) and while the goal of this study was not to contrast the multitude of different methodological options for exploring and validating spatial models, it is important to identify areas where improvements can be made.

In this study, creation of maps of algal distribution and stand height were possible when trends with depth were accounted for, particularly for areas where *Cladophora* was the only target. Improvements could likely be made through the use of additional predictors. For example, stratified kriging could be employed had accurate maps of substrate type been generated from the 120 kHz system, as trends between percent *Cladophora* cover and depth are not likely to be similar on soft substrates compared to hard substrates. Furthermore, removal of acoustic data associated with macrophytes may facilitate better kriging estimates (both of predicted values and error variance) as trends between percent cover and depth and percent cover and stand height are much different for macrophytes than for filamentous algae such as *Cladophora*. However, these study sites were dominated by hard substrate, and in areas where macrophyte growth was present, it was generally minor in nature, and isolated. Improvements are likely to be minor in these cases, but may offer improvement for other study sites with more variable substratum.

3.5.1 Current distribution of nuisance *Cladophora* growth in Lake Huron, Erie and Ontario

Nuisance *Cladophora* growth was evident at all sites in Lake Erie and Ontario, including the offshore shoals in each lake. The maximum depth where consistent detection of *Cladophora* was possible with the acoustic system was ~ 5 - 6 m at Lake Erie shoreline sites, 6 - 7 m for western Lake Ontario, and up to 9 m at Presqu'ile Provincial Park in eastern Lake Ontario and the offshore shoal sites in Lake Erie and Ontario. These ranges of depths where nuisance biomass occurred are consistent with results of surveys in 1995 and 2001-02 reported by (Higgins et al. 2005b) where nuisance biomass of *Cladophora* (e.g., > 50 g m^{-2}) were widespread to depths of 5 m at a variety of sites along the East Basin of Lake Erie. While a data set with similarly intensive depth sampling is not available for western Lake Ontario, the depth specific extent is consistent with modeled peak biomass from 2004 and 2005 for a site at Oakville (Malkin et al. 2008). The apparent greater depth of detection at Presqu'ile is difficult to reconcile given the relatively lower water clarity measured at this site, and the tendency for long shore transport of eroded bluff material from western Lake Ontario that often results in turbid waters in Wellington Bay (e.g., Martini and Kwong 1985). Nonetheless, these results are consistent with the limited quantitative data available for this site. For example, biomass reaching 84 g m^{-2} at depths of 9.1 m was recorded in July of 1999 (DeJong 2000). While data are not available for comparison with either

of the shoal sites (Nanticoke or Dobbs Bank), the depth limits for detection of nuisance *Cladophora* with the acoustic system is in general agreement with available quantitative studies.

In contrast to the lower lakes, nuisance *Cladophora* growth was not detected with the acoustic system at any of the sites in Lake Huron or Georgian Bay during this study. This does not mean that the lake bed at these sites were entirely devoid of *Cladophora* growth. On the contrary, small quantities of *Cladophora* were observed at 6 of 9 stations at the Southampton site and at stations 800 and 801 at the Cape Chin site with the aid of the underwater camera. These small growths of *Cladophora* were generally short (i.e < 5 cm in length) and of limited areal extent (approx. 10s of cm^2). While quantitative data on *Cladophora* biomass at these sites is lacking, it is likely that the attached biomass at the time of study was well below the detection limit for the acoustic system. The failure to detect nuisance *Cladophora* biomass at these sites may be due in part to the comparatively fewer surveys conducted at these sites relative to those in Lake Erie and Ontario, but also the later seasonal timing of the surveys may have not been ideal to capture peak biomass conditions. However, recent work along the Ontario shore of Lake Huron produced estimates of *Cladophora* biomass ranging from 0 to 15 g m^{-2} at depths ranging between 0.5 and 3 m (S.N. Higgins, University of Wisconsin, unpubl. data) well below "nuisance" quantities. Furthermore, shoreline surveys by the Ontario Ministry of the Environment between 2003 and 2005 found only localized nuisance growth of *Cladophora* in proximity to known nutrient sources (Howell 2004). The combination of the survey results and the observations discussed previously do suggest that at the current time, C*ladophora* does not reach nuisance biomass levels in Lake Huron.

3.5.2 Distribution of nuisance *Cladophora* in relation to water chemistry, land use and dreissenid mussels

The upper limit of *Cladophora* biomass in the Great Lakes has historically been and continues to be set by P supply and light availability (Auer and Canale 1982a, Higgins et al. 2005a, Malkin 2007, Higgins et al. 2008a). Prior to the implementation of the GLWQA and mandated P control strategies, high P concentrations were characteristic of many near shore areas of the Great Lakes (Gregor and Rast 1982). In Lakes Erie and Ontario, TP concentrations routinely exceeded 15 µg L^{-1} (Gregor and Rast 1982; Ontario Ministry of Environment 1975, Ontario Ministry of Environment 1986). In contrast, few near shore areas in Lake Huron were characterized by TP concentrations in excess of 10 - 15 µg L^{-1} and these were mainly limited to Saginaw Bay (Gregor and Rast 1982) and areas near the Ausable and Maitland Rivers along the Ontario coast of southern Lake Huron (Stevens et al. 1985) where proximity to major tributaries

and municipal effluent discharges ensured persistent high nutrient concentrations (Stevens et al. 1985, Jackson et al. 1985, Ross and Chatterjee 1977). The resultant patterns of *Cladophora* growth during this time period were generally consistent with the trends in nutrient concentrations; nuisance biomass was often locally associated with known point or shoreline sources in Lake Huron (Auer et al. 1982, Jackson 1988) whereas in the lower lakes (Erie and Ontario) nuisance *Cladophora* growth was widespread, in concordance with widespread elevated nutrient concentrations (Taft and Kishler 1973).

Considerable strides reducing nutrient loads to the Great Lakes were made in the 1970s and 80s in part by controlling point source discharges of P such as waste water treatment plant effluent (Stevens and Neilson 1987, Neilson et al. 1995). These improvements were possible due in part to the ease in identifying point sources, but also in implementing effective controls. On the other hand, the control of point sources of P did not necessarily end the eutrophication problem (Schindler 2006). It was widely recognized that diffuse non-point sources of nutrients such as agricultural runoff and internal recycling of P persisted in some areas (Schindler 2006). As far back as the 1970s, the International Joint Comission (IJC) estimated that ~ 50 % of the nutrient load originated from non-point sources (IJC 1980). The effectiveness of non-point source controls is difficult to determine because a) it is difficult to identify the exact source of nutrient pollution within a watershed (Sharpley and Rekolainen 1997) and 2), reductions often require changes to agricultural practices or revitalization of wetlands and riparian areas, which can take several years to implement and therefore demonstrate a measureable effect. Compounding such efforts is the fact that the pace of land use change (often from natural cover to agricultural or urban cover) is rapidly changing, exceeding that predicted by population growth in the Great Lakes basin (e.g., Wolter et al. 2006).

While it is well recognized that the conversion of forested land to agricultural land (even pastured land) is known to increase the nutrient fluxes from the watershed (Dillon and Kirchner 1975), the dynamics of land use has changed dramatically. For example, prior to the 1940s, most farming communities were self sufficient, producing enough feed locally to meet animal requirements and recycling animal nutrients to meet crop needs (Sharpley et al. 2001). The advent of mechanized farming and concentrated farming systems has lead to a transfer of P from areas of grain production to animal production, effectively creating regional surpluses of P inputs (fertilizer and feed) over outputs (crop and animal produce) (Sharpley et al. 1998). These regional P imbalances are further exacerbated by the inefficient utilization of P in feed by by many animals (~30%; Sharpley et al. 1998). As a result much of the P entering livestock operations ends up in animal manure which is often applied locally and designed to meet crop N needs. This

results in a build-up of soil P above the amount needed by crops and increases the potential for P loss in runoff as well as leachate to subsurface systems. The net result of these changes withing agricultural lands has been a gradual evolution from net sinks of P to net sources of P (Sharpley et al. 2001).

Conversion of natural land or agricultural land to urban land can also increase the flux of nutrients from the watershed. In general, developed lands, (residential, commercial or industrial) increase the amount of impervious surface area which promotes high runoff during precipitation events and reduces the potential attenuation of nutrients in these areas (Sorrano et al. 1996). Sewage inputs can also be a key source of P inputs from urban areas, particularly if the sewage infrastructure (e.g., combined sewer overflows; CSO) are not able to accommodate the increased volume of water that results from expansion of impervious surface area (Marsalek and Rochefort 2004).

In this study, significant relationships between land use and NO_3^- concentrations were found at differing spatial extents. The relationship observed between NO_3^- concentrations and agricultural land use is well documented and is thought to result from the high loadings and low retention of nitrogenous fertilizers in cultivated fields (Howarth et al. 1996). The significant relationship observed between % urban land use and NO_3^- concentrations at the coastal scale (~ 5 km) likely reflects the fact that many of these highly urbanized shorelines are still situated within primarily agricultural watersheds (see for example, Table 3.1). This is largely consistent with the findings of Danz et al. (2007) who found a strong relationship between agricultural stress and TN in Great Lakes coastal areas and the findings of Peterson et al. (2007) who found N^{15} of benthic organisms closely resembles the N^{15} of the adjacent watersheds. Upward trends in NO_3^- concentration observed in tributaries within these urban watersheds around Lake Ontario (Ontario Ministry of Environment 1999) are also consistent with these patterns.

The lack of strong relationships between land use type and near shore P concentrations observed in this study does not exclude the possibility that catchment loading has not increased. The strong correlations between urban land use and summer TSS and kPAR are certainly not inconsistent with increased connectivity of the urban areas to the lake (Sorrano et al. 1996). Associations between P concentrations in receiving waters and land use are less universal than those typically described for N (Sorrano et al. 1996, Vanni et al. 2007). Watersheds with comparable land uses can vary greatly with respect to nutrient fluxes or instream conditions (Vanni et al. 2007, Fraterrigo and Downing 2008). Further compounding this variation is the observation that nutrient fluxes can show appreciable temporal variation, often corresponding to precipitation mediated changes in discharge. Simple sampling regimes such as the one employed

in this study are insufficient to characterize such events and their subsequent effects on near shore nutrient chemistry.

The nutrient concentrations measured in the near shore are a function of biological processes (Edsall and Charlton 1997), the magnitude of loads from the catchment (Gregor and Rast 1982), dynamics of hydrologic transport to the lake (Harremoes 1988) and the mixing and dispersion created by hydrodynamic forces (see Rao and Schwab 2007 for a review) which will determine the distribution of nutrients once in the lake. Although the open near shore areas (such as the ones sampled in this study) are thought to be sufficiently well mixed such that specific sources of nutrient pollution can be difficult to identify (Peterson et al. 2007), given the limitations of such a limited temporal sampling regime, the lack of response for P concentrations and land use classes may simply reflect the fact that P remains the limiting nutrient for algal growth in the Great Lakes and is therefore subjected to high biological demand, particularly during the summer months. The strong negative correlation that was observed between estimated *Cladophora* biomass and TP during the summer supports this interpretation.

The widespread nature of *Cladophora* growth in Lakes Erie and Ontario suggests that shorelines with differing land uses (e.g., urban and rural/agricultural; Lake Ontario, and agricultural; Lake Erie) can experience nuisance *Cladophora* biomass accumulation. While this is certainly not inconsistent with historical patterns, the current patterns in water chemistry and nuisance *Cladophora* growth in near shore areas are not easily reconciled. For example, phytoplankton chlorophyll a remains low in both near shore and offshore waters and in many places (e.g., this study, Depew et al. 2006, Hall et al. 2003) and compelling evidence for increasing nutrient concentrations in Lakes Erie or Ontario is lacking (e.g., North 2008, Malkin et al. submitted). In this study, TP only exceeded the GLWQA concentration of 10 $\mu g\ L^{-1}$ at Lake Erie shore line sites during the spring and at Southampton (Lake Huron site) during the summer. TP measured at the remainder of the sites was often less than 10 $\mu g\ L^{-1}$, and SRP was low, even falling below the detection limit (~ 0.35 $\mu g\ L^{-1}$) in Lake Erie during the summer. These patterns are consistent with the hypothesis that near shore water chemistry can be strongly affected by biological activity. For example, nuisance *Cladophora* growth was lacking along the Lake Huron shoreline at Southampton where one of the most heavily farmed watersheds in Ontario (Saugeen River) drains into the lake. The Saugeen River watershed is ranked 6th in the country for N production from manure (35 kg ha^{-1}) and 7th in the country for P production from manure (10 kg ha^{-1}) (Statistics Canada 2001). This site had the highest measured nutrient concentrations (TP and NO_3) in this study, but also had low dreissenid abundance and nuisance *Cladophora* growth was absent. In contrast, the upper Grand River watershed is ranked 3rd in the country for N production

from manure (46 kg ha^{-1}) and 4th in the country for P production from manure (12 kg ha^{-1}) (Statistics Canada 2001). At the Grand River site, luxuriant *Cladophora* growth was clearly widespread, yet some of the lowest P concentrations (summer) were measured at this site. This is clearly a change when contrasted against historical studies and is remarkably consistent with the near shore shunt hypothesis (e.g., Hecky et al. 2004) that attributes these paradoxical patterns (excessive benthic algal growth and unremarkable water chemistry) to alterations of nutrient and energy cycling mediated by mussels. The high densities and biomass of dreissenids in near shore areas of Lakes Erie and Ontario are well documented (e.g., Patterson et al. 2005, Wilson et al. 2006, Ozersky et al. 2009), although the abundances of mussels in the east basin of Lake Erie is likely lower than the numbers reported here for the year 2002 due to predation by round gobies (e.g., Barton et al. 2005). Less well known are the abundances of mussels in Lake Huron or Georgian Bay, and their potential impact on the ecology of the upper lakes. The estimates of mussel abundance for Lake Huron and Georgian Bay from this study are low compared to Lake Erie and Ontario, but comparable to densities observed by Pothoven and Nalepa (2006) and Nalepa et al. (2007) at deeper depths (31 to 50 m) in Lake Huron. When dreissenids are present at high abundances, numerous studies have documented their ability to filter large amounts of particulate matter and increase water clarity (Howell et al. 1996), reduce phytoplankton chlorophyll a concentrations (Hall et al. 2003, Depew et al. 2006), generate large quantities of fecal material (Stewart et al. 1998a) and recycle N and P (e.g. Arnott and Vanni 1996, Ozerksy et al. 2009). At lower abundances, however, such effects may not be as large, and on the surface the differences in dreissenid abundance appears to explain the pattern of nuisance *Cladophora* growth well. Although Barbiero et al. (2009) suggest that even mussels have had a profound effect on nutrients and the pelagic food web in Lake Huron, the bulk of dreissenid biomass appears to be located at depths > 30 m (e.g., Pothoven and Nalepa 2006, Nalepa et al. 2007) and the positive effects of enhanced nutrient supply from profundal dreissenids to *Cladophora* in the littoral areas is likely inconsequential.

Further support for the dreissenid link is provided by observations of nuisance growth at offshore shoals (e.g. Nanticoke Shoal and Dobb's Bank). Although these were not studied historically, given the relatively restricted depth of colonization observed in Lake Erie and Ontario durig the 1970s and 1980s, it is unlikely that these shoals were heavily overgrown by *Cladophora*. These shoals are also well removed from the local influences at the shoreline, and are characterized by nutrient conditions that closely resemble offshore conditions. The results of this study clearly demonstrate that even the low nutrient conditions that have been measured in

the offshore (e.g., North 2008, Malkin et al. submitted) are sufficient to support *Cladophora* growth, which is clearly a change from conditions in the 1960s and 1970s.

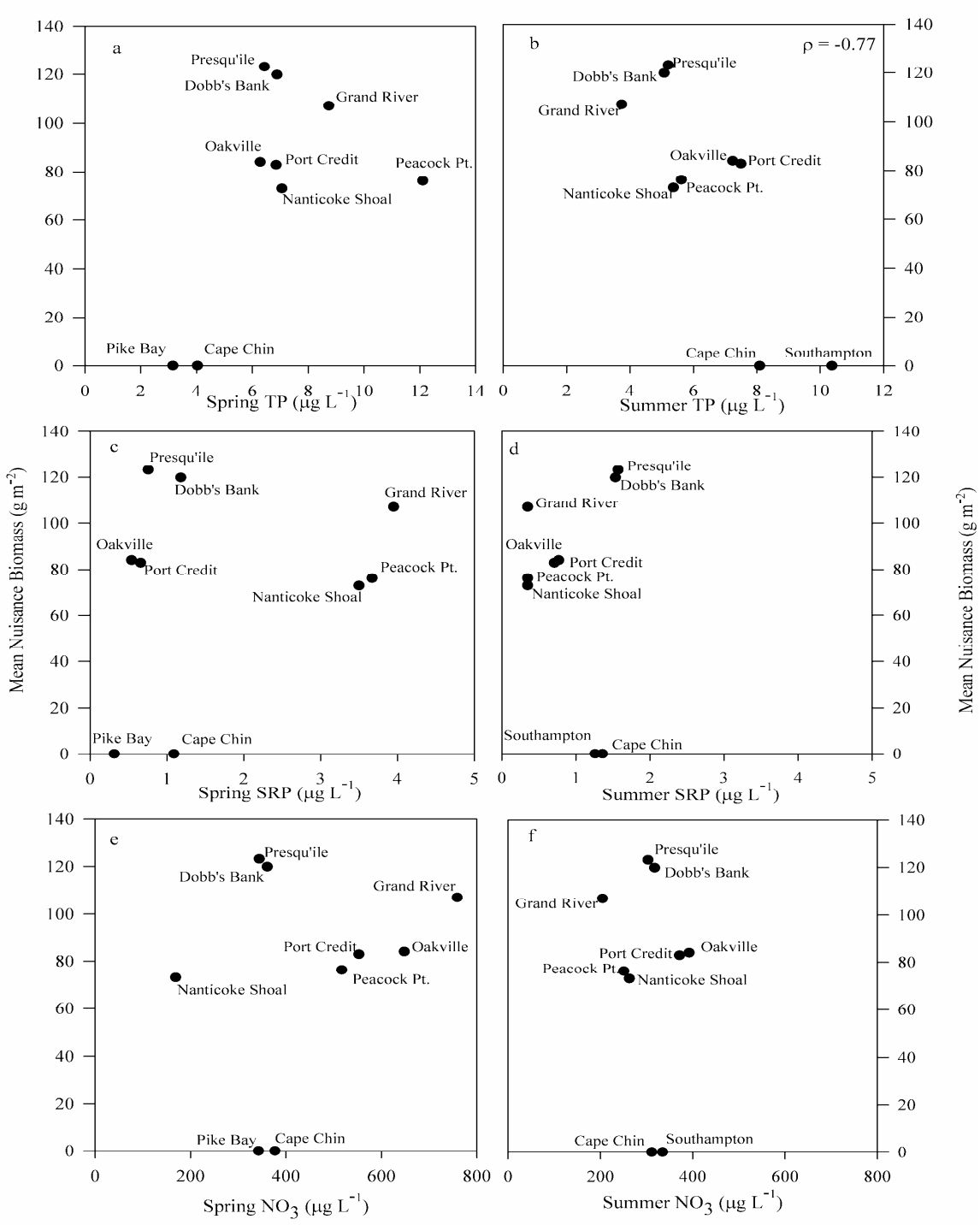

Figure 3.17. Scatterplots of mean nuisance *Cladophora* biomass estimated from acoustic methods with a) Spring total P, b) summer TP, c) Spring SRP,) summer SRP, e) spring NO_3^-, f) summer NO_3^-. Significant (p <0.05) Spearman correlation coefficients are given in the upper right corner of panel.

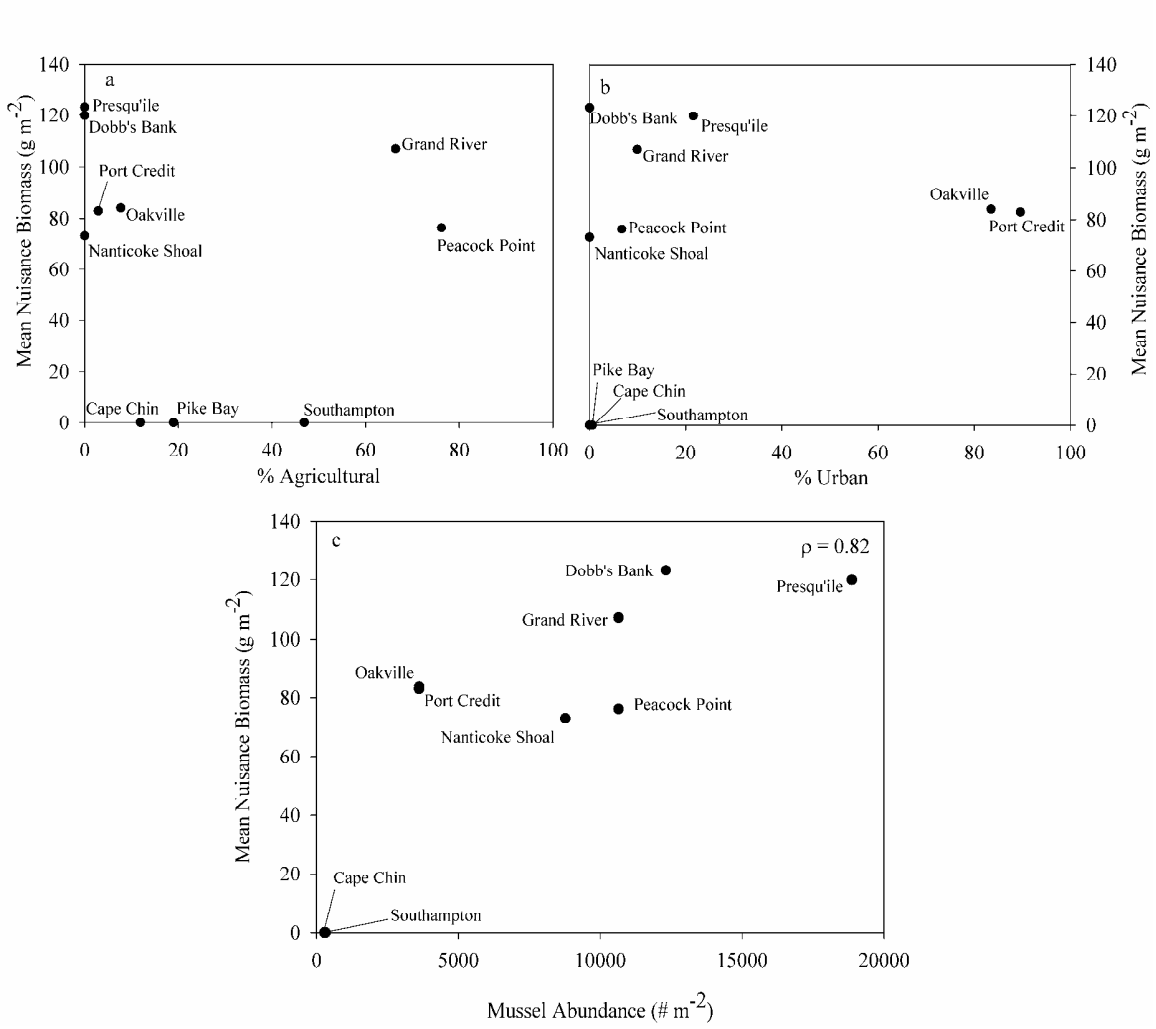

Figure 3.18. Scatterplots of mean nuisance *Cladophora* biomass estimated from acoustic methods with a) % agricultural land use, b) % urban land use, c) dreissenid mussel abundance. Significant ($p < 0.05$) Spearman correlation coefficients are given in the upper right corner of panel.

3.6 Summary and Conclusions

The ambient nutrient conditions and differences in land use measured among sites do not readily explain the regional differences in nuisance *Cladophora* growth and biomass, nor do they offer much insight into the nature of *Cladophora* growth within Lakes Erie and Ontario. These results show a stronger correlation between nuisance *Cladophora* biomass with dreissenid mussel abundance than with ambient near shore nutrient concentrations, or land use types at the coastal or watershed level.

These results also suggest that nuisance *Cladophora* growth extends into waters 6 to 9 m deep. Although comparable data from the 1960s and 70s are scarce, this is deeper than historical depths determined from modeling studies (e.g., Higgins et al. 2005b, Malkin et al. 2008). The expansion of *Cladophora* into deeper waters is also consistent with the results of a recent bi-national modeling study (Auer et al. submitted) that concluded the gains made through phosphorus loading reduction have been offset by the dreissenid mediated changes in water clarity and phosphorus cycling that increase the depth of colonization of *Cladophora*, thereby increasing the total production. Lacking a demonstrable increase in nutrient loading from catchments or point sources (e.g., Ontario Ministry of the Environment 1999, Medieros and Molot 2006), the patterns of *Cladophora* growth and water chemistry observed in this study are better explained by the patterns of dreissenid mussel abundance and the near shore shunt hypothesis (Hecky et al. 2004).

Chapter 4

Distribution of nuisance benthic algae (*Cladophora*) along urban shorelines: Can the resurgence be linked to nutrient sources?

4.1 Overview

Two shorelines in the heavily urbanized western basin of Lake Ontario were surveyed with a high frequency hydroacoustic echosounder to assess the spatial patterns of water quality and the nuisance benthic filamentous algae (e.g., *Cladophora*) to evaluate whether potential point sources (e.g., municipal waste water treatment plant outfalls) and shoreline point sources of nutrients (e.g., tributaries and storm drains) contribute to the patterns of nuisance algal growth. Results from these surveys indicate that nutrient concentrations are spatially heterogeneous in the near shore areas of Lake Ontario but do not regularly exceed GLQWA target concentrations during the summer growing period of *Cladophora*. Nuisance biomass (> 50 g m^{-2}) of *Cladophora* is widespread along large areas of these heavily urbanized shorelines and these accumulations are not spatially associated with identifiable point sources (e.g., WWTP outfalls) of nutrients. While some degree of spatial association was observed between nuisance *Cladophora* biomass and tributaries at one site, the widespread nature of nuisance *Cladophora* growth indicated that autochthonous recycling of P is likely important. These results are consistent with prior surveys in Lakes Huron, Erie and Ontario that suggest dreissenid mussels are a key link governing the contemporary distribution of nuisance *Cladophora* in the Great Lakes.

4.2 Introduction

Historically, nutrient loading to the Great Lakes occurred primarily via point sources such as municipal waste water treatment plants and industrial discharges, and non-point sources such as agricultural and urban runoff, that are derived from a multitude of catchment sources (Neilson et al. 2003). For Lake Ontario, nearly 60 % of the P load to the lake in the mid 1960s was attributed to municipal sources (International Lake Ontario - St Lawrence River Water Pollution Board 1969), with the remaining 30% attributed to the Niagara River, and upstream Lake Erie (International Lake Ontario - St Lawrence River Water Pollution Board 1969). Approximately 70 % of the total P load to Lake Ontario was estimated to be derived from detergent phosphates, and due to the locations of the discharges, these primarily occurred in shallow near shore areas as direct discharge to surface waters via municipal WWTP outfalls or tributary discharge at the shoreline (Stevens and Neilson 1987). As a result, both the production and biomass of phytoplankton increased (Glooshenko et al. 1974, Stadelmann et al. 1974), particularly in near shore areas near nutrient inputs where nutrient concentrations were the highest. In addition to high phytoplankton biomass, excessive amounts of the filamentous green algae (*Cladophora*) were commonly observed across large areas of the Lake Ontario shoreline where hard substrate dominated (Neil and Owen 1964, Wezernak and Lyzenga 1975, Painter and Kamaitis 1987).

Intensive research on *Cladophora* in Lake Huron (see Auer et al. 1982a for a review) and in Lake Erie (Neil and Jackson 1982) concluded that phosphorus was the key nutrient controlling *Cladophora* growth in the Great Lakes. Phosphorus abatement programs were implemented in the early 1970s to reduce the phosphate content of detergent from 20 % to ~ 5 % (Municipal Abatement Task Force 1983). In addition, the signing of the Great Lakes Water Quality Agreement (GLWQA) in 1972 outlined additional remediation measures necessary to control P input to the Lakes; including regulating the effluent concentrations from municipal waste water treatment plants (WWTP) discharging in excess of 1 million gallons day^{-1} to 1 mg L^{-1} of P (Stevens and Neilson 1987). These strategies were largely effective at reducing both near shore (Nicholls et al. 2001) and open lake phosphorus concentrations in Lake Ontario (Lean et al. 1990). Although less intensively monitored, there is evidence that P control contributed to a decline in *Cladophora* biomass and tissue P content in Lake Ontario (Painter and Kamaitis 1987).

Over the last two decades, Lake Ontario has experienced significant reductions in phosphorus loading with a concomitant shift to oligotrophy and a dramatic increase in water clarity resulting from both nutrient reduction and after the mid-1990's a proliferation of the filter

feeding dreissenid mussels (Mills et al. 2003). In the late 1990s and into the early 2000s, reports of shoreline fouling by *Cladophora* were increasing in the western basin of Lake Ontario (Malkin et al. 2008), despite off shore nutrient concentrations remaining at or below the levels set in the GLWQA (Malkin et al. submitted). Similar reports of increased *Cladophora* growth in Lakes Erie (Higgins et al. 2005) and Michigan (Bootsma et al. 2005) suggested that this was not a localized phenomenon, and may be a result of extensive dreissenid mussel colonization (Hecky et al. 2004). Due to the high biomass that dreissenid mussels have attained in the lower Great Lakes, mussels have been credited with increasing water clarity and re-distributing nutrients and organic matter from the pelagic environment to the benthic environment (Hecky et al. 2004). These effects are thought to be particularly strong in the shallow near shore waters of the Great Lakes underlain by hard substratum, which is suitable for dreissenid and *Cladophora* colonization, and the perception that increased benthic algal growth has resulted from dreissenid colonization has become widespread.

The degree to which this perception is accurate, however, is unclear. Phosphorus flux from catchments is known to increase with land disturbance, soil erosion, and increases of impervious surface area (Byron and Goldman 1989). While agricultural and urban areas may be quantitatively similar in the magnitude of P loading, they are qualitatively different in their linkage to receiving surface waters. Many urban landscapes consist of a mosaic of land uses varying at a fine spatial scale, ranging from impervious surfaces to pervious landscapes like parks, lawns, athletic fields and golf courses. Urban areas are often tightly coupled to surface waters via storm sewers, and impervious surfaces that increase runoff to waterways, thus urban areas may export P during relatively small precipitation events that agricultural land would attenuate. Urban areas are also known to export a larger fraction of dissolved P compared to agricultural areas where the majority of P is transported in particulate form (Stone and English 1993). This dissolved P is presumably more readily available for uptake by *Cladophora*, unlike particulate nutrients which may sink out of the water column (Sonzogni et al. 1982).

For heavily urbanized areas of the Lake Ontario catchment, this has naturally lead to questions whether the resurgence of *Cladophora* in Lake Ontario might be driven by increased P loading in runoff from urbanized areas. Additionally, increased P loading from municipal waste water treatment plants (WWTP) is of concern as population continues to increase in urban areas, because WWTP must manage this increased load to keep effluent concentrations at mandated levels. But, mandated effluent concentrations are set for the effluent discharging from the end of the outfall pipe and not the total load. Consequently, the total load may go up unless increased treatment efficiencies are imposed by the WWTP. For example, the total volume of waste water

discharged by the city of Toronto increased 4 % from 1987 to 1999, even though per capita waste water discharge was declining, indicating that rising populations can lead to increased discharge volumes (Sahely et al. 2003).

In this study I use a high frequency hydroacoustic method (Chapter 2) to map nuisance benthic algal (*Cladophora*) cover and stand height along two segments of Lake Ontario shoreline in 2006 and 2007 to assess the patterns of nuisance algal growth. A regression model developed in Chapter 3 is used to estimate attached *Cladophora* biomass, and the spatial patterns of *Cladophora* growth in relation to potential nutrient sources are examined for spatial associations. Specifically, if nuisance *Cladophora* growth is directly related to known nutrient sources (e.g. municipal WWTP outfalls) or potential nutrient sources (e.g. tributary and storm sewer locations) then management strategies for specific problem areas can be investigated. In contrast, if nuisance *Cladophora* growth is ubiquitous, then this indicates that ambient conditions are adequate to support nuisance *Cladophora* growth and alternative strategies are needed. Preliminary surveys in 2005 at Oakville and Port Credit (Chapter 3) suggest that *Cladophora* growth may be widespread during mid summer periods along urbanized shorelines. In 2006, monthly surveys from May to October were conducted at high spatial resolution at the Oakville site sampled in 2005. In 2007, a similar survey protocol was followed on a bi-weekly schedule at a site near Pickering from May to October.

4.3 Materials and Methods

4.3.1 Site Selection and Descriptions

The western end of Lake Ontario is a near continuous urban landscape that stretches from Oshawa, east of Toronto, all around the west end of Lake Ontario to St. Catharine's near the Niagara River. With a population of approximately 4 million (Rao et al. 2003), this highly urbanized part of the Lake Ontario watershed features extensive areas of impervious land cover, often extending right to the shoreline of the lake. Municipal water intakes and waste water treatment plant discharges are situated in a narrow band of the lake, extending at most, a few kilometers offshore (Rao et al. 2003). In addition, the shoreline features numerous tributaries, creeks and storm sewers that discharge a mixture of both urban and agricultural runoff to the near shore waters.

The first site, adjacent to the town of Oakville (Figure 4.1) features moderately steep bathymetry with a substratum composed primarily of bedrock and cobble. Within the study site there are two active waste water treatment plant (WWTP) outfalls (Southeast WWTP; situated 300 m from shore at a depth of 4 m and Clarkson WWTP; situated ~ 1 km from shore at a depth of 16.5 m) and 20 storm sewers discharging at the lake shore (Figure 4.1a). An additional 49 storm sewers discharged into a tributary or creek that eventually discharged into the near shore waters (Figure 4.1a; Griffiths 1990). The main tributary for this shoreline (16 Mile Creek) has a mean annual discharge (1960 – 2008) of 2.76 $m^3 s^{-1}$ and discharges into Lake Ontario at ~ the 5 m contour because of the harbour channel breakwalls. 16 Mile Creek is in the approximate middle of the survey area (Figure 4.1a).

The second site in Lake Ontario was located 32 km east of Toronto in the vicinity of the Pickering Nuclear Generating Station (PNGS) and the outflow of the Rouge River (Figure 4.1b and c). Substrate at this study site was considerably more diverse than at Oakville, and consisted of a mixture of compact clays, sand and gravel in Frenchman's Bay, changing to larger cobble and rock overlying a primarily sandy substrate east of the PNGS. Further east from where Duffin's Creek entered the lake, substrate was a mixture of rock at moderate depths (2 to 10 m) and a mixture of sand and gravel in the shallows (< 2 m). The accumulations of softer substrate here are likely a conseuquence of depositional material from the tributaries (e.g., Rouge River and Duffins Creek) but also settled material that had eroded from bluffs further west (e.g., Scarborough Bluffs; Rukavina 1976). One major WWTP outfall (Duffins WWTP) is located to the east of PNGS, and Duffins Creek is the major tributary at this study site with a mean annual

discharge (1947 – 2008) of 2.82 m^3 s^{-1} and dischares directly at the shoreline. Several storm drains are present along the shoreline, but at a lower density that at Oakville (Figure 4.1a). Substrate at the Rouge River survey site was dominated by sand and silt, but areas of hard substrate were present northeast of the river outflow (personal observation).

Table 4.1. Summary of the surveys in 2006 and 2007. Survey data indicated date of acoustic survey, WQ date; date of water quality sampling.

Year	*Site*	*Survey Dates*	*WQ Dates*
2006	Oakville	April 11	April 11
			April 13
			April 20
			April 27
		May 8	May 8
			June 8
		June 23	June 23
		July 11	July 11
		August 1	August 1
		September 14	September 14
		October 15	October 15
2007	Pickering		May 14
		June 11	June 6
		June 22	June 20
		July 17	July 12
		July 25	July 24
		August 8	August 10
		September 17	September 6
			October 22

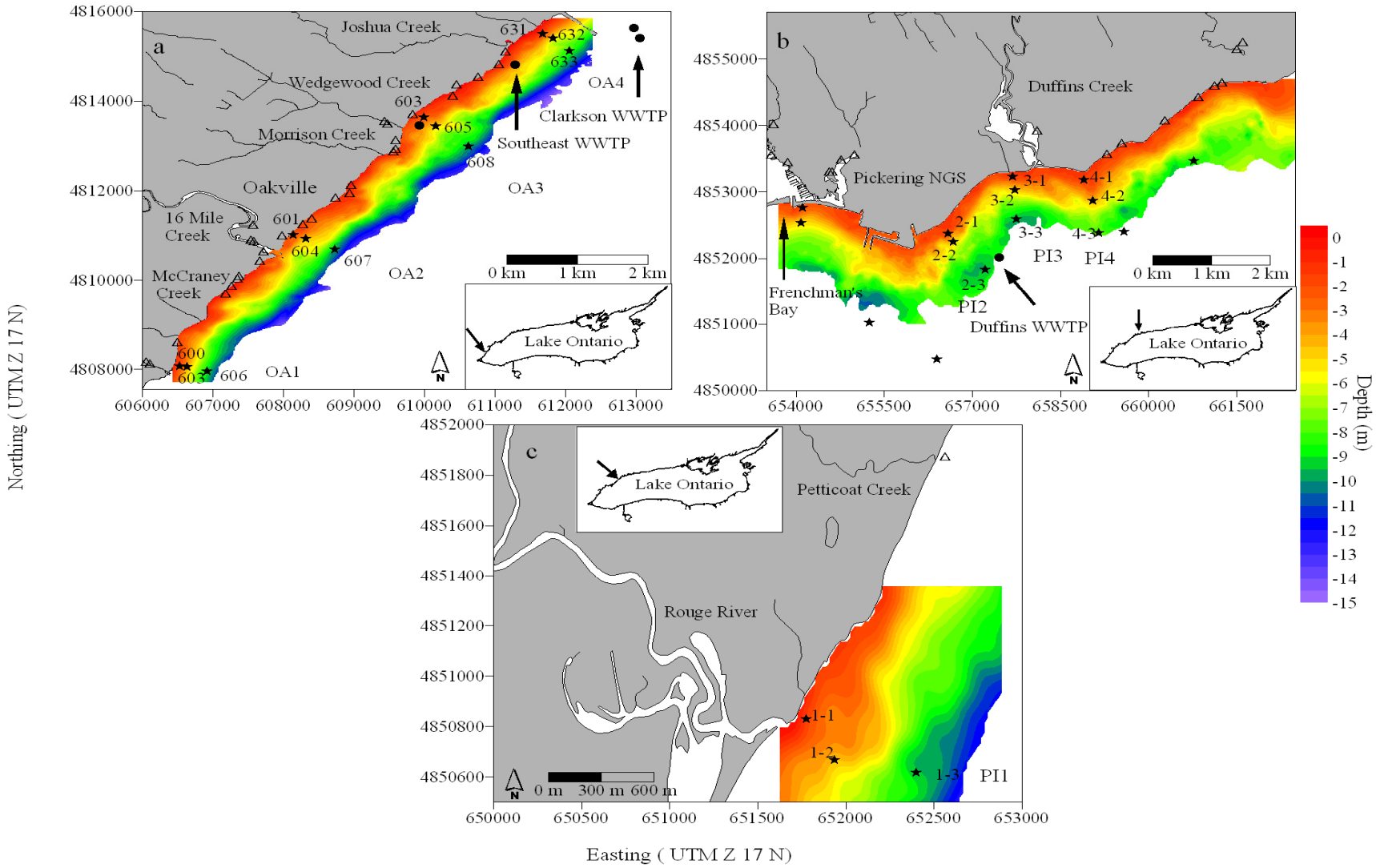

Figure 4.1. Map of the sites surveyed for this study; a) Oakville b) Pickering (main portion) and c) Rouge River area (west of Pickering). Maps show water sampling stations (★), storm sewers (△), municipal outfalls (●), and major tributaries are labeled. Bathymetric contours delineate the area covered by the acoustic surveys. Inset panel denotes the location of the study site (arrow) within Lake Ontario. All labeled municipal outfalls are currently active. Note: transect labels (e.g., OA1 – OA4, and PI1 – PI4) indicate transect number.

4.3.2 Physical and Chemical Measurements

In 2006, sampling and surveys were conducted exclusively at the Oakville site (Figure 4.1a). In addition to the regular transect sampling program (described below), surface waters were sampled during the spring runoff period to assess the conditions in the near shore of an urban area during the thermal bar period. From 13 April to 27 April, surface waters (nominal depths 0.5 m) were sampled along the Oakville shoreline on a weekly basis. Surface grab samples were collected in 4 L carboys at selected near shore locations along the Oakville shoreline in proximity to tributaries, storm sewers and along the axis of the turbidity plume that emanated from 16 Mile Creek. The plume was easily spotted due to the high levels of turbidity. Water samples were processed for TP, SRP, TDP, NO_3, Cl^-, TSS, and chlorophyll a as described below.

In 2006, water sampling was conducted exlusively at the Oakville site. Sampling transects were located near 14 Mile Creek (OA1), 16 Mile Creek (OA2), Wedgewood Creek (OA3) and the Portland Cement Pier (OA4). In 2007 water sampling was conducted exclusively at the Pickering site. Although I again used a similar sampling strategy as in previous years, a greater number of offshore sampling stations to characterize the offshore region for modelling studies necessitated two separate days for water sampling and acoustic surveys (see Table 4.1). For comparative purposes to the Oakville study, I only use the data from the 4 transects at Pickering. Transects for this study were located near the Rouge River (PI1), PNGS (PI2), Duffins Creek (PI3) and Simcoe Point (PI4) (Figure 4.1b and c).

Water quality stations were located at each transect at the 2, 5 and 10 m depth contours (Figure 4.1). At each station, CTD profiles were taken using aYSI-6600 profiler to characterize the physical structure of the water column. Photosynthetically active radiation (PAR) profiles were measured with a LI-COR underwater cosine quantum sensor (LI-COR, Lincoln, NB, USA) at 0.5 m to 1 m intervals from the surface to the lake bottom, and light attenuation coefficients were calculated as from linear regressions of the natural logarithm of irradiance vs depth. A 6 L Niskin bottle was used to collect ~ 15 L of water at a depth equal to 50% of the mixed layer depth (determined from CTD cast). Water was transferred to covered carboys and stored in coolers until transported to the laboratory (Univ. Waterloo). Samples for total dissolved P (TDP) and soluble reactive P (SRP) were filtered through a 0.2 µm polycarbonate filter, particulate P (Part P) by filtering 500 mL of lake water onto acid soaked (5% HCl ~ 4 hr) Whatman GF/F filters (nominal pore size ~ 0.8 µm). Total P (TP) and all composite fractions (TDP, SRP, Part P) were determined according to Stainton et al. (1977). Samples for other particulate nutrients (carbon – Part C, nitrogen – Part N) were determined by filtering 500 mL of lake water onto pre-combusted

(500 C ~ 4hr) GF/F filters and assayed using a CEC-440 Elemental Analyzer (Exeter Analytical, MA). Phytoplankton chlorophyll *a* was measured using a Turner Designs 10-AU fluorometer (Smith, et al 1999). Additional ions (NO_3^-, Cl^-) were determined using ion chromatography (Dionex DX 500, Dionex AS17 and AG17 guard column). Ammonium was determined following the fluorometric method of Holmes et al. (1999) on a Turner Designs TD-700 fluorometer. Total suspended solids (TSS) were determined by filtering 2 to 5 L of lake water onto pre-combusted (500 C for 4 hr) pre-weighed GF/F filters, drying at 65 °C to a constant weight and re-weighing. AFDW was determined after combustion at 500 °C for 4 hrs.

4.3.3 Acoustic Surveys

Acoustic surveys to assess the spatial patterns of *Cladophora* growth were conducted using a BioSonics® DTX system with a 430 kHz 10.2° beam width (full beam angle, source level 213 dB re 1μPa at 1 m) and a 120 kHz 7° beam width (full beam angle, source level 216 dB re 1μPa at 1 m) single beam echo sounders. Both transducers were set to ping with pulse lengths of 0.1 ms (430 kHz) and 0.4 ms (120 kHz) using the software Visual Acquisition 5.1 (BioSonics Inc, Seattle, WA). The ping cycle was increased from 5 Hz (Chapter 2) to 8 Hz, to better characterize the uneven nature of the rocky substrate that dominated the bottom. Due to signal saturation, data from the 120 kHz transducer could not be used for substrate classification. Analysis of the 430 kHz acoustic data was performed using a graphical user interface (GUI) written in Matlab v7.2 (see Chapter 2). In 2006 and 2007, acoustic surveys were conducted by running acoustic transects approximately parallel to shore, with a inter-transect spacing of ~50 – 75 m, from ~ the 1.5 m depth contour to the 10 m depth contour. The change in survey transects was necessitated since the focus of the 2006 and 2007 surveys was primarily geared toward delineating the patterns of *Cladophora* growth that could result from a potential shoreline source of nutrients (e.g., tributaries and storm sewers) and other point sources (municipal WWTP outfalls), a dense, but regularized series of data points in the vicinity of the sources would help to better characterize the resultant spatial patterns of algal growth. During the 2006 surveys at Oakville, schools of baitfish (possibly emerald shiner) were commonly observed between 23 June and 1 August, occasionally swimming under the boat (and subsequently into the beam path of the transducer), generating strong echoes that obscured the presence of *Cladophora* on the lake bottom. Because it was impossible to tell where the fish echoes ended and the algal canopy began, these data were manually removed prior to geo-statistical analysis and mapping. Similar interference from schools of fish was not a common phenomenon during the 2007 study at Pickering, however, excessive water column noise was imparted by the high velocity of water from the thermal

discharge on the east side of PNGS (Figure 4.1b). These data was also removed prior to geo-statistical analysis.

4.3.4 Geostatistical Methods

The fundamentals of geostatistical analysis, with emphasis on the assumptions and methodology involved are thoroughly explained in several publications (e.g., Isaaks and Srivastava 1989, Cressie 1991, Webster and Oliver 2001) and summarized in Chapter 1, so only a brief summary will be provided here. In this study, I employed a spatial correlation function called the "semivariogram" (Cressie 1991) to characterize the spatial autocorrelation of the data collected. The semivariogram is derived from the experimental data, taking into account the spatial position of the samples by the following equation;

$$\gamma(h) = \frac{1}{2N(h)} \sum_{i=1}^{N(h)} \{Z(x_i) - Z(x_i + h)\}^2 \qquad (4.1)$$

where $Z(x_i)$ is the value of the variable Z at location x_i, h is a lag distance over which the local average is taken and $N(h)$ is the number of point pairs at the lag distance (h) (Cressie 1991). The semivariogram is the average of the Euclidean distance between pairs of samples (h) plotted against average variance at distance h. The presence of extreme values or outliers can seriously distort the real variation patterns present in the data, especially when biological data are considered (Rufino et al. 2005). The robust semivariogram method was originally developed to reducing the effect of outliers without removing them from the dataset (Cressie and Hawkins 1980). The robust estimation method is based on the fourth power of the square root of absolute differences as in equation (4.2);

$$\bar{\gamma}(h) = \frac{\left\{ \frac{1}{2 \mid N(h) \mid} \sum_{i=1}^{N(h)} \{Z(x_i) - Z(x_i + h)\}^{1/2} \right\}^4}{0.914 + (0.988 / \mid N(h) \mid)} \qquad (4.2)$$

This particular semivariogram estimator is robust to contamination by outliers, greatly enhances semivariogram continuity and has been successfully used to model spatial distributions of animal densities, which often have data sets characterized by overdispersion and non-normal distributions (Maravelias et al. 1996, Rufino et al. 2005).

Once a semivariogram estimator is chosen and semivariances for all point pairs computed either by equation 4.1 or 4.2, a function (the theoretical spatial covariance function or semivariogram model) is fit to the empirical semivariogram through an automated fitting procedure. In this study, the weighted least squares method (WLS) of fitting the semivariogram model was employed as it typically defines the behavior of the semivariogram model at the origin

most clearly, which is essential for prediction (Cressie 1991). I used either spherical or exponential semivariograms for all data given by the following equations;

$$\gamma(h;\theta) = \begin{Bmatrix} 0, & h = 0 \\ C_0 + C_s\ ((3/2)(\|h\|/\alpha_s) - (1/2)(\|h\|/\alpha_s)^3), & 0 < \|h\| \le \alpha_s \\ C_0 + C_s, & \|h\| \ge \alpha_s \end{Bmatrix} \quad (4.3)$$

$$\gamma(h;\theta) = \begin{pmatrix} 0, & h = 0 \\ C_0 + C_e(1 - \exp(-\|h\|/\alpha_e)), & h \neq 0 \end{pmatrix} \quad (4.4)$$

These spatial covariance models are defined by three essential parameters: the nugget (C_0) (indicating the variance not explained by the spatial model), the sill C_s (indicating the variance explained by the spatial model) and the range α (distance beyond which spatial autocorrelation is no longer significant). After computation of the semivariograms for each of the respective variables, the spatial models were used with block kriging to predict the value of algal cover and stand heights for grid cells of size 10 m by 10 m for 2006 surveys and 20 m by 20 m for 2007 surveys.

Exploratory data analysis was conducted on the acoustic data prior to spatial modeling using scatter plots, histograms and correlations to assess the presence of possible predictive trends. With a sampling frequency of 8 Hz, a summary cycle output every 16 pings, a full day of surveying (0600 to ~ 2000 hrs) yielded an average of 13,000 to 19,000 individual geo-referenced datum reports. Unlike the data from the 2005 surveys, the frequency distributions of the percent cover and stand height variables derived by acoustic analysis were strongly overdispersed. This was likely a function of 1) the increased ping frequency that generated more data, 2) the change in survey design which collected more data at deeper depths where detection of *Cladophora* with acoustics was difficult, and 3) surveys at times of the year when biomass was not maximal often generated a large number of zeros. To rectify this, the geo referenced data were condensed by averaging records within 5 m of one another, thereby increasing the average spacing of data from 3-5 m apart to 8 to 13 m apart. This was primarily done to reduce the computational effort involved in solving large kriging matrices, but also to reduce the degree of overdispersion of the acoustic variables (percent cover and height).

Experimental semivariograms were computed using the robust estimator (Cressie and Hawkins 1980) with a 10 m lag for interpolation onto grids of 10 m by 10 m for 2006 surveys, and 20 m by 20 m grid for 2007 surveys. Preliminary comparisons suggested that the classical semivariogram estimator did not perform as well as the robust estimator (data not shown), though I could not determine a threshold for use of one or the other. I computed both directional

semivariograms by limiting all point pairs within a directional tolerance (0° to 135°, 45° ± 22.5° step tolerance) in addition to the omni-directional semivariogram to assess the degree of anisotropy.

Relationships between depth and percent cover when biomass was detectable with acoustics (in the summer months) for all years (2006, 2007) were moderately strong and generally linear in nature (r^2 0.3 to 0.7). Strong correlations were evident between percent cover and height ($r^2 > 0.64$) when coverage was moderate or high. To account for these potentially non-stationary processes, I performed block regression kriging on percent cover using depth as a predictor. Briefly, a Generalized Linear Model (GLM; Gotway and Stroup 1997) was used with a quasi-Poisson family of probability distributions due to the over dispersion in the data distribution. The GLM model trend was subtracted from the percent cover data and simple kriging (SK) was performed on the residuals (i.e. the mean of the residuals should be "0"). The GLM model trend was then added back to the kriged residuals to generate the predicted surface map. Algal stand height was interpolated using KED, with percent cover as a predictor. Bathymetric grids for each survey site were generated using universal kriging (coordinates as predictors) of the acoustically determined bottom depth from the individual surveys. All bathymetric survey grids were clipped using the lake shorelines and the 10 m depth contour as downloaded from the National Geophysical Data Center Great Lakes Bathymetry ArcIMS web server (http://map.ngdc.noaa.gov/website/mgg/greatlakesbathy/viewer.htm). All exploratory data analysis, regression and variogram modeling, and subsequent kriging computations were performed using the statistical software R (R Core Development Team 2007) and the R package *gstat* (Pebesma 2004).

4.3.5 Nuisance *Cladophora* biomass and association to nutrient sources

Kriged surfaces of percent cover and stand height were used to estimate *Cladophora* biomass as outlined in Chapter 3. Approximate standard errors of biomass estimates were computed following Heuvelink (2002). *Cladophora* polygons were created from the estimated biomass maps using the following procedure. The *Cladophora* biomass grids were imported into SAGA-GIS (http://www.saga-gis.org/en/index.html) and contours delineating estimated *Cladophora* biomass were created at intervals of 50 g m^{-2}, starting at 50 g m^{-2}. Each contour line was then closed, converted to a polygon, and the centroid (center of mass) of the polygon determined. For each date where polygon centroids were successfully computed, proximity to the nearest waste water treatment plant outfall, storm sewer and tributary mouth were determined by computing the minimum Euclidean distance to the nearest respective potential nutrient source.

Spatial associations between *Cladophora* polygon centroids and proximity to potential nutrient sources were assessed using a partial Mantel test. The partial Mantel test is a nonparametric partial regression approach based on dissimilarity matrices of the predictor and response variables (Smouse et al. 1986). The advantage of the partial Mantel test is that it can explicitly account for spatial autocorrelation in both predictor and response variables as well as inter-correlations among possible predictor variables. While Mantel and partial Mantel tests have been used for causal modelling (Legendre and Trousselier 1989), in this study, results from the partial Mantel tests served to test alternative hypotheses governing the spatial patterns of excessive *Cladophora* growth (e.g., polygon centroids), environmental controls (e.g., depth and bathymetric slope) and proximity to potential nutrient sources (tributary mouths, storm sewers and municipal outfalls). The locations of tributary mouths were determined by selecting the coordinates where the tributary entered the lake from the Ontario Basic Mapping ArcIMS data layer (http://www.geographynetwork.ca/website/obm/viewer.htm). Storm sewer and municipal outfall locations for Oakville and Pickering were provided by the Ontario Ministry of Environment (Griffiths 1990) and Gary Bowen (Toronto Region Conservation Authority).

Euclidean distances were computed for the geographic distance matrix (Universal Transverse Mercator Zone 17 N, NAD 1983) as well as the matricies for depth, slope and distances to nutrient sources. The Manhattan distance was used to construct the distance matrix for the biomass polygon centroids since these were effectively converted to classes of 50 g m^{-2} intervals. Partial Mantel tests were performed using the package *ecodist* (Goslee and Urban 2007) in the statistical software "R" (R Core Development Team 2007). The significance of the partial Mantel tests was assessed using a permutation procedure using 10,000 permutations (Jackson and Somers 1989) as outlined in Legendre (2000). The p value was adjusted for the number of tests conducted (e.g., Bonferroni adjustment, $\alpha/6 = 0.0083$).

4.3.6 Statistical Analyses

Early season surface water sampling was assessed using Kendall's τ to detect trends as a function of distance from source. Source locations were the same as outlined above. Distances were computed as the minimum Euclidean distance from the nearest respective source. For the remainder of the water chemistry data, analysis was performed using two-way ANOVA (station depth and date as factors) on $\log_{10}$ transformed variables for each year. Transects were treated as replicates, since the null hypothesis for these tests was that there would be no differences in parameter concentrations across the range of depths (i.e., distance from shore). If the interaction term (e.g., depth x date) was not significant, Tukey's multiple comparison procedure was used to

compare within the main effects. If the interaction term was significant, multiple comparison tests were done at the individual level (e.g., date x depth) to assess where the patterns changed. All statistical calculations were performed using the base stats package in 'R' (R Core Development Team 2007). Separate two way ANOVAs were run for each site due to the differences in sampling frequency.

4.4 Results

4.4.1 Physical and Chemical conditions during thermal bar at Oakville

The early season sampling in 2006 (April 13 to April 27) was designed to reveal spatial patterns in water quality at the Oakville site during the period of spring runoff and thermal bar formation. Although a CTD failure prevented a complete characterization of the water column at all sampling sites on each date, based on the profiles collected surface temperatures along the shoreline range between 5.5 °C and 10 °C (data not shown), and suggested that all of the sites (within 1 m to 15 m depth) were on the inside of the thermal bar. Concentrations of total phosphorus (TP) ranged from 4.75 µg L^{-1} to 13.95 µg L^{-1} and did not show a strong relationship with distance from the nearest tributary (Figure 4.2a, Kendall's $\tau = 0.04$, $p = 0.59$). No relationships were observed between total dissolved phosphorus (TDP) or soluble reactive phosphorus (SRP) concentrations and distance to a tributary (Figure 4.2b and c, Kendall's $\tau = 0.002$, $p = 0.51$ and $\tau = 0.04$, $p = 0.73$ respectively).

In contrast to phosphorus concentrations, a stronger influence of distance to tributaries was observed for chloride (Cl^-), nitrate (NO_3^-), as evidenced by their negative relationship with distance from the nearest tributary (Figure 4.2 d and e, Kendall's $\tau = -0.27$, $p<0.0001$, $\tau = -0.25$, $p<0.0001$). Total suspended solids (TSS) (Figure 4.2 f) appeared to also decline as distance from tributaries increased, however the relationship was not significant (Kendall's $\tau = -0.02$, $p = 0.78$), but this may reflect the changing nature of the turbidity plume between sampling dates, as it was observed to be flowing northward on two of the three sampling dates. Of the tributaries along the section of surveyed coastline, 16 Mile Creek appeared to generate the strongest signal compared to the smaller tributaries, and the zone of influence appeared to extend upwards of 500 m away.

No significant spatial associations were found for the two municipal water treatment plant outfalls (Figure 4.3a through f). Kendall's correlation analyses were all non significant for TP, SRP, Cl^-, NO_3^- and TSS ($p> 0.2$). A marginally significant association was observed for TDP (Kendall's $\tau = -0.18$, $p = 0.11$), but this appears to be the result of a single sample (Figure 4.3b).

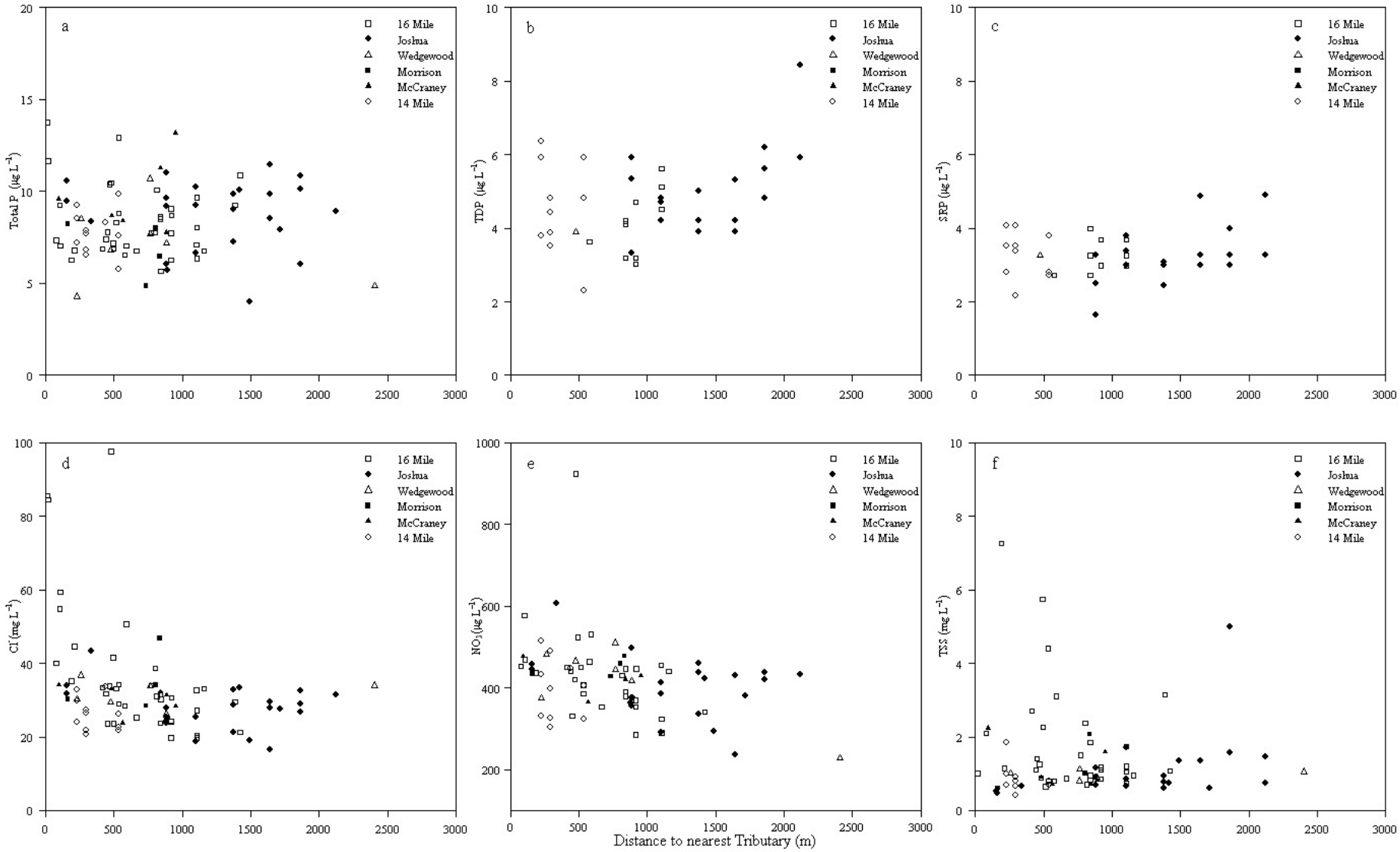

Figure 4.2. Scatter plots of a) Total Phosphorus (TP; µg L^{-1}) , b) Total dissolved Phosphorus (TDP; µg L^{-1}), c) Soluble Reactive Phosphorus (SRP; µg L^{-1}), d) Chloride (Cl; mg L^{-1}), e) Nitrate (NO_3; µg L^{-1}), and f) Total suspended solids (TSS; mg L^{-1}) as a function of distance to the nearest tributary mouth along the Oakville shoreline. Note: Data collected 13 April 2006 to 27 April 2006. Distance here is computed as the minimum Euclidean distance.

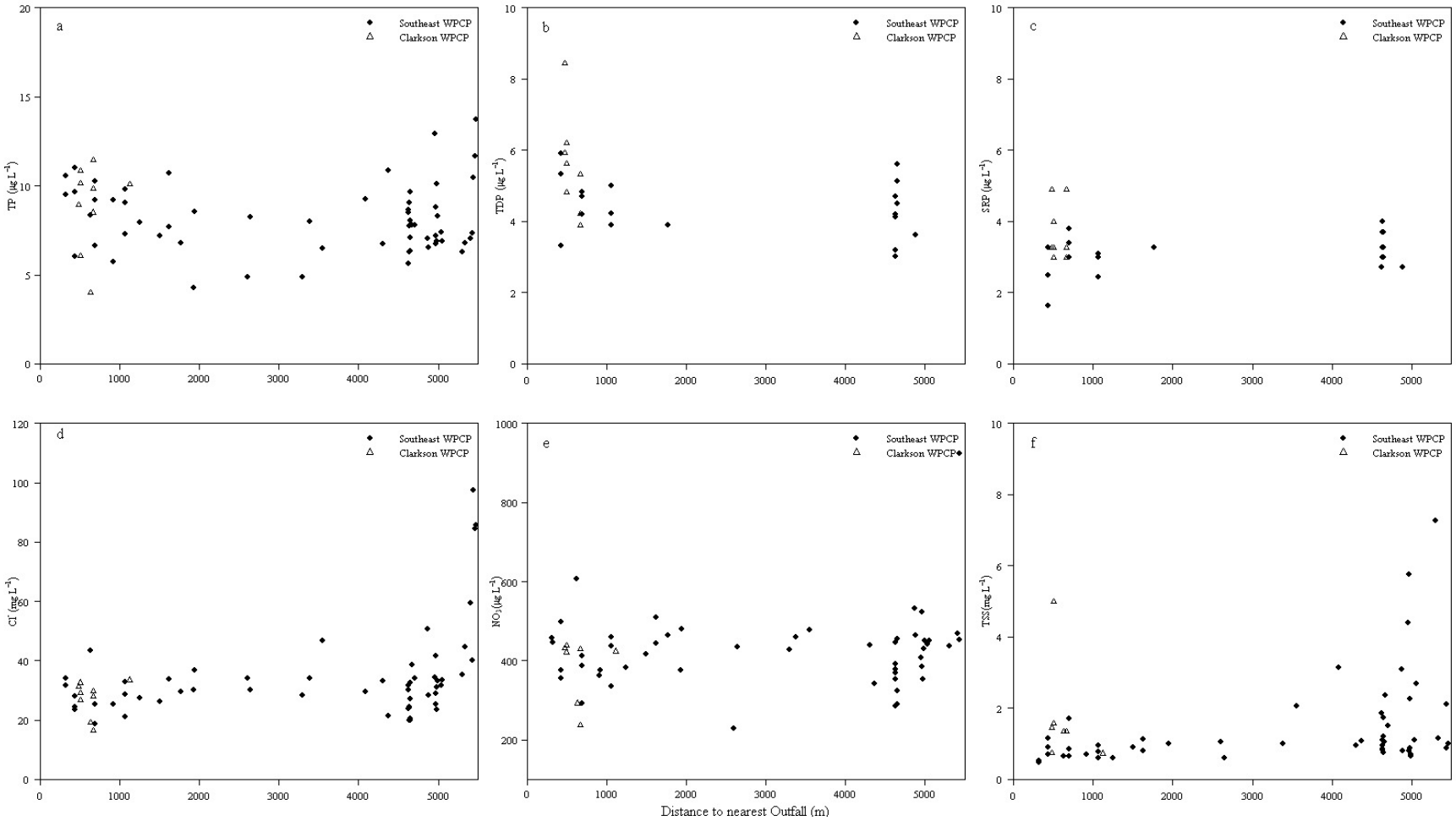

Figure 4.3. Scatter plots of a) Total Phosphorus (TP; µg L^{-1}) , b) Total dissolved Phosphorus (TDP; µg L^{-1}), c) Soluble Reactive Phosphorus (SRP; µg L^{-1}), d) Chloride (Cl; mg L^{-1}), e) Nitrate (NO_3; µg L^{-1}), and f) Total suspended solids (TSS; mg L^{-1}) as a function of distance to the nearest outfall along the Oakville shoreline. Note: Data collected 13 April 2006 to 27 April 2006. Distance here is computed as the minimum Euclidean distance**.**

4.4.2 Physical and chemical conditions at Oakville during the growing season

Much of the variability in water chemistry and physical conditions is imparted by seasonal variation (Figure 4.4; Table 4.2). The effects of upwelling were clearly evident on at least two of the sampling dates as water temperatures fell from ~ 18 °C on 8 June to approximately 10 to 15 °C on 23 June and 11 July (Figure 4.4a). Total suspended solids were lowest soon after the upwelling event on 23 June, and again on 14 September when downwelling of low chlorophyll offshore water occurred (Figure 4.4b). Despite relative stability in TSS, the variability in light attenuation (kPAR) was primarily governed by depth (e.g., distance from shore; Figure 4.4c and Table 4.2), with significantly higher light attenuation always occurring at the 2 m isobath (Table 4.2). Significant seasonal variation was also observed for kPAR, with higher light attenuation in October (Table 4.2). Cl^- was also significantly related to depth and date, with higher concentrations observed closer to shore (Figure 4.4d; Table 4.2), particularly during the early part of the season (8 May and 8 June; Table 4.2). Concentrations of chlorophyll a displayed a markedly reverse pattern; significantly higher concentrations were observed at the 10 m stations compared to the 2 and 5 m stations (Figure 4.4e; Table 4.2), but seasonal variation was much larger than the variation among depth (Table 4.2). Concentrations of TP did not vary across the range of station depths sampled (Table 4.2) but did show appreciable seasonal variation, with the highest concentrations observed during September and October (Figure 4.4f; Table 4.2). TDP and SRP followed much the same pattern as TP (Figure 4.4g and h) with appreciable seasonal variation in TDP and SRP. The interaction term in the ANOVA for SRP was significant ($p<0.05$), and is likely a result of the higher concentrations closer to shore in September and October (Figure 4.4h). NO_3^- showed a significant seasonal decline until October (Figure 4.4i; Table 4.2) and did not vary significantly across the range of station depths (Table 4.2).

Although seasonal patterns strongly influenced the concentrations of chemical parameters during this study, some spatial patterns are noticeable. Variability in surface temperatures was indistinguishable across the four transects (Figure 4.5a). TSS did not show consistent patterns across transects at Oakville (Figure 4.5b), but kPAR appeared to show the greatest variability at transects closest to the major tributary (16 Mile Creek) for the study region (transects OA1 and OA2) (Figure 4.5c). Spatial trends in Cl^- (Figure 4.5d) and chlorophyll a concentrations (Figure 4.5e) were not evident across transects, but displayed diverent patterns with distance from shore; Cl^- was generally higher at 2 m sites, while for chlorophyll a, clear increases with distance from shore are apparent (Figure 4.5d). TP concentrations were most variable at the 2 m site on transect OA1 and the 5 and 10 m sites on transect OA2 (Figure 4.5e). Similar spatial patterns were evident

for TDP and SRP (Figure 4.5g and h). These transects bracket the major tributary to this study site (16 Mile Creek), and the increased variability at these transects may reflect the periodic reversals of along shore currents where the tributary plume from 16 Mile Creek is discharged and mixed. Comparable spatial patterns were not observed for NO_3^- concentrations (Figure 4.5i).

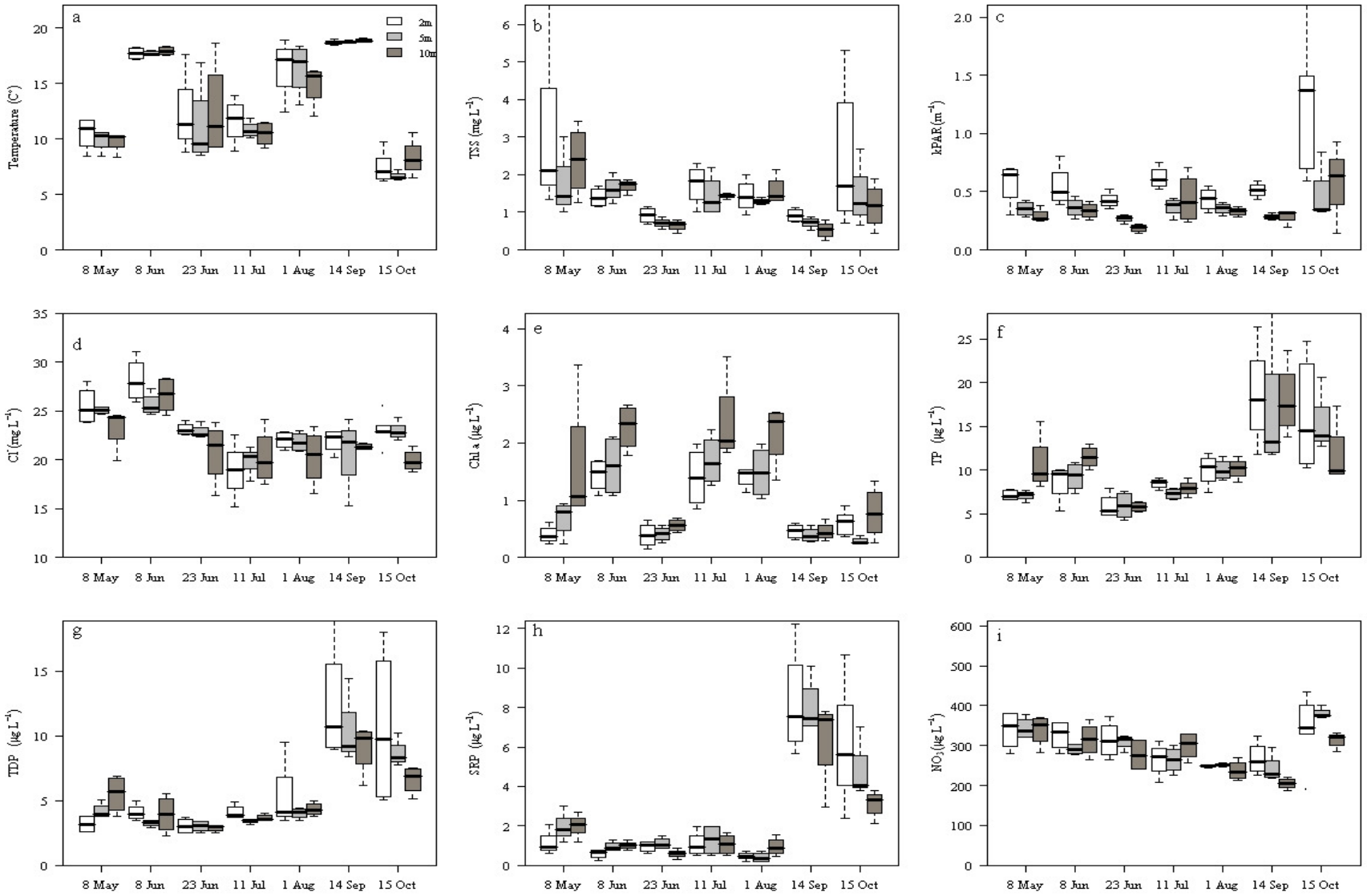

Figure 4.4. Seasonal boxplots of a) surface temperature (°C), b) TSS (mg L^{-1}), c) light attenuation (kPAR; m^{-1}), d) chloride (Cl; mg L^{-1}), e) Chlorophyll a (Chl a; µg L^{-1}), f) total phosphorus (TP; µg L^{-1}), g) total dissolved phosphorus (TDP; µg L^{-1}), h) soluble reactive phosphorus (SRP; µg L^{-1}) and i) nitrate (NO_3; µg L^{-1}) for the 2006 study at Oakville. Legends as in panel a).

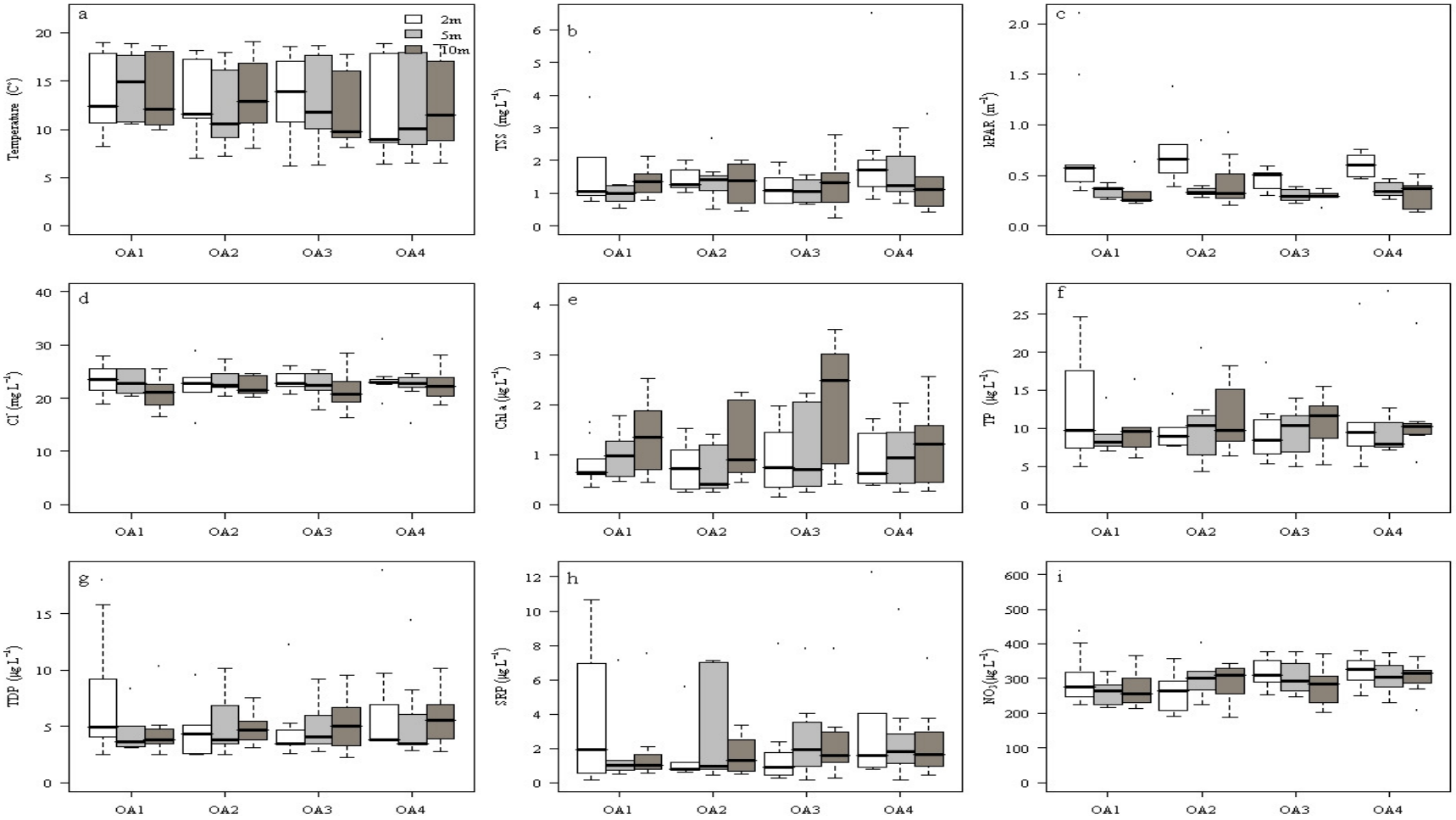

Figure 4.5. Spatial boxplots of a) surface temperature (°C), b) TSS (mg L^{-1}), c) light attenuation (kPAR; m^{-1}), d) chloride (Cl; mg L^{-1}), e) Chlorophyll a (Chl a; µg L^{-1}), f) total phosphorus (TP; µg L^{-1}), g) total dissolved phosphorus (TDP; µg L^{-1}), h) soluble reactive phosphorus (SRP; µg L^{-1}) and i) nitrate (NO_3; µg L^{-1}) for the 2006 study at Oakville. Legends as in panel a).

Table 4.2. Results from the two-way ANOVA for 2006 Oakville surveys. Note: superscripts on multiple comparison tests indicate not significantly different at the p <0.05 level.

Variable	*Factor*	*df*	*F*	*p*	*Post*	*hoc*	*tests*				
TSS	Depth	2	2.73	0.07							
	Date	6	10.78	<0.001	8 May^{b}	8 Jun^{b}	23 Jun^{a}	11 Jul^{b}	1 Aug^{b}	14 Sept^{a}	15 Oct^{b}
	Date x Depth	12	0.78	0.66							
kPAR	Depth	2	24.25	<0.001	2	5^{a}	10^{a}				
	Date	6	7.83	<0.001	8 May^{a}	8 Jun^{a}	23 Jun^{a}	11 Jul^{a,b}	1 Aug^{a}	14 Sept^{a}	15 Oct^{b}
	Date x Depth	12	0.73	0.71							
Cl^-	Depth	2	3.48	<0.05	2^{a}	5^{a,b}	10^{b}				
	Date	6	14.05	<0.001	8 May^{a}	8 Jun^{a,b}	23 Jun^{b,c}	11 Jul^{d}	1 Aug^{c,d}	14 Sept^{c,d}	15 Oct^{b,c,d}
	Date x Depth	12	0.94	0.51							
Chl a	Depth	2	12.21	<0.001	2^{a}	5^{a}	10				
	Date	6	34.74	<0.001	8 May^{a}	8 Jun^{b}	23 Jun^{a}	11 Jul^{b}	1 Aug^{b}	14 Sept^{a}	15 Oct^{a}
	Date x Depth	12	1.59	0.11							
TP	Depth	2	0.83	0.44							
	Date	6	29.42	<0.001	8 May^{a}	8 Jun^{a}	23 Jun	11 Jul^{a}	1 Aug^{a}	14 Sept^{b}	15 Oct^{b}
	Date x Depth	12	1.35	0.22							
TDP	Depth	2	0.88	0.41							
	Date	6	37.42	<0.001	8 May^{b}	8 Jun^{a,b}	23 Jun^{a}	11 Jul^{a,b}	1 Aug^{a,b}	14 Sept^{c}	15 Oct^{c}
	Date x Depth	12	1.46	0.16							
SRP	Depth	2	0.68								
	Date	6	51.99								
	Date x Depth	12	2.22	<0.05							
NO_3^-	Depth	2	1.25	0.29	8 May^{a}	8 Jun^{a,b}	23 Jun^{a,b}	11 Jul^{b,c}	1 Aug^{c}	14 Sept^{c}	15 Oct^{a}
	Date	6	13.48	<0.001							
	Date x Depth	12	1.26	0.26							

4.4.3 Physical and chemical conditions at Pickering during the growing season

Much like at Oakville, upwelling appeared to be a prominent feature here based on surface temperatures (Figure 4.6a). Compared to Oakville, significant depth dependent variability in TSS was observed at Pickering, with higher concentrations at the 2 m stations (Figure 4.6b; Table 4.3). kPAR at Pickering transects nearly replicated the pattern for TSS, with highest attenuation observed at the shallow 2 m sites (Figure 4.6c; Table 4.3). Date of sampling was also a significant determinant in light attenuation, but the seasonal variation was far less than that associated with depth (Table 4.3). Cl^- varied significantly only with date, with the highest concentrations observed in May. The effect of depth on Cl^- was only marginally significant (Figure 4.6d; Table 4.3). Chlorophyll a concentrations displayed strong seasonal variation (Figure 4.6e) but unlike Oakville did not show a significant relationship with depth (Table 4.3). Total P concentrations showed no significant relationship with depth, and only a marginally significant relationship with date (Figure 4.6f; Table 4.3). TDP and SRP varied strongly with date, but not with station depth (Figure 4.6g and h; Table 4.3), and highest values for both were recorded in October (Table 4.3). NO_3^- appeared to follow a similar seasonal decline as observed at Oakville before rebounding to higher concentrations in October (Figure 4.6i; Table 4.3).

Like Oakville, seasonal variation strongly influenced the variability in parameter concentrations through the growing season. This is further supported by data from offshore reference stations (ranging in depth from 15 m to 40 m) that displayed comparable patterns for nearly all water chemistry variables (data not shown). Despite this, some spatial patterns were evident at Pickering, and several of these differed from the pattern observed at Oakville. Surface temperatures did not appear to vary systematically by transect (Figure 4.7a), somewhat suprising given the proximity of transect PI2 to the warm water discharge at PNGS, and the proximity of transects PI1, PI3 and PI4 to major tributaries (Rouge River, and Duffins Creek respectively). TSS and kPAR were distinctly elevated at 2 m sites at transects PI1 PI3 and PI4 (Figure 4.7b and c). Although re-suspension of sediment or along shore transport of eroded material from the bluffs west of the study site can contribute to high turbidity here, the high turbidty is most likely attributable to high suspended sediment loads from the tributaries. Transect PI2 did not show the same variation in either TSS or kPAR, and the substratum at transect PI4 is comprised of > 90% rock. Both these observations can be explained by a predominantly eastward migration of the turbidity plumes. Despite evidence that both the Rouge River and Duffins Creek imparted significant suspended sediment signals at near shore sites, Cl^- concentrations were frequently higher at the 2 m site for transect PI1 (Figure 4.7d), and may reflect differing degrees of

urbanization within the separate watersheds. A similar pattern was observed for chlorophyll a (Figure 4.7e) and may be a result of the marsh near the outflow of the Rouge that can contribute phytoplankton to transect PI1 during high flow periods (spring or during heavy precipitation events). TP concentrations were also generally elevated at transect PI1, but these concentrations were not significantly greater than those measured at the other transects further east. The patterns of spatial variability (greater variation at transects PI2 and PI3 at all depths) do suggest that tributaries can contribute considerably to TP concentrations (Figure 4.7f). TDP was most variable at transects PI2 and PI3 (Figure 4.7g). Whether this is a result of the proximity of these stations to the Duffins Creek WWTP outfall is not known, but Duffins Creek itself cannot be ruled out. In contrast to TP and TDP, SRP varied relatively little at all transects (Figure 4.7h) except for 22 October when concentrations increased dramatically (Figure 4.6h). Much like Oakville, concentrations of NO_3^- did not display great spatial variation among transects (Figure 4.7i).

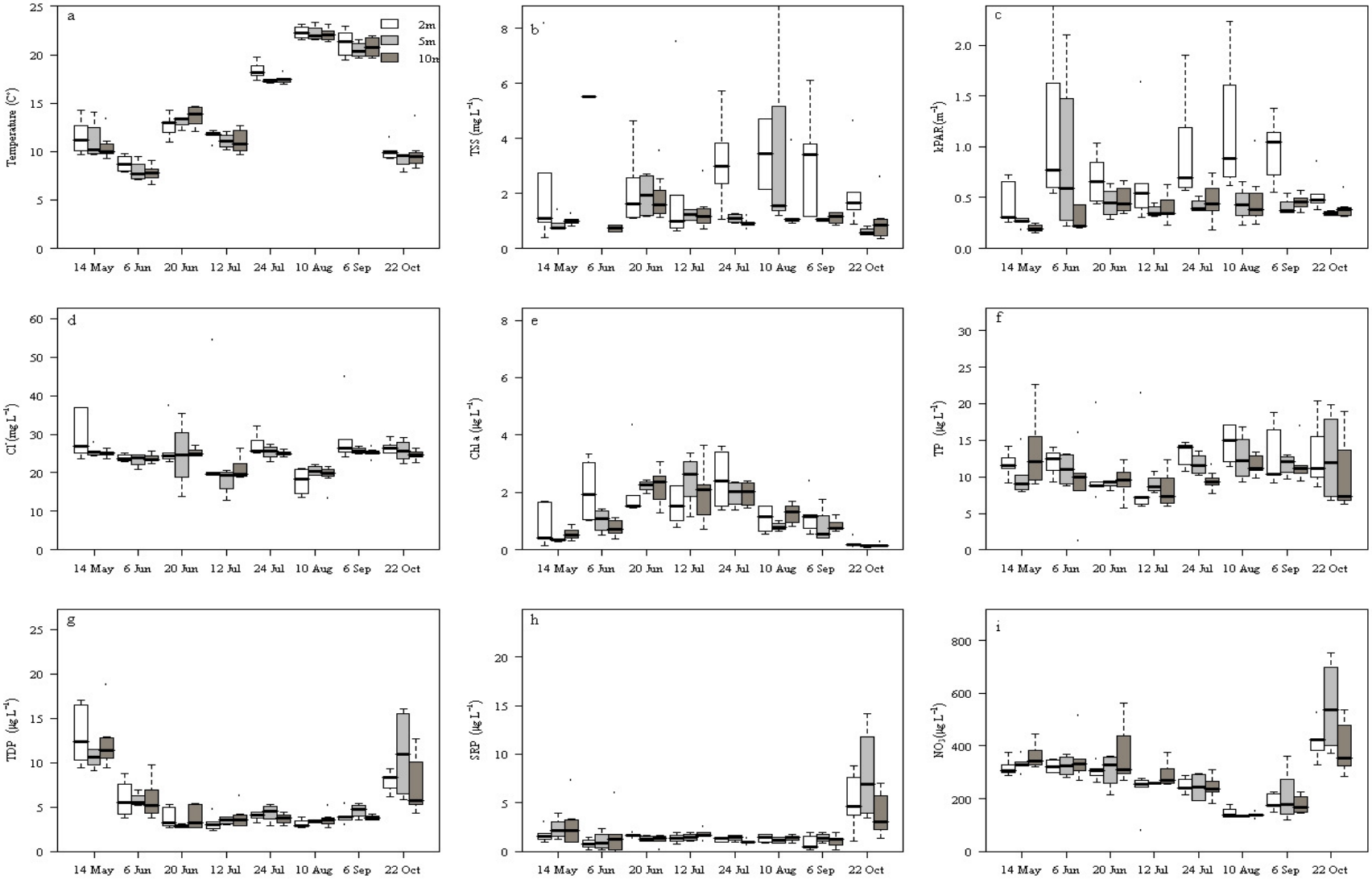

Figure 4.6. Seasonal boxplots of a) surface temperature (°C), b) conductivity (µS cm^{-1}), c) light attenuation (kPAR; m^{-1}), d) chloride (Cl; mg L^{-1}), e) Chlorophyll a (Chl a; µg L^{-1}), f) total phosphorus (TP; µg L^{-1}), g) total dissolved phosphorus (TDP; µg L^{-1}), h) soluble reactive phosphorus (SRP; µg L^{-1}) and i) nitrate (NO_3; µg L^{-1}) for the 2007 surveys at Pickering. Legends as in panel a).

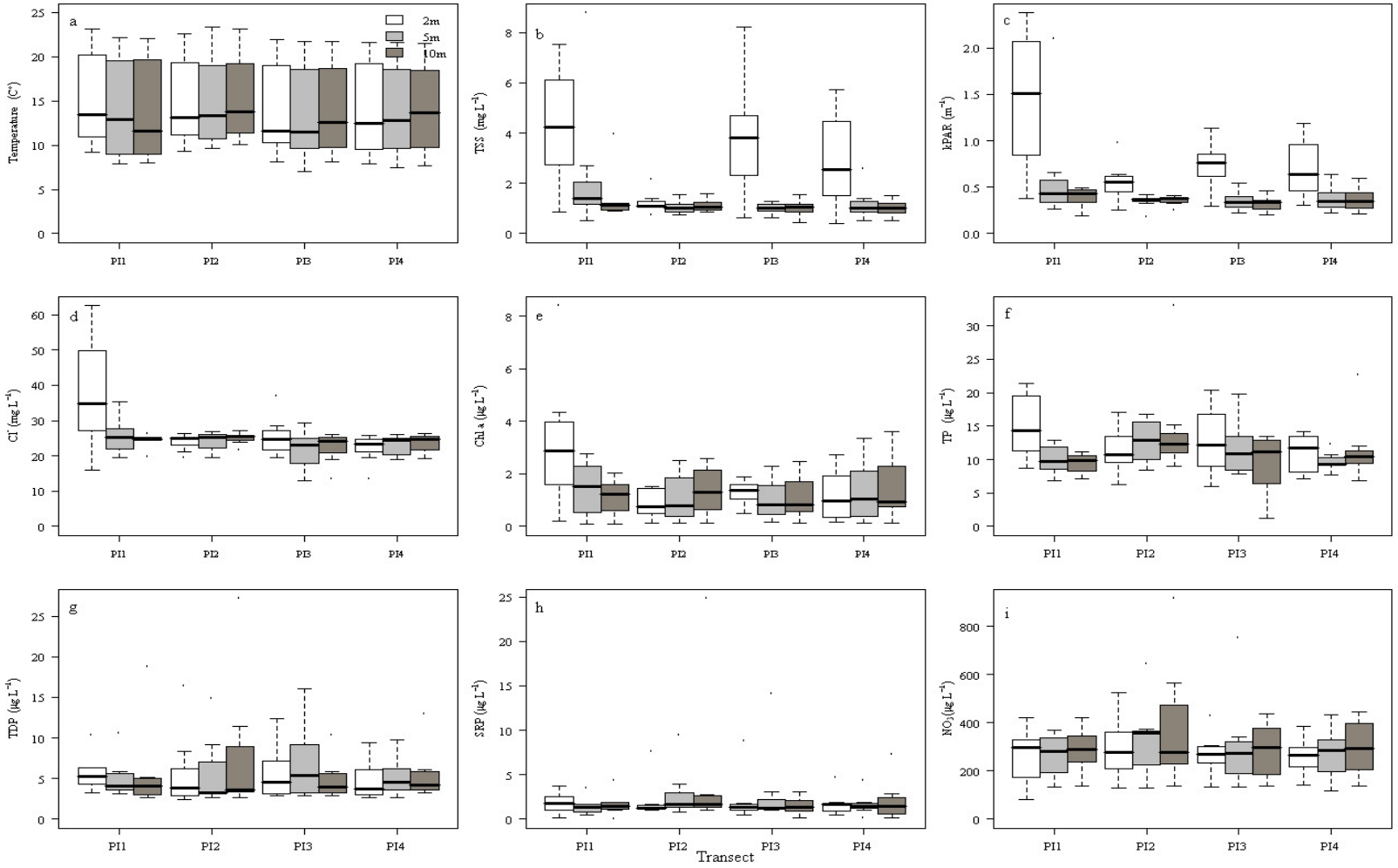

Figure 4.7. Spatial boxplots of a) surface temperature (°C), b) TSS (mg L^{-1}), c) light attenuation (kPAR; m^{-1}), d) chloride (Cl; mg L^{-1}), e) Chlorophyll a (Chl a; µg L^{-1}), f) total phosphorus (TP; µg L^{-1}), g) total dissolved phosphorus (TDP; µg L^{-1}), h) soluble reactive phosphorus (SRP; µg L^{-1}) and i) nitrate (NO_3; µg L^{-1}) for the 2007 surveys at Pickering. Legends as in panel a).

Table 4.3. Results from the two way ANOVA for 2007 Pickering surveys. Note: superscripts on multiple comparisions tests indicate not significantly different at the p <0.05 level.

Variable	*Factor*	*df*	*F*	*p*	*Post*	*hoc*	*Tests*					
TSS	Depth	2	13.39	<0.001	2[a]	5[b]	10[b]					
	Date	7	2.13	0.057								
	Date x Depth	13	0.78	0.67								
kPAR	Depth	2	31.26	<0.001	2[a]	5[b]	10[b]					
	Date	7	3.33	<0.005	14 May[a]	6 Jun[b]	20 Jun[b]	12 Jul[a,b]	24 Jul[b]	10 Aug[b]	6 Sept[b]	22 Oct[a,b]
	Date x Depth	13	0.66	0.80								
Cl^-	Depth	2	2.84	0.06								
	Date	7	4.98	<0.001	14 May[a]	6 Jun[a,b,c]	20 Jun[a,b]	12 Jul[b,c]	24 Jul[a,b]	10 Aug[c]	6 Sept[a,b]	22 Oct[a,b]
	Date x Depth	13	0.73	0.73								
Chl a	Depth	2	2.89	0.06								
	Date	7	39.16	<0.001	14 May[a]	6 Jun[b,c]	20 Jun[c]	12 Jul[c]	24 Jul[c]	10 Aug[b]	6 Sept[a,b]	22 Oct[d]
	Date x Depth	13	0.89	0.57								
TP	Depth	2	1.58	0.21								
	Date	7	1.88	0.08								
	Date x Depth	13	0.69	0.77								
TDP	Depth	2	0.19	0.82								
	Date	7	32.63	<0.001	14 May[b]	6 Jun[a]	20 Jun[b]	12 Jul[b]	24 Jul[b]	10 Aug[b]	6 Sept[a,b]	22 Oct[c]
	Date x Depth	13	0.74	0.73								
SRP	Depth	2	0.16	0.85								
	Date	7	19.25	<0.001	14 May[d,e]	6 Jun[a]	20 Jun[b,c,d]	12 Jul[b,c,d]	24 Jul[b,c]	10 Aug[b,c,d]	6 Sept[a,b]	22 Oct[e]
	Date x Depth	13	0.63	0.83								
NO_3^-	Depth	2	1.57	0.21								
	Date	7	29.89	<0.001	14 May[b,c]	6 Jun[b]	20 Jun[b,c]	12 Jul[a,b]	24 Jul[a,b]	10 Aug	6 Sept[a]	22 Oct[c]
	Date x Depth	13	0.80	0.66								

4.4.4 Structural analysis and semivariograms

By repeating acoustic surveys over a period of time at the two survey sites, changes in the spatial structure of *Cladophora* growth can be appreciated on a seasonal dynamic. Semi-variogram models and associated parameters for each survey where detection and characterization of *Cladophora* with acoustics was successful are summarized in Table 4.4. Initial modeling of directional semivariograms for the Oakville surveys indicated strong anisotropic behavior at 45°. This is geometric anisotropy expressing the same degree of spatial continuity for different ranges. In its simplest form, this is akin to elliptically shaped zones wherein the data values are correlated; that is, zones that are "stretched" in the direction of maximum range. This elliptical "stretching" of the spatial correlation may be due inpart to the survey design (transects running approximately 45°, e.g. parallel to shore) but also may reflect a strong influence of bottom depth (e.g., light availability) in structuring algal growth patterns. Directional semivariograms computed for the Rouge River site were also anisotropic at 45°, despite the survey transects having a more regular grid pattern than truly parallel to shore. In contrast, directional semivariograms at the main Pickering site were not strongly anisotropic, but surveys toward the latter part of the summer (e.g., July and August) generated semivariograms that displayed weak anisotropy at 90° (parallel to shore). While also potentially resulting from primarily shore parallel transects or the effect of depth (e.g., light availability), the weaker anisotropy here may be due to a more diverse substratum (e.g., sand, gravel, silt) in the shallow areas where shoreline irregularities allow for deposition of softer susbtrates in protected locations that do not typically support *Cladophora* attachment. Furthermore, areas that are structurally complex (e.g., characterized by large boulders and rapidly fluctuating bottom depths) pose diffilculties for acoustic detection of *Cladophora* due to the interaction of the acoustic beam with a complex substrate. These features (diverse substratum composition or substratum complexity) were generally not present at the Oakville site, but did occur in areas near at the main portion of the Pickering site, particularly around the Duffins WWTP (sand and presence of large boulders) and from PNGS eastward to Duffins Creek (predominantly sand bottom with scattered boulders). Semivariograms for percent cover from the main Pickering site indicated the presence of mild non-stationarity. This increased toward August 8, and is due to the large area of macrophyte growth that developed over the summer in outer Frenchman's Bay (see Figure 4.8 and Figure 4.12 to Figure 4.19). No improvement was observed by including easting (e.g., X coordinate) as a coavariate in the semivariogram model (data not shown).

Semivariogram model parameters at Oakville were generally similar across all three surveys. The range parameter varied little, and the sill reached a maximum on 11 July before declining on 1 August for both percent cover and height residuals. The high sill on 11 July for both percent cover and height residuals indicates that the greatest variability was observed on this date. The degree of spatial dependency ($1 - C_0 / C_0 + C$) for percent cover and height residuals declined from 11 July to 1 August, and is consistent with a decline in spatial variability, perhaps as biomass is gradually detached from the lakebed. At Pickering, semivariogram parameters were generally similar to those observed at Oakville, but displayed greater variability, perhaps owing to a more frequent sampling interval (bi-weekly as opposed to monthly). The higher nugget variance and sill values observed consistently at Pickering were likely due to the presence of macrophytes within the survey area growing despositional areas dominated by soft substrate (e.g., outer Frenchman's Bay; see figures below). The influence of macrophytes is much more evident in the sill parameter for the height residuals, which displayed a consistent increase from the first survey (11 June) to the last (8 August) to values far exceeding those observed at Oakville. The decline in spatial dependence that was observed at Oakville was not observed at Pickering (Table 4.4), because much of the *Cladophora* biomass had yet to slough from the lakebed, but also because areas of macrophyte growth continued to increase through the study period. Major sloughing at Pickering occurred on 9 August, the day after the acoustic survey (C. Gregoris, Ontario Power Generation, Picking Nuclear, personal communication).

Semivariogram models for the smaller survey area at the Rouge River outflow featured a similar if not smaller range of autocorrelation, but a much higher nugget variance and sill than observed at Oakville or the main Pickering site (Table 4.4). This is characteristic of data that present a highly clustered patch surrounded by areas with little variability, which at this site was induced by large areas characterized by sand substrate, which was not suitable for attachment of *Cladophora*. Although not directly comparable with parameters from the Pickering site, the temporal pattern of semivariogram parameters at the Rouge River site suggested that height (e.g., a proxy of biomass) peaked on July 17, approximately 2 weeks prior to that at the Pickering site.

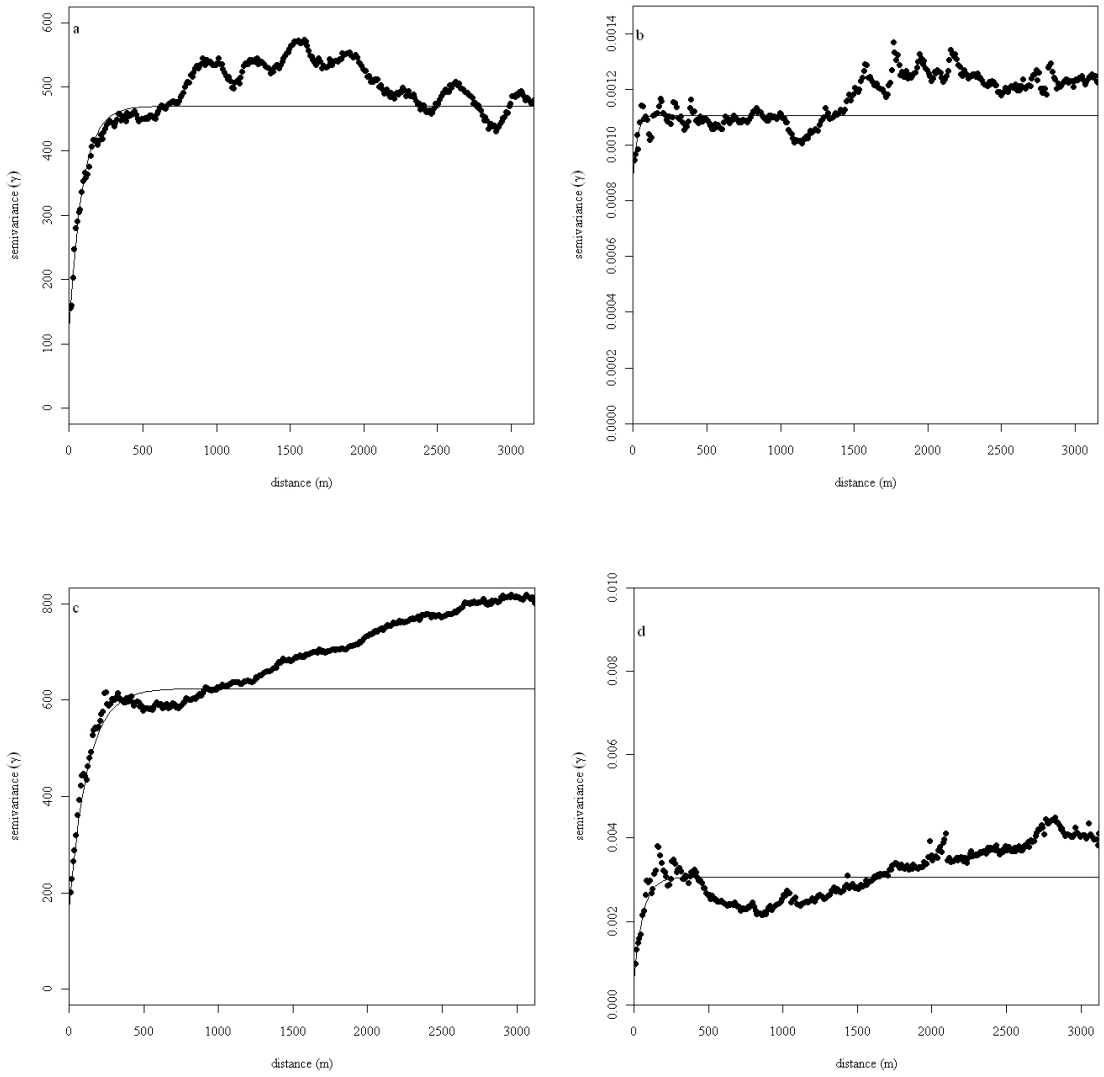

Figure 4.8. Sample residual semivariograms for percent cover (a) and canopy height (b) at Oakville, June 23 2006 and percent cover (c) and canopy height (d) at Pickering, July 25 2007. Note the oscillation in the semivariance for percent cover at Oakville as discussed in text. Note also the difference in scale for the semivariance in the height residuals at Pickering.

4.4.5 Patterns of nuisance algal growth at Oakville

Although short tufts of *Cladophora* growth were visually observed on the lake bottom during the May 8 survey, these were clearly < 5 cm in height and far too short to be detected with acoustics. Similarly, acoustic surveys on 14 September and 15 October failed to detect *Cladophora* biomass with the acoustic unit, and observations of the lake bottom generally confirmed the substrate was devoid of significant *Cladophora* cover and the remaining filament tufts were only a few centimeters in height.

Kriged surfaces of percent *Cladophora* cover, *Cladophora* stand height, estimated biomass and approximate biomass standard errors for three of the survey dates (23 June, 11 July and 1 August) when *Cladophora* biomass was sufficient for successful detection and characterization with the acoustic system are presented in Figure 4.9 to **Figure 4.11**. On 23 June, percent *Cladophora* cover varied widely and exceeded 80 % in several places along the Oakville shoreline (Figure 4.9a). Expansive areas of high percent cover were observed south of 16 Mile Creek, midway between 16 Mile Creek and Morrison Creek, and between Wedgewood and Joshua Creek (Figure 4.9a). Percent *Cladophora* cover ranged between 30 and 60 % for much of the rest of the shoreline at depths < 4 m. *Cladophora* stand heights were generally < 15 cm for much of the shoreline (Figure 4.9b), but did exceed 20 cm in several areas, most notably in the three areas previously identified where *Cladophora* cover was high (Figure 4.9b). At one location, stand height exceeded 30 cm (midway between 16 Mile Creek and Wedgewood Creek) but only for a limited area (~ 800 m^2) (Figure 4.9b). Estimated biomass at this point reached a maximum of ~ 685 g m^{-2}, but for the rest of the survey area, biomass was generally estimated to be < 150 m^{-2}, and only exceeded this in areas with tall *Cladophora* stands (Figure 4.9c). The partial Mantel test revealed significant spatial associations between *Cladophora* biomass and storm sewers, as well as bathymetric slope. No spatial associations were observed for tributary mouths or municipal outfalls (Table 4.5).

On 11 July, percent *Cladophora* cover varied widely but appeared to be much more spatially variable than on 23 June, and reached values > 30 % at deeper depths (~ 6 to 7 m) (Figure 4.10a). The expansive areas with very high percent cover (e.g., > 80%) observed on 23 June had either reduced in size or to levels of percent cover < 80% (Figure 4.10a). *Cladophora* stand heights reached maximum values of 20 cm (Figure 4.10b) but these appeared to be widely scattered. Areas with very tall stands (e.g., > 30 cm) were not observed (Figure 4.10b). Estimated biomass reached > 150 g m^{-2} in some shallow areas, but several areas exceeded 50 g m^{-2} at depths up to 6 m (Figure 4.10c). Partial Mantel tests failed to find significant spatial associations

between *Cladophora* biomass and storm sewers, tributaries or outfalls, but did detect significant effects of depth (Table 4.5).

By 1 August, percent *Cladophora* cover was declining along much of the shoreline, but did remain moderately high (>60 %) at the three areas where expansive heavy cover was first observed on 23 June (**Figure 4.11**a). *Cladophora* stand heights during this survey were much more uniform, and did not exceed 15 cm (**Figure 4.11**b). Accordingly, estimated *Cladophora* biomass was generally below 100 g m^{-2} for much of the shoreline, but did exceed 100 g m^{-2} at the three areas where cover had increased relative to 11 July (**Figure 4.11**c). Partial Mantel tests again indicated that strong spatial associations between algal biomass and distance to storm sewers, but again failed to find any relationship to tributary mouths or outfalls. Interestingly, the areas where *Cladophora* cover remained high occurred in the same locations where cover was extensive on 23 June (Table 4.5).

Table 4.4. Semivariogram parameters and kriging cross validation results for 2006 and 2007 surveys. Date and site give the location of the acoustic surveys. C_0 denotes the nugget variance, C denotes the sill, and α the range (m). Sp% is the degree of spatial dependence described by the fitted semivariogram model. Model Type indicates the form of model fitted to the experimental semivariogram."Exp" denotes exponential model, and "Sph" denotes spherical model.

Site	*Date*	*Variable*	C_0	C	α	*% Sp*	*Model*
Oakville	June 23	Cover	127.3	346.31	93.98	73 %	Exp
Oakville	June 23	Height	8.8×10^{-4}	2.2×10^{-4}	113.22	20 %	Exp
Oakville	July 11	Cover	77.94	366.47	87.37	83 %	Exp
Oakville	July 11	Height	7.6×10^{-4}	3.2×10^{-4}	39.75	29 %	Exp
Oakville	August 1	Cover	90.28	119.87	90.16	57 %	Exp
Oakville	August 1	Height	7.5×10^{-4}	1.8×10^{-4}	155.06	27 %	Exp
Pickering	June 11	Cover	162.94	27.34	244.65	14 %	Sph
Pickering	June 11	Height	1.2×10^{-3}	8.7×10^{-4}	136.04	41 %	Exp
Pickering	June 22	Cover	89.03	231.86	93.25	72 %	Exp
Pickering	June 22	Height	6.3×10^{-4}	4.9×10^{-4}	52.10	44 %	Exp
Rouge Area	June 22	Cover	222.32	360.70	58.75	62 %	Sph
Rouge Area	June 22	Height	1.1×10^{-3}	3.8×10^{-4}	41.85	26 %	Exp
Pickering	July 17	Cover	132.48	433.48	52.46	76 %	Exp
Pickering	July 17	Height	8.6×10^{-4}	1.3×10^{-3}	67.05	60 %	Exp
Rouge Area	July 17	Cover	314.50	755.00	119.14	71 %	Exp
Rouge Area	July 17	Height	2.0×10^{-3}	1.7×10^{-3}	55.22	46 %	Exp
Pickering	July 25	Cover	166.54	461.37	105.51	73 %	Exp
Pickering	July 25	Height	6.0×10^{-4}	2.5×10^{-3}	58.58	80 %	Exp
Rouge Area	July 25	Cover	370.81	1003.48	116.57	73 %	Exp
Rouge Area	July 25	Height	1.4×10^{-3}	7.0×10^{-4}	47.93	33 %	Sph
Pickering	Aug 8	Cover	157.40	437.41	76.58	74 %	Exp
Pickering	Aug 8	Height	1.8×10^{-3}	1.5×10^{-2}	213.78	89 %	Exp

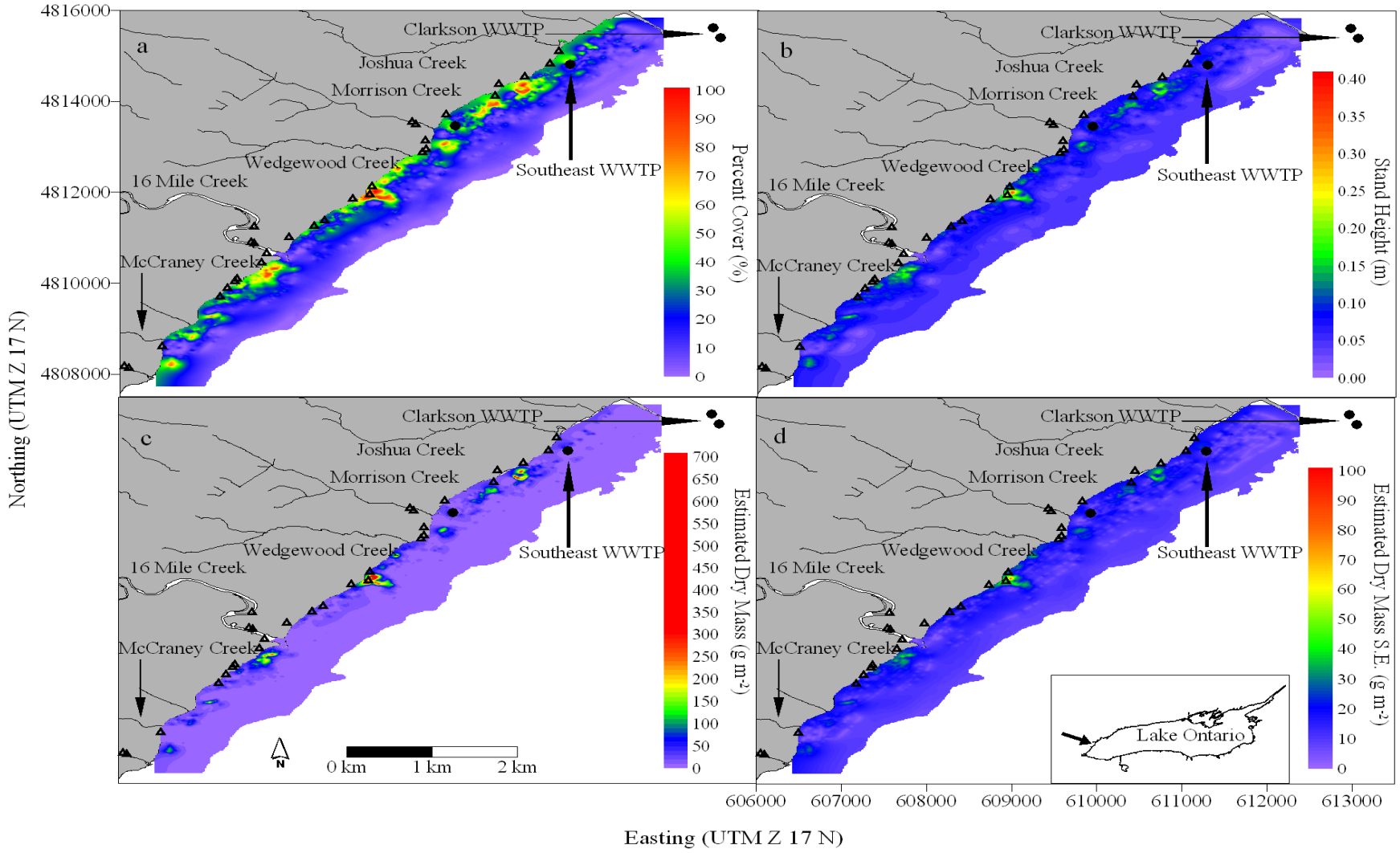

Figure 4.9. Kriged maps showing a) percent cover b) stand height c) estimated biomass, and d) approximate standard error of the biomass estimate for Oakville, June 23 2006. Note the difference in scale for biomass (panel c) in the following figures.

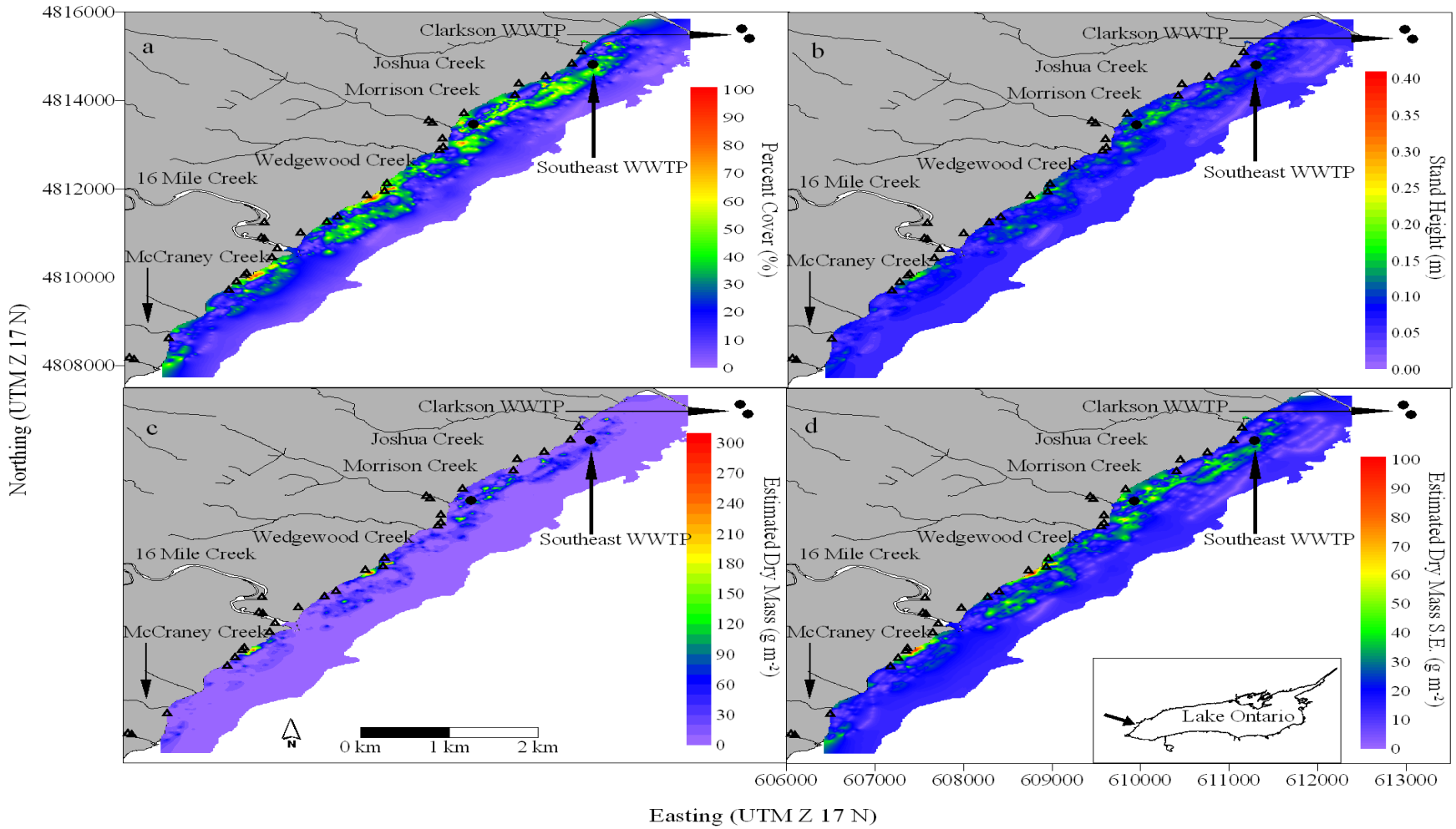

Figure 4.10. Kriged maps showing a) percent cover b) stand height, c) estimated biomass and d) approximate standard error of the biomass estimate for Oakville, July 11 2006.

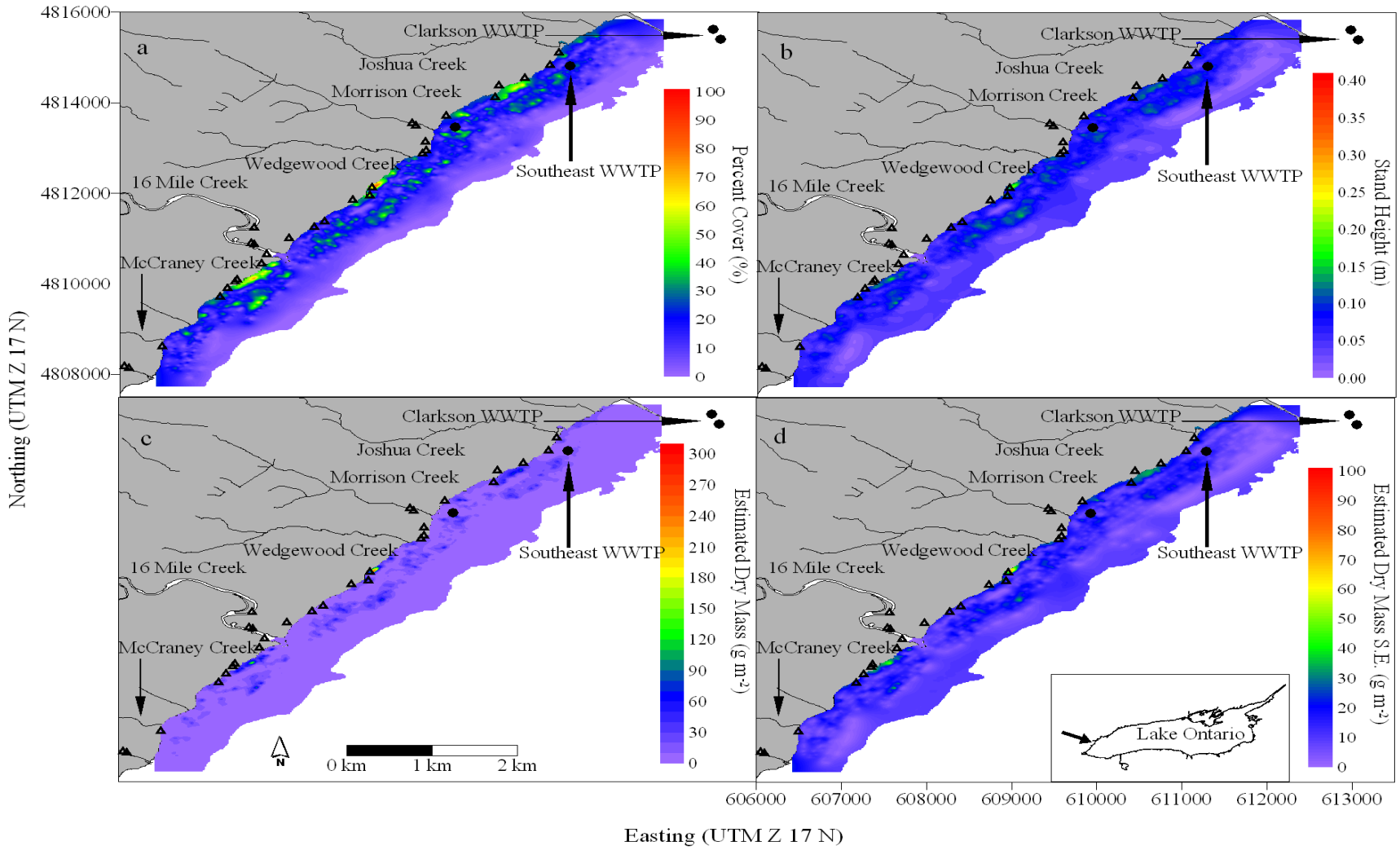

Figure 4.11. Kriged maps showing a) percent cover b) stand height, c) estimated biomass and d) approximate standard error of the biomass estimate for Oakville, August 1 2006.

Table 4.5. Results of partial Mantel tests for Oakville surveys in 2006. r_{splenv} denotes pure partial Mantel correlation coefficient, *p* denotes significance of permuted Mantel correlation coefficient, ns denotes not significant at the $p = 0.0083$ level. Covariates indicate covariate tested against while all others are paritaled out. X + Y are Easting and Northing (m) (e.g., geographic location), Sewer indicates minimum distance to storm sewer (in m), Slope indicates bathymetric slope (degrees), Tributary indicates distance to nearest tributary mouth (in m), Outfall indicates distance to nearest municipal WWTP outfall (m), and depth indicates depth of lake where polygon centroid resides (m). Number in brackets below the date denotes the number of polygon centroids available.

Covariate	*June 23*		*July 11*		*Aug 1*	
	(106)		*(167)*		*(35)*	
	r_{splenv}	*p*	r_{splenv}	*p*	r_{splenv}	*p*
X + Y	0.004	ns	0.19	0.003	0.04	ns
Sewer	0.26	0.0001	0.08	ns	0.29	0.001
Slope	0.12	0.0081	-0.06	ns	0.04	ns
Tributary	0.00	ns	0.01	ns	-0.16	ns
Outfall	-0.03	ns	-0.15	ns	0.06	ns
Depth	-0.05	ns	-0.03	ns	-0.23	ns

4.4.6 Distribution of nuisance *Cladophora* at Pickering

Attached *Cladophora* growth during the 11 June survey was generally at or below the detection limit of the acoustic system. Percent *Cladophora* cover was generally < 30 % along much of the shoreline, though small, localized areas exceeded 40 % in some areas (Figure 4.12a). These localized areas characterized by higher percent cover (e.g., 40 – 50 %) and stand height (e.g., 10-15 cm) were observed near the outflow of Carruthers Creek, the thermal discharge of PNGS and the inner Frenchman's Bay (Figure 4.12a and b). Some detached algal material was observed in the shallow water on sandy substrate, but this was later confirmed to be *Spirogyra*. Based on inspection of the echograms and underwater video, the area in Frenchman's Bay characterized by relatively high percent cover was primarily macrophytes rather than algal (Figure 4.12a,b) though *Cladophora* was observed to be growing within the macrophyte beds where hard substrate existed. Estimated biomass at this time was generally low (< 60 g m^{-2}) for much of the shoreline where *Cladophora* was dominant (except where macrophytes were growing in outer Frenchman's Bay) (Figure 4.12). Partial Mantel tests did not find any significant associations with storm sewers, tributary mouths or the Duffins WWTP outfall (Table 4.6).

By 22 June, percent *Cladophora* cover continued to increase in the areas where early season growth was noted, but additional growth was evident along much of the shoreline (Figure 4.13a). Percent *Cladophora* cover exceeded 60 % adjacent to the PNGS thermal outflow and at the outflow of Carruthers Creek (Figure 4.13a). The area of macrophyte growth in outer Frenchman's Bay continued to expand, and estimated stand height reached 0.4 m (Figure 4.13b). *Cladophora* also appeared to grow reasonably well in outer Frenchman's Bay, particularly toward the shallow portion where the substrate changed to gravel, but also in among the macrophytes. Estimated biomass did not exceed 100 g m^{-2} except in outer Frenchman's Bay where macrophyte growth was more common, and much of the biomass was restricted to depths < 5 m (Figure 4.13c and d). Partial Mantel tests again failed to find any significant spatial associations between estimated biomass and potential nutrient sources (Table 4.6).

On the same date, a smaller survey at the Rouge River site revealed percent *Cladophora* cover ranging between 20 to 70 % out to a depth of ~ 5 m, comparable to levels observed at the Pickering site (Figure 4.14a). Detached algal material was noted on the predominantly sandy bottom near the outflow of the Rouge River (Figure 4.14a), but macrophytes were not observed in this limited survey area. Estimated stand heights were consistently < 14 cm (Figure 4.14b), and estimated biomass at the Rouge River site was comparable to that estimated for the Pickering site (outer Frenchman's Bay excluded, Figure 4.14c and d).

On 17 July, percent cover continued to increase in previously identified areas, reaching coverage values in the high 80 to 90 % for many of the larger patches, and formed a nearly continuous band of heavy *Cladophora* cover from Duffins Creek eastward to Carruthers Creek at depths of 2 - 3 m. (Figure 4.15a). Some changes in the size of the patches were noted adjacent to the thermal discharge and next to Carruther's Creek (Figure 4.15a). Percent cover also increased to 40 to 50 % at depths of 5 to 6 m. *Cladophora* stand height generally remained below 20 cm for most of the shoreline east of PNGS, but the continued growth and expansion of macrophytes in outer Frenchman's Bay produced stands heights close to 1 m (Figure 4.15b). Estimated biomass remained below 150 g m^{-2} for much of the shoreline, except in outer Frenchman's Bay (Figure 4.15c). Here, *Cladophora* was observed growing epiphytically on macrophyte stems, but also interspersed among macrophytes and in larger aggregations where hard substratum predominated. Unlike the previous surveys, the partial Mantel tests detected a significant association between estimated biomass and depth, and estimated biomass and location (Table 4.6), likely induced by the large and expanding macrophyte stands in outer Frenchman's Bay.

At the Rouge River site, heavy Cladophora cover (> 70 %) was observed to depths of ~ 7 m (Figure 4.16a), and Cladophora stand height reached to nearly 40 cm in the shallows. Stand heights between 10 and 20 cm were widespread (Figure 4.16b). Estimated biomass reached a maximum of ~ 550 g m^{-2} in a localized spot where the stand heights were tallest, but in general, biomass appeared to be greater here than at the Pickering site (except in outer Frenchman' Bay) (Figure 4.16c).

By July 25, percent *Cladophora* cover at Pickering reached moderate values (~ 40 %) at depths of 8 m (Figure 4.17a) and remained above 80 % in many areas. Estimated stand heights suggest that much of the growth east of PNGS remained below 25 cm, while in outer Frenchman's Bay, macrophyte growth continued to expand, reaching stand heights of 0.5 to 1 m (Figure 4.17b). Estimated biomass at this time appeared somewhat lower in the shallow depths, but large patches of biomass in excess of 150 g m^{-2} were observed near the outflow of Duffin's Creek and midway between Duffins and Carruthers Creek (Figure 4.17c). Partial Mantel tests found a significant spatial association with location, and also detected a significant association with distance to the nearest tributary mouth (Table 4.6).

Percent *Cladophora* cover remained high at the Rouge River site, but was less uniform than on 17 July (Figure 4.18a), although it did extend to depths of 7 m. *Cladophora* stand heights were lower than observed on 17 July, but still frequently exceeded 15 cm (Figure 4.18b). Estimated biomass was comparable to that observed at the Pickeirng site, but did not reach very the high values observed on 17 July (Figure 4.18c).

On 8 August, percent *Cladophora* cover remained high along much of the shoreline although cover was reduced in shallow waters and areas east of PNGS (Figure 4.19a). Areal cover in outer Frenchman's Bay reached a maximum at this time, and based on stand heights and underwater video, macrophytes dominated much of the area (Figure 4.19b). Tall stands of *Cladophora* (e.g., ~ 20 cm) were still present along the shore, but some of these areas also supported occasional macrophytes, particularly in the shallows adjacent to Carruthers Creek (Figure 4.19b). Estimated biomass did not reach comparable levels as on July 25, though values > 150 g m^{-2} were observed near Carruthers Creek (Figure 4.19c). Much like the prior survey, partial Mantel tests indicated a strong spatial association with location and distance to a tributary mouth (Table 4.6).

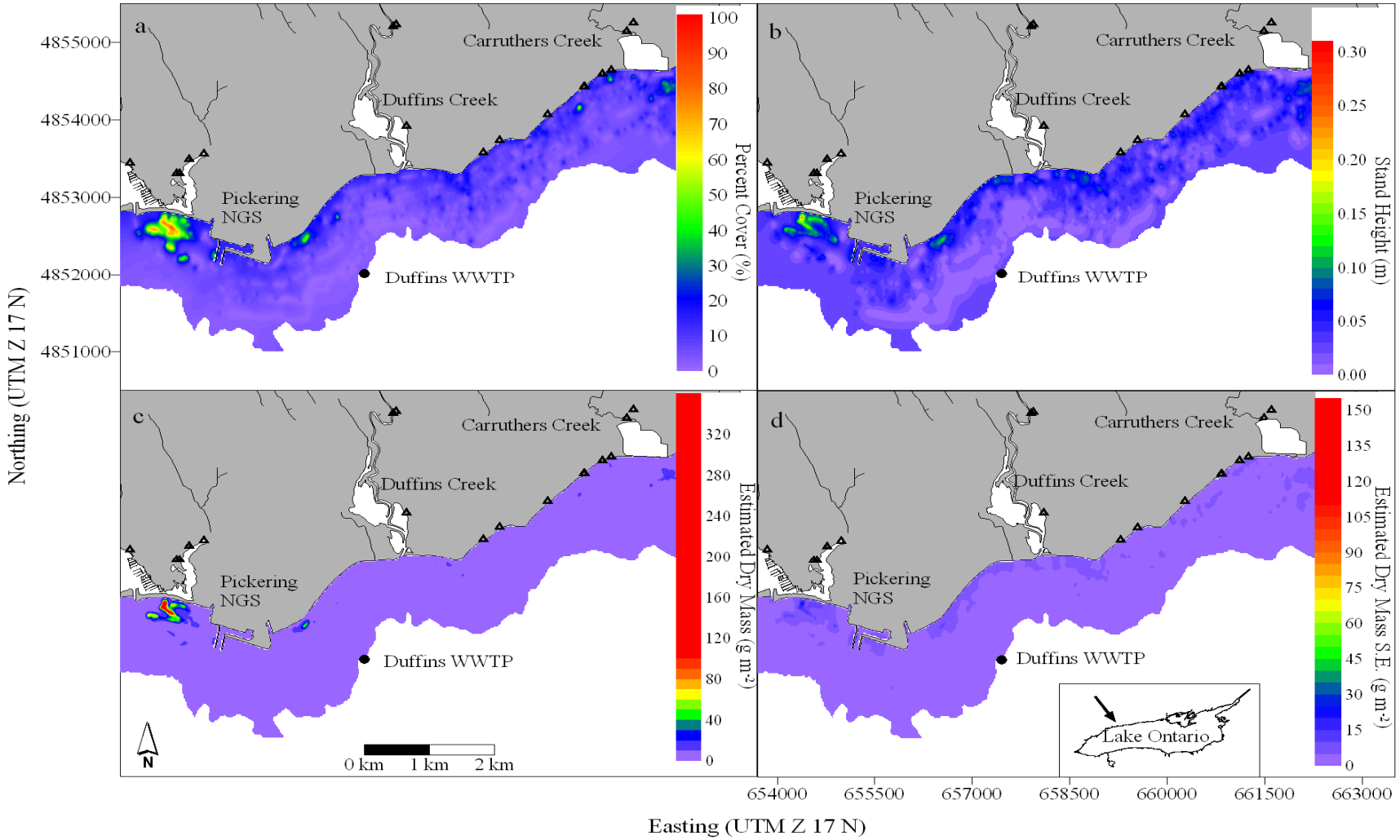

Figure 4.12. Kriged maps showing a) percent cover b) stand height, c) estimated biomass and d) approximate standard error of the biomass estimate for the Pickering site June 11 2007.

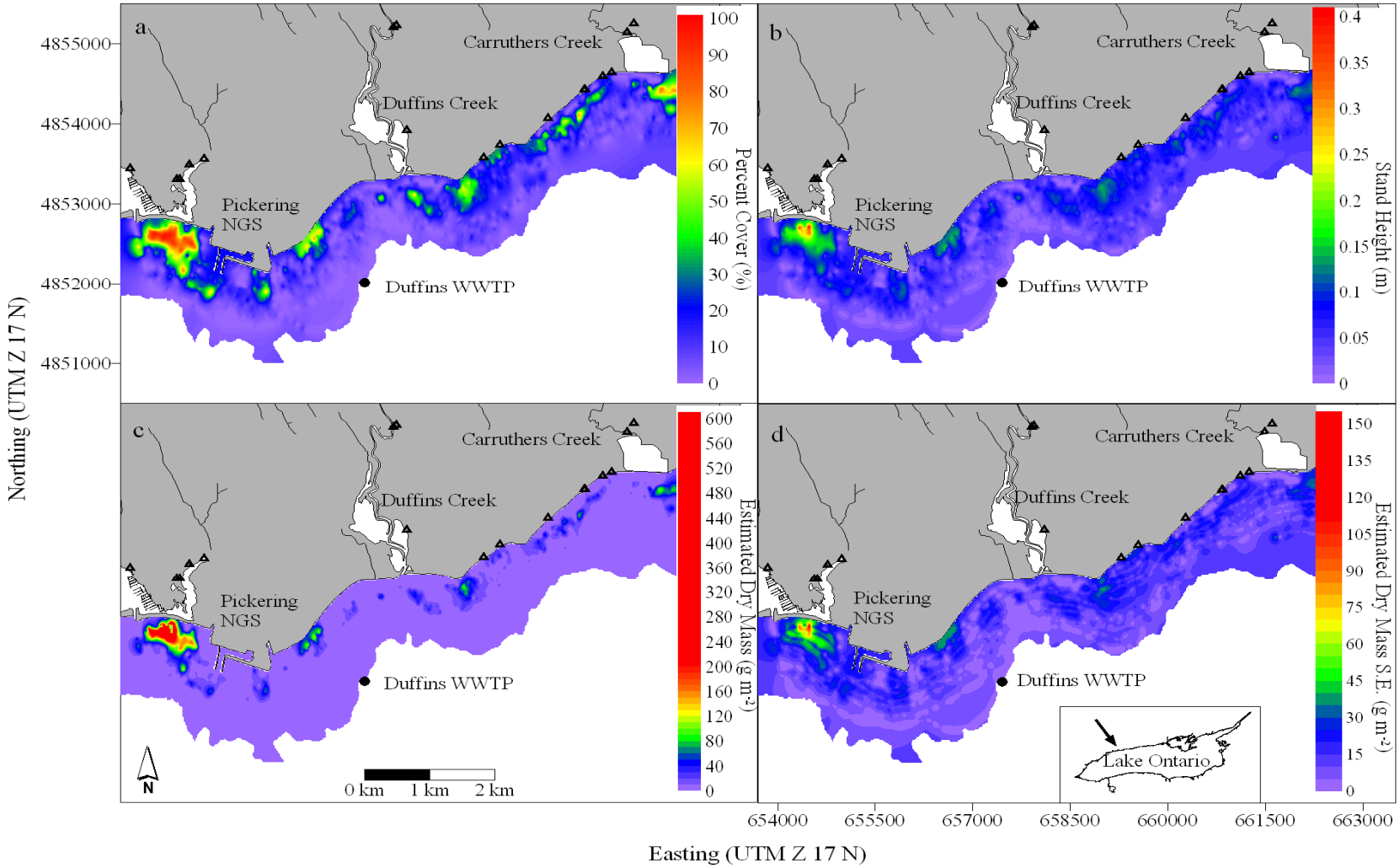

Figure 4.13. Kriged maps showing a) percent cover b) stand height, c) estimated biomass and d) approximate standard error of the biomass estimate for the Pickering site June 22 2007.

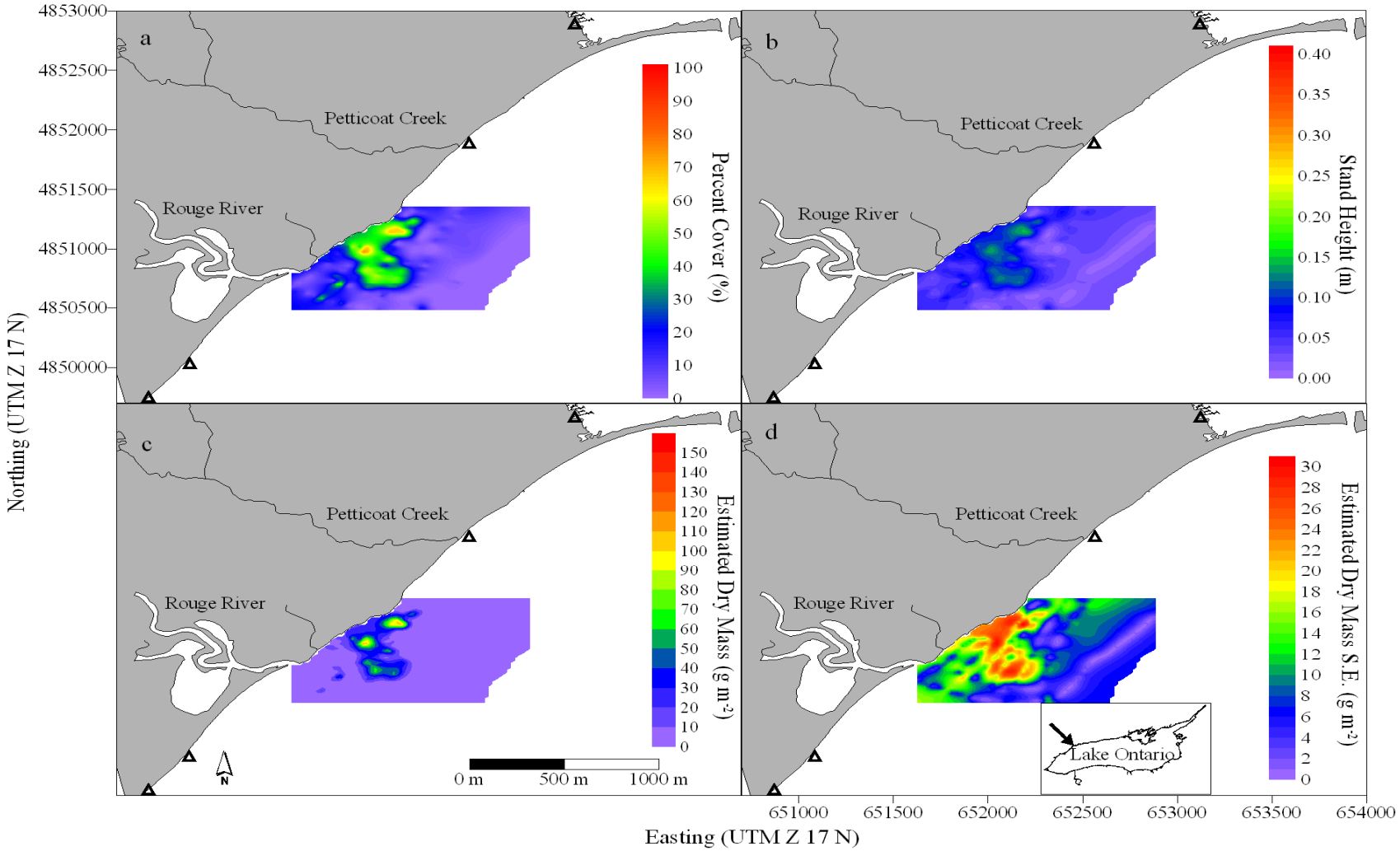

Figure 4.14. Kriged maps showing a) percent cover b) stand height, c) estimated biomass and d) approximate standard error of the biomass estimate for the Rouge River site June 22 2007.

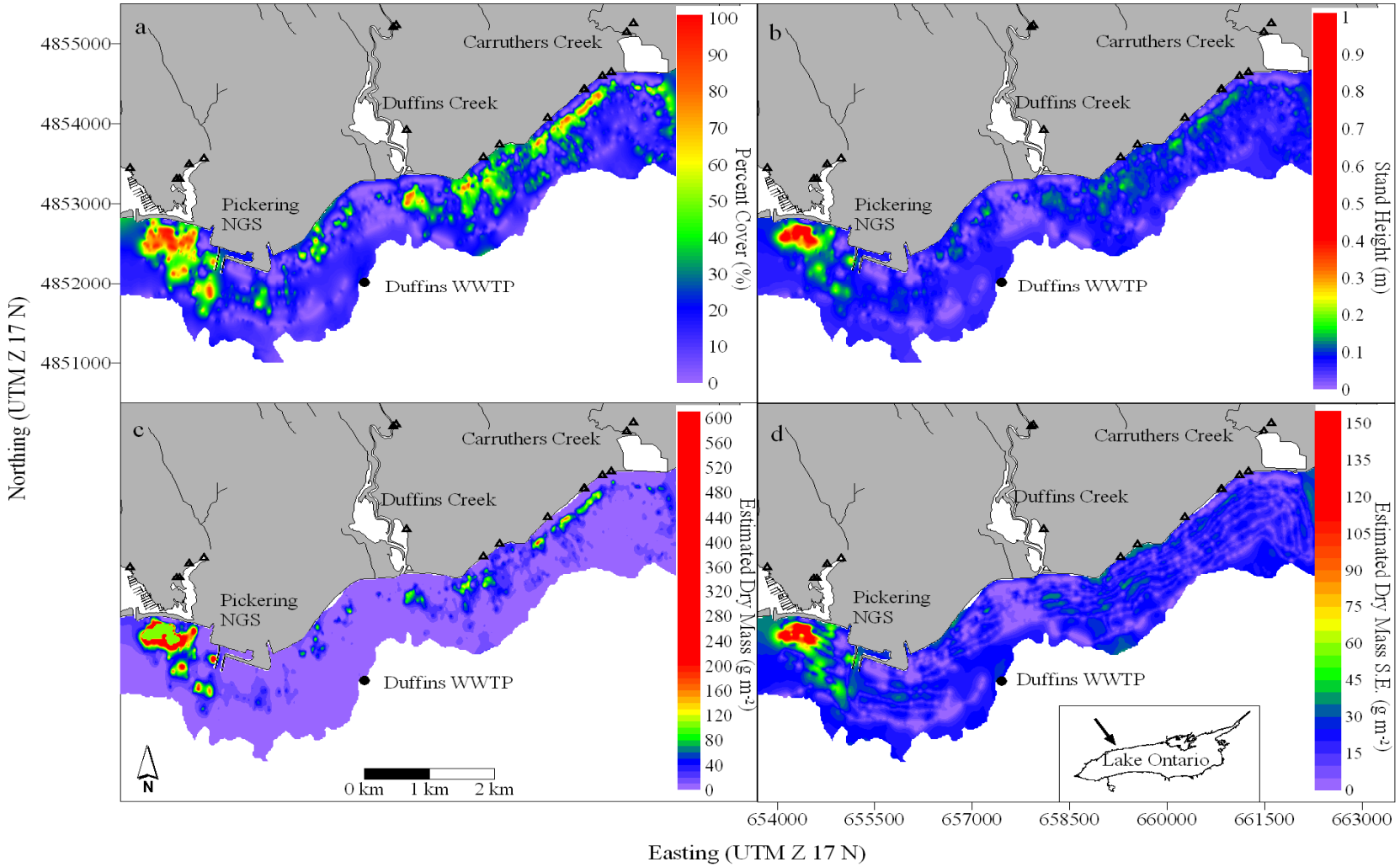

Figure 4.15. Kriged maps showing a) percent cover b) stand height, c) estimated biomass and d) approximate standard error of the biomass estimate for the Pickering site July 17 2007.

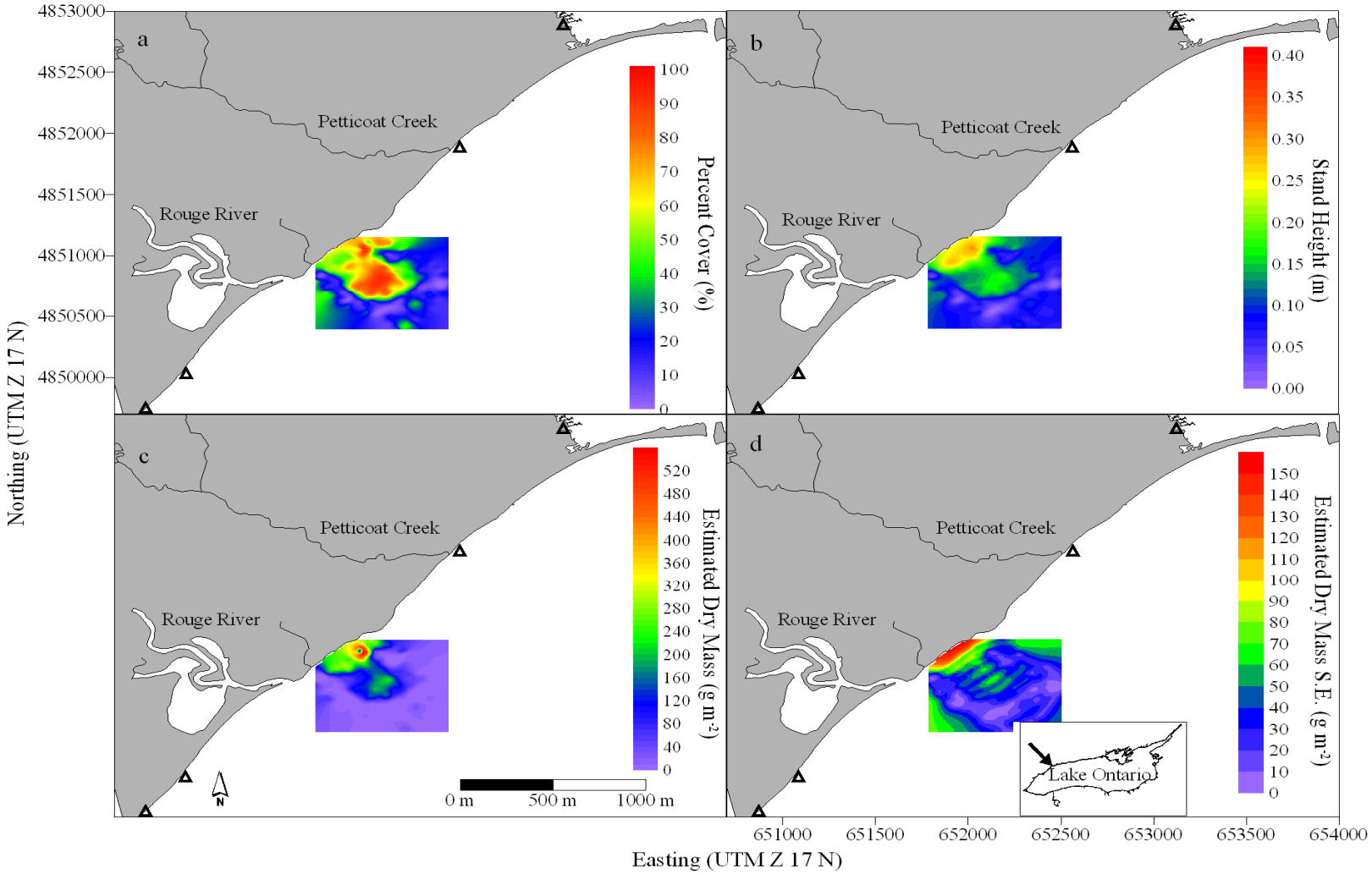

Figure 4.16. Kriged maps showing a) percent cover b) stand height, c) estimated biomass and d) approximate standard error of the biomass estimate for the Rouge River site, July 17 2007.

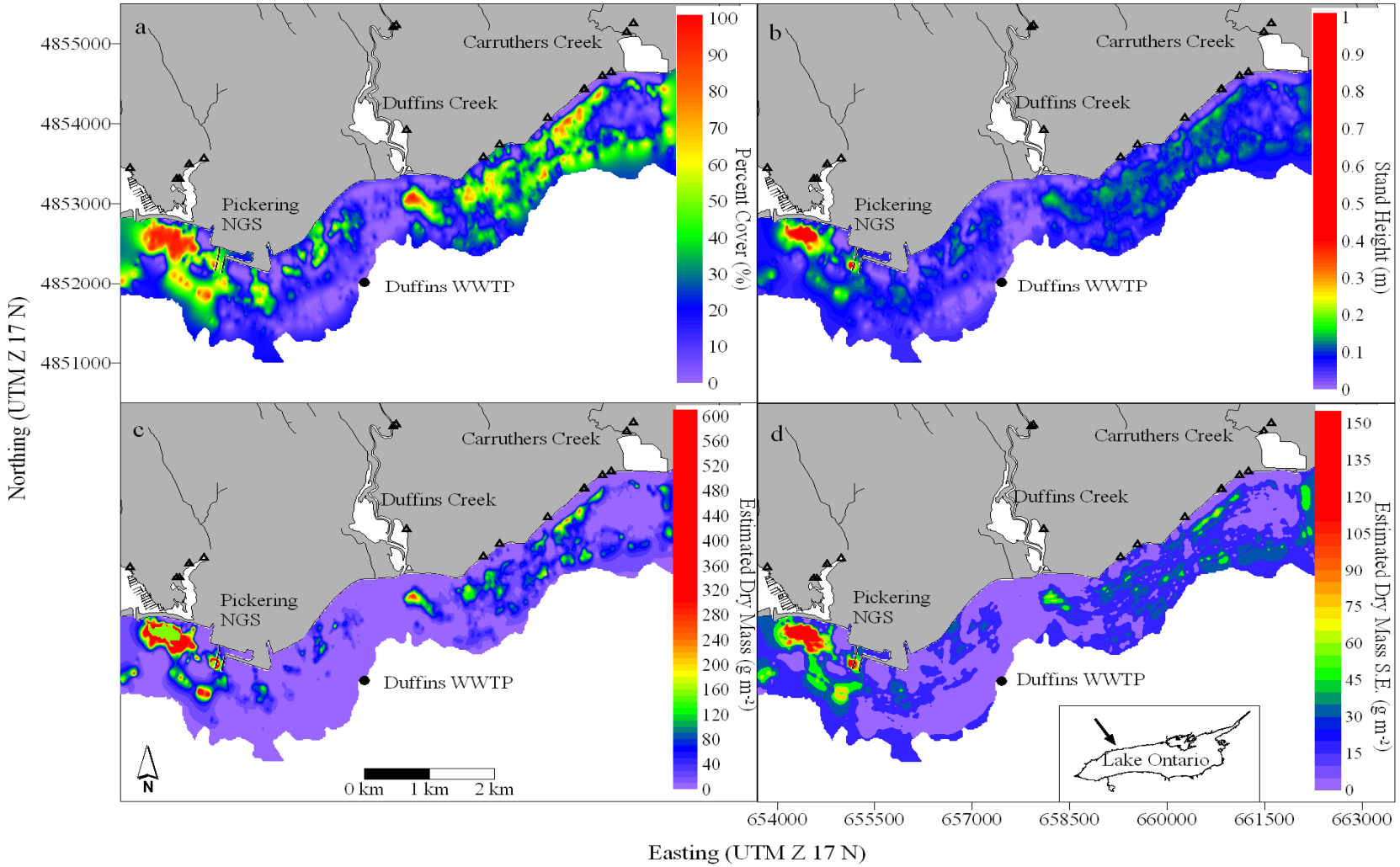

Figure 4.17. Kriged maps showing a) percent cover b) stand height, c) estimated biomass and d) approximate standard error of the biomass estimate for the Pickering site, July 25 2007.

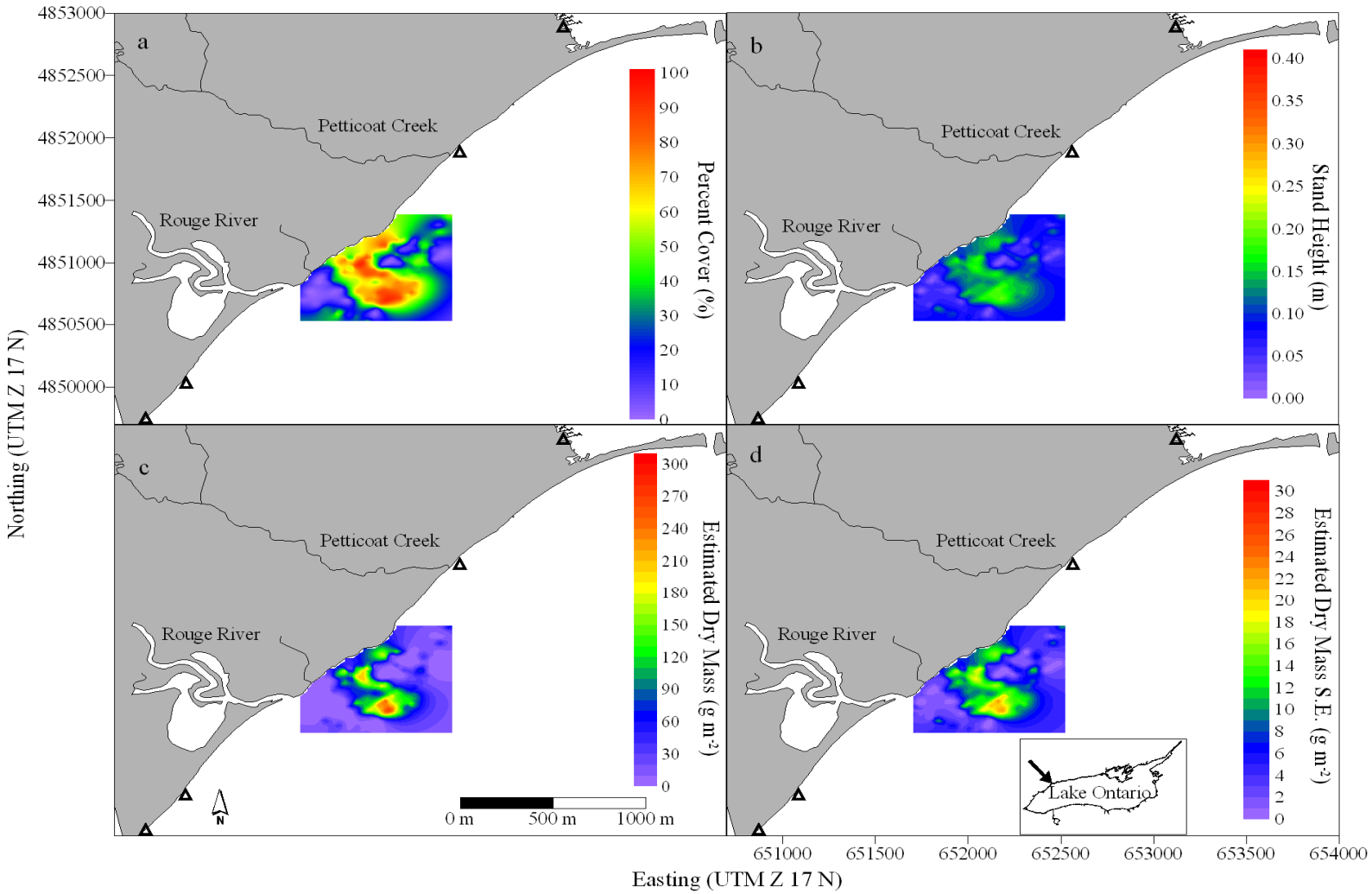

Figure 4.18. Kriged maps showing a) percent cover b) stand height, c) estimated biomass and d) approximate standard error of the biomass estimate for the Rouge River site, July 25 2007.

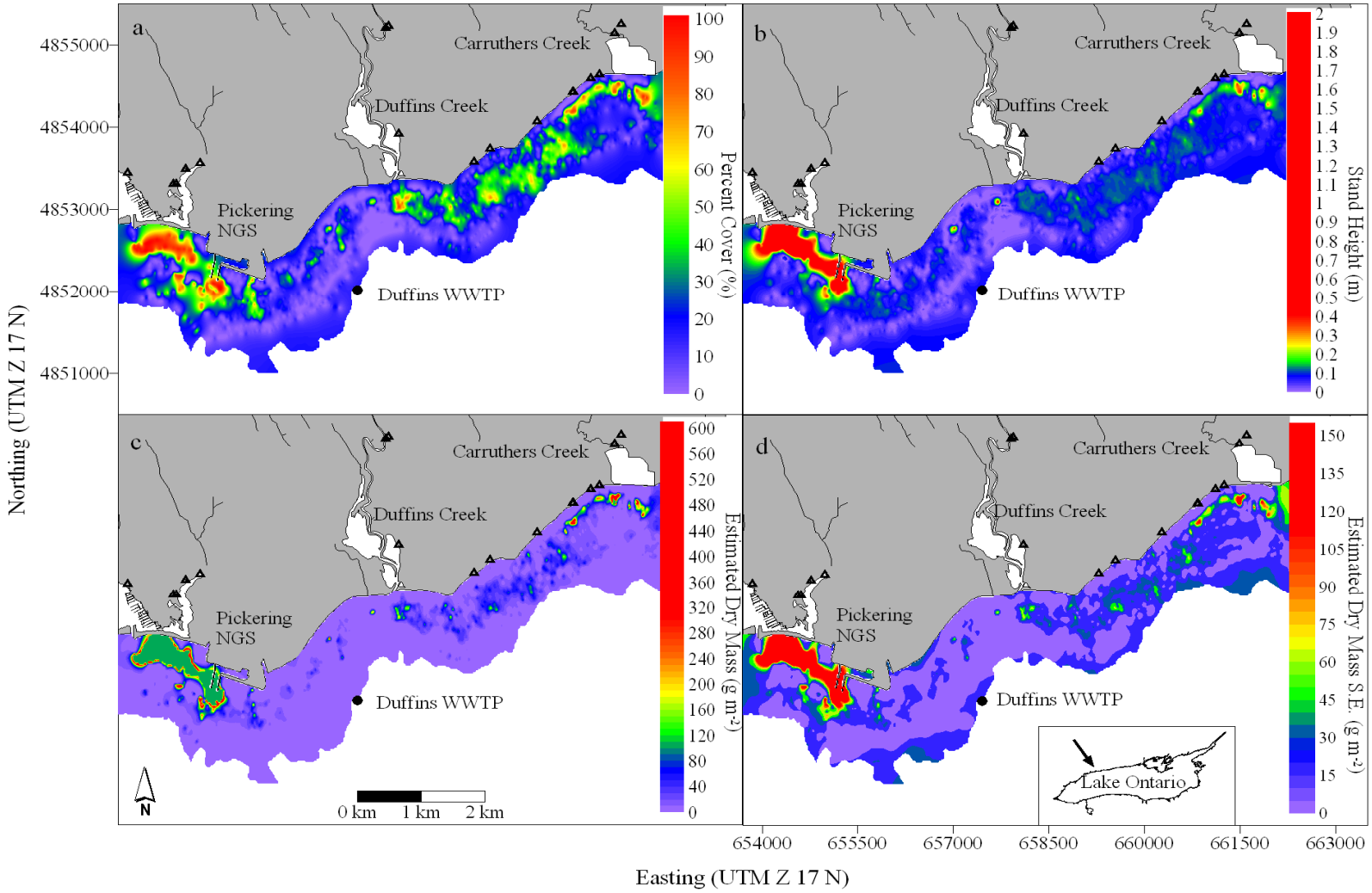

Figure 4.19. Kriged maps showing a) percent cover b) stand height, c) estimated biomass and d) approximate standard error of the biomass estimate for the Pickering site, August 8 2007.

Table 4.6. Results of partial Mantel tests for Pickering surveys in 2007. r_{splenv} denotes pure partial Mantel correlation coefficient, *p* denotes significance of permuted Mantel correlation coefficient, ns denotes not significant at the $p = 0.0083$ level. Covariates indicate covariate tested against while all others are paritaled out. X + Y are Easting and Northing (m), Sewer indicates minimum distance to storm sewer (in m), Slope indicates bathymetric slope (degrees), Tributary indicates distance to nearest tributary mouth (in m), Outfall indicates distance to nearest municipal WWTP outfall (m), and depth indicates depth of lake where polygon centroid resides (m).Number in brackets below the date indicates the number of polygon centroids available.

Covariate	*June 11*		*June 22*		*July 17*		*July 25*		*Aug 8*	
	(16)		*(46)*		*(164)*		*(221)*		*(282)*	
	r_{splenv}	*p*	r_{splenv}	*p*	r_{splenv}	*p*	r_{splenv}	*p*	r_{splenv}	*p*
X + Y	0.11	ns	0.15	ns	0.18	0.0001	0.28	0.0001	0.10	0.0001
Sewer	0.03	ns	0.04	ns	-0.08	ns	-0.04	ns	0.03	ns
Slope	-0.13	ns	-0.06	ns	-0.01	ns	0.05	ns	0.00	ns
Tributary	0.24	ns	-0.03	ns	0.04	ns	0.17	0.0001	0.06	0.0001
Outfall	-0.17	ns	-0.14	ns	-0.06	ns	-0.08	ns	0.00	ns
Depth	-0.16	ns	-0.08	ns	0.09	0.002	-0.05	ns	0.03	ns

4.5 Discussion

The primary advantage of the hydroacoustic survey method as employed in this study is the rapid sampling and characterization of benthic algal growth (in this case, primarily *Cladophora*) over moderately large to large areas with good spatial coverage. The subsequent geostatistical analyses employed here extend the utility of the collected data to delineate the spatial distribution and pattern of *Cladophora* growth, and provide spatially explicit estimates of *Cladophora* biomass, which cannot be derived from quadrat sampling without considerable effort. The geostatistical analyses demonstrated that considerable spatial structure is apparent in nuisance *Cladophora* growth at these study sites, and the high degree of spatial dependence observed for percent *Cladophora* cover and stand height underscores the variability inherent in the near shore areas that may not be adequately characterized even by an intensive quadrat sampling design.

A model was used to calibrate the measures of *Cladophora* stand height to areal biomass in the previous chapter (Chapter 3). This provides a biologically meaningful measure that is comparable to previous studies which use more traditional sampling methods. These spatial estimates of *Cladophora* distribution and biomass can them be examined to investigate patterns that are suggestive of physical or biological factors that influence the distribution of excessive *Cladophora* growth. In this study, the patterns of principal interest were those related to the spatial distribution of nuisance *Cladophora* biomass and relationships to known nutrient sources (e.g., municipal WWTP outfalls) and potential shoreline point sources of nutrients (e.g., tributaries and storm sewers).

The response of *Cladophora* growth and biomass accrual to point sources of nutrients or localized inputs of non-point source nutrients is strongest when ambient nutrient concentrations are low (Canale and Auer 1982). The kinetics of limiting nutrient uptake (for *Cladophora* in the Great Lakes, this is almost always P; see references in Higgins et al. 2008a) are well documented (e.g., Auer and Canale 1982x, Rosmarin 1982), and clearly show that growth rate potential is hyperbolic in nature with respect to P content of the algal tissue (Gerloff and Fiztgerald 1976, Auer and Canale 1982y). Thus, at high nutrient availability, nutrient uptake rates tend to decline as nutrient content of the tissue increases. Above a threshold level (for *Cladophora*, this is ~ 0.16 % by DW; c.f. Higgins et al. 2008a) growth potential is high, and providing other environmental factors are sufficient, high biomass accrual can result. This effectively describes the situation in Lakes Ontario and Erie during the 1960s through 1970s when elevated nutrient concentrations (compared to current nutrient concentrations) were widespread (e.g., Kwiatkowski 1984, Ontario

Ministry of Environment 1982) and supported excessive *Cladophora* growth on much of the available substrate when light availability did not limit growth (Wezernak and Lyzenga 1975). Conversely, at low nutrient availability, nutrient uptake rates are generally high, but tissue P content may remain low. Growth potential is therefore very sensitive to changes in external P concentration that drive changes in internal P content (Gerloff and Fitzgerald 1976, Auer and Canale 1982y). Relationships between excessive *Cladophora* biomass and known nutrient sources were well defined in Lake Huron, where ambient nutrient concentrations were not nearly as high as those found in the lower Lakes (e.g., Auer et al 1982a). In Lake Huron, nuisance *Cladophora* biomass declined with increasing distance from the nutrient source, both in an alongshore and offshore direction, and the range where clearly defined gradients in water column SRP and *Cladophora* tissue P content existed was ~ 250 to 500 m (Auer et al. 1982a).

An assessment of whether such spatial patterns in relation to point sources or shoreline sources of nutrient might occur in present day near shore Lake Ontario is therefore predicated on establishing that both current water column nutrient concentrations and *Cladophora* tissue P content are indeed lower than historical levels. In the 1970s, near shore and offshore TP concentrations in Lake Ontario were high, ranging from 18 to 30 $\mu g\ L^{-1}$, while SRP ranged between 3 and 10 $\mu g\ L^{-1}$ (Ministry of Environment 1980, Haffner et al. 1984, Malkin et al. submitted). During this study, concentrations of TP in the near shore at Oakville averaged close to the 10 $\mu g\ L^{-1}$ GLWQA target (mean $10.62 \pm 4.96\ \mu g\ L^{-1}$), and SRP was below 3 $\mu g\ L^{-1}$ (mean $2.25 \pm 2.82\ \mu g\ L^{-1}$) for much of the growing season (May to September), with higher concentrations observed during spring or late fall months. At Pickering, TP tended to be slightly higher, ranging from 6 to 22 $\mu g\ L^{-1}$, but average concentrations (mean $11.59 \pm 4.31\ \mu g\ L^{-1}$) were comparable to those at Oakville. SRP concentrations at Pickering also followed a comparable seasonal trend as at Oakville, but were more variable, and generally did not exceed 3 $\mu g\ L^{-1}$ during the May – August period (mean $1.92 \pm 2.47\ \mu g\ L^{-1}$). Interestingly, P concentrations observed in the months of September and October at both study sites are consistent with enrichment of the coastal zone, but the proximate cause remains unknown and is difficult to determine. That such enrichment is not observed during the June – August period may reflect the biological demand for P by *Cladophora* and the trapping of particulate material by dreissenid mussels.

Much like the reduced nutrient concentrations in Lake Ontario, measured *Cladophora* tissue P content also declined from lakewide averages of 0.49 % in 1972, to 0.20 % in 1983 (as ash free dry weight; Painter and Kamaitis 1987). Current estimates of tissue P at Oakville rarely exceeded 0.16 % (by dry weight; Houben 2007) unless at depths of 10 m. Although not reported

in this chapter, tissue P (by dry weight) at Pickering averaged 0.17 % (n=80) and exceeded 0.16 % only at depths of 5 m or greater, or in the months of September and October (Leon et al. 2009). The decline of tissue P during the summer months in shallow waters indicates that dilution through growth exceeds supply at that time. Given the relatively low nutrient and tissue P concentrations observed during the summer months when *Cladophora* is actively growing, this suggests that spatial associations between nuisance *Cladophora* and potential nutrient sources might well occur at the study sites.

4.5.1 Patterns of nuisance *Cladophora* growth and municipal WWTP outfalls

Although this study did not find strong evidence that WWTP outfalls could impact water chemistry on a local scale (e.g., < 1 km), follow-up studies at Pickering in 2008 were able to detect a considerable influence of the Duffins WWTP on local water quality, primarily through the effect of higher TP and SRP concentrations (Leon et al. 2009). However, it is important to note that this effect is not constant; rather it seems to vary depending on the ambient conditions at the time of sampling. The primary goal of a WWTP outfall diffuser system is to rapidly mix the discharged effluent stream with the lake water, thereby minimizing any potential localized enrichment (Rao et al. 2003). Mixing of effluent from a WWTP diffuser is generally accomplished by two processes 1) intense mixing and dilution created by the turbulence from the diffuser and 2) the mixing of the waste field by the hydrodynamic forces generated within the lake. Depending on the density of the effluent and the density of the receiving lake water, this waste field may boil to the surface or remain trapped at a depth of neutral buoyancy (Murthy and Csanady 1971, Rao et al. 2003). For most outfalls, studies have shown that at distances of < 1000 m, water quality and bacteriological parameters are comparable to background concentrations, and suggest that mixing is generally thorough (Murthy and Csanady 1971, Rao et al. 2003). Rao et al. (2003) determined the optimal depth for outfall placement in the western basin of Lake Ontario to be 14 m depth and 1200 m from shore to achieve efficient dilution and mixing.

The lack of a consistent outfall effect during the surveys at Oakville and Pickering likely results from a) stations situated beyond the 1000 m distance which translates into a low probability of "detecting" a waste plume, and b) the observation that infrequent sampling (monthly at Oakville, bi-weekly at Pickering) may not be of sufficient to fully characterize the dynamics. In both study sites, the WWTP have been identified as the largest local source of P to the immediate study areas (e.g., Aquafor Beech 2006, Leon et al. 2009). Despite this, the concentrations of P that were measured in this study averaged close to the GLWQA target of 10 $\mu g\ L^{-1}$, and rarely exceeded 15 $\mu g\ L^{-1}$ during the summer months (June – August) when

Cladophora growth is most prominent. Very high P concentrations (15 – 30 μg L^{-1}) were observed, however, during September and October at both study sites, but this does not necessarily implicate WWTP as the proximate source. It is entirely possible that P discharged by the WWTP outfalls is quickly assimilated by phytoplankton, but the chlorophyll a concentrations measured in this study do not provide compelling evidence for this.

In this study, no spatial association between nuisance *Cladophora* biomass and WWTP outfalls was found for either the Oakville site or the Pickering site. Based on the depths of the outfalls at the Oakville site (Southeast WWTP outfall; ~ 4 m depth, 300 m from shore, Clarkson WWTP outfall; ~ 16 m depth; 1.4 km from shore) stronger patterns might be expected to occur in relation to the Southeast WWTP outfall, as it is closer in proximity to shore and large piers at the north end of the study site likely disrupt along shore currents commonly observed in this area. However, much of the excessive biomass occurred at distances in excess of 2 km away, and was clearly not locally restricted to the vicinity of either the Southeast or Clarkson WWTP outfall. At Pickering, the Duffins WWTP outfall is the major outfall influencing this study site. Although nuisance *Cladophora* biomass was found not to be spatially associated with this outfall at any of the survey periods, the lack of suitable substrate immediately adjacent to the diffuser complicates interpretation. *Cladophora* growth within a 1.5 km radius of the outfall is substrate limited, as much of the lake bottom between Duffin's Creek and the WWTP outfall is sand, particularly in the shallow depths (< 5m) (D. Depew, unpubl. data). Some hard substratum does exist, primarily in patchy aggregations of large rocks and boulders. If more suitable substratum were available in close proximity to the outfall, accumulation of *Cladophora* at distances closer than 1000 m might well occur, especially given the high P concentrations that have been periodically measured in the vicinity of the outfall (Leon et al. 2009).

4.5.2 Nuisance *Cladophora* biomass and shoreline nutrient sources

In contrast to the placement and mixing conditions at WWTP outfalls, mixing and dispersion of effluent is much less efficient for shoreline based discharges such as storm sewers and tributaries. Both numerical and experimental evidence suggests that a given effluent plume will tend to closely follow the shoreline in response to flow patterns influenced by lake wide circulation (Csanady 1970). With high nutrient loading, this can ultimately result in a situation of coastal entrapment, creating gradients in nutrient and contaminant concentrations that increase toward shore. Depending on the discharge volume and concentration, this can form a widespread zone of enrichment (Csanady 1970). Seasonal changes also influence these processes, the prime example being the coastal entrapment of nutrients by the thermal bar (Rao et al. 2004). With the

thermal bar, an additional impediment to horizontal mixing is provided by the presence of the dense band of 3.98 °C water that gradually moves offshore as the near shore waters warm in the spring (Rao et al. 2004). Combined with the high discharges that are characteristic during the spring, the potential for a highly enriched near shore zone is high. The early spring sampling at Oakville in April 2006 was designed to evaluate the thermal bar period. Parameters that can be considered tracers of tributary input (e.g., NO_3^- and Cl^-) displayed strong gradients in concentration that decreased as distance from the tributary increased. Not surprisingly, the highest concentrations were generally observed for the largest tributary (16 Mile Creek) and were observed within 500 m of the tributary mouth. However, P concentrations did not comparable spatial gradients and concentrations were generally unremarkable (mean TP 8.31 ± 1.91; range 4.75 - 13.95 μg L^{-1}). The lack of a similar pattern for concentrations of TP, TDP and SRP suggests either that tributary input of P during the spring were not characterized by high concentrations, or that P inputs quickly sink out of the water column or are quickly taken up. The observation that P concentrations in tributaries in these urbanized catchments are decreasing or remaining stable while concentrations of Cl^- and NO_3^- are increasing (e.g., Ontario Ministry of Environment 1999) support the former.

For much of the growing season (May – October) patterns in near shore water quality can vary considerably. Hydrodynamic features common to the Great Lakes (e.g., upwelling and downwelling) can and do periodically disrupt the formation of near shore enrichment zones (Rao and Schwab 2007). In general, dilution of effluents discharged directly at the shoreline by currents is generally quite poor due to the friction imparted by the bottom on very near shore currents (Csanady 1970). This low frequency of mixing with offshore waters was likely the cause of widespread near shore enrichment in the lower Great Lakes during the 1950s and 1960s, when nutrient loading from point sources and non-point sources to the lake via tributaries was high (Gregor and Rast 1982). If tributaries and storm sewers are providing a considerable nutrient load from non-point sources, higher nutrient concentrations in shallow waters should be a reasonable expectation along these urban shorelines.

Patterns of water chemistry suggestive of chronic near shore nutrient enrichment were generally not evident at the two study sites. Other parameters such as Cl^- at Oakville, and TSS at Pickering were elevated at 2 m sites relative to 5 and 10 m sites, and are consistent with the near shore trapping of discharge from storm sewers and tributaries and such patterns are detectable up to several hundred meters away form the source(s). This is consistent with a similar study conducted at the outflow of Cooksville Creek (near Port Credit, ONT; see Chapter 3) during the summer of 2004. Here, strong spatial patterns demonstrating elevated concentrations of TSS, Cl^-

and TP up to 500 m away from the mouth of the creek were evident across much of the season (Hiriart-Baer et al. 2009). Although the patterns observed for Cl^- and TSS at these sites were consistent with those observed by Hiriart-Baer et al. (2009) at Cooksville Creek, similar trends for TP, TDP or SRP at Oakville and Pickering were not apparent. These contrasting patterns may arise from differing geomorphology of the shorelines and the subsequent effects on currents that disperse tributary discharge. For example, a large man-made harbor is adjacent to Cooksville Creek. This provides a moderately protected area inset from the main portion of the lake (e.g., see Figure 3.3b), while the Oakville and Pickering sites are much more exposed and subjected to wind and wave action (Pickering) and un-impeded along shore flow (Oakville). Cooler, wet summers with heavy precipitation can also result in continued measures of high P concentrations near tributaries (e.g., Malkin 2007). 2004 was also identified as an abnormally cool and wet summer with higher discharge from 16 Mile Creek (Oakville, May – September mean discharge = 1.71 ± 1.63 m^3 s^{-1}, Water Survey of Canada stations 02HB004 and 02HB005) and higher concentrations of TP were measured at the Oakville site in 2004 compared to 2005 (which was warmer and drier, May – September mean discharge = 0.95 ± 0.53 m^3 s^{-1}) (e.g., Malkin 2007; Malkin et al. submitted). Given the close geographical proximity of Cooksville Creek and 16 Mile Creek (~ 16 km) it is likely that Cooksville Creek experienced comparable regional meteorology as Oakville, and therefore higher tributary discharge and presumably nutrient loading in 2004. The limited sampling conducted at Oakville and near Cooksville during an earlier study in 2005 (Chapter 3) demonstrated low P concentrations and is consistent the trends in tributary discharges observed at Oakville. Unfortunately, discharges for 2006 are not available for 16 Mile Creek. Inter-annual differences in meteorology may therefore affect nutrient concentrations in near shore waters by increasing (wet) or decreasing (dry) discharge.

Other local phenomena may also influence the patterns of near shore water quality at Oakville and Pickering. At Pickering, the re-suspension of sand and softer substrate via wind and wave action, the transport of eroded sediments from the Scarborough bluffs in an eastward direction (e.g., Martini and Kwong 1985) may also influence water quality. The degree to which this occurred during this study is not easily assessed. However, the lack of comparable variation in TSS at PI2 as compared to the other transects in addition to the general lack of soft substratum at transect PI4 suggest the high TSS measured at these transects is likely derived from tributaries (e.g., Rouge River at PI1, and Duffins Creek at PI3 and PI4) rather than re-suspension or long shore transport of eroded sediments At Oakville and Pickering, the influence of upwelling was evident in water temperatures, but less so on water chemistry. Historically, upwelling of cooler metalimnion or hypolimnion water often increased P concentrations as remineralized P was

injected into near shore regions (Haffner et al. 1984b, Lean et al. 1990). However, as early as the late 1980s, upwelling of hypolimnion water was characterized by low nutrient concentrations (e.g., Lean et al. 1990). Without samples collected within minutes of upwelling it is difficult to assess the potential for P inputs from upwelled water, but based on recent offshore water chemistry trends (e.g., Malkin et al. submitted) and limited near shore sampling conducted soon after upwelling (e.g., Malkin 2007), P inputs via upwelling can be assumed to be negligible.

Despite a generally widespread distribution of nuisance *Cladophora* biomass, on 23 June and 1 August, *Cladophora* biomass did show significant spatial association with storm sewers at the Oakville site. Stom sewers are known to transport both particulate and soluble forms of P (Bannerman et al. 1993, Sorrano et al. 1996) and the significant association between nuisance Cladophora biomass and proximity to storm sewers may suggest some influence of storm sewers as contributing to the spatial patterns of *Cladophora* growth. However, significant association between nuisance *Cladophora* biomass and bathymetric slope was also observed on 23 June and complicates the interpretation. Partial Mantel tests conducted for these dates explicitly to examine relationships between bathymetric slope and proximity to storm sewers also revealed a highly significant relationship for 23 June and 11 July, but not 1 August (partial Mantel $r = 0.18$ and $r = 0.08$, $p<0.0005$ and $p<0.05$ respectively). This suggests that areas adjacent to storm sewers at Oakville often had relatively flat bathymetry. Such flat areas may support excessive *Cladophora* biomass by slowing the loss of *Cladophora* biomass by attenuating wave energy or allowing for deposition of detached biomass. The lack of a significant relationship between proximity to storm sewers and slope in August may be a reflection of the small sample size (Table 4.5) or it may indicate a potential importance of periodic discharges of nutrients by storm sewers during the summer for localized areas.

At Pickering, significant relationships between nuisance *Cladophora* biomass and proximity to storm sewers were not obseved. The lack of a relationship at Pickering may simply be due the general lack of suitable substratum in proximity to storm sewers. Much of the substratum in depths of 1- 2 m along the shoreline where storm sewers are numerous is composed of sand and the maps indicate that these areas generally remained devoid of growth for much of the study period (see Figures 4.11 to 4.19). However, it is clear from the maps that *Cladophora* does grow well at distances far removed from storm sewers, and these do not appear to be contributing to growth patterns at this site.

Despite the obvious presence of a large patch of heavy cover and high biomass immediate south of 16 Mile Creek, *Cladophora* biomass did not show significant relationships in proximity to tributaries at Oakville. This may be due to a non-linear pattern in biomass

distribution when examined as a function of proximity to tributary mouth. This would not be inconsistent with the patterns of growth induced by a tributary plume that generates persistent highly turbid water immediately adjacent to the tributary mouth. Here, light is limiting and the tributary plume likely has a negative effect on *Cladophora* growth, even in the presence of excess nutrients. Further from the tributary mouth, as heavier particles settle and finer particles are further diluted, light limitation is likely alleviated. Therefore, a strongly linear relationship between *Cladophora* biomass and proximity to tributaries is not necessarily expected. However, it is difficult to infer the stability and persistence of such turbidity plumes since tributary plumes are generally transient. Tributary plumes are subjected to flow reversals and hydrodynamics once in the lake (Rao and Schwab 2007). This may include changes in direction on the order of 5 -8 days (Rao and Schwab 2007) or trapping near surface during and after an upwelling event (Fong and Geyer 2002).

At Pickering, significant relationships between *Cladophora* biomass and proximity to tributaries were observed on three of the survey dates. Interestingly, these relationships were only observed during the surveys when macrophyte growth in outer Frenchman's Bay had expanded to near maximum coverage. Repeating the partial Mantel tests with the Frenchman's Bay tributary source removed, the partial Mantel tests were all non significant for all surveys, including the three dates where Frenchman's Bay induced a significant result (July 25, $r = -0.04$, and August 8, $r = -0.04$, $p > 0.9$ respectively). This suggests that the significant association between *Cladophora* biomass and proximity to tributaries at Pickering was induced largely by the large area of macrophyte and *Cladophora* growth west of PNGS in outer Frenchman's Bay.

4.6 Summary and Conclusions

The current distribution of nuisance *Cladophora* growth at two highly urbanized shorelines in Lake Ontario (Oakville and Pickering) is widespread and not well explained by proximity to known point sources or shoreline nutrient sources. At these study sites, the local WWTP are the largest P contributors in terms of seasonal nutrient load (Aquafor Beech 2006, Leon et al. 2009), followed by the major tributaries (e.g., 16 Mile Creek at Oakville, Aquafor Beech 2006, and Duffins Creek at Pickering; Leon et al. 2009) and storm sewers as the smallest (Aquafor Beech 2006, Leon et al. 2009). Near shore water chemistry measured during the typical *Cladophora* growing season (May – August) does not appear to have returned to levels measured during the 1970s and early 80s (e.g., Ontario Ministry of Environment 1980), and the current patterns of widespread growth are difficult to reconcile with recent measures of P concentrations. The absence of strong consistent patterns of *Cladophora* growth at these sites in relation to these

known and potential nutreint sources does not necessarily preclude the dependence of *Cladophora* growth on nutrients from theses sources, but rather that there is no compelling evidence that these known nutrient sources are contributing to current growth patterns of excessive *Cladophora* biomass. There is little evidence that WWTP in the west basin of Lake Ontario have significantly increased their loading of P to the lake with the discharge of treated effluent because of improvements to treatment facilities (Medeiros and Molot 2006), and monitored tributaries and calculated loads from the major tributaries at these study sites appear to have declined relative to loads experienced in the 1970s and early 1980s (Malkin et al. submitted) when high P concentrations were widespread along much of the Lake Ontario near shore. A companion study of *Cladophora* nutrient content conducted at the Oakville site is consistent with the results of this study; little spatial variation in *Cladophora* tissue P or N existed, except that which was imparted by depth (e.g., light limitation). This suggests that along the shoreline, the nutrient content (and thus general availability of nutrients) was homogeneous and did not indicate localized areas of continued enrichment (Houben 2007).

Dreissenid mussels could account for the current pattern of *Cladophora* growth, largely because they are relatively ubiquitous on hard substrate at these sites (e.g., Ozersky et al. 2009, T.Ozerksy unpubl. data) and the rates of in situ nutrient supply have been estimated to be sufficient to meet *Cladophora* demand for P (Ozersky et al. 2009). Yet, it is not a simple task to determine whether or not *Cladophora* is solely dependent on dreissenid supplied nutrients, nor is it simple to determine wether or not dreissenids can influence the mobility of catchment derived nutrients once they enter the lake form tributaries or storm sewers. During the thermal bar period, high P concentrations were not commonly observed at Oakville, despite clear patterns in NO_3^- and Cl^- that could be attributed to 16 Mile Creek. The thermal bar has been hypothesized to be important for *Cladophora* by providing conditions suitable for luxury uptake and storage of P by *Cladophora* for later growth in the summer (Rao et al. 2004). However, there are two fundamental problems with this assumption. First, *Cladophora* biomass must be sufficiently large in order to sequester enough P to support the nuisance growths that occur in the summer months. Second, since internal P content of *Cladophora* during the early spring is generally already high (e.g., Higgins 2005, Malkin 2007), further uptake is not likely to occur without an increase in growth (which is likely temperature limited at the ambient temperatures observed in the thermal bar; Hoffmann and Graham 1984) because slow growing, P rich tissue is already saturated and unable to sequester significant P (Auer and Canale 1982b). Therefore, P inputs from the catchment during the thermal bar are unlikely to directly benefit *Cladophora*. Wether or not dreissenid mussels might be effective at trapping and retaining such P inputs during this time

period remains unanswered, but does provide one mechanism for the retention of spring runoff derived nutrients in the near shore.

Unfortunately, it is not possible to discern from the data in this study if a particular shoreline nutrient source might be problematic (see for example the storm sewers and high biomass at Oakville). Exposure to transient P sources such as periodic urban runoff and tributary plumes may provide sufficient P to support a ten fold increase in *Cladophora* biomass (Auer and Canale 1982b) but further site specific work with more frequent temporal sampling and a finer spatial scale analysis would be required to elucidate such effects and quantify their importance to the seasonal pattern of growth (if any). This study does, however, provide a starting point by identifying potential areas of interest where such work could be done.

The results of this study do not support the hypothesis that the current patterns of nuisance biomass of *Cladophora* along these urban shorelines in Lake Ontario is driven by nutrient loading from known point or shoreline based sources. These results are consistent with previous surveys both at the same location (Oakville), other urbanized areas (Port Credit) and other sites in Lake Ontario and Lake Erie that show widespread accumulation of nuisance Cladophora at sites that are characterized by high abundance of dreissenid mussels. Future work at finer temporal and spatial scales would be beneficial for conclusively separating the effects of near shore nutrient sources and dreissenids to *Cladophora* in the Great Lakes.

.

Chapter 5

Spatial structure in a complex coastal zone: New methods for elucidating controls on water quality and phytoplankton

5.1 Overview

Nighttime surveys of a 4 to 6 km long section of western Lake Ontario shoreline were conducted with a small boat equipped with instruments configured to sample at high spatial resolution to assess the spatial patterns of benthic algal distribution, phytoplankton photosynthetic efficiency, dissolved gases (e.g., CO_2 and O_2) and water masses in the shallow areas of the littoral zone (1 to 10 m depth). In early September, after the sloughing of benthic algal growth, downwelling of offshore waters dominated, resulting in a spatially homogeneous water mass characterized by warm surface temperatures, high concentrations of TP (mean 17.71 ± 5.60 μg L^{-1}) and a phytoplankton community with high photosynthetic efficiency (mean F_v/F_m = 0.62). In contrast, during a mid-summer period characterized by exstensive heavy cover of benthic algae, upwelling of cooler metalimnetic waters in the near shore combined with warmer tributary discharge, resulted in a significantly higher spatial variability of water quality, phytoplankton community composition, and phytoplankton photosynthetic efficiency (mean F_v/F_m ~ 0.43), with much of the spatial pattern oriented along shore. Patterns driven by both seasonal variability and physical processes are apparent in the near shore of Lake Ontario. Signals in water column dissolved gases (e.g., CO_2, O_2) at times of high benthic algal cover suggest that patterns in the near shore may be further influenced by biota. Results from this study provide a unique method for characterizing the relevant spatial scales of ecosystem processes in a highly dynamic, complex costal zone.

5.2 Introduction

Coastal ecosystems, both freshwater and marine, are under serious threat from many human related stressors (Niemi et al. 2007). The Great Lakes coastal regions are highly dynamic ecosystems which link the terrestrial and aquatic environments, facilitating the exchange of energy and materials between coastal and pelagic ecosystems (Edsall and Charlton 1997). The coastal regions of the Great Lakes provide a vital role in many ecosystem processes that have lake wide importance. Coastal regions may be important for primary and secondary production (Mackey and Goforth 2005), provide crucial habitat for fish (Randall and Minns 2002), resources for anthropogenic uses (e.g., potable water and cooling water for industry; Edsall and Charlton 1997), and areas with intrinsic recreational value for the near 35 million residents of the costal regions of the Great Lakes (Niemi et al. 2007). These near shore regions are therefore of much greater importance than their relatively limited spatial extent would suggest (Mackey and Goforth 2005). Although much of the previous scientific attention has primarily focused on the open waters of the Great Lakes, there has been a renewed emphasis to include coastal components in lake wide monitoring programs (Neilson et al. 2003), but much of the ecology and dynamics remain poorly understood, especially in the exposed near shore areas (Randall and Minns 2002). This limited understanding of near shore ecology and the processes controlling the variability is therefore a serious impediment to coastal zone management and restoration.

A recurring challenge to ecologists is to understand, and ultimately predict, the factors that determine structure in natural and managed communities (Menge et al. 1997). At present, the understanding of near shore ecology in the Great Lakes is based largely on research at relatively small spatial scales (e.g., transects, or single sampling sites). However, the influence of biotic and physical factors can vary across spatial scales, and the interpretations based on small scale studies often need modification when large scales are considered. Therefore, further elucidation of the determinants of near shore spatial patterns will depend on the study of links between small scale and large scale processes. Presently, the limited understanding of near shore ecology in the open near shore of the Great Lakes is due to the historical bias toward offshore sampling, logistical difficulty conducting adequate surveillance, and the inherent spatial and temporal variability imposed by climate and meteorologically driven physical processes that dominate in the near shore environment (Rao and Schwab 2007). Moreover, the perception of many open near shore environments as “wet deserts” (Brazner and Beals 1997) that support little biodiversity in comparison with other more productive areas (e.g., embayments, wetlands) ultimately makes the definition of the near shore, measurement and interpretation of patterns within it extremely

challenging. Robust assessment and monitoring methods are therefore needed to characterize near shore areas. Without comprehensive knowledge of the spatial variability, conditions in the near shore, and linkages to the open waters of the lake, it is difficult to effectively devise management strategies that lead to demonstrable improvements in near shore conditions.

In this study, methods to systematically sample tracers for water masses (e.g., temperature, conductivity), biological processes (dissolved gases CO_2, O_2), phytoplankton community structure and condition (e.g., spectral fluorescence and active fluorescence), and benthic algae cover and canopy height at high resolution in a highly complex coastal zone were evaluated. Geostatistical methods are employed to evaluate and characterize the spatial structure of the data collected, create snapshot maps of the distribution of the above parameters in the near shore, and test hypotheses about factors that may control the spatial structure in a highly dynamic near shore zone. Specifically, this work seeks to define the relevant scales of spatial variability in phytoplankton community structure and condition in the near shore, and evaluate the potential for recognizable spatial patterns to be imparted by nuisance crops of benthic algae at times of high biomass and cover. To date, such data are not available for the open near shore of the Great Lakes. Consequently, the tools and methods employed in this study may be adapted and applied to other areas to assess the linkages between near shore biological communities and the physical characteristics of the near shore environments.

5.3 Materials and Methods

5.3.1 Study site and sampling design

Nighttime (2200 hrs to 0600 hrs) surveys were conducted along the Oakville shoreline in western Lake Ontario (Figure 5.1) on two dates (September 14-15 2006, and June 25-26 2007). This site is underlain by boulder and cobble substrate and supports moderate abundances of dreissenid mussels (~ 3500 m^{-2}; Ozersky et al. 2009) and heavy growth of *Cladophora* is common during the summer months (Chapter 2, Chapter 3, Malkin et al. 2008).

Surveys were performed on a 21 ft aluminum vessel outfitted with two acoustic transducers and a flow through system set up to measure surface water (~ 0.3 m below surface) pCO_2, conductivity, temperature, dissolved O_2, and both spectral and variable chlorophyll *a* fluorescence. In 2006, the acoustic survey was completed during daylight hours. The night time survey covered a greater range of depths (to 30 m) and transects were run perpendicular to shore, spaced between 75 and 150 m apart. In 2007 both the acoustic and night time survey were conducted concurrently, running transects parallel to shore, spaced ~ 50 to 75 m apart. All surveys were conducted with the vessel traveling between 1.8 and 2.3 m s^{-1}. Acoustic data to characterize benthic algal growth was analyzed using a Matlab based GUI (Chapter 2).

5.3.2 Flow through system and set-up

All underway data (acoustics excluded) were measured on inflowing water from a 12 V pump (Cyclone pump, Proactive Environmental Products, Bradenton FL, USA, 10 L min^{-1}) attached to an intake pipe (18 mm diameter), mounted on the bow of the vessel. The intake pipe was located ~ 0.3 m below the surface and ~ 0.5 m in front of the vessel so as to sample water that was not disturbed by boat passage. The intake pipe and was covered with nylon screen (~ 2.3 mm aperture size) to prevent large clumps of detached *Cladophora* and other detritus from fouling the system. Lake water was pumped through 10 mm ID opaque polyethylene tubing to a stainless steel pre-filter (124A-SC, 100 μm mesh, Spraying Systems Co. Chicago IL, USA) before being diverted to a three way splitting valve for diversion to a series of probes and other instruments (Figure 5.2). During the surveys, a DGPS (JRC212, Japan Radio Co.) provided fix updates at 1 second intervals (positional error < 5 m; Japan Radio Co.). Because of different sensitivities and reporting cycles with different GPS units, I elected to use the DGPS data to co-locate all data collected by other instrumentation. All instrument clocks and laptop clocks were synchronized to the clock time from the DGPS satellites using NMEATime v1.2 (VisualGPS LLC, Orange, CA).

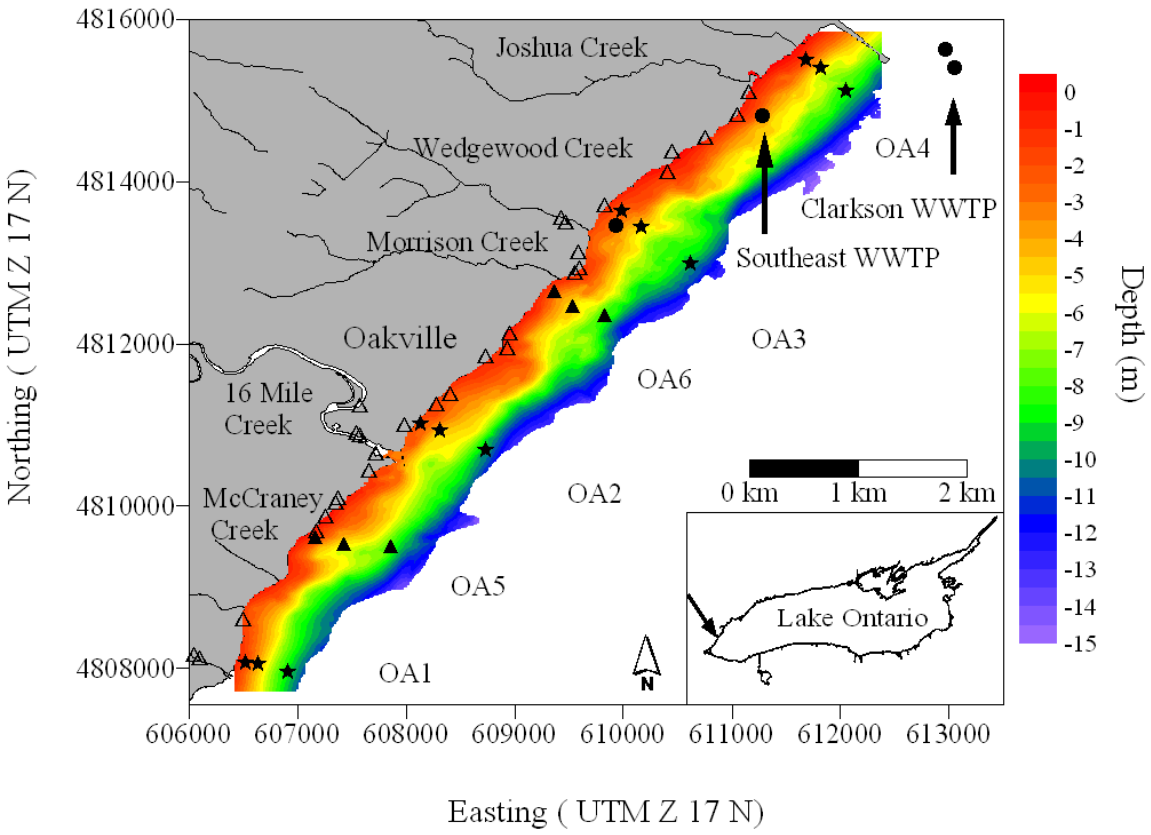

Figure 5.1. Map of the study site at Oakville, ON. Inset panel denotes location of the study site in Lake Ontario. Sites sampled for water chemistry in 2006 are denoted by (★). Sites sampled for water chemistry in 2007 include transects OA1, OA2, and two additional transects (OA5, and OA6) denoted by (▲). Storm sewers are represented on the map by (△) and municipal waste water treatment plant outfalls by (●).Note only active municipal WWTP outfalls are labeled.

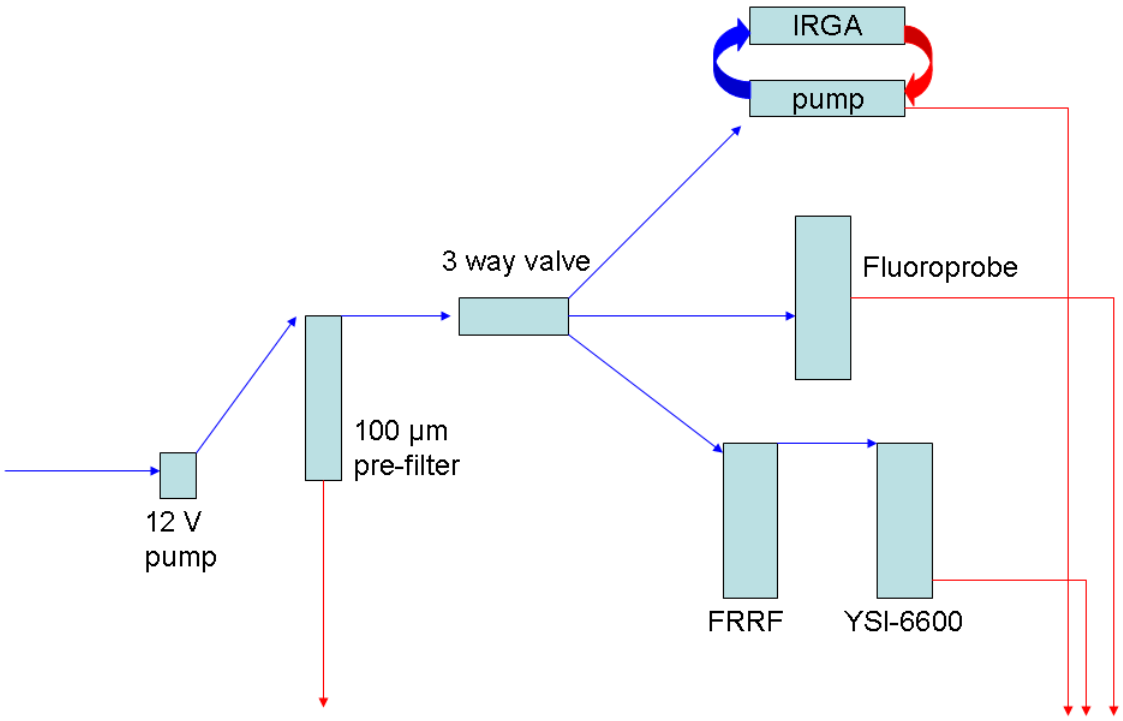

Figure 5.2. Schematic diagram of the flow through system employed during the study. Note that for the 2006 survey, the Fluoroprobe and YSI-6600 were not online due to logistical problems. Blue arrows indicate incoming lake water (intake pipe located ~ 0.3 m depth, 0.5 m in front of vessel). Red arrows indicate outflowing water that was diverted back into the lake. Note that the peristaltic pump for the IRGA also contained an air inlet for measuring atmospheric CO_2 prior to commencing water flow.

pCO_2

Measurements of atmospheric, surface pCO_2 and water temperature were made using an apparatus designed by Morris Holoka and Ray Hesslein (Department of Fisheries and Oceans, Winnipeg, Canada). This unit consisted of a datalogger (CR10X, Campbell Scientific, Edmonton, Alberta), a peristaltic pump, and a non-dispersive infra-red gas analyzer (IRGA; Li-820, Li-Cor, Lincoln, Nebraska, USA). Inflowing water from the intake pump flowed first past a thermistor (P107, Campbell Scientific) then through a membrane contactor (Liqui-Cel, Membrana, Charlotte, NC, USA). The membrane contactor extracted the dissolved gas by increasing the pressure of the air stream, and the extracted gas was circulated using an air pump via a separate system, first through Nafion tubing (PermaPure Toms River, NJ, USA) to remove moisture, then via tygon tubing through the IRGA which measured the molar fraction of CO_2 (xCO_2) of the gas stream and gas pressure (atm). Gas removed from the water, once passed through the IRGA was returned to the outflowing water stream before being pumped over the side of the vessel. Measurements of water temperature, gas pressure and xCO_2 were recorded on the data logger at 20 second intervals. The data logger was also connected to a solenoid which directed either atmospheric air or the airstream from the membrane contactor into the IRGA, a reverser which designated the direction of water flow, and a pair of mechanical switches to control these components. The peristaltic pump pushed water through at a rate of 1.2 L min^{-1}, varying slightly with battery charge. The water volume housed in the tubing was never more than 0.02 L. The IRGA analyzer was calibrated for a range of 0 to 1000 ppm on a bi-weekly basis using a CO_2 standard gas (Praxair Inc., Cambridge, ON.).

Conductivity, dissolved O_2, water temperature

Measurements of conductivity, temperature (YSI 6560), and dissolved O_2 (YSI-6150 ROX DO) were measured using a YSI-6600 multiprobe. The YSI probe sensors were immersed into a 33 cm long cylinder of ABS pipe (closed at the bottom end; 14 cm diameter) and connected to one inflowing water line. The displacement volume of the YSI probes and instrument body was sufficient to keep the volume of water contained in the ABS pipe to less than 1 L, allowing for complete flushing within 15 seconds. Recorded data were therefore averaged over 15 second intervals prior to analysis and merging with the DGPS string.

Spectral Fluorescence measurements

Measures of phytoplankton pigment fluorescence were made at 5 wavelengths using a Fluoroprobe (bbe Moldaenke, GmbH). The fluoroprobe contains five light emitting diodes (450, 525, 570, 590 and 610 nm) for excitation of pigments present in phytoplankton and a UV-blue

LED (370 nm max, range 350 to 440 nm) for the differential excitation and correction for fluorescence emitted by dissolved organic matter (DOM). The excitation spectrum is compared to fingerprint curves for four different phytoplankton groups based on their response to multi-wavelength excitation, and is reported as chl a ($\mu g\ L^{-1}$) equivalents (Beutler et al. 2002). Although there are conflicting reports on the efficacy of the Fluoroprobe at distinguishing phytoplankton taxa in the Great Lakes (e.g., Ghadouani and Smith 2005, Pemberton et al. 2007), the use of the Fluoroprobe in this study was not specifically to evaluate the accuracy of the measurements, but to monitor substantial changes in spectral fluorescence that may indicate significant changes in community composition. In addition, I hypothesized that the UV-blue LED would be moderately effective at identifying fluorescent compounds of terrestrial origin near substantial tributaries (bbe Moldaenke, 2004). The Fluoroprobe was immersed into a pail (volume of water ~ 2.3 L) and the flow rate into the pail was adjusted to provide a flushing time of ~ 15 to 20 seconds. The Fluoroprobe was programmed to measure every 5 seconds, and data aggregated over 15 second intervals prior to merging with the DGPS string.

Active fluorescence measurements

Measurements of active fluorescence of phytoplankton were made using a fast-repetition rate fluorometer (FRRF; Chelsea Technologies Group, UK). Maximal and minimal fluorescence, F_m and F_0 respectively, were measured on water from the flow through system (Figure 5.2) passed through darkened tygon tubing (3/4" ID) into the dark chamber of a FRR fluorometer (Mark I, Chelsea Technologies Group, SN 182055) operated in benchtop mode. The FRRF measurement protocol consisted of a gradient of pump flashes that delivered 100 excitation flashes within 280 µs, and 20 relaxation flashes within 50 µs. A series of 8 flash sequences were internally averaged and repeated every 5 seconds. The dark chamber under normal use has a flushing time of 0.2 to 1 second, depending in configuration and profiling speed. The three way valve system was used to adjust the flow rate so that complete flushing occurred within ~ 2 seconds, which is sufficient time for 8 acquisition sequences before complete flushing occurs. The ratio F_v/F_m (where $F_v = F_m - F_0$) measures the maximal quantum efficiency of photosystem II (PSII) (Kolber and Falkowski 1993). F_v/F_m is considered to reach a theoretical maximum value of 0.65 when all PSII reaction centers are open (Kolber and Falkowski 1993). Variability in F_v/F_m is associated with the physiological condition of the phytoplankton (Olaizola et al. 1996) and has been linked to nutrient limitation in some waters (Geider et al. 1993). The functional absorption cross section of PSII (σ_{PSII}) is a measure of photochemical target size of PSII and is the product of absorption by the suite of PSII antennae pigments and the probability that an exciton within the antenna will cause a photochemical reaction (Kolber et al. 1998). Considerable taxonomic

variability of σ_{PSII} is observed; and, in addition, other factors such as photoacclimation and nutrient status can also affect this parameter (Greene et al. 1991, Kolber et al. 1998, Suggett et al. 2004). During daylight hours, dark adapted fluorescence may be affected by the activation of non-photochemical pathways, depending on the duration of the dark adaption period. Because these surveys were conducted at night, phytoplankton were considered to be already dark adapted, and measures of F_v/F_m reported in this study are somewhat unique since they represent "true" dark adapted (ie. night-time) measures of photosynthetic efficiency because phytoplankton are not containerized for the purposes of dark adaption prior to measurement. Downloaded FRRF data were analyzed using the V6 software (run in Matlab; provided by Sam Laney), which represents an updated version of the V5 software (Laney 2003). Raw data were quality controlled by eliminating any data collected on gains higher than 16, and during times when the DGPS unit was not recording. F_v/F_m was calculated on data processed to account for instrument noise (IRF) but not for blanks (see below).

Effect of blanks

Determination of an appropriate fluorescence blank, i.e. the signal associated with the absence of chlorophyll *a*, is recognized as an important issue in oceanographic research, particularly in low chlorophyll waters (Cullen and Davis 2003). Because this study had a significant spatial component to it, collecting an equivalent number of sample blanks was not possible. I therefore sought to evaluate the effect of blanks on survey data by collecting blanks at transect stations (Figure 5.1), which cover a range of depths and presumably the conditions encountered during the survey. Samples for blanks were collected from the outflow of the FRRF dark chamber into 60 mL dark polycarbonate bottles, and stored in a cooler. Upon return to the laboratory, blanks were filtered using a peristaltic pump and a pleated cartridge filter (polysulfone membrane, pore size 0.2 μm; Pall Corporation, Ann Arbor MI, USA). Filtered lake water blanks were run on the same instrument gain as the survey data was collected on (gains 4 and 16; except in the mouth of 16 Mile Creek, where the FRRF was ranged to a gain of 1). No significant differences in baseline or maximal fluorescence were found between the cartridge filtration procedure described above at pressures below ~ 3 mm Hg, and gravity filtration with a 0.2 μm polycarbonate filter (D. Depew, unpubl. data). Fluorescence from the filtered lake water blanks averaged between 3.6 and 32.5 % of the measured fluorescence signal, and increased at levels of low sample F_0 and F_m (Figure 5.3). This dependence was similar to that observed by (Suggett et al. 2006) and has been observed in Lake Erie as well (G.M. Silsbe, University of Waterloo, Waterloo, ON, pers, comm.). Values of F_0 and F_m were corrected using the equation from Figure 5.3 prior to computation of F_v/F_m.

5.3.3 Water chemistry

Water samples to characterize the ambient chemical and nutrient conditions at the time of the survey were collected and analyzed for total and soluble phosphorus (TP and SRP), nitrate (NO_3^-), chloride (Cl^-), ammonium (NH_4^+), phytoplankton chlorophyll a (chl *a*), particulate carbon, nitrogen and phosphorus (Part C,N,P). These samples were collected in 4 L polyethylene carboys at the same transect stations where the FRRF blanks were collected (see Figure 5.1). Upon return to the laboratory, samples were processed as described in Chapters 3 and 4.

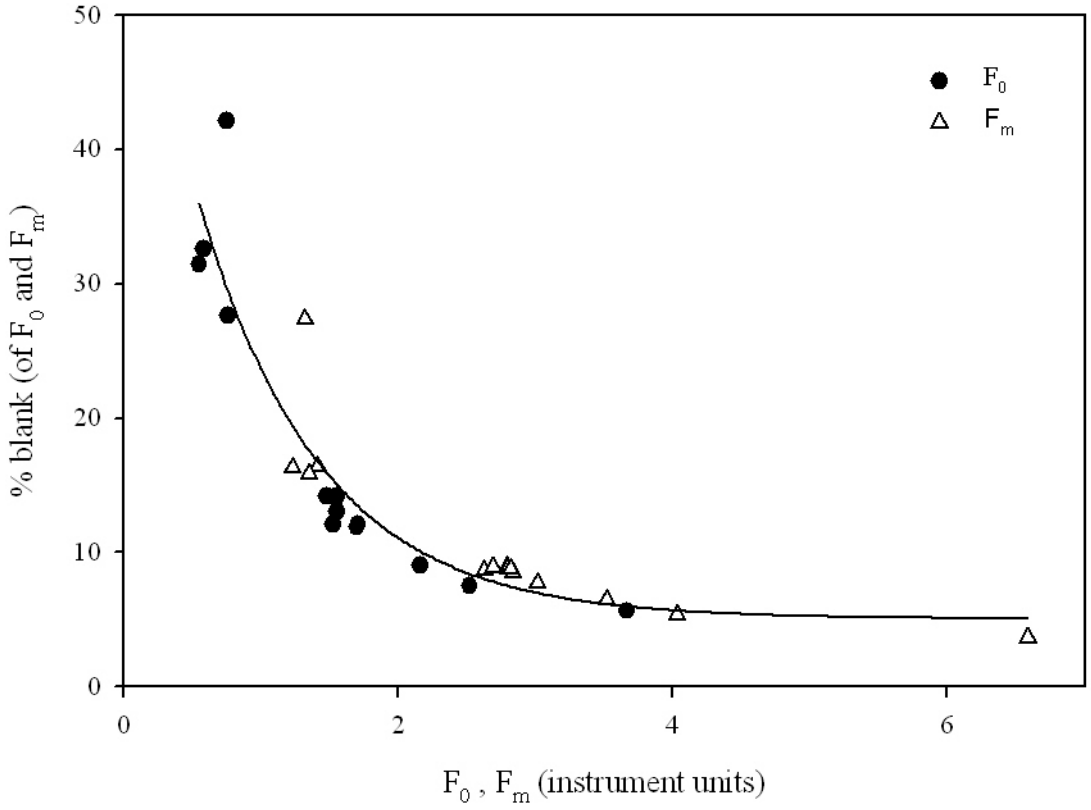

Figure 5.3. Blank fluorescence as a percentage of sample fluorescence from the surveys in 2006 and 2007. One equation was fit to the data, $\%Blank_F = 5.084 + 57.38e^{-1.13SampleF}$, n=28, $p<0.0001$.

5.3.4 Geostatistical Analyses

The fundamentals of geostatistics, with emphasis on the assumptions and methodology involved are well explained in several publications (e.g., Isaaks and Srivastava 1989, Cressie 1991, Webster and Oliver 2001), so only a short summary will be provided here. In this study, I employed a spatial correlation function called the "semivariogram" (Cressie 1991) to characterize the spatial autocorrelation of the data collected. The semivariogram is estimated from the data, taking into account the spatial position of the samples by the following equation;

$$\gamma(h) = \frac{1}{2N(h)} \sum_{i=1}^{N(h)} \{Z(x_i) - Z(x_i + h)\}^2 \qquad (5.1)$$

where $Z(x_i)$ is the value of the variable Z at location x_i, h is a lag distance over which the local average is taken and $N(h)$ is the number of point pairs at the lag distance (h). The semivariogram is the average of the euclidean distance between pairs of samples (h) plotted against average variance at distance h. Once the semivariogram is computed, a function (the theoretical spatial covariance function or semivariogram model) is fitted to the empirical semivariogram through an automated fitting procedure. In this study, I employed the weighted least squares method of fitting the semivariogram model as it typically defines the behaviour of the semivariogram model at the origin most clearly, which is essential for prediction (Cressie 1991). I used either spherical or exponential semivariograms for all data given by the follwing equations;

$$\gamma(h;\theta) = \begin{Bmatrix} 0, & h = 0 \\ C_0 + C_s\ ((3/2)(\|h\|/\alpha_s) - (1/2)(\|h\|/\alpha_s)^3), & 0 < \|h\| \le \alpha_s \\ C_0 + C_s, & \|h\| \ge \alpha_s \end{Bmatrix} \qquad (5.2)$$

$$\gamma(h;\theta) = \begin{pmatrix} 0, & h = 0 \\ C_0 + C_e(1 - \exp(-\|h\|/\alpha_e)), & h \neq 0 \end{pmatrix} \qquad (5.3)$$

These spatial covariance models are defined by three essential parameters: the nugget (C_0) (indicating the variance not explained by the spatial model), the sill C_s (indicating the variance explained by the spatial model) and the range α (distance beyond which spatial autocorrelation is no longer significant). After computation of the semivariograms for each of the respective variables, the spatial models were used with kriging (either ordinary kriging; OK, or kriging with external drift; KED; see Chapter 1 for a discussion of the different kriging variants).

Mantel test

In addition to characterizing the spatial structure of the data collected to produce maps, I sought to assess the degree of correspondence between FRRF derived photosynthetic parameters

(e.g. F_v/F_m and σ_{PSII}) and other data collected during this study (e.g., % algal cover, algal stand height, phytoplankton classes as measured by Fluoroprobe, water temperature, conductivity, pCO_2 and dissolved O_2). To accomplish this, a partial Mantel test (Smouse et al. 1986) was employed. The partial Mantel test is a nonparametric partial regression approach based on dissimilarity matrices of the predictor and response variables rather than the variables themselves. The advantage of the partial Mantel test is that it can explicitly account for spatial autocorrelation in both predictor and response variables as well as inter-correlations among possible predictor variables. While Mantel and partial Mantel tests have been used for causal modelling (Legendre and Trousselier 1989), in this study, results from the partial Mantel tests served to test alternative hypotheses governing the spatial patterns of F_v/F_m and σ_{PSII}. Euclidean distances were computed for the geographic distance matrix (Universal Transverse Mercator Zone 17N, NAD 1983) and the Manhattan distance was used to construct distance matrices for biological and environmental variables (as recommended in Legendre and Legendre 1998). Partial Mantel tests were performed using the package *ecodist* (Goslee and Urban 2007) in the statistical software "R" (R Core Development Team 2007). The significance of the partial Mantel tests was assessed using a permutation procedure using 10,000 permutations (Jackson and Somers 1989) as outlined in Legendre (2000), and the p value was adjusted for the number of tests conducted (e.g., Bonferroni adjustment, α/n).

5.4 Results

September 2006 survey

September 2006 was characterized by relatively warm surface temperatures (18 to 20 °C) (Figure 5.4a) with little spatial variability, as noted by the very low sill value and large range parameter (nearly 4 km) (Table 5.2). A weak gradient of cooler temperatures toward the shore is consistent with more rapid cooling of shallow waters expected to occur seasonally at this time. Surface pCO_2 varied little across the survey area, but was generally above atmospheric saturation (atmospheric ~ 394 to 407 ppm) for much of the area surveyed (Table 5.2; Figure 5.4b). Surface pCO_2 appeared to increase toward the Southeast WWTP outfall, and was also higher than at the outflow of Wedgewood and Morrison Creeks (Figure 5.4b), and within the mouth of 16 Mile Creek (Figure 5.4b).

Despite the apparent low spatial variability in surface temperatures, considerable variability was observed for concentrations of TP and SRP. TP and SRP were generally elevated across all four transects (OA1, OA2, OA3, OA4) but the highest TP (26.02 ± 2.12 µg L^{-1}; mean and stdev) and SRP (9.70 ± 2.50 µg L^{-1}) concentrations were measured at transect OA4 which is near two WWTP outfalls and Joshua Creek (Figure 5.1). Concentrations of Cl^- and NO_3^- displayed considerably less variability than P, but NO_3^- concentrations still spanned a range of nearly 150 µg L^{-1} along this relatively small segment of shoreline. Although nutrient concentrations were high (Table 5.1) chlorophyll a was not, averaging 0.43 µg L^{-1} (Table 5.1). Particulate nutrient ratios (e.g. C:P and N:P) indicated that despite this relatively low biomass (chl a), phytoplankton communities did not appear to be strongly P limited based on the thresholds defined by Guildford and Hecky (2000) (Table 5.1).

Spatial variation was present in both F_v/F_m and σ_{PSII} (Figure 5.4c and d). The semivariogram parameters for both F_v/F_m and σ_{PSII} indicated the presence of a large nugget variance (Table 5.2). I interpret this high proportion of unexplained variance as a result of the low chlorophyll a concentration that was present at this time (Table 5.1). As a result of the high nugget variance, there was little spatial variation in F_v/F_m and σ_{PSII} beyond the mouth of 16 Mile Creek (Figure 5.4c and d). The lowest values of both F_v/F_m and σ_{PSII} were measured in the mouth of 16 Mile Creek (F_v/F_m ~ 0.31, σ_{PSII} ~ 121 x 10^{-20} m^{-2} $photon^{-1}$; Figure 5.4c and d), but quickly increased beyond the harbor to average values for F_v/F_m of ~0.62 and σ_{PSII} of ~ 365 x 10^{-20} m^{-2} $photon^{-1}$. A small decline in F_v/F_m to values near 0.55 was observed toward transects OA3 and OA4, in the vicinity of the WWTP outfall and nearby tributaries, which may have been due to a higher level of pheophytin:chlorophyll a (Figure 5.6). σ_{PSII} appeared to increase in the same area,

but the relatively high nugget variance (Table 5.2) obscures much of the spatial variation in σ_{PSII} (Figure 5.4d).

The acoustic survey for *Cladophora* was completed during the preceding daylight hours, and covered a more restricted area (only from 1 m depth contour to 10 m depth contour) than the nighttime survey (out to 30 m contour). Attached biomass of *Cladophora* was below the detection limit for the hydroacoustics at this time because much of the algal material that was present in earlier surveys (e.g., Chapter 4) had detached (personal observation). Accordingly, maps showing the absence of any benthic algae have not been created.

June 2007 survey

In contrast to conditions the previous September, heavy cover of *Cladophora* was evident along much of the shoreline in June, and covered much of the lakebed between 1.5 m depth and 7 m depth, before falling below the detection limit of the acoustic system in deeper waters. In some areas, *Cladophora* sp. mats exceeded 30 cm in thickness (Figure 5.5 a and b). Surface temperatures measured during the June survey present a far more complex pattern than that observed in September, with cooler temperatures (11 to 16 °C; Figure 5.5c) and a far greater spatial variability (much higher sill parameter, and a much lower range; Table 5.3). The higher spatial variance appears to be related to two factors; 1) warm water entering the lake from the mouth of 16 Mile Creek and possibly other tributaries along the shore, and 2) cooler water immediately adjacent to shore (Figure 5.5c). This pattern of surface temperature is highly suggestive of warmer water trapped near the surface overlying cooler water that is present after an upwelling event. Conductivity generally showed the same response as temperature (i.e. high sill indicating high spatial variance, and a range parameter similar to that observed for temperature; Table 5.3 and Figure 5.5d), and there were pockets of low conductivity associated with areas of cooler water (Figure 5.5d). The pattern of UV fluorescence from the Floroprobe (Figure 5.5c) also suggests some influence of tributaries, but the spatial patterns are not coherent with those of temperature and conductivity (Figure 5.5c).

Surface pCO_2 was far more variable that the prior September, although the range of variation between the two surveys was comparable (Table 5.3). In contrast to pCO_2 during the September 2006 survey, here, pCO_2 was widely undersaturated, particularly in shallow areas, although it once again peaked in the mouth of 16 Mile Creek as in September (Figure 5.5f). Dissolved O_2 displayed an opposite pattern to pCO_2, remaining above saturation for much of the survey area (except in the mouth of 16 Mile Creek), but was particularly elevated along shore, at depths less than 3 m (Figure 5.5h). Dissolved O_2 also varied over much shorter distances

compared to pCO_2 (see Table 5.3), and interestingly displayed no correspondence with chl a (a proxy of phytoplankton biomass).

Nutrient conditions were significantly different during this survey when compared to the previous September survey (Table 5.1). Concentrations of TP and SRP were significantly lower and did not show an increasing trend toward the northeast as in September, although the survey area was smaller than that in 2006. Despite lower P concentrations that in September, phytoplankton chlorophyll a was on average 4 fold higher during the June survey, and stoichiometric ratios (C:P and N:P) indicated a state of moderate P deficiency in the phytoplankton. NO_3^- concentrations, although higher than the previous September, varied by a nearly identical amount (Table 5.1; CV ~ 15%).

F_v/F_m and σ_{PSII} displayed less overall variability than in September (as estimated by the sill; Table 5.3). Part of the reduced variability is due to a higher chlorophyll a concentration which reduced the nugget variance to 0 for F_v/F_m and to 525 for σ_{PSII} (Table 5.3), but also the range of F_v/F_m and σ_{PSII} was more constrained than that observed in September (Figure 5.5h and i). Average F_v/F_m throughout much of the survey area was ~ 0.43. Unlike the previous September, F_v/F_m in the mouth of 16 Mile Creek was higher (~ 0.58) than values measured in the lake. Several shore parallel streaks of low F_v/F_m were observed, some in the vicinity of tributaries, but one area near the 10 m contour at the northeast edge of the survey grid. σ_{PSII} was generally higher than values measured in September (mean 413 x 10^{-20} m^{-2} $photon^{-1}$). σ_{PSII} in 16 Mile Creek did not fall below 300 x 10^{-20} m^{-2} $photon^{-1}$, and generally appeared to be higher toward the outer edge of the survey area (Figure 5.5i).

Spectral fluorescence signatures from the Floroprobe indicated the presence of a alongshore plume of increased chlorophyll a that originated at the north edge of the survey area and extended down the coastline at depths ranging from shore to the 5 m contour (Figure 5.5j). Based on the taxonomic differentiation assessed by the Floroprobe, the algal taxa within the high chlorophyll plume were mainly chlorophytes (Figure 5.5k) diatoms (Figure 5.5l) and cyanophytes (Figure 5.5n). Algal taxa that were not abundant within the plume consisted primarily of cryptophytes (Figure 5.5m).

Factors affecting spatial variability of F_v/F_m and σ_{PSII}

The partial Mantel tests found significant associations between F_v/F_m and σ_{PSII} with surface temperature in 2006 (Table 5.4). For F_v/F_m, this indicated that F_v/F_m declined toward shore, where surface temperature was cooler. For $\sigma_{PSII,}$ this indicated a decline in σ_{PSII} areas of cooler water (e.g. near the shore). In 2007, partial Mantel tests again found a significant

association between F_v/F_m, σ_{PSII} and temperature. This indicates that water masses (in this case, shore parallel parcels) were characterized by similar values of F_v/F_m and σ_{PSII}. A significant association between F_v/F_m, σ_{PSII} and depth also confirms the similar values were oriented in a shore parallel pattern. A significant association was found between F_v/F_m and pCO_2, but the same pattern did not exist for σ_{PSII}. Both F_v/F_m and σ_{PSII} were also significantly associated with UV fluorescence (Table 5.5). No significant associations were observed between F_v/F_m and σ_{PSII} with percent algal cover, algal canopy height, phytoplankton classes (as measured by the Fluoroprobe) conductivity or dissolved O_2 (Table 5.5).

Table 5.1. Summary of environmental characteristics at the study site during the night surveys. Bolded variables indicate significant differences between the two surveys (two-way ANOVA; depth + year factors, $p < 0.05$). Note that significant differences were not detected between 2, 5 or 10 m station depths for any variables, thus significant differences refer to differences between September 2006 and June 2007 only. Note samples size "n" is 12 for both 2006 and 2007.

Year	*Variable*	*min*	*mean*	*max*	*CV*
2006	**Chl a (µg L^{-1})**	0.29	**0.43**	0.67	30 %
	TP (µg L^{-1})	11.80	**17.71**	27.93	32 %
	SRP (µg L^{-1})	2.95	**7.55**	12.24	29 %
	NO_3 (µg L^{-1})	187.30	**237.93**	323.50	17 %
	Cl^- (mg L^{-1})	20.28	21.35	22.90	10 %
	Part_C (µg L^{-1})	181	**231**	304	19 %
	Part_N (µg L^{-1})	26	**35**	54	26 %
	Part_P (µg L^{-1})	2.95	**4.45**	7.68	29 %
2007	**Chl a (µg L^{-1})**	0.37	**1.32**	1.99	35 %
	TP (µg L^{-1})	7.72	**11.66**	14.74	19 %
	SRP (µg L^{-1})	0.99	**1.64**	2.47	32 %
	NO_3 (µg L^{-1})	234.21	**307.36**	397.09	15 %
	Cl (mg L^{-1})	ND	ND	ND	
	Part_C (µg L^{-1})	358	**454**	557	13 %
	Part_N (µg L^{-1})	57	**72**	80	9 %
	Part_P (µg L^{-1})	4.69	**5.96**	7.94	16 %

*Note ND implies No data available

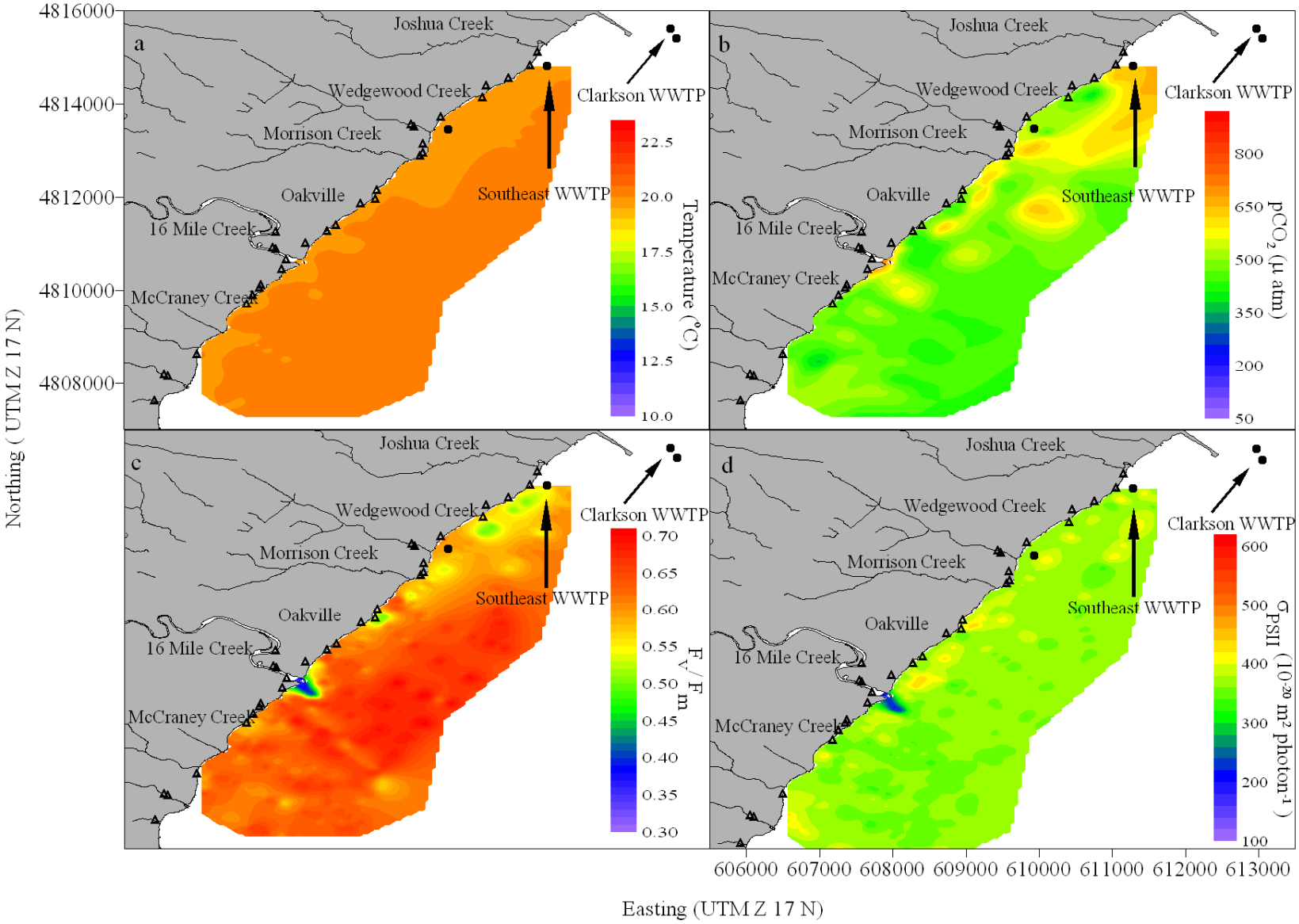

Figure 5.4. Kriged surfaces of a) Water Temperature, b) pCO_2, c) F_v/F_m and d) σ_{PSII} during the September 2006 survey.

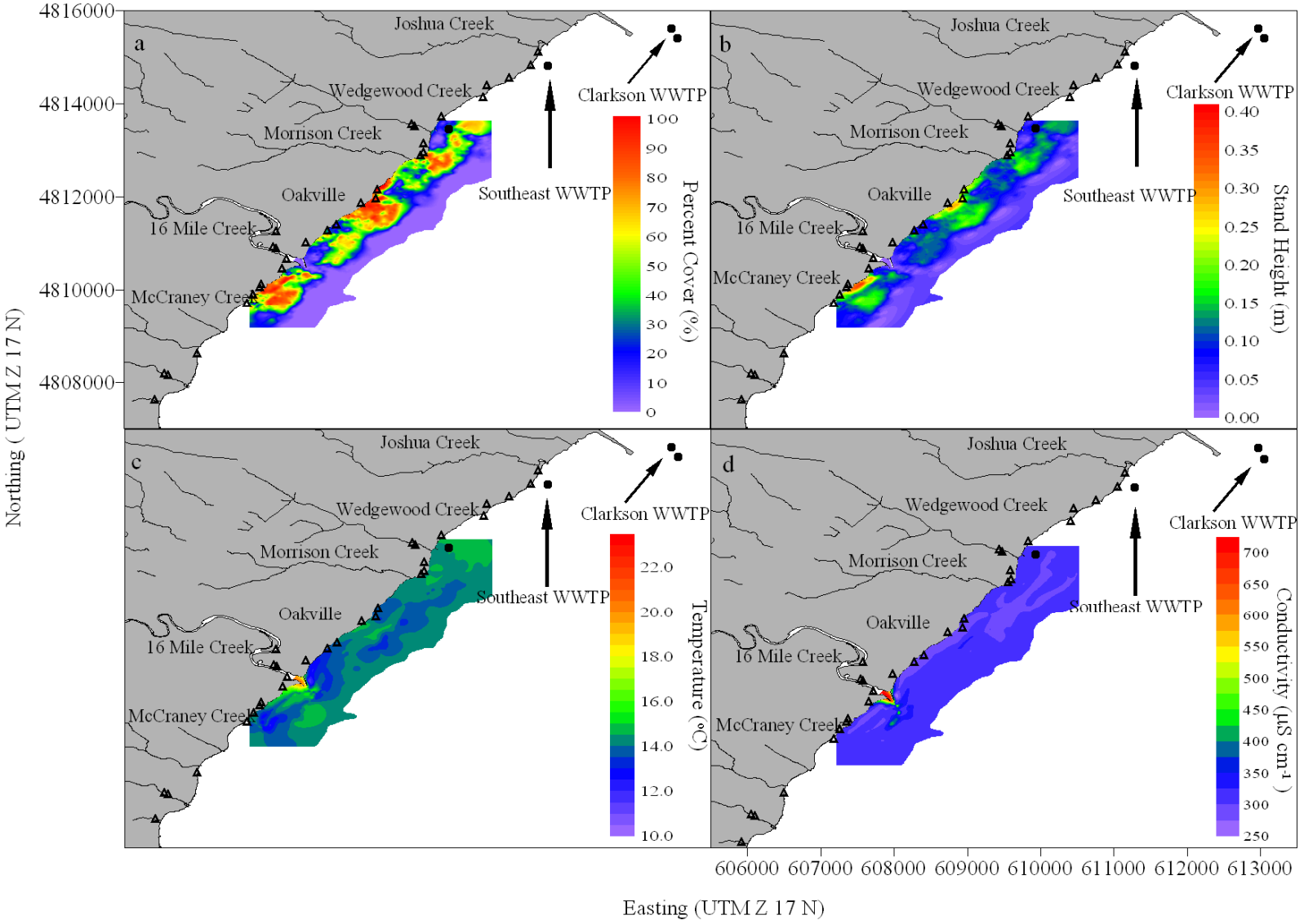

Figure 5.5. Kriged surfaces of a) % algal cover, b) algal canopy height , c)surface temperature, and d) Conductivity during the June 2007 survey.

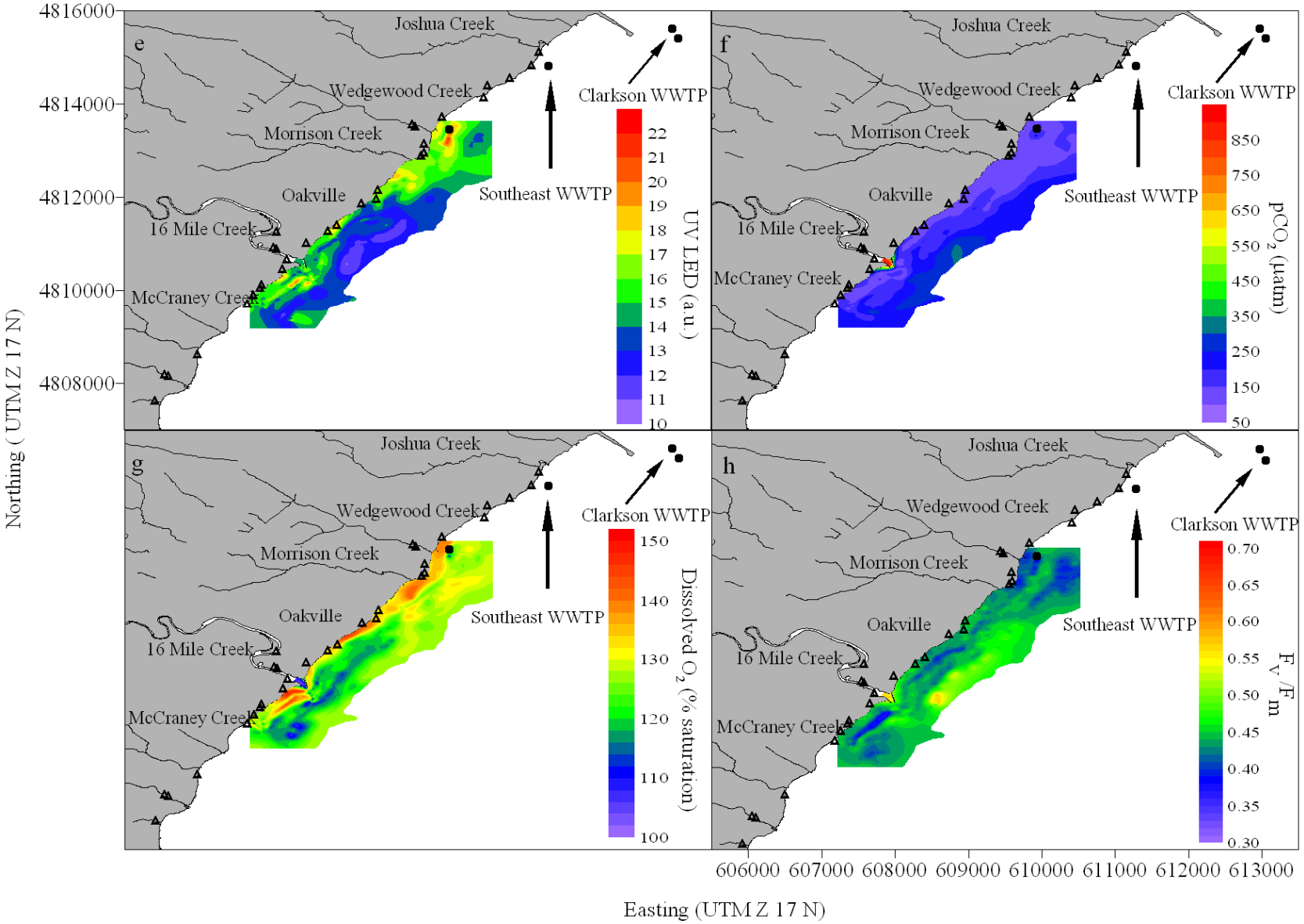

Figure 5.5.cont Kriged surfaces of e) UV LED fluorescence (from Fluoroprobe), f) pCO_2 , g) dissolved O_2 saturation , h) F_v/F_m during the June 2007 survey.

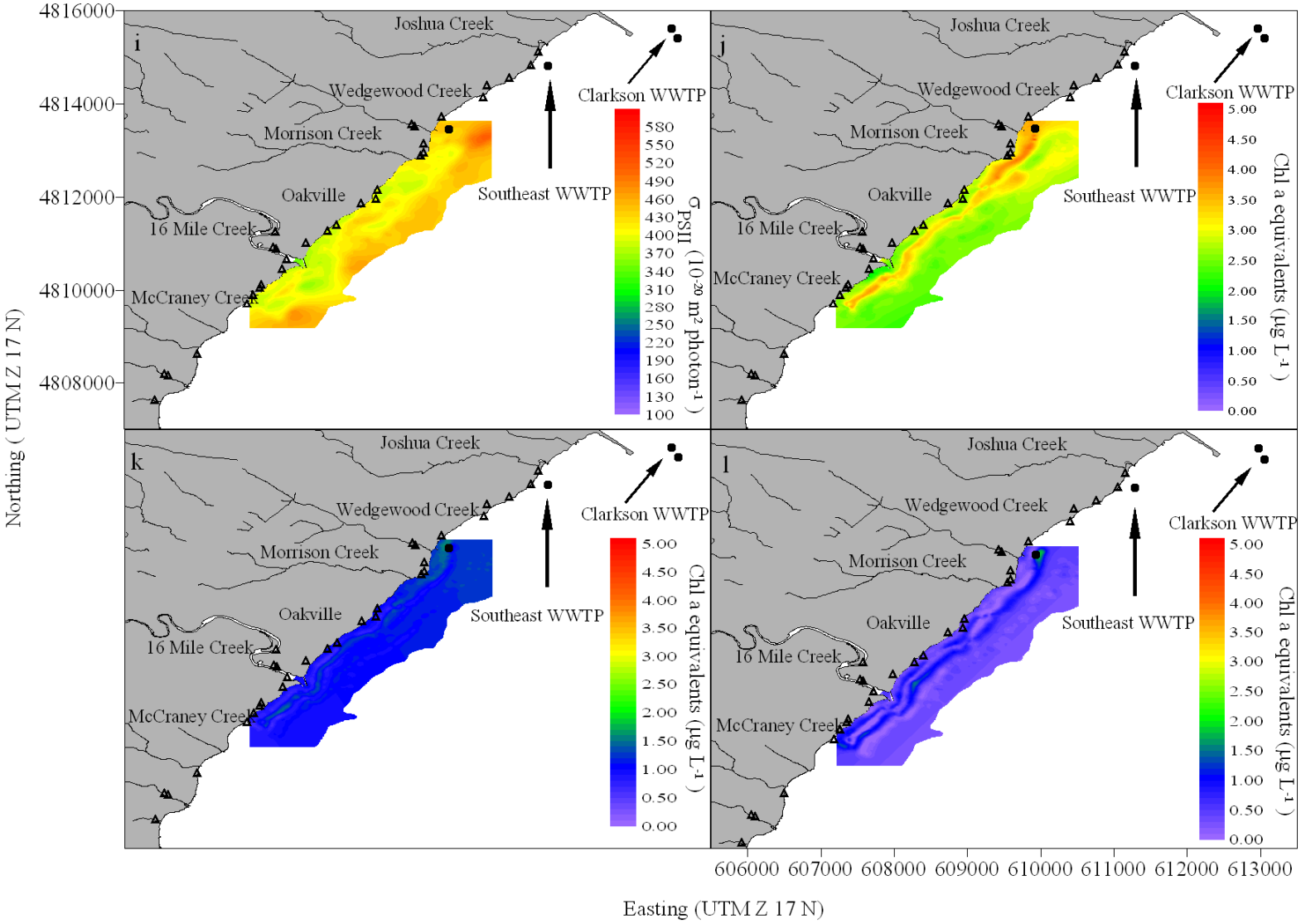

Figure 5.5. cont.. Kriged surfaces of i) $\sigma_{PSII,}$ j) floroprobe estimated total chlorophyll a, k) floroprobe estimated chlorophyte algae, l) floroprobe estimated diatom algae during the June 2007 survey. Note that panels j,k and l represent pigment responses suggestive of the algal taxa.

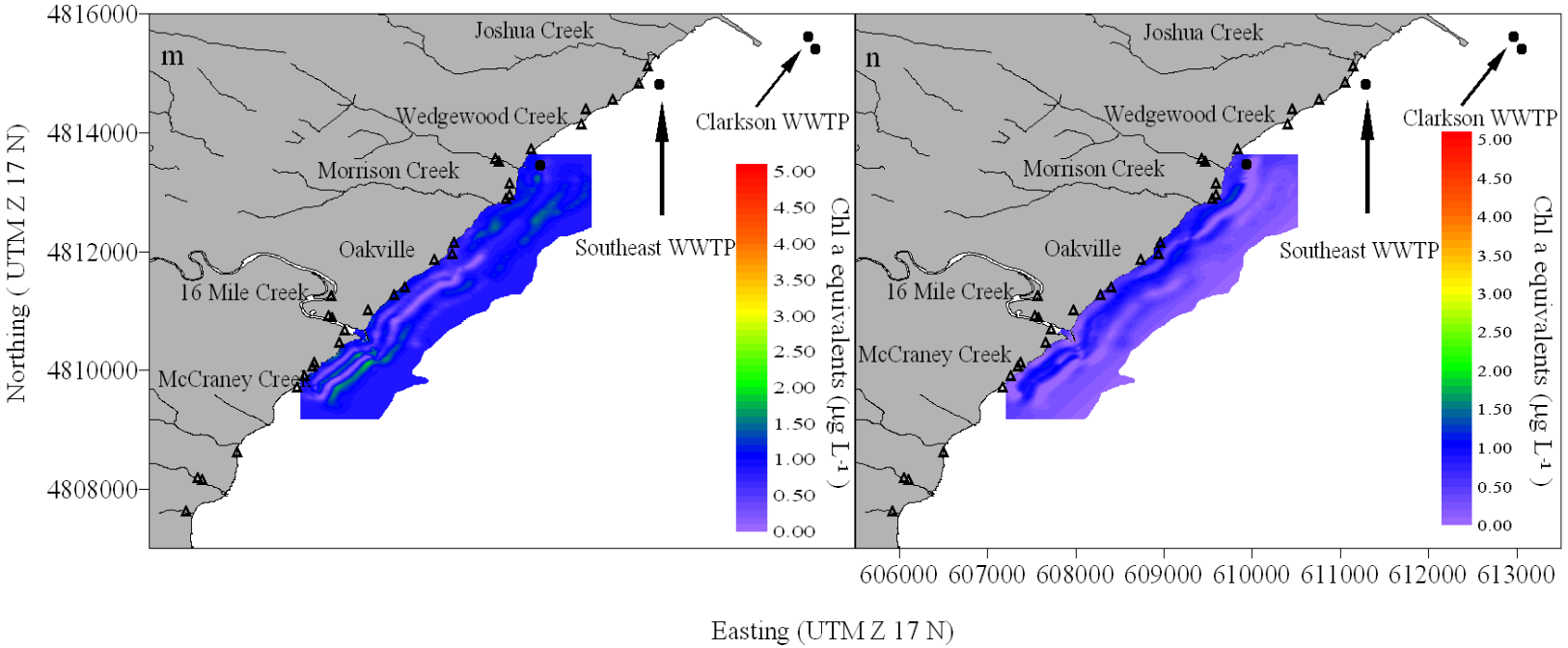

Figure 5.5 cont. Kriged surfaces of m) floroprobe estimated cryptophyte algae, n) floroprobe estimated cyanophyte algae during the June 2007 survey. Note that panels m and n represent pigment responses suggestive of algal taxa.

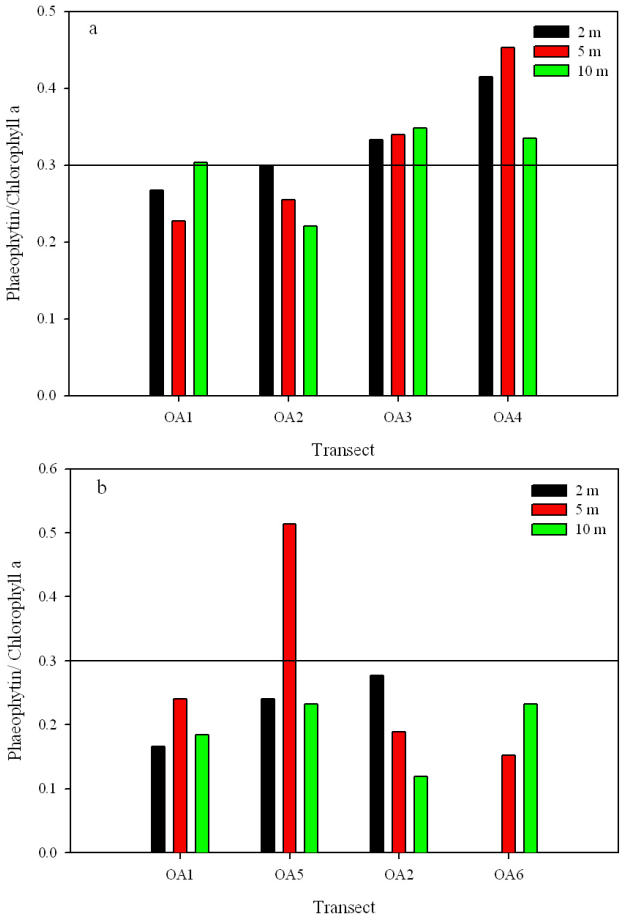

Figure 5.6. Bar plots of phaeophytin :chlorophyll a ratio for the transect stations in 2006 (a) and 2007 (b). Note: transects names correspond to those in Figure 4.1. and proceed from southwest to northeast. Solid line denotes a ratio of 30% above which corrections to F_v/F_m are suggested.

Table 5.2 Semivariogram model parameters and cross validation statistics for variables measured during the September 2006 survey. Covariate identifies the trend variable if KED was used, otherwise implies OK. C_0 is the nugget, C is the sill, α is the range (m), Sp is the spatial dependency, and model defines the semivariogram function.

Variable	***Covariate***	***C_0***	***C***	***α***	***Sp***	Model
Temperature		0.003	0.06	3820	94%	Exp
pCO_2	Easting + Northing	0	3362	1043	100%	Exp
F_v/F_m		2.5×10^{-3}	3.2×10^{-3}	239	56 %	Exp
σ_{PSII}		3006	1235	109	29 %	Exp

Table 5.3. Semivariogram model parameters and cross validation statistics for variables measured during the June 2007 survey. Covariate identifies the trend variable if KED was used, otherwise implies OK. C_0 is the nugget, C is the sill, α is the range (m), Sp is the spatial dependency, ME is the mean error, MSPE is the mean prediction error, Z is the normalized residual error, and model defines the semivariogram function.

Variable	***Covariate***	***C_0***	***C***	***α***	***Sp***	Model
Temperature		0.016	0.901	219	99 %	Exp
pCO_2		0	19948	1158	94 %	Exp
Conductivity		0	2233.50	343	100 %	Exp
DO		0	55.06	119	100%	Exp
F_v/F_m		0	0.001	227	100%	Exp
σ_{PSII}		525.46	739.24	901	58 %	Sph
%Cover	Depth	210.36	880.56	566	81 %	Sph
Height	Cover	0.0006	0.0012	373	67 %	Sph
Green algae		0.003	0.030	143	97 %	Sph
Blue Green		0.008	0.123	254	98 %	Sph
Diatoms		0.009	0.130	185	98 %	Sph
Cryptophyte		0.002	0.142	187	99 %	Sph
Total Chl a		0	0.103	278	100 %	Sph
UV		0.25	2.89	337	92 %	Exp

Table 5.4. Partial Mantel test results for variable fluorescence measurements and other environmental variables. r_{splenv} denotes pure partial Mantel correlation (accounting for space and inter-correlations among variables). p denotes significance at the $\alpha = 0.01$ level, ns denotes not significant.

FvFm	r_{splenv}	***p***	σ_{PSII}	r_{splenv}	***p***
Depth	ns	ns	Depth	ns	ns
pCO_2	ns	ns	pCO_2	ns	ns
Temperature	0.107	0.0001	Temperature	0.080	0.0001
% cover	ns	ns	% cover	ns	ns
height	ns	ns	height	ns	ns

Table 5.5. Partial Mantel test results for variable fluorescence measurements and other environmental variables from the June 2007 survey. r_{splenv} denotes pure partial Mantel correlation (accounting for space and inter-correlations among variables). p denotes significance at the α=0.0042 level, ns denotes not significant.

FvFm	r_{splenv}	***p***	σ_{PSII}	r_{splenv}	***p***
Depth	0.12	0.0001	Depth	0.20	0.0001
Temperature	0.07	0.0001	Temperature	0.07	0.0001
Conductivity	ns	ns	Conductivity	ns	ns
DO	ns	ns	DO	ns	ns
pCO_2	0.15	0.0001	pCO_2	ns	ns
UV	0.11	0.0001	UV	0.094	0.0001
Greens	ns	ns	Greens	ns	ns
BlueGreens	ns	ns	BlueGreens	ns	ns
Diatoms	ns	ns	Diatoms	ns	ns
Cryptophytes	ns	ns	Cryptophytes	ns	ns
% Cover	ns	ns	% Cover	ns	ns
Height	ns	ns	height	ns	ns

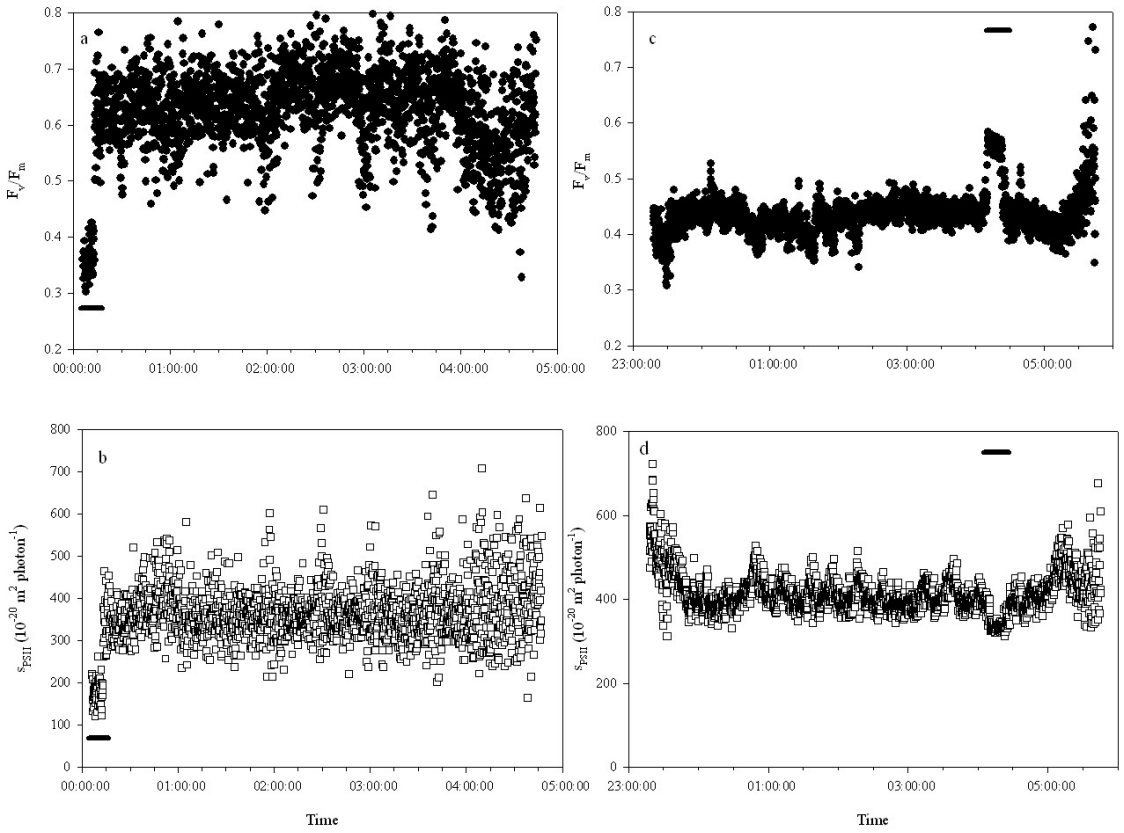

Figure 5.7. Time series plots of a) F_v/F_m and b) σ_{PSII} for 2006 survey, and c) F_v/F_m and d) σ_{PSII} for the 2007 survey. Solid bar denotes sampling of 16 Mile Creek. Note: the larger scatter evident in 2006 data (left panels) is presumably due to the lower biomass present at the time of the survey (see Table 5.1). Note upward drift in F_v/F_m in panel c) occurred 5 to 10 min prior to sunrise.

5.5 Discussion

Apparent scales of spatial pattern observed here varied among variables and sampling periods, from 100 to >1000 meters, while both physical and biological controls on spatial patterns appeared to be operating. This is the first resolution of such spatial pattern in the coastal zone of any large lake, but interpretations depend on a number of factors including the non-instantaneous nature of the surveys, as this study attempts to provide a spatial description of a moving water body. Taylor's Frozen Turbulence Approximation (Taylor 1938) essentially links spatial data to time series data, and is frequently used to deduce spatial information from time series measurements of single probes (Tennekes and Lumley 1999). It is based upon the hypothesis that a time series from a stationary probe can be regarded as a spatial series due to the advection of a "frozen" pattern past the probe with a mean speed U_T (m s^{-1}). In this case, the probe(s) are not stationary, but rather moving through a turbulent field (the water mass), and this presents a case where the opposite condition applies; that is, if the measurement location (i.e. the probe attached to the boat) is moving, then the speed of a probe [U_P (m s^{-1})] traversing the turbulent field (the lake surface) must be large compared to the velocity of the turbulent field (e.g the lake) [U_T (m s^{-1})] for the data collected to be considered a stationary "snapshot" of the spatial field. This is made possible by the substitution of t=x/U where t is time (s) and x is position (m) (Tennekes and Lumley 1999; p253). Given that the current velocities in the coastal regions of Lake Ontario are generally in the range of 0.05 to 0.25 m s^{-1} (Simons and Schertzer 1987) and the speed of the boat during the surveys was between 1.8 and 2.3 m s^{-1}, this approximates the condition of $U_P >> U_T$.

5.5.1 Physical structure and differences in hydrodynamic regimes

The range and distribution of surface temperatures observed between the two surveys indicate the presence of two very different hydrodynamic regimes. In 2006, the near shore was characterized by widespread, warm (e.g. > 18 °C) surface temperatures which displayed little spatial variation. A Fluoroprobe cast at a control station located at the 35 m contour earlier in the day indicted that the entire water column was well mixed to a depth of 35 m, with a change in temperature across the entire water column of 1.1 °C. Because the seasonal thermocline in Lake Ontario is generally between the 15 to 20 m depth (Simons and Schertzer 1987), the presence of near surface temperatures at the lake bottom is strongly suggestive of a period of downwelling. In contrast, the surface temperatures in 2007 suggest this survey took place some time after a recent upwelling event. Upwelling and downwelling are common phenomena along the northern and northwestern shores of Lake Ontario (Rao and Murthy 2001, Rao and Schwab 2007; Wilson et al. 2006). Satellite imagery (e.g., Mortimer 1988) indicates that periods of strong offshore winds

induce upwelling of deep coastal water in all the Laurentian Great Lakes and that upwelling usually persists between 2 to 6 days afterwards. In contrast, downwelling during the summer months tends to occur with strong on-shore winds, and can last longer than upwelling due to strong westward flowing shore parallel currents (Rao et al. 2003). Records from the Lake Ontario meteorological buoy (C45139; 43° 15' 36" N, 79° 32' 24"W) indicate that moderate (20 to 35 km h^{-1}) winds from the east to southeast direction dominated in the days leading up to the September 14 2006 survey (September 11 to September 13) and winds 15 to 35 km h^{-1} from a west to northwest direction dominated prior to the June 25 2007 survey (June 19 to June 23), and strongly suggest that much of the differences in spatial structure that I observed in the near shore zone during this study may have in fact been driven by these two physical processes.

5.5.2 Factors affecting F_v/F_m and σ_{PSII}

Before interpreting the patterns of F_v/F_m and σ_{PSII} observed in this study, it is important to consider potential factors which may influence the quantities of the measured parameters. Variability in F_v/F_m and σ_{PSII} in coastal waters has typically been attributed to variations in the degree of nutrient limitation (e.g., Kolber et al. 1988, Kolber et al. 1990, Greene et al. 1994), differences in taxonomy (Moore et al. 2003, Moore et al. 2005) and photo adaptive status (Moore et al. 2006). Multiple lines of laboratory work (e.g., Greene et al. 1991, Berges et al. 1996, Lippemeier et al. 1999, Beardall et al. 2001) suggest that nutrient limitation (Fe, N, Si and P) induces a decline in F_v/F_m, as the relative fluorescence per unit Chl a increases in response to nutrient stress (Cleveland and Perry 1987). Upon the addition of the limiting nutrient, recovery of F_v/F_m to near maximal values within a matter of hours is commonly observed (Greene et al. 1991, Sylvan et al. 2007), thus low values of F_v/F_m co-occurring with high values of σ_{PSII} in the field are not inconsistent with the hypothesized relationship to nutrient limitation. However, some laboratory studies (e.g., Parkhill et al. 2001, Kruskopf and Flynn 2006) suggest that F_v/F_m is not a valid indicator of nutrient stress, particularly under balanced growth conditions (Parkhill et al. 2001).

In addition to nutrient stress, other factors may also produce a decline in F_v/F_m. These include photoinhibition, photoprotection, diel variability, changes in community composition, dissolved fluorescence, and fluorescence from chlorophyll a degradation products (e.g. Geider et al. 1993, Olaizola et al. 1996, Fuchs et al. 2002, Moore et al. 2005). As the surveys were conducted at night, photoinhibtion and photoprotective mechanisms are not likely to exert a significant effect on the measured values of F_v/F_m since the surveys were initiated at least 2 h after sunset, and photo protective processes (e.g. xanthophyll cycle) are likely to be reversed

within 30 minutes of dark adaptation (Kolber et al. 1990). Likewise, diel effects should be minimized, since the surveys occurred during the natural dark period for phytoplankton.

Changes in community composition can alter the measured values of F_v/F_m and σ_{PSII} (Suggett et al. 2009). A recent review (e.g., Suggett et al. 2009) found that among laboratory and field data, a unique taxonomic signature is often superimposed on physiological variability, which suggests that measures of F_v/F_m and σ_{PSII} on natural communities cannot be interpreted on the basis of nutrient stress alone. Under nutrient replete conditions, F_v/F_m and σ_{PSII} are known to vary considerably among algal taxa (Suggett et al. 2009), with high values (~ 0.50 to 0.70) observed for diatoms and chlorophytes (Koblizek et al. 2001), and lower values (0.1 to 0.4) observed mainly for cyanobacteria (Campbell et al. 1998). The low values of F_v/F_m and σ_{PSII} associated with cyanobacteria may be due to the presence of phycobilisomes as the primary light harvesting antennae for PSII (Suggett et al. 2009). For cyanobacteria that contain appreciable amounts of phycocyanin, the poor overlap between the FRRF excitation light and the absorbance by phycobilisomes can lead to very low values of σ_{PSII} (Raateoja et al. 2004). Low values of F_v/F_m can also result from fluorescence emission from phycocyanin, or chlorophyll a fluorescence originating from PSI in cyanobacteria (Campbell et al. 1998).

Other non-physiological interferences may also influence the computation of F_v/F_m but these do generally not affect the computation of σ_{PSII} (Fuchs et al. 2002). The coastal regions of the Great Lakes receive allochthonous dissolved organic matter (DOM) from the surrounding catchments (Hiriart-Baer et al. 2008). This terrestrial DOM is often highly aromatic (fulvic or humic acids) and has a strong absorbance in the UV and blue wavebands (Kirk 1994), and may thus be stimulated to fluoresce with the FRRF excitation light (blue). The comparisons of sample blank fluorescence against UV fluorescence from the Fluoroprobe (Figure 5.8) suggest that the filtered lake water blanks are relatively constant and low, across the range of UV fluorescence encountered during this study. Similar insensitivity of sample blanks has been noted by (Bibby et al. 2008) who found that the FIRe instrumentation (similar to FRRF) was insensitive to background fluorescence when compared to fluorescence measured by a Turner Designs 10-AU. However, even with a relatively stable and constant blank the contribution of the sample blank to measured fluorescence increases as the magnitude of fluorescence declines (Figure 5.3). I was able to characterize this response sufficiently and correct measures of F_0 and F_m prior to computing F_v/F_m. Since both F_0 and F_m are reduced by the same amount, this should have no effect on the value of σ_{PSII} (Fuchs et al. 2002).

While dissolved fluorescence appears to contribute little to variability in F_v/F_m here, the presence of chlorophyll a degradation products (e.g. pheopigments) can also reduce the value of

F_v/F_m when the ratio of pheopigments to total chlorophyll a exceeds 30% (Fuchs et al. 2002). During this study, phaeophytin:total chlorophyll a ratios were generally below 30 %, similar to values reported for this region in the 1970s (Glooschenko et al. 1972). The prevalence of pheophytin:chlorophyll a ratios below the 30% value suggests that for most of the areas sampled, correction of F_v/F_m is not likely to be necessary. In the few areas where pheophytin:chlorophyll a ratios were high (Figure 5.8) in 2006, applying the correction factor in Fuchs et al. (2002) mostly raises the value of F_v/F_m to levels seen in the surrounding waters (e.g. at transects OA3 and OA4). In contrast, the correction of the low F_v/F_m values observed at approximately the 5 m contour during the 2007 survey only increased from 0.33 to 0.36, which does not account for the low values here. The proximate cause of high pheophytin:total chlorophyll a ratios is not immediately obvious, but there are a number of possibilities that will be discussed in the following sections.

Other factors that may affect F_v/F_m on a more local scale in the study area include the presence of waste water treatment plant (WWTP) effluent which has been demonstrated to be toxic to natural phytoplankton assemblages in Lake Ontario (Munawar et al. 1993), contaminants from urban watersheds such as metals (West et al. 2003), herbicides (Devilla et al. 2005) and PAH's (Marwood et al. 1999). In most cases, these substances act to reduce F_v/F_m, even though nutrients supplied form WWTP effluent may increase F_v/F_m. These effects should be strongest in proximity to the source (e.g., tributaries, storm sewers, WWTP outfalls), yet characteristic patterns pointing to such effects were not apparent during either survey.

5.5.3 Spatial patterns during downwelling

For downwelling events, the structure and flow of water within the coastal boundary layer in Lake Ontario is strongly westward due not only to the nature of the on shore winds, but also the propagation of internal Kelvin waves in a counter-clockwise direction (Rao and Murthy 2001). For relatively open areas of shoreline (such as the one sampled in this study) downwelling may therefore thoroughly mix the waters in the coastal boundary layer, smoothing the spatial variability over large areas. The results for the most part tend to confirm this, as September surface temperatures varied little and maximal variability was encountered at scales close to 4 km. Although the ranges of variation for pCO_2, F_v/F_m and σ_{PSII} are clearly less than that for surface temperature (Table 5.2), this is mostly due to changes in these parameters across the gradient established by the inflow of 16 Mile Creek into the lake. For example, the largest magnitude of changes in pCO_2, F_v/F_m and σ_{PSII} on a short spatial scale were clearly seen at the transition from 16 Mile Creek into the lake. Once in the lake, variability of F_v/F_m and σ_{PSII} dropped considerably, with only a gentle decline toward transects OA3 and OA4 at the north boundary of the survey area. Variability in pCO_2 within the lake appeared to be similar to that

observed across the transition from 16 Mile Creek. However, the presence of potential sources of CO_2 enriched water within the study area (municipal waste water treatment plant outfalls, storm sewers and tributaries) may influence the patterns of pCO_2 on a finer scale than temperature, Furthermore, the presence of the large piers at the northeast end of the study site may serve to disrupt shore parallel flow, creating a quiescent area where CO_2 rich water can accumulate.

Nutrient conditions during the period of downwelling were characterized by unusually high TP and SRP concentrations. Data collected from a reference station at the 35 m contour (~ 3 km offshore) also revealed comparable TP (20.6 $\mu g\ L^{-1}$) and SRP (7.5 $\mu g\ L^{-1}$) concentrations. Offshore total P concentrations in the western basin of Lake Ontario at this time of year are usually close to 15 $\mu g\ L^{-1}$ (Gouvea et al. 2006, Bocaniov 2007) and SRP concentrations are generally close to 2 $\mu g\ L^{-1}$ (Pemberton et al. 2007). While the exact cause of such high TP and SRP concentrations is difficult to resolve, the widespread nature of high P concentrations combined with low tributary discharge and precipitation (Sept 11 – 15 2006, 19.3 mm, Climate ID# 6155PD4) suggests that nutrient loading from the catchment is not likely the cause. Effluent from the numerous WWTP outfalls that discharge within 2 to 3 km of the lake shore is another possibility (Rao et al. 2003), but regular sampling at Oakville over several years has not detected such effects on a consistent basis (Chapter 4; Malkin 2007), and high concentrations (when present) are generally confined to distances within 0.5 km of the outfall (Pickering 2007 and 2008 data, S. Malkin, unpubl. data). High concentrations of TP and SRP are often also found along the southern shore of Lake Ontario where the Niagara River discharges into the lake (e.g., Malkin et al. submitted), but advection of this nutrient rich water toward the western shore from the southern shore seems unlikely. Re-mineralized P from decaying *Cladophora* tissue (e.g., Paalme et al. 2002) and fecal matter from dreissenids are a more likely explanation. Further support for this hypothesis is provded by the data from the Pickering surveys in 2007, where September and October TP and SRP were comparably high, after the majority of *Cladophora* had sloughed from the lake bottom.

The variability of F_v/F_m and σ_{PSII} was high in September primarily because of a larger range in measured values, but also because of a noisy data set, due to low chlorophyll a concentrations at this time (Table 5.1). This is clearly illustrated by the high nugget variance for both F_v/F_m and σ_{PSII} during the September survey (Table 5.2). Spatial dependence for F_v/F_m and σ_{PSII} was generally low (59% for F_v/F_m and 29 % for σ_{PSII}) and combined with a high nugget variance yielded a scenario with very little spatial variability (Figure 5.4c and d) which is consistent with strong controls mediated by downwelling regimes. The moderate to high values of F_v/F_m (0.50 to 0.80, mean ~ 0.62) observed in during the September survey are consistent with a

high maximal photosynthetic efficiency under conditions of adequate nutrients as reflected by indicators of phytoplankton nutrient status (e.g., C:P and N:P; Guildford and Hecky 2000) and measures of nutrient concentrations. A recent study by Pemberton et al. (2007) in the offshore waters of Lake Ontario (including the western basin) reported F_v/F_m in the range of 0.45 to 0.50 during late August to early September in 2004 and attributed the near optimal condition of the phytoplankton communities to a mild degree of P stress (Pemberton et al. 2007). Similarly, a study in Lake Erie suggested that by September, the deepening mixed layer and lower light levels mark the beginning of a period where phytoplankton are no longer severely P stressed (Rattan 2009).

Strong taxonomic variation from 16 Mile Creek into the lake may indeed exist, but I lack the data to confirm this. The generally widespread and relatively high values of F_v/F_m coupled with moderate values of σ_{PSII} suggest that strong taxonomic variation at this time is not likely. While I do not have spatial data on taxonomic distribution, vertical Floroprobe casts at the near shore sites and the offshore reference site revealed chlorophyll a concentrations that were uniformly low, and estimated the community composition to be dominated by cryptophytes. This is not inconsistent with data from Pemberton et al. (2007) for offshore Lake Ontario, where cryptophytes were abundant, F_v/F_m was moderately high, and σ_{PSII} was comparable.

5.5.4 Spatial patterns during upwelling

During periods of upwelling, along shore flow in the coastal boundary layer is much weaker and generally toward the east. These weak flows may also reverse in direction soon after an upwelling event (Rao and Murthy 2001). The advection of cooler water from the metalimnion or hypolimnion into the near shore, coupled with weak along shore flow, can therefore allow for a large increase in spatial variability in water masses in the near shore. Spatial variation may be further exacerbated by input of warmer tributary water, as this warmer water mass will become trapped near the surface and remain buoyant (Masse and Murthy 1992). Water Survey of Canada discharge records for 16 Mile Creek indicate that flows were above base flow conditions of 0.3 $m^3\ s^{-1}$ for the period 19 June to 30 June 2007 (range 1.3 to 0.55 $m^3\ sec^{-1}$) so surface plumes originating from local tributaries may have been responsible for the part of the significant patchiness observed during this survey. Mixing of these surface trapped plumes is usually enhanced as the plume migrates toward the offshore, becoming thinner and closer in temperature to that of the underlying water (Fong and Geyer 2001), however, these results suggest that these surface trapped plumes were not migrating offshore, but rather flowing toward the west in an alongshore direction, consistent with a possible flow reversal in the post-upwelling period (Rao and Murthy 2001). The much shorter range of variability in surface temperatures (219 m), far

higher spatial variance, and overall cooler temperatures compared to the conditions during the September downwelling strongly support this hypothesis.

Nutrient conditions during the upwelling period were moderate, with TP and SRP more comparable to summer conditions commonly observed along this section of shore line (e.g. Malkin et al. 2008, Chapter 3, Chapter 4). Historically, upwelling often injected nutrient rich waters into the near shore of Lake Ontario (Lean et al. 1990), but no evidence of this is apparent from these data, which is consistent with the results of Malkin (2007) and supports the evidence of continual declines in offshore nutrients (Malkin et al. submitted). Chlorophyll a concentrations were higher than the prior September, and interestingly, the water sample values displayed a similar variability in concentration despite the obvious changes in spatial variability of the lake surface. Higher chlorophyll during the June survey may have been partly facilitated by the thick overstory of benthic algae that could reduce grazing efficiency of dreissenids.

With the increased chlorophyll a concentrations, there was far less noise in the measured fluorescence, and F_v/F_m and σ_{PSII} were characterized by a much lower nugget variance and sill (Table 5.3). Spatial dependence of F_v/F_m and σ_{PSII} was nearly double that observed during the lower chlorophyll a, downwelling regime, and resulted in a highly structured pattern of variation, as shown in Figure 5.5h and i. The highly structured patterns of F_v/F_m and σ_{PSII} displayed significant associations with other variables that indicated a strong along shore variation. For example, partial Mantel tests indicated significant associations for F_v/F_m and σ_{PSII} with depth, surface temperature and UV fluorescence that displayed patterns consistent with dominant along shore flow, and indicates that spatial organization was oriented in this manner. Despite these significant associations, the patterns of variability in F_v/F_m and σ_{PSII} still suggest the interplay of several factors. The values of F_v/F_m and sigma measured in the June survey were on average lower (mean ~ 0.43) and more consistent with values typically observed in offshore waters of Lake Ontario (e.g. Pemberton, et al 2007). Coupled with moderate nutrient availability, higher stochiometric ratios (e.g. N:P, C:P) and a significant negative correlation between F_v/F_m and $\sigma_{PSII,}$ these are not inconsistent with a greater degree of nutrient limitation.

Low F_v/F_m occurred in elongated patches along the shore near the 5 m contour. I also observed high pheophytin:chlorophyll a ratios in at least one of these areas (e.g. transect OA5). The proximity to 16 Mile Creek strongly suggests that the low F_v/F_m was a characteristic of the plume emanating from 16 Mile Creek, yet F_v/F_m within the harbor was high (~ 0.58). Explaining the higher pheophytin:chlorophyll a ratio here is difficult without additional data, but might indicate enhanced grazing by zooplankton (Carpenter et al. 1986). Zooplankton are known to migrate into surface waters to feed at night (McNaught and Hasler 1966), although many pelagic

species may also avoid the near shore areas (c.f. Wetzel 2001). Pelagic species however, can be advected into near shore areas by the tilting of the thermocline during an upwelling event (Megard et al. 1997). In Lake Ontario, the displacement of the surface layer by upwelling changes the composition of near shore zooplankton temporarily, with copepods becoming more abundant (Haffner et al. 1984). Coupled with the physical changes during upwelling (e.g., trapping of tributary plumes near surface) this can result in significant spatial variability in zooplankton biomass (Pinel-Alloul and Ghadouani 2007). In marine systems, tributary plumes create frontal boundaries where river and ocean water meet. These areas are frequently populated by high zooplankton abundances, presumably for feeding (Peterson and Peterson 2008) or in response to density gradients (Woodson et al. 2005). Whether such a phenomenon occurs in Lake Ontario is not known, but does at least provide a plausible hypothesis why F_v/F_m appears to be low in these elongated patches relative to F_v/F_m closer to shore or in deeper waters. Applying the correction factor suggested by Fuchs et al. (2002) however, does not adequately compensate (8 % increase from 0.33 to 0.36) suggesting other factors may be involved.

Although the partial Mantel test failed to find a significant relationship with taxonomic classes as estimated by the fluoroprobe, the spectral florescence signatures from the Fluoroprobe clearly indicated the presence of an alongshore high chlorophyll a plume, occupied by a more diverse assemblage than observed during the previous September. In some parts, F_v/F_m appeared to be low where cyanophyte biomass (as chlorophyll a equivalents) was high, but the patterns were largely inconsistent. The putative cause for the lack of a significant result from the partial Mantel test with F_v/F_m and σ_{PSII} and the Fluoroprobe data is not known, but may be related to the meandering nature of the chlorophyll plume. As the kriged surfaces show (Figure 5.5 j to n), adjacent transects were often characterized by very different spectral and active fluorescence. This would not be inconsistent with a meandering plume along the shore, drifting close to shore over time. Because I did not use a pre-set navigation system for transects, occasional overlapping at a later time lead to awkward, streaked patterns suggesting major changes to community composition, water chemistry and active fluorescence variables, yet these are still predominantly consistent with a dominant along shore flow pattern.

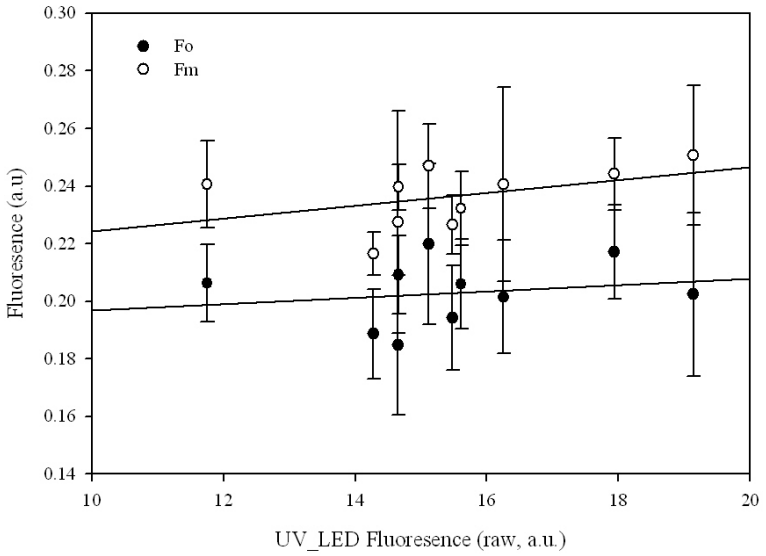

Figure 5.8. Relationship between FRRF fluorescence of 0.2 um filtered lake water (blanks) vs UV (370 nm) excited fluorescence as measured by the Fluoroprobe for samples collected in 2007. Data plotted are the mean (error bars; standard deviation) of 50 replicate F_0 and F_m measurements for sample blanks. Neither relationship was significant (F_0 = 0.001*UV + 0.186, r^2=0.038, F=0.319, *p*=0.59 and F_m=0.002*UV + 0.202, r^2=0.18, F=1.81, *p*=0.21).

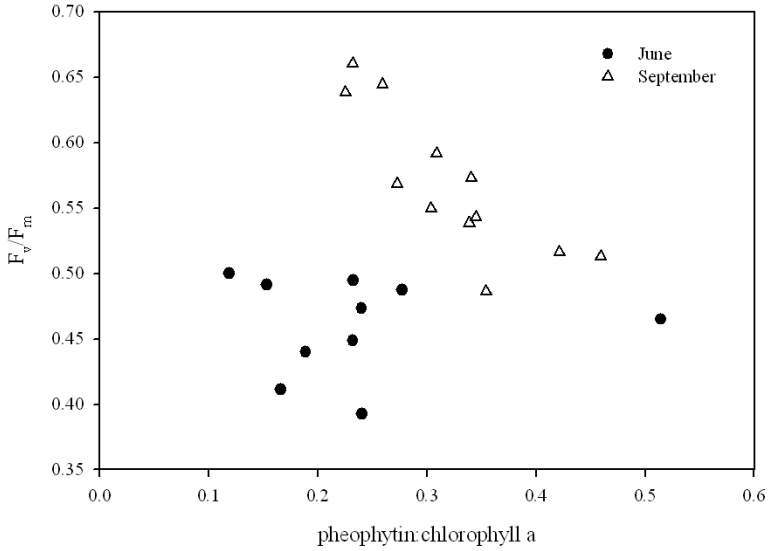

Figure 5.9. Relationship between F_v/F_m and % pheophytin. Note the higher sensitivity in September when phytoplankton biomass (measured as chlorophyll a) is lower.

5.5.5 Potential for benthic-pelagic interactions in near shore Lake Ontario

Although it appears that hydrodynamics and tributary influence play key roles in structuring the patterns of spatial variability of phytoplankton communities in the near shore environment, in this study, the extensive crops of benthic algae (e.g., *Cladophora*) that colonize the substrate during the summer may also exert a structuring effect on the spatial distribution of water quality variables, particularly in shallow waters where biomass is high. At times of appreciable *Cladophora* biomass, the potential for competitive interactions with phytoplankton exists. The absence of nuisance *Cladophora* biomass during the September survey in combination with the downwelling regime do not allow for elucidation of such patterns But, in June, *Cladophora* was approaching the typical midsummer biomass peak (Malkin et al. 2008) and I did observe some evidence that *Cladophora* can impart a signal on the water column. For example, the spatial distribution clearly shows a band of water with supersaturated dissolved O_2 along the shore, at depths < 3 m. This is consistent with the observations of Malkin (2007) and Davies and Hecky (2005) that *Cladophora* can achieve high photosynthetic rates, particularly at shallow depths where light is not limiting for much of the photoperiod. Once a significant biomass of benthic algae has accumulated, it may exert strong effects on dissolved O_2 saturation. A partial Mantel test on dissolved O_2 saturation did suggest a marginally significant association with percent *Cladophora* cover ($r=0.032$, $p=0.06$). The lack of correlation with total chlorophyll a and the proximity to the shore suggest that *Cladophora* rather than phytoplankton are responsible for the elevated dissolved O_2. The weak correlation with percent *Cladophora* cover is likely affected by the smearing of this highly saturated band of water by along shore currents into areas that are low in *Cladophora* cover.

With potential effects on dissolved O_2 saturation seemingly evident in shallow waters where *Cladophora* cover is high, by extension, a similar pattern with respect to pCO_2 might be expected, since *Cladophora* is thought to dominate the C flux at depths < 6 m (Malkin 2007). The distribution of surface pCO_2 during the June survey is not inconsistent with this, as pCO_2 was widely undersaturated, down to levels approaching 100 ppm in the shallow areas near the shore. An increase in pCO_2 was clearly observed toward the offshore, and into the mouth of 16 Mile Creek, suggesting a drawdown in the shallow waters was present. Although upwelling normally injects metalimnetic or hypolimnetic that is super saturated with pCO_2 along this shoreline (Malkin 2007, D. Depew unpubl. data.) the widespread under saturation of pCO_2 so soon after an upwelling event implies that the C demand by *Cladophora* in the near shore is substantial. Unlike dissolved O_2 saturation, no significant association was observed between percent algal cover and surface pCO_2 (partial Mantel test, $r=-0.04$, $p>0.9$), however, once pCO_2 is drawn down to low

levels, *Cladophora* may switch to other forms of inorganic C (e.g. HCO_3^-) (Choo et al. 2002). The pH and buffering capacity of the alkaline waters of Lake Ontario yields a nearly endless supply of total dissolved inorganic C (Malkin 2007) and at the low concentrations observed during the June survey (100 ppm ~ 5 uM) *Cladophora* probably switches to other forms of inorganic C, particularly in shallow waters where the energetic costs of HCO_3^- uptake are likely to be met by light availability (Malkin 2007).

Because *Cladophora* attaches primarily to hard substrate, sequestration of nutrients from the water column is the primary means of nutrition (Whitton 1970). If competition between *Cladophora* and phytoplankton is important in the near shore, I expected to see some patterns that would be consistent with nutrient stress of the phytoplankton communities, either over areas with heavy growth of *Cladophora* or perhaps along a depth gradient. While distinct signals in F_v/F_m and σ_{PSII} were not observed over short spatial scales that could be interpreted as competitive interactions, the possibility of competitive interactions for P cannot be ruled out. The ability of macroalgae to sequester large quantities of nutrients has been primarily linked to light availability (McGlathery et al. 1997, McGlathery and Pedersen 1999). For example, increased light availability has been shown to boost NH_4 uptake in *Chaetomorpha linum* (McGlathery et al. 1997) and P uptake kinetics in periphyton (Hwang et al. 1998). The increase in water clarity associated with dreissenid filtering activity (Howell et al. 1996) and the potential for nutrient supply from the benthos (Ozersky et al. 2009) may have effectively tipped the balance toward benthic algal dominance in the Great Lakes (Hecky et al. 2004).

Without a detailed analysis of the phytoplankton community present during each survey, I cannot conclusively link the differences in F_v/F_m between September and June solely to differences in nutrient sufficiency, though the responses are generally consistent with those described in the literature (e.g., Geider et al. 1993, Kolber et al. 1990). It is apparent from the results of this study that physical forcing plays a large role in structuring the variability of water quality and phytoplankton communities in the near shore. Super-imposed on these dynamic processes are seasonal variations driven by differences in nutrient supply and species interactions. Seasonal variation aside, distinct differences between alternating periods of downwelling and upwelling lead to very different circumstances of spatial structure and variability in measured paramters. Downwelling appears to be strong enough to successfully homogenize conditions over large areas of the near shore, while upwelling tends to produce high spatial variability, largely due to the slowing of current speeds and the injection of cooler water into the near shore where it must intereact with often much warmer tributary waters.

While further work is required to confirm the regularity of such responses, this study provides a framework on which to move forward with such studies. Geostatistical methods and partial Mantel tests were able to detect significant spatial variability in many parameters during the surveys. The semivariance modeling and subsequent kriging produced spatial snapshots that capture much of the spatial variability in physical (e.g., temperature), biological (e.g., benthic algal cover, phytoplankton pigment groups), chemical (e.g., conductivity), and perhaps physiological parameters (e.g., variable fluorescence, dissolved gases) along an open coastline of Lake Ontario. These results suggest that physical forcing plays a large part in structuring the spatial variability in the near shore, and provide a means to quantify and characterize such conditions. In addition, these results suggest that benthic algae may exert a significant effect on water column properties, further compounding the spatial variability in an already complex ecosystem.

Chapter 6

Cladophora in Lake Simcoe: Why does it not reach nuisance proportions?

6.1 Overview

In recent years, a resurgence of filamentous benthic algae (e.g., *Cladophora*) in the Laurentian Great Lakes has been perceived as a consequence of dreissenid mussel invasion and subsequent alterations to ecosystem nutrient and energy cycling. Here, I conduct high resolution hydro-acoustic surveys at two sites in Lake Simcoe to assess the presence and extent of excessive benthic algal growth on hard substrate in the post dreissenid mussel period. Despite comparable dreissenid abundance, water clarity and phosphorus concentrations to sites in the lower Great Lakes known to suffer extensive *Cladophora* fouling during the summer months, only trace amounts of *Cladophora* were found in the surveyed areas. While the proximal cause for the lack of excessive *Cladophora* growth in Lake Simcoe remains elusive, distinct differences in water chemistry and top down pressure from potential algal grazers separate Lake Simcoe from the near shore areas of the lower Great Lakes, and these factors may be relatively more important for structuring the benthic algal communities in Lake Simcoe. Overall, the results of this study and other recent studies in Lake Simcoe are not inconsistent with the near shore shunt hypothesis that predicts dreissenid mussels enrich the benthic environment, but the manifestation of the shunt in Lake Simcoe is vastly different than the manifestation observed in the lower Great Lakes.

6.2 Introduction

Excessive growth and biomass of the ubiquitous filamentous green alga *Cladophora* is generally considered to be symptomatic of eutrophication (Dodds and Gudder 1992). Perhaps one of the better known North American cases occurred in the Laurentian Great Lakes, where *Cladophora* reached nuisance proportions due to cultural eutrophication in the 1950s and 1960s (Shear and Konasewich 1975) and public complaints over shoreline fouling by decaying mats of *Cladophora* were a major driver for phosphorus (P) abatement programs that were implemented in the Great Lakes Water Quality Agreement (GLWQA) (Painter and Kamaitis 1987). Lake Simcoe also underwent considerable ecosystem degradation during the 1960s and 1970s due to excessive nutrient loading (Evans et al. 1996). P loading during pre-settlement years (~1800s) was estimated at approximately 30 T yr^{-1} (Johnson and Nicholls 1989), and by the early 1980s, external P loading had effectively tripled to over 100 T yr^{-1} (Evans et al. 1996, Winter et al. 2007), before stabilizing near the 75 T yr^{-1} target since the early 2000s (Winter et al. 2007).

In contrast to the lower Great Lakes, historical records of *Cladophora* growth in Lake Simcoe are scarce. While *Cladophora* has been recorded in qualitative surveys (Jackson 1982, Jackson 1985, Sheath et al. 1988) quantitative data for Lake Simcoe are limited to one report, summarized by Jackson (1982). Jackson (1982) surveyed multiple locations in 1976 and 1980 and found that while *Cladophora* was present at many sites (particularly in the splash zone), accumulation of excessive biomass was consistently found only at one location, adjacent to the sewage discharge from the town of Orillia, in Shingle Bay. This is in stark contrast to conditions in Lakes Erie and Ontario where accumulation of excessive *Cladophora* biomass was widespread (Neil and Owen 1964, Taft and Kishler 1973, Neil and Jackson 1982), but such a sporadic occurrence as seen in Lake Simcoe was consistent with patterns of nuisance growth in Lake Huron at that time (Auer et al. 1982a).

In the lower Great Lakes there is widespread perception that since the establishment of the invasive dreissenid mussels over the past 15 years, benthic algal (in particular *Cladophora*) biomass and extent has increased (e.g., Higgins et al. 2005a, Malkin et al. 2008). Due to the high biomass achieved by dreissenids in the lower Great Lakes (e.g., Patterson et al. 2005, Wilson et al. 2006, Ozersky et al. 2009), mussels have been credited with altering nutrient distributions by filtering suspended matter and excreting re-mineralized nutrients, and depositing mucus-bound particulate nutrients in the benthos (Hecky et al. 2004). The clearing of the particles from the water column enhances water clarity (e.g., Howell et al. 1996) and solar energy flux to the benthos, potential importance of benthic producers, and therefore, potential energy flow through

benthic organisms (Vanderploeg et al. 2002). Yet, attributing these remarkable changes observed in the Great Lakes near shore regions solely to dreissenids has been difficult due to the paucity of data for the time period immediately before as after their successful invasion, and is further complicated by concurrent P abatement strategies to reduce the P loads to the lakes. Decreased nutrient loading can also act to decrease phytoplankton biomass and increase water clarity (Nicholls and Hopkins 1993, Nicholls et al. 2001) and therefore have a similar net result of enhancing the relative importance of benthic primary producers.

Lake Simcoe provides a unique opportunity to examine the response of the benthic producer community to changes induced by dreissenid invasion. In particular, water quality in Lake Simcoe has been consistently and continually monitored since the 1980s (Eimers et al. 2005) well before the invasion of dreissenid mussels, which began in 1995 (Nicholls 1998). Consequently the additive effects of mussel grazing and nutrient regeneration can be appreciated relative to the impact of nutrient reductions that were well underway. In this study, a novel hydro-acoustic method (Depew et al. 2009) is employed to survey the littoral areas adjacent to the two largest islands in the lake, Georgina and Thorah Island. These areas are exposed to the open lake, and are characterized by small to moderately sized cobble and gravel substrate, suitable for the attachment of dreissenid mussels (Ozersky et al. submitted) and *Cladophora* (Whitton 1970). These surveys were designed to be comparable to surveys conducted in the near shore regions of Lakes Ontario, Erie and Huron in 2005 to assess the extent of *Cladophora* growth and biomass accumulation (Chapter 3).

Current estimates of dreissenid abundance on areas of hard substrate in Lake Simcoe (e.g., Ozersky et al. submitted) are similar to those reported in Lake Ontario (e.g., Wilson et al. 2006, Ozersky et al. 2009) and less than those reported for Lake Erie (e.g., Patterson et al. 2005), but higher than those reported for Lake Huron (Nalepa et al. 2007). *Dreissena polymorpha* rather than *Dreissena bugensis* is the numerically dominant species in Lake Simcoe (Ozersky et al. submitted) whereas *D. polymorpha* has become a relatively minor member of the dreissenid assemblages in the lower Great Lakes (Patterson et al. 2005, Wilson et al. 2006, Ozersky et al. 2009). Nonetheless, I hypothesized that given a suitable time since dreissenid invasion, a similar abundance of dreissenids, and an environment with suitable environmental conditions, excessive *Cladophora* growth should manifest itself on hard substrata on which they dominate in the lower Great Lakes.

6.3 Materials and Methods

6.3.1 Study Locations

Lake Simcoe has a surface area of 722 km^2, and is the fifth largest inland lake in Ontario (Evans et al. 1996). The main basin of the lake is the largest, and has a maximum depth of 33 m (Evans et al. 1996). Kempenfelt Bay is a narrow, deep bay with a maximum depth of 42 m oriented in a southwest to northeast direction. Cook's Bay is a relatively shallow (maximum depth 15 m), soft bottom bay at the south end of the lake near the Holland Marsh, that is carpeted by macrophyte growth to depths up to 9 m (Chapter 7). The lake generally stratifies in areas deeper than 15 m, however, parts of the lake are shallower than 15 m; including most of Cook's Bay and the east portion of the main basin. Consequently, these parts of the lake are well mixed to the bottom for the ice free season. Agriculture is the dominant land use in the catchment (47 %; Lake Simcoe Conservation Authority 2009) and consists mainly of livestock and crop production, but urban areas have been expanding rapidly (~ 8 km^2 per year since 1985; Winter et al. 2002) and comprise ~ 6% of the catchment (Lake Simcoe Region Conservation Authority 2009). P loading to the lake is well monitored, and has declined in recent years to a relatively stable annual load of 68 ± 7 T yr^{-1} (Winter et al. 2007), with more recent estimates of loading between 70 and 75 T yr^{-1} (Lake Simcoe Region Conservation Authority 2009). Dreissenid mussels were first identified in the lake in 1993, and were widely established in 1996 (Nicholls 1998). Since the establishment of mussels, phytoplankton biovolume has declined, and water clarity has increased (Eimers et al. 2005). Recent water quality data indicate that the main basin of the lake can be described as oligo-mesotrophic (e.g., Eimers et al. 2005; Guildford et al. submitted).

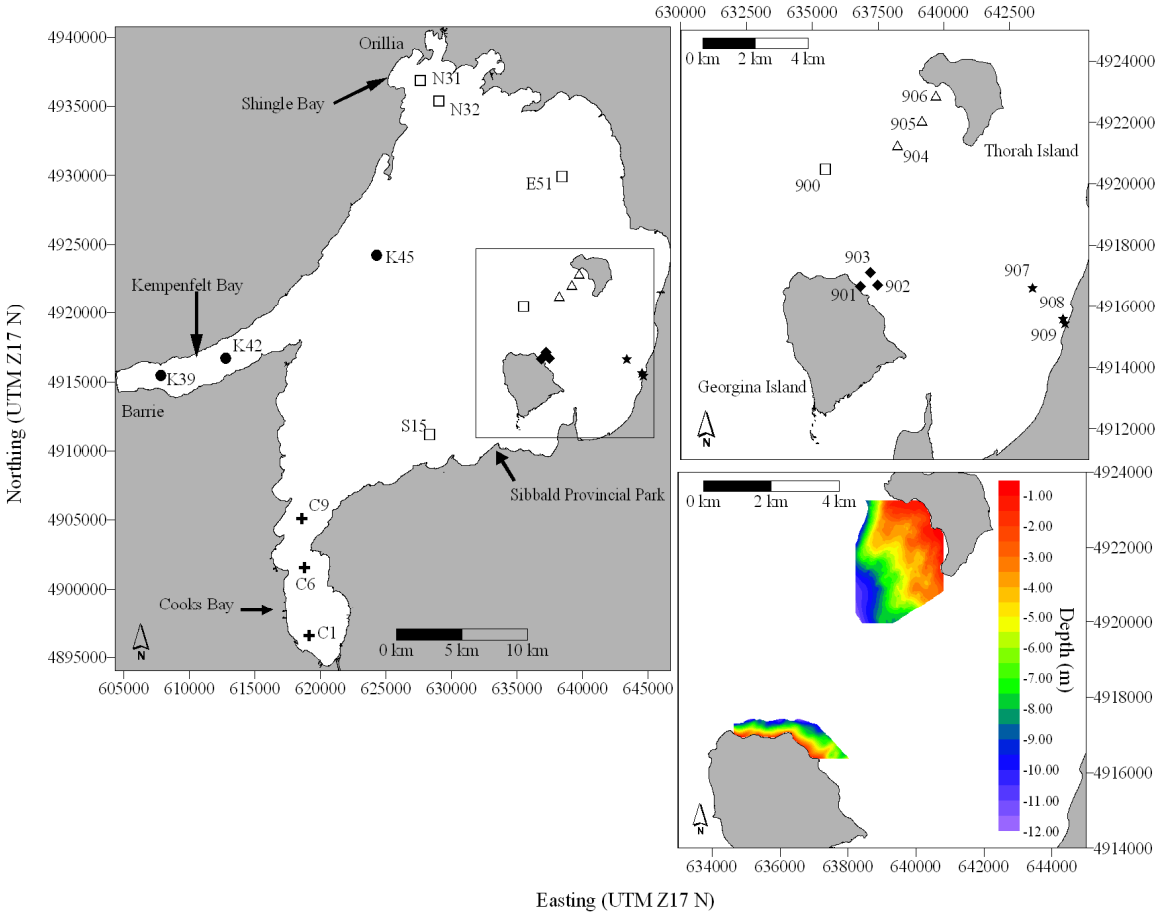

Figure 6.1. Map of Lake Simcoe showing sampling sites. Kempenfelt Bay stations denoted by (●), Cooks Bay stations denoted by (✚) and main lake stations denoted by (◘). Transect stations at Georgina Island (◆), Thorah Island (△) and Pefferlaw (★) are show in the inset panel (upper right). Bathymetric contours generated via universal kriging of echosounder depth records (easting and northing as covariates) for the acoustic survey areas at Georgina and Thorah Island are shown in the lower inset panel. Note that stations in Cook's Bay, Kempenfelt Bay and the main basin of the lake are long term MOE stations (station 900 excluded).

6.3.2 Physical and Chemical conditions

Physical and chemical conditions were monitored at long term Ministry of Environment (MOE) stations (e.g., Eimers et al. 2005; Figure 6.1) and at 9 additional stations located in the southeast quadrant in 2006 (May 16 and August 8) and 2007 (May 22-23, July 4-6 and August 21-23) (Figure 6.1). At each station, CTD profiles were taken using aYSI-6600 profiler, and analyzed to determine the depth of the mixed layer. Photosynthetically active radiation (PAR) was measured with a LI-COR cosine sensor at 0.5 m to 1 m intervals from the surface to the lake bottom. The vertical attenuation coefficient for PAR (kPAR) was determined by linear regression of the natural logarithm of irradiance vs. depth (Kirk 1994).

A 6 L Niskin bottle was used to collect ~ 15 L of water at a depth equal to 50% of the mixed layer depth as determined from CTD cast. Hypolimnion samples were collected ~ 2 m off bottom during summer months when a thermocline was confirmed to be present. Water was transferred to covered carboys and stored in coolers until transported to the laboratory (OMNR fisheries assessment unit; Sibbald Provincial Park) for processing and storage. Samples for total dissolved P (TDP) and soluble reactive P (SRP) were filtered through a 0.2 µm polycarbonate filter, particulate P (PartP) by filtering 500 mL of lake water onto acid soaked (5% HCl ~ 4 hr) Whatman GF/F filters (nominal pore size ~ 0.8 µm). Total P (TP) and all composite fractions (TDP, SRP, Part P) were determined according to the molybdate blue method (APHA 1998). Samples for other particulate nutrients (carbon – Part C, nitrogen – Part N) were determined by filtering 500 mL of lake water onto pre-combusted (500 C ~ 4hr) GF/F filters and assayed using a CEC-440 Elemental Analyzer (Exeter Analytical, N. Chelmsford, MA). Phytoplankton chlorophyll *a* was measured using a Turner Designs 10-AU fluorometer calibrated yearly against pure chlorophyll a (Smith et al. 1999). Additional ions (NO_3^-, Cl^-) were determined using ion chromatography (Dionex DX 500, Dionex AS17 and AG17 guard column). Ammonium was determined on a Turner Designs TD-700 fluorometer following the methods of Holmes et al. (1999). Total suspended solids (TSS) were determined by filtering 2 to 5 L of lake water onto pre-combusted (500 °C for 4 hr) pre-weighed GF/F filters, drying at 65 °C to a constant weight and re-weighing. AFDW was determined after combustion at 500 °C for 4 hrs.

6.3.3 Acoustic Surveys and Data Processing

Acoustic surveys at Georgina and Thorah Island were conducted on May 16 2006 and August 8 2006 (Figure 6.1) during daylight hours (0800 – 2000 hrs) using a 7 m aluminum vessel. Acoustic data were collected using a BioSonics Inc. (Seattle WA, USA) DTX deck unit

connected to two single beam transducers that were mounted on 2 m long adjustable sliding mounts attached to the side of the vessel with a series of clamps and bolts. The first transducer (430 kHz, 10.2° full beam angle, source level 213 dB re 1 μPa at 1m) was set to ping at a frequency of 5 Hz with a pulse length of 0.1 ms, and was used for detection of filamentous algae (see Chapter 2). The second transducer (120 kHz, 7.1° full beam angle, source level 216 dB re 1 μPa at 1m) was also configured to ping at 5 Hz with a pulse length of 0.4 ms and was intended to be used for substratum characterization. Unfortunately, the high transmission power of the 120 kHz transducer caused near complete saturation of the returned acoustic signal at depths < 6 m, thus separation of substratum types using standard echo analysis algorithms (e.g., RoxAnn) was not possible.

Acoustic survey transects were run in a back and forth pattern from the 1.5 m depth contour to the 10 m depth contour, approximately parallel to the shoreline of the islands. Transects were spaced ~ 50 m apart. During the acoustic surveys vessel speed was kept between 1.5 to 2.3 m sec^{-1}. Differentially corrected GPS locations were provided at a fix update interval of 1 sec from a JRC DGPS212 (Japan Radio Company).

Acoustic data from the surveys were processed using a Graphical User Interface (GUI) written in MATLAB® 7.2 (Chapter 2). A threshold setting of -88 dB was used to characterize the top of the algal canopy, and a threshold setting of -56 dB was used to characterize the substratum. Although the threshold settings used for detection of filamentous algae (e.g., *Cladophora*) are of lower energy than that used for vascular macrophytes (~ -65 dB), lower acoustic thresholds will still correctly classify macrophytes if they are present (Sabol et al. 2002b). The minimum height of a *Cladophora* canopy that can be detected by acoustics is theoretically determined from the acoustic resolution of single targets (for example, two separate fish, or a fish and the bottom). This is calculated according to $R = c\tau/2$ (i.e. speed of sound in medium, c, [~1500 m s^{-1}] x pulse length, τ, [0.1ms] / 2 = 0.075 m; Simmonds and MacLennan 2005). This distance R is often referred to the "acoustic dead zone" based on the difficulty of discriminating fish echoes from bottom echoes (Ona and Mitson 1996). How this affects the detection of vegetation is not clear, as plants tend to occupy the entire area from the canopy top right to the substrate and thus are not spatially separated from the bottom. However, this method has been extensively tested and validated in the lower Great Lakes (Chapter 2, 3 and 4) where excessive *Cladophora* growth is a seasonal occurrence during the summer months. It is, however, important to note that *Cladophora* stands that do not reach the height threshold for acoustic detection (~7.5 cm) will be missed entirely, but characterization of algal stands in excess of this threshold are well characterized.

6.3.4 Geostatistical Analysis

The recent availability of high resolution data from acoustic systems has allowed exploration of various methods to interpolate between data points to provide a surface of predicted values. Guan et al. (1999) and Valley et al. (2005) have evaluated different methods and concluded that kriging provides the most robust method for regularly spaced data collected using acoustic methods. The prediction of spatial variation from point measurements over surface areas requires some realistic interpolation techniques. Deterministic and geo-statistical methods are the two main groupings of interpolation techniques to produce a continuous surface from point measurements. Deterministic interpolations create surfaces from measured points using mathematical functions which are based on the extent of similarity (inverse distance weighting) or the degree of smoothing (radial basis functions). Geostatistical methods (i.e. kriging) utilize both the mathematical and statistical properties of the measured points (Isaaks and Srivastava 1989). For a detailed and in depth discussion of geostatistics and the underlying theory, the reader is referred to Journel and Huijbergts (1978) and Isaaks and Srivastava (1989). The basic assumption required for geostatistics is that the process under study is stationary, and that the observed values are simply one of many possible random realizations of the process (Webster and Oliver 2001). In addition, spatial autocorrelation must be present (i.e. one point should be able to provide some information about neighboring points).

The initial step in geostatistical analysis is the construction of the semivariogram. The semivariogram is a graphical representation of half the average squared variance between sample points as a function of separation distance *(h)* and is defined in equation 1

$$\gamma(h) = \frac{1}{2N(h)} \sum_{i=1}^{N(h)} \left[Z(x_i) - Z(x_i + h) \right]^2 \qquad (1)$$

where $\gamma(h)$ is the semivariance for lag (h), $Z(x_i)$ is the measured value at location x_i, $Z(x_i+h)$ is the measured value at location (x_i+h) and $N(h)$ is the total number of paired samples for a given lag (h) (Cressie 1991). The experimental semivariogram has important characteristics that reveal the kind of spatial variation present in an area, for the variable under study. Generally, the semivariance increases as the lag distance (h) increases to a maximal value, after which the semivariance is frequently flat. This lag distance is known as the range and it represents the limit of spatial autocorrelation. By definition, $\gamma(h)=0$ when $h=0$, however any smooth curve that approximates values of γ as h approaches 0 is unlikely to pass through the origin. This value (i.e when $h=0$) is termed the nugget variance. The nugget variance is a combination of measurement error and variation at distances smaller than the shortest sample spacing which cannot be

resolved. The value of γ where γ reaches its maximum is called the sill (*C*), and represents the maximum semivariance.

To describe the spatial variation at distances other than just the lag distances, a mathematical function is fit to the experimental semivariogram data, usually using weighted least squares (Cressie 1991). Two of the three more common models were used: the spherical and exponential model. These two models in terms of the semivariogram are given in equation (2; spherical model) and equation (3; exponential model);

$$\gamma(h;\theta) = \begin{Bmatrix} 0, & h = 0 \\ C_0 + C_s\ ((3/2)(\|h\|/\alpha_s) - (1/2)(\|h\|/\alpha_s)^3), & 0 < \|h\| \le \alpha_s \\ C_0 + C_s, & \|h\| \ge \alpha_s \end{Bmatrix} \quad (2)$$

$$\gamma(h;\theta) = \begin{pmatrix} 0, & h = 0 \\ C_0 + C_e(1 - \exp(-\|h\|/\alpha_e)), & h \neq 0 \end{pmatrix} \quad (3)$$

where *C* is the sill of the variogram that represents the maximal variation (C_s for the spherical model and C_e for the exponential model), α is the range of the variogram beyond which data are no longer autocorrelated (α_s and α_e as before), and C_0 is the nugget effect. A variogram model can also be nested, i.e. it can be a combination of two or more component models such as nugget and exponential. Most variograms are nested in this manner, although more complex models (i.e. a double spherical with nugget) are sometimes used. Once the semivariogram function has been defined and fit, it can be used to weight predictions in the kriging system of equations to yield the best linear unbiased estimator of the target variable. For more information on the various forms of kriging the reader is referred to Webster and Oliver (2001).

Exploratory data analysis was conducted on raw acoustic data before variogram modeling and analysis. Data from the preliminary surveys in May 2006 were comprised of nearly all zeros, as there was insufficient growth for characterization with the acoustic unit. Strong relationships between percent cover and bottom depth were observed for data collected in August at both sites. Following the general framework provided in Hengl et al. (2004), block regression kriging was used to provide interpolated surfaces of percent cover and stand height for blocks of nominal size 25 m by 25 m. Breifly, this involved using generalized linear models (GLM) to characterize the relationship between percent cover and bottom depth, and stand height and percent cover. GLM with a poisson distribution (log-link function) were used as the data sets displayed non-normal distributions with over dispersion (Gotway and Stroup 1997). Block kriging was conducted on the model residuals, and the GLM trend was then added back to the interpolated surface of the residuals to generate the interpolated surfaces. All regression modeling, semivariogram

calculations, variogram model fitting, and subsequent kriging computations were performed in the statistical software R (R Core Development Team 2007) using the base stats package and the *gstat* package (Pebesma 2004).

6.3.5 *Cladophora* sampling and internal nutrient analyses

Samples of benthic algae were collected at stations 901, 902, 904 and 905 during May and July of 2007 during follow up water quality surveys. Additional samples collected during an additional survey in Cook's Bay on August 9 2006 are also compared here. Samples were collected via snorkeling or with the assistance of a sampling rake for deeper stations. Samples were placed in a small Ziploc bag, and stored in coolers until returned to the laboratory. Upon return to the lab, samples were washed in a mesh sieve (mesh size ~ 1 mm) to remove debris and sediment. Invertebrates were removed with forceps. A representative algal sample was placed in a 20 mL scintillation vial and fixed in 2 % glutaraldehyde solution for later identification and the remaining tissue was frozen at -20 °C pending analysis at the University of Waterloo. Algal material was examined under a dissecting microscope (magnification 4 to 25 x) to confirm that the sample was indeed primarily composed of *Cladophora* and not other filamentous chlorophytes. Prior to analysis, algal tissue was freeze dried (Modulyo D, ThermoSavant, Holbrook, NY) at -50 °C for 48 hours. Dry tissue was then ground using a ball and mill grinder, and homogenized sub-samples were combusted at 450 °C for 1 hour and then autoclaved for 30 minutes in distilled water with 4% potassium persulfate solution added to a final concentration of 0.16%. Following digestion, solubilized P was measured spectrophotmetrically using the molybdate blue method (APHA 1998). Tissue content of C and N was assayed using an elemental analyzer (CEC-440, Exeter Analytical, N. Chelmsford, MA).

6.3.6 Statistical Analyses

The resulting unbalanced design of the sampling for water quality variables (variable number of stations in each region) complicates statistical comparisons. Nonetheless, to contrast conditions in Lake Simcoe with those encountered in the Great Lakes, a one way ANOVA was used to compare average water chemistry and physical parameters of interest. Data were $\log_{10}$ transformed to equalize variances and stations were binned into corresponding "site" groupings. In Lake Simcoe, groupings consisted of Cook's Bay (C1, C6, C9), Kempenfelt Bay (K39, K42, K45) and the main lake stations (S15, E50, E51, 900, N31, N32). Additional stations to characterize near shore variability were composed of the transect stations at Georgina (901, 902, 903), Thorah Island (904, 905, 906) and near Pefferlaw River (907, 908, 909). For comparative

purposes, data from near shore areas of the Great Lakes sampled in 2005 (Chapter 3) were used to characterize differences between the Great Lakes and Lake Simcoe nutrient chemistry. Great Lakes sites comprised of a site in Georgian Bay (Cape Chin), two sites in Lake Huron (Southampton and Pike Bay), three sites in Lake Erie (Nanticoke shoal, Peacock Point, and Grand River) and four sites in Lake Ontario (Oakville, Port Credit, Presqu'ile Provincial Park, Dobb's Bank). Data were further binned into seasonal groupings based upon the month of sampling and thermal regime of the water body in question. Spring covered the period from mid April to early June in the Great Lakes data, but only May samples were classed as spring for the Lake Simcoe data. Summer covered the months of July and August for both Lake Simcoe and the Great Lakes sites. While recognizing that these are somewhat crude classifications, obvious differences in nutrient and chemical conditions should nonetheless be apparent. ANOVA was run using the base *stats* package in the statistical software R (R Core Development Team 2007). Post-hoc comparisons were conduced using a Tukey-Kraemer test with an α level set to 0.05.

6.4 Results

6.4.1 Water chemistry and physical conditions

Considerable variability in thermal structure is imparted by the variability in basin morphometry and the seasonal thermocline in Lake Simcoe appears to be between 12 and 15 m deep (data not shown). Patterns of surface temperature varied predictably within the lake and within the months of sampling, with shallow areas of the lake (e.g., Cook's Bay, eastern portion) warming more quickly than deeper areas (e.g., Kempenfelt Bay). Surface temperatures measured at the Island transects and Pefferlaw transect stations in May 2006 were ~ 10 °C, with temperatures at bottom ranging from 6 to 8 °C. Surface temperatures in the summer months (July and August) were generally quite stable with one exception. Surface temperatures in August 2007 were considerably lower and more variable among the stations (19.16 ± 1.18 °C) than in August 2006 (24.44 ± 0.71 °C). Strong north easterly winds during the August 2007 sampling may have caused upwelling of cooler water from the main basin hypolimnion into the east portion of the lake.

Light attenuation in Lake Simcoe is comparable to that in Lakes Erie and Ontario during both spring and summer (Figure 6.2a, Figure 6.3a). Higher PAR attenuation in Cook's Bay and at Pefferlaw during the spring was due to re-suspended sediment, as the macrophyte overstory was not yet fully developed. The main lake and other shallow areas (< 10 m) in Lake Simcoe have similar attenuation coefficients for near shore Great Lakes areas. In Simcoe, these shallow areas (e.g. Georgina, Thorah and Pefferlaw transects) can also experience high turbidity (and thus high light attenuation) due to re-suspension of material from the lake bottom even in the summer when accompanied by strong winds in August 2007 (Figure 6.3a; see Thorah and Georgina Island transects).

Concentrations of chlorophyll a in Lake Simcoe were remarkably similar to Great Lakes sites during both spring and summer (Figure 6.2b, Figure 6.3b). Patterns of variation were not consistent among sites, or within lakes, however higher chlorophyll was observed in Cooks Bay and Kempenfelt Bay during the summer compared to the main lake and the transect sites which are located in shallow waters over dreissenid colonized substrate.

Spring TP in Lake Simcoe was generally similar to concentrations in the Great Lakes sites, but were higher than concentrations measured in Georgian Bay and Lake Huron (Figure 6.2c). In contrast, summer TP in Lake Simcoe was generally the same as at the highly agricultural Southampton site in Lake Huron, but was higher than all sites in Lake Erie and Ontario (Figure

6.3c). Spring soluble reactive P (SRP) did not vary considerably within areas of Lake Simcoe, and was comparable to SRP measured at all the Great Lakes sites (Figure 6.2dFigure 6.3). In the summer, SRP in Lake Simcoe was comparable to concentrations in Georgian Bay, Lake Huron and Lake Ontario. Lake Erie SRP was not detectable in any of the samples (Figure 6.3d).

In contrast to weak variation among sites with respect to P concentrations, there were remarkable differences between NO_3^- and SiO_2 concentrations (Figure 6.2e and f, and Figure 6.3e and f). NO_3^- concentrations in the spring in Lake Simcoe were remarkably low (< 10 $\mu g\ L^{-1}$ to 70.8 $\mu g\ L^{-1}$), and dropped to concentrations at or below the detection limit (~ 10 $\mu g\ L^{-1}$) in the summer (Figure 6.2e, Figure 6.3e). This is in stark contrast to the Great Lakes sites, where NO_3^- concentrations were significantly higher in both spring and summer (Figure 6.2e, Figure 6.3e). Spring SiO_2 concentrations in Lake Simcoe are similar to those observed in Georgian Bay and Lake Huron, and greatly exceed concentrations found in Lakes Erie and Ontario (Figure 6.2f). This pattern continues into the summer, although the magnitude of concentrations differs, SiO_2 is still quite high in Lake Simcoe (Figure 6.3f).

6.4.2 Acoustic surveys

Maps displaying the kriged surfaces for percent cover and estimated canopy height derived from the analysis of acoustic data at Georgina and Thorah Island are shown in Figure 5. During the spring survey at these sites, I failed to detect any growth of either filamentous algae or macrophytes using the acoustic system. Observations made during the survey with under water video (SplashCam; Ocean Systems, Everett, WA, see Ozersky et al. submitted) at each of the water quality sites (Figure 6.1) and randomly selected locations along survey transects showed a substratum comprised of small to medium sized cobble, colonized by dreissenid mussels. Based on visual examination of the underwater video, the substratum was not heavily colonized by periphyton, and the presence of filamentous algae could not be confirmed visually. Isolated stems of macrophytes (mostly *Myriophyllum spicatum*) were observed growing in areas underlain predominantly by hard substratum, perhaps rooting between rocks or interstitial spaces created by dreissenid shells. Many of these single macrophytes probably escaped detection by acoustics due to a sparse distribution, low biomass, and close association with the substratum.

The August surveys were far more successful for detection of submerged vegetation with acoustics. Isolated patches of moderate to high percent cover were evident along both islands but the areal extent of growth at Thorah Island was significantly larger due to the much gentler bathymetric slope when compared to Georgina Island (Figure 6.4 and Figure 6.1). Nearly all the growth in these areas was characterized by bed heights in excess of 20 cm, and was confirmed to

be largely due to macrophyte growth with the aid of the underwater camera system. Some growth of *Cladophora* was observed at Thorah Island, but it did not reach sufficient height for detection with the acoustic system. Similar conditions were encountered during follow-up water quality surveys during 2007.

In the few areas where *Cladophora* was confirmed to be present either by visual observation or with the underwater camera, samples were collected for tissue nutrient analysis via snorkeling or rake sampling. Compared to *Cladophora* collected from Cook's Bay and Shingle Bay where it was growing epiphytically on macrophytes, *Cladophora* from the Island sites in May and July of 2007 appeared to be heavily encrusted with epiphytic diatoms. These samples also had the lowest tissue nutrient content (both P and N) (Figure 6.5a), yet did not appear to be greatly P deficient when compared to samples from near shore areas of the Great Lakes (Figure 6.5b,c,d). Low tissue N and P content (as a % of AFDW) may have been due to a high inorganic content, as these samples were characterized by low organic content (LOI ~ 41-47 %) when compared to samples found elsewhere in Lake Simcoe and the Great Lakes (LOI ~ 65 – 89 %).

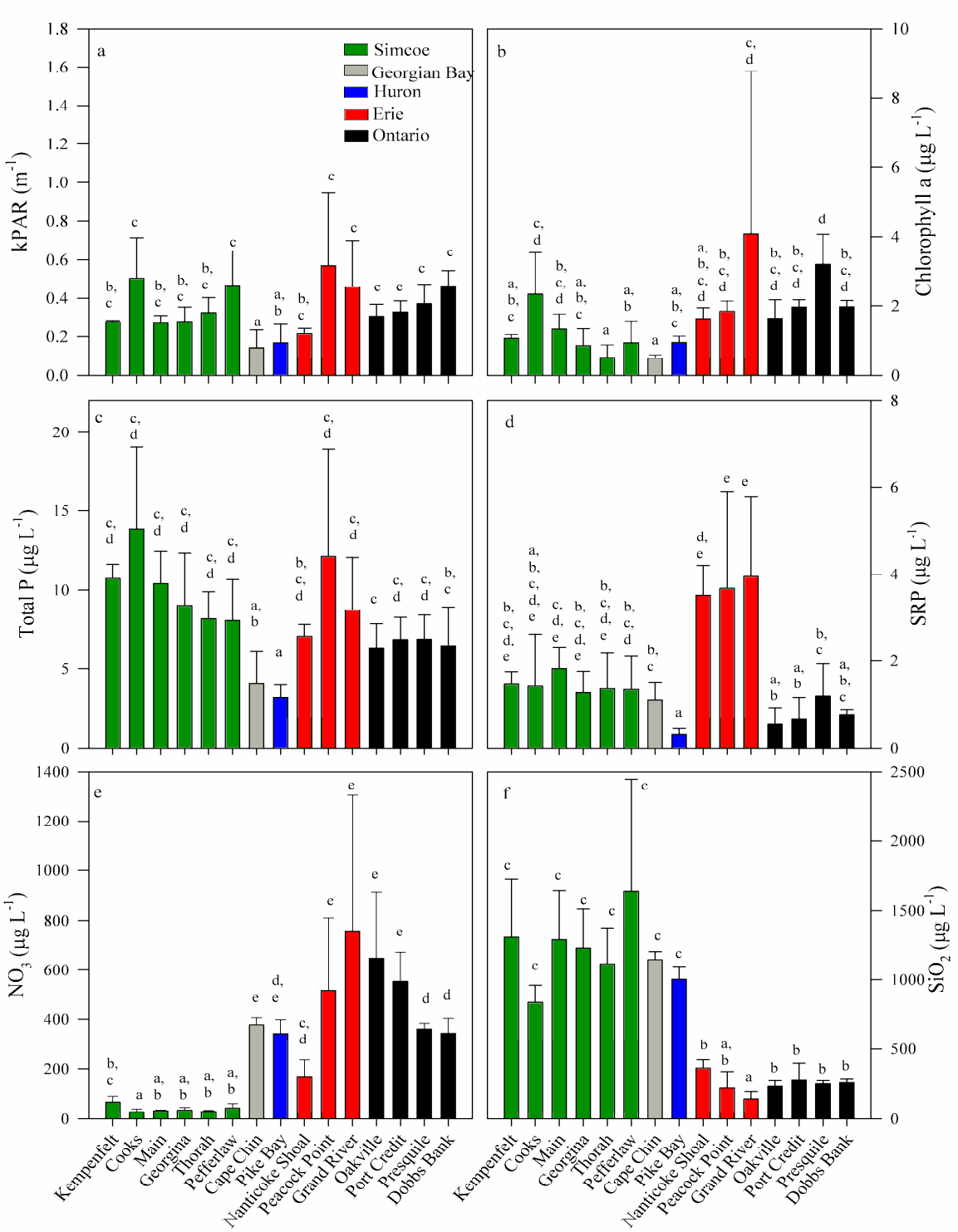

Figure 6.2. Plots of average a) light attenuation (kPAR; m^{-1}), b) Chlorophyll a (µg L^{-1}), c) TP (µg L^{-1}) , d) SRP (µg L^{-1}), e) NO_3 (µg L^{-1}), f) SiO_2 (µg L^{-1}) in Lake Simcoe and selected nearshore areas of the Great Lakes for spring periods (April – early June). Lake Simcoe data are compiled from 2006 and 2007, Great Lakes data from 2005. Note color of bar denotes the water body as in panel a).Superscript letters denote values not significantly different at p=0.05.

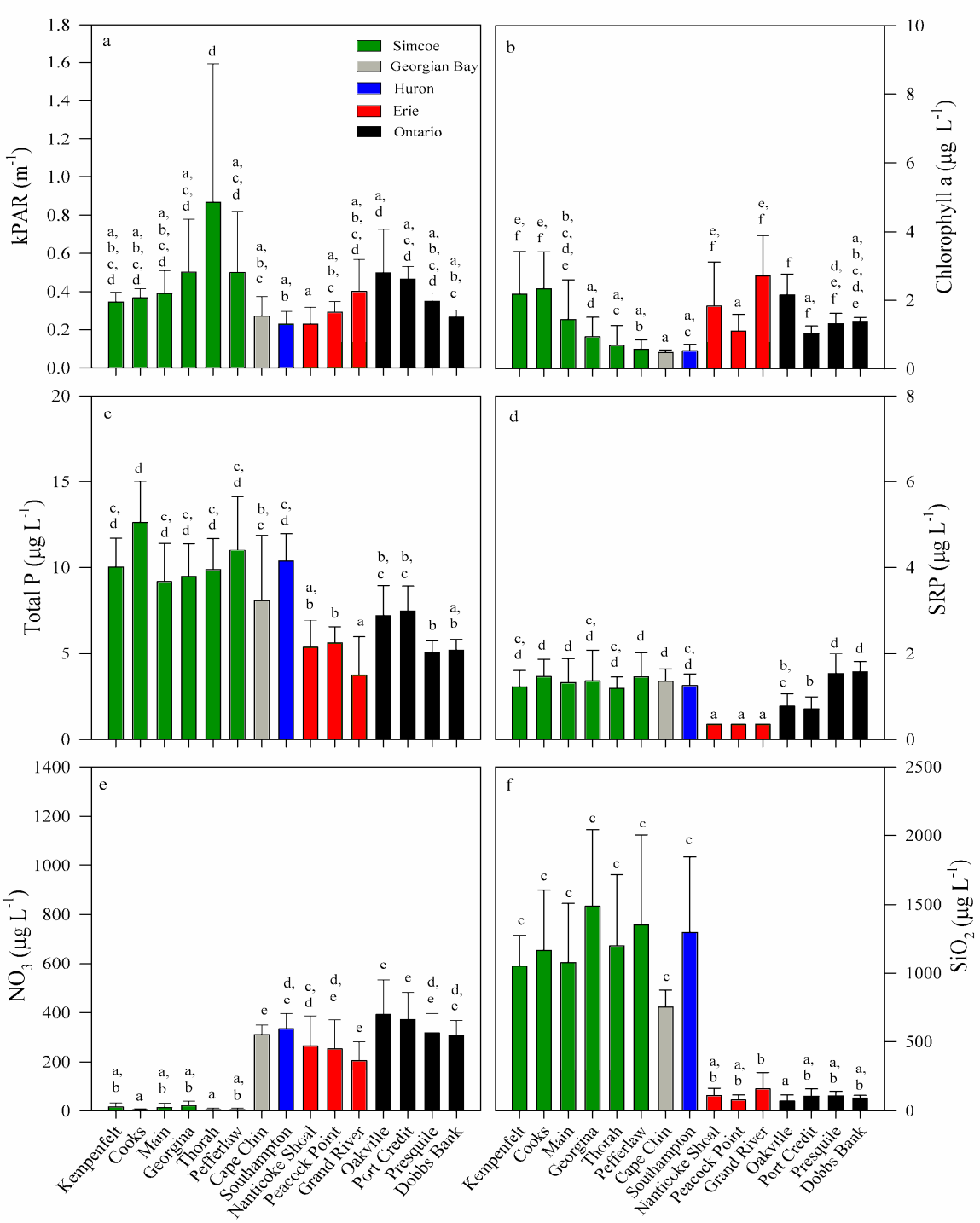

Figure 6.3. Plots of average a) light attenuation (kPAR; m^{-1}), b) Chlorophyll a (µg L^{-1}), c) TP (µg L^{-1}) , d) SRP (µg L^{-1}), e) NO_3 (µg L^{-1}), f) SiO_2 (µg L^{-1}) in Lake Simcoe and selected nearshore areas of the Great Lakes for summer periods (July to August). Lake Simcoe data are compiled from 2006 and 2007, Great Lakes data from 2005. Note color of bar denotes the water body as in panel a). Superscript letters denote values not significantly different at p=0.05.

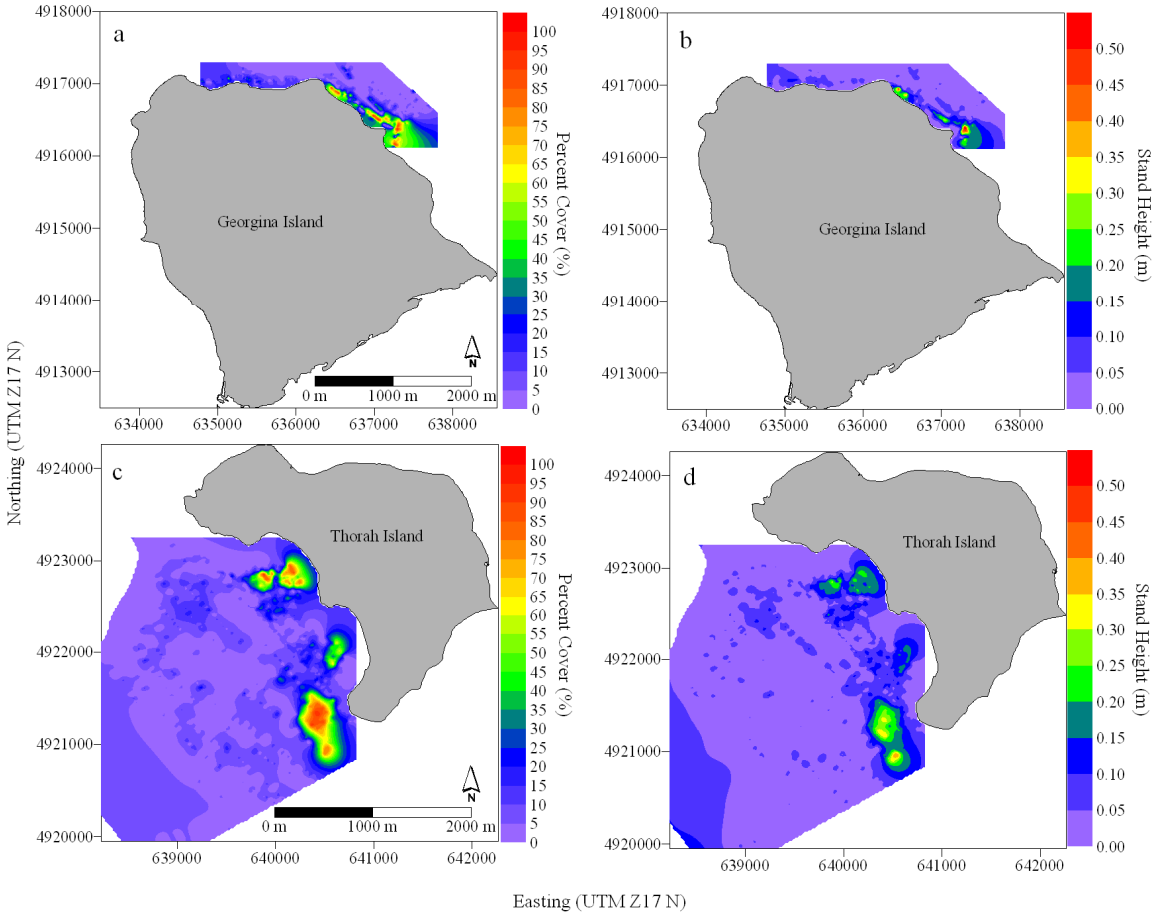

Figure 6.4. Maps of kriged surfaces showing percent cover at Georgina Island (a), canopy height at Georgina Island (b) and percent cover at Thorah Island (c), and canopy height at Thorah Island (d) on August 9 2006.

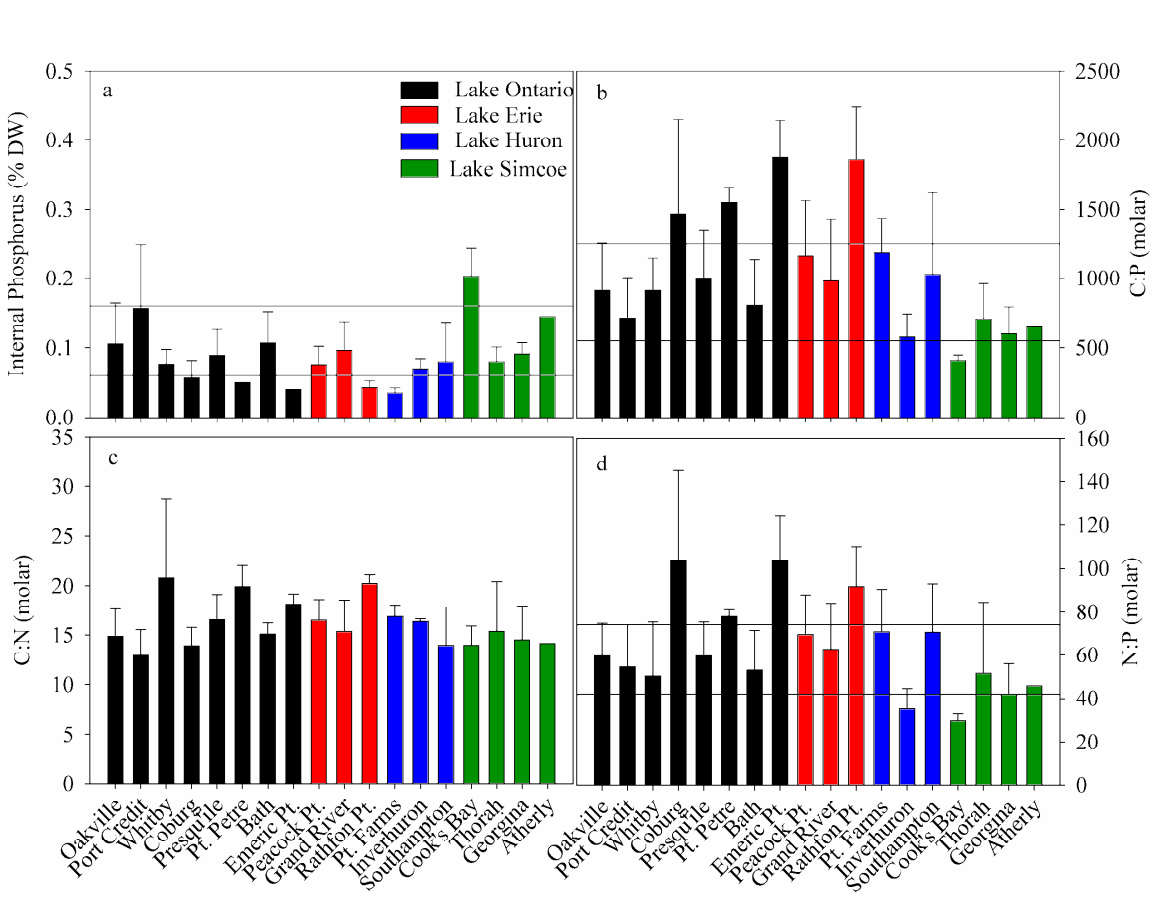

Figure 6.5. Bar plots of a) % tissue P b) tissue C:P ratio ,c)tissue C:N ratio and d) tissue N:P ratio of Cladophora tissue samples from Lake Simcoe and other locations in the Great Lakes. Data from Lake Ontario, Erie and Huron were collected during 2005 and 2006 and are summarized from Houben (2007) and Higgins et al. (2008). Data below upper specification line in panel a) indicate P limit growth (< 0.16% P DW) and below the lower specification indicate levels corresponding to zero net growth (< 0.06% DW). Data above upper line in panel b) and d) indicate C:P > 1550 and N:P > 74 determined by Houben (2007) to correspond to zero net growth. Data above the lower line in panel b) and d) indicate C:P > 550 and N:P > 42 determined by Houben (2007) to correspond to P limited growth.

6.5 Discussion

The initial goal of this study was to apply the hydroacoustic survey methodology developed in Chapter 2 to areas in Lake Simcoe with conditions that were hypothesized to be conducive to *Cladophora* growth. Although other filamentous chlorophytes such as *Ulothrix zonata* (Weber and Mohr) Kützing, *Stigeocolonium tenue* (Ag.) Kützing and *Spirogyra* are common members of the benthic algal assemblage in the Great Lakes rocky littoral areas, their occurrence as nuisance blooms is less well documented (Graham 1982). The dominance of *Cladophora* in these highly turbulent environments is thought to arise by virtue of its physical attributes (e.g., tenacious holdfasts and robust mature thalli) as well as its rapid growth rate (Garwood 1982). Finer, un-branched filamentous algae (e.g., *Stigeocolonium tenue*, *Spirogyra* and *Ulothrix*) have delicate filaments and lack the robust holdfasts characteristic of *Cladophora,* and therefore may not be able to withstand the physical turbulence common in rocky littoral areas (Rosemarin 1982, Garwood 1982, Lowe and Pillsbury 1995). Recent work using molecular markers (e.g., Ross 2006) has confirmed that the dominant filamentous alga of the dreissenid infested littoral zones of the Great Lakes is indeed *Cladophora glomerata* (L.) Kützing, and this particular species is responsible for the excessive nuisance blooms in recent years in Lakes Erie (e.g., Higgins et al. 2005a), Ontario (e.g., Malkin et al. 2008) and Michigan (e.g., Bootsma et al. 2004).

As mentioned in the introduction, the apparent resurgence of shoreline fouling by *Cladophora* in the Great Lakes occurred in the mid 1990s, approximately 5 to 8 years after dreissenid mussels became established (Higgins et al. 2008a and references therein). Reconciling the return of excessive *Cladophora* growth to the near shore regions of the Great Lakes in the presence of continued declines in offshore nutrient concentrations (e.g., Malkin et al. submitted) is complicated by the lack of data on *Cladophora* biomass and distribution in the intervening periods between P control and the invasion of dreissenid mussels (Higgins et al. 2008a). However, the apparent response of *Cladophora* biomass and distribution to P control in Lake Ontario in the early 1980s (Painter and Kamaitis 1987) coupled with lake wide declines in near shore P concentrations (Nicholls et al. 2001) suggest that reductions in *Cladophora* biomass were likely to have occurred elsewhere, and that the current resurgence is perhaps best explained by the shunt hypothesis that links the *Cladophora* resurgence to ecosystem changes mediated by dreissenids (Hecky et al. 2004).

Part of the rationale for this study was that the extensive annual monitoring conducted by the Ministry of Environment since 1980 (Eimers et al. 2005) covered time periods of high

nutrient loads, declining nutrient loading, dreissenid invasion, and currently a period of established mussels and relatively stable P loadings (Winter et al. 2007). Therefore, trends in water clarity and nutrients are characterized sufficiently during periods of P loading reduction and the subsequent invasion of dreissenid mussels to attribute some obvious changes to mussels rather than nutrient reductions (Eimers et al. 2005). For example, while improvements in phytoplankton bio-volume and water clarity were noted prior to the establishment of dreissenid mussels, major increases in water clarity were noted in the following years (Nicholls 1998). Phytoplankton bio-volume declined and became much less variable than prior to the dreissenid period (Eimers et al. 2005). Such changes are consistent with observations from water intake monitoring in the Great Lakes before and after dreissenid colonization (e.g., Nicholls et al. 1999) and support the hypothesis that dreissenids are having a significant impact on the ecology of Lake Simcoe. Likewise, major increases in water clarity were noted in 1996 and 1997 on a lake wide basis (e.g., Eimers et al. 2005) and are more consistent with the effects of dreissenid filtering, as nutrient loading during that time did not decline significantly compared to prior years (Winter et al. 2002).

Although *Cladophora* has historically been a shoreline nuisance in Lake Simcoe (Jackson 1982), these surveys failed to detect significant amounts of *Cladophora* with the acoustic system during the surveys. While it must be acknowledged that *Cladophora* at low biomass (e.g., $< 31 \pm 18$ g m^{-2} the estimated detection limit from Chapter 2) or not of sufficient height for detection with acoustics (< 7.5 cm) will escape detection, in my experience, underwater video and visual observations in shallow water can frequently confirm the presence or absence of *Cladophora* in these cases.

Despite surface temperatures during the May 2006 survey near 10 °C and temperatures at 10 m depth ranging from 6 to 8 °C, the substratum remained mostly devoid of filamentous algal growth. Vegetative growth of *Cladophora* generally begins as water temperatures exceed 5 °C (Graham et al. 1982) and optimal photosynthetic rates are not achieved until water temperature exceeds 15 °C (Graham et al. 1982), so excessive biomass of *Cladophora* is not expected to be found so early in the season. In Lake Ontario, growth of the first cohort of *Cladophora* is generally underway at these temperatures, and although areal biomass is low (< 20 g m^{-2}; c.f. Malkin 2007), the growing *Cladophora* covers nearly 100% of the substratum with the characteristic dark green filaments (Malkin 2007). Moreover, other filamentous chlorophytes (e.g., *Ulothrix zonata, Spirogyra*) are known to colonize areas with hard substrate during early season (e.g., April and May) when water temperatures are cooler (Graham et al. 1985, 1995, Higgins et al. 2005a), yet such growths were conspicuously absent in Lake Simcoe during this study.

As the water temperature warms, *Ulothrix* and *Spirogyra* generally suffer reduced rates of photosynthesis (Graham et al. 1985,1995) and their relative contribution to the total macroalgal biomass during summer months appears to be low (e.g., Sheath et al. 1988, Jackson et al. 1990, Higgins et al. 2005, Malkin et al. 2008). The inability of *Ulothrix* and *Spirogyra* to maintain high rates of positive net growth during warm water periods (> 15 °C; Graham et al. 1985, 1995) may create an opportunity for *Cladophora* to become the dominant filamentous alga during summer months. In temperate lakes and rivers, *Cladophora* generally reaches maximal biomass in mid-summer (e.g., Higgins et al. 2005a, Malkin et al. 2008), sometimes followed by a second peak in the autumn (Whitton 1970). *Cladophora* was indeed observed during the August 2006 survey, and again during follow up water quality surveys in July and August of 2007, but *Cladophora* did not accrue to excessive biomass. This suggests that either biomass simply does not accumulate to excessive amounts in Lake Simcoe, or that perhaps biomass had detached and washed ashore prior to the surveys.

In the Great Lakes, sloughing (detachment of *Cladophora* filaments from substratum) is a common occurrence following the mid-summer biomass maxima, with much of the algal material deposited on shore (Higgins et al. 2008a). Such a phenomenon was indeed noted by Jackson (1982) during his seasonal study in Lake Simcoe in 1976 and 1980. While debate continues on the exact mechanism responsible (Higgins et al. 2008b), it is generally recognized that sufficient biomass must accrue prior to major sloughing events. While it is possible that the failure to locate nuisance biomass of *Cladophora* at the Island sites may be due to prior detachment of algal biomass, significant shoreline accumulations along the island shorelines were not obvious at the time (personal observation) and the lack of complaints from shoreline residential communities (J. Winter, Ontario Ministry of Environment, personal communication) do not support this hypothesis. Furthermore, no mention of excessive *Cladophora* growth was made during invertebrate sampling in the fall of 2005 at multiple shoreline sites around the lake (e.g., Kilgour et al. 2008), suggesting that *Cladophora* probably does not currently achieve nuisance levels in Lake Simcoe at the present time.

Causes for the apparent lack of nuisance biomass of *Cladophora* are unknown, but several possible explanations exist. The proximate factors controlling benthic algal biomass can be categorized into those regulating the process of biomass accrual and those regulating the processes that lead to biomass loss (Biggs 1996). The factors that lead to biomass accrual are generally at the level of resources (e.g., nutrients and light), while the main factor leading to biomass loss is disturbance related (e.g., excessive turbulence, abrasion, or grazing).

6.5.1 Nutrient control of *Cladophora*

Phosphorus and nitrogen are the most commonly limiting nutrients for benthic algae, although carbon limitation can be a factor in soft water lakes (Turner et al. 1995). Because Lake Simcoe is a hard water system with pH and total alkalinity comparable to shallow near shore areas in Lakes Ontario and Erie (Lake Simcoe mean pH = 8.3 ± 0.1, mean total alkalinity 2.10 ± 0.05 meq L^{-1}; c.f. Houben 2007, Lake Ontario mean pH = 8.3 ± 0.3, mean total alkalinity 1.77 ± 0.09 meq L^{-1}; c. f Houben 2007, and mean Lake Erie pH = 8.2 ± 0.4, mean total alkalinity 1.86 ± 0.11 meq L^{-1}; c.f. Depew 2003), and the observation that *Cladophora* is able to utilize HCO_3^- (Choo et al. 2002), carbon limitation of *Cladophora* growth is not likely.

Although there are reports of nitrogen limitation of *Cladophora* growth in the literature (e.g., Millner et al. 1982), nearly all studies on *Cladophora* in freshwaters indicate that phosphorus is the principal growth limiting nutrient (Auer and Canale 1982a, Painter and Kamaitis 1987, Parker and Maberly 2000). Concentrations of both TP and SRP measured during this study in Lake Simcoe are similar to concentrations measured in 2005 in near shore areas of Lakes Ontario and Erie, where excessive *Cladophora* growth is a seasonally recurrent phenomenon (e.g., Chapter 2, Chapter 3, Higgins et al. 2005, Malkin et al. 2008). Yet, NO_3^- concentrations in Lake Simcoe are far lower than those measured in the Great Lakes (Figure 6.2 and Figure 6.3). While perhaps somewhat peculiar given the dominance of agricultural land use in the catchment (Eimers et al. 2005) and the well defined trend of increasing NO_3^- concentrations in the geographically close water bodies of the Great Lakes (e.g., Millard et al. 2003, Finlay et al. 2007), these values are comparable to those collected since 1980 on an annual basis by the MOE (A. Landre, Ontario Ministry of Environment, personal communication) and are not likely erroneous. The low NO_3^- concentrations may reflect the ability of smaller lakes to denitrify or bury most external NO_3^- or DON inputs (e.g., Molot and Dillon 1993, Lepisto et al. 2006) better than large lakes (Finlay et al. 2007).

The small number of *Cladophora* tissue samples collected in this study makes statistical comparisons to other areas difficult, but current measures of tissue P are generally lower than historical data (tissue P range 0.03 to 0.65 % DW; Jackson 1982), and remain between the 0.06 % DW and 0.16 % DW values suggested for zero growth (Gerloff and Fitzgerald 1976) and P limited growth (Wong and Clark 1976). Tissue N from the Lake Simcoe samples were generally above the 1.1 % DW critical level defined by Gerloff and Fitzgerald (1976). Based on the nutrient ratio thresholds determined by Houben (2007) for Great Lakes *Cladophora*, Lake Simcoe *Cladophora* can be considered P limited (Figure 6.5), although perhaps to a lesser extent than some areas in the Great Lakes. This is not inconsistent with Lake Simcoe's status as a

mesotrophic water body. Historical N:P ratios averaged between 10 and 17 (Jackson 1982), which are far lower than current N:P ratios (mean N:P = 39, range 26 – 74, n = 11), further confirming that *Cladophora* in Lake Simcoe remains P limited at present.

Despite comparable P concentrations to near shore areas of the Great Lakes and an apparent state of P limitation in Lake Simcoe *Cladophora*, other factors such as turbulence can affect the transport of limiting nutrients to the cell surface (Vogel 1994). For epilithic algae such as *Cladophora*, their attachment to chemically inert substratum necessitates the acquisition of nutrients from the water column, and thus they are susceptible to physical controls on the thickness of the benthic boundary layer (Whitton 1970). The diffusion of nutrients across the benthic boundary layer is dependent on the thickness of the boundary layer, which may vary from mm to cm depending on the velocity of the overlying water and turbulence (Riber and Wetzel 1987) and the concentration gradient from the water column to the cell surface (Vogel 1994). Although SRP concentrations in Lake Simcoe are similar to concentrations measured in the lower Great lakes, Lake Simcoe is considerably smaller, and may not experience sufficient turbulence to overcome nutrient demand in the lack of a considerable concentration gradient. SRP concentrations in Lake Simcoe during the 1970s and early 1980s were generally in the 4 to 8 µg L^{-1} range, but concentrations >150 µg L^{-1} were observed at the site adjacent to the Orillia sewage treatment plant discharge where nuisance growth was most common (Jackson 1982). Insufficient turbulence was cited by Jackson (1982) as the primary reason for the sudden cessation of nuisance *Cladophora* growth beyond a depth of 3 m in Shingle Bay. While insufficient turbulence may explain the lack of nuisance *Cladophora* growth in sheltered shoreline areas of Lake Simcoe, the two locations surveyed in this study were far more exposed that the site Jackson (1982) sampled in Shingle Bay. The average fetch distance for the exposed portions of the island sites was 16 km, and measurements of current velocity in 2005 from an ADCP moored due west of the study sites suggest that surface currents averaged between 5 and 10 cm sec^{-1}, and 3 to 10 cm sec^{-1} at a depth of 10 m, with maximal values ~ 25 cm sec^{-1} during high wind events (Baird 2006). These current velocities are comparable to those measured in the near shore regions of the Great Lakes (Rao and Schwab 2007) and suggest that at least for these study sites, physical turbulence was likely sufficient for *Cladophora* growth at the attendant nutrient conditions.

Additional consideration of benthic boundary layer dynamics must consider the effects of nutrients excreted by dreissenids or re-mineralized in the benthos. In Lake Simcoe, dreissenid abundance and nutrient excretion rates measured *in situ* are comparable to those observed in Lake Ontario (Ozersky et al. submitted, Ozersky et al. 2009), and dreissenids appear to excrete at an N:P molar ratio of 19, which is close to the optimal ratio for benthic algae (Hillebrand and

Sommer 1999; Kahlert 1998). Even if turbulence was insufficient to maintain a supply of nutrients to *Cladophora* from the overlying water column, insufficient turbulence would conceivably prolong the duration that nutrients are available for uptake in the benthic boundary layer. Visual observations of the substratum in Lake Simcoe suggest that there is an extensive epilithic algal film present, comprised mainly of diatoms. Such epilithic biofilms are often enmeshed with hydrated glycocalyx and other mucopolysaccharides that are excreted by bacteria and other algae which can enhance nutrient retention of ammonium and phosphorus (Avnimelech et al. 1982). Reduced C:P and N:P ratios of benthic diatoms growing on dreissenids compared to bare substrate in Lake Erken (Kahlert and Pettersson 2002) are also consistent with the hypothesis that nutrients excreted by dreissenids can be assimilated by benthic algae close to the substratum surface. Based on the tissue P and nutrient stoichiometry, *Cladophora* in Lake Simcoe does not appear to be more severely P limited than *Cladophora* from the Great Lakes and suggests that perhaps other factors may be more important in controlling the accumulation of nuisance *Cladophora* biomass in Lake Simcoe.

6.5.2 Light availability

Control of *Cladophora* biomass at the resource level can also be influenced by the availability of light. Since one of the major ecosystem changes attributed to dreissenid mussel filtering activity is a substantial increase in water clarity (e.g., Howell et al. 1996, Zhu et al. 2006), an expanded habitat range and enhanced light availability at depth could reasonably be hypothesized to result in an increase in *Cladophora* biomass accrual (Higgins et al. 2008a). Although I lack direct measures of photosynthetic capacity for *Cladophora* growing in Lake Simcoe, experimental work from Lakes Erie (e.g., Higgins et al. 2008b) and Huron (e.g., Graham et al. 1982) suggest that photosynthesis is light saturated at intensities ranging from 205 to 300 $\mu E\ m^2\ s^{-1}$. Based on the PAR attenuation coefficients measured at the Island transects (average ~ $0.35\ m^{-1}$), an average surface irradiance of 807 $\mu E\ m^2\ s^{-1}$ (Lorenz et al. 1991), light limitation of growth would occur around a depth of 2.8 to 3.9 m. This approximates the depth of light limitation of growth in both Lakes Erie (Higgins et al. 2008b) and Ontario (Malkin 2007), and suggests that comparable levels of light energy are reaching the benthos.

The amount of light available to benthic algae is not solely dependent on the attenuation and scattering within the overlying water column, but also by the attenuation and scattering induced by the presence and quantity of epiphytic colonization (Sand - Jensen and Søndergaard 1981). The cellulosic cell wall of *Cladophora* and upright growth form provides a suitable substrate for a diverse epiphyte flora which often becomes structurally complex with populations

of bacteria, prostrate and adnate diatoms, and multicellular filaments of green algae (Lowe et al.1982, Stevenson and Stoermer 1982). A modest diversity of epiphyte species has been found on *Cladophora* in the Great Lakes (e.g., Lowe et al. 1982, Stevenson and Stoermer 1982, Malkin et al. 2009) and the dominant group is often primarily siliceous diatoms (e.g., *Cocconeis*) that adhere to the *Cladophora* filaments and are thus able to stay attached in high energy environments (Bergey et al. 1995, Malkin et al. 2009). Since light must first pass through the epiphyte layer, competition for light between *Cladophora* and its epiphytes is therefore a strong possibility (Dodds and Gudder 1992). Dodds et al. (1999) estimated the maximal extinction coefficient for a 30 µm thick layer of *Cocconeis* to be ~ 4500 m^{-1}, and heavy coatings of epiphytes have been shown to reduce *Cladophora* photosynthesis at light intensities < 500 uE m^{-2} s^{1} (Dodds 1991). Whether the negative effects of a heavy epiphyte coating is due to direct competition for light (e.g., Sand-Jensen 1977) or by infilling between the filaments that acts to impede current flow and presumably nutrient transport to the filaments (Nowell and Jumars 1984), is not known. While other factors obviously affect the light dependency of photosynthesis (e.g., current velocity, nutrient supply, temperature, etc), a heavy encrustation of diatom epiphytes may significantly reduce photosynthesis and restrict the ability of *Cladophora* to achieve maximal growth rates at all but very shallow depths.

The potential importance of epiphytes to *Cladophora* biomass accrual in Lake Simcoe becomes more important with the observation that silica concentrations in Lake Simcoe are significantly higher than silica levels measured in the lower Great Lakes (e.g., Lake Erie and Ontario). In Lakes Erie and Ontario, dissolved silica concentrations generally fall well below the threshold thought to limit siliceous alga (e.g., diatoms and chrysophytes) of 0.4 mg L^{-1} (Schelske et al. 1986) during the summer months (Figure 6.3). No such mid-summer decline was observed during the two years in this study, and silica concentrations never dropped below 0.5 mg L^{-1}. The scarcity of silica during the summer months in the lower Great Lakes may therefore allow *Cladophora* to outgrow its epiphyte layer (Malkin et al. 2009). Further support for this hypothesis is provided in a study of Danish lakes where filamentous green algae (e.g., *Oedogonium*, *Ulothrix, Spirogyra, Zygnema*) were dominant only in lakes with low silica concentrations or did not flourish until the spring diatom bloom had exhausted the available silica (Sand-Jensen and Søndergaard 1981). The few samples of *Cladophora* collected in this study appeared brownish and heavily encrusted by epiphytes. This is in remarkable contrast to the description of samples collected at the Orillia sewage treatment plant by Jackson (1982) of “dark green and healthy”, and those that I observed at numerous locations in Lake Ontario and Lake Erie in previous years. While I did not attempt to enumerate the epiphytes or assay the silica content (Malkin et al.

2009), these samples had a much lower organic content (LOI: 41 to 47 %) compared to *Cladophora* collected in Cook's Bay and Shingle Bay (LOI: 65 to 86 %). While not a direct measure of epiphyte colonization, LOI will be lower when siliceous epiphytes are present and it does indirectly suggest that *Cladophora* growing at the Island sites may been heavily encrusted by epiphytes and experiencing strong light limitation.

6.5.3 Grazer control of *Cladophora*

The principal mechanism controlling biomass removal of *Cladophora* in the Great Lakes is physical turbulence that tears the elongated filaments from the substratum during wind and wave action (Higgins et al. 2008a). Top down control of *Cladophora* by grazers is thought to be limited because *Cladophora* is generally considered to be a poor, non-preferred food source (Dodds and Gudder 1992). Compared to diatom rich periphyton, *Cladophora* has a much lower content of amino acids and essential fatty acids (Dodds and Gudder 1992), and may contain toxic fatty acids (e.g., LaLonde et al. 1979). Further deterrence to grazing may be provided by the large size of the filaments relative the size of the grazer (Dodds and Gudder 1992). Despite this, many species from varied taxonomic groups do graze *Cladophora* in freshwaters (reviewed in Dodds and Gudder 1992), although Dodds (1991) notes that accidental ingestion of filaments during epiphyte consumption cannot be ruled out. Grazers may also indirectly increase algal biomass by selectively removing epiphytes (e.g., Sarnelle et al. 1993) and by recycling nutrients within the algal mat (e.g., Hillebrand 2002). However, when the abundance of grazing animals is high enough, consumptive losses will far outweigh any potential benefits produced by the grazers themselves (Hillebrand 2002).

The importance grazers as controlling agents of *Cladophora* biomass in Lake Simcoe is particularly relevant since the biomass of macro-invertebrate grazers appears to have nearly quadrupled (D.R. Barton, Dept. of Biology, University of Waterloo, unpubl. data) since the period prior to the invasion by dreissenids (e.g., Rawson 1930). The significant increase in macro-invertebrate abundance, biomass and diversity (138 taxa, including sensitive species such as mayflies (e.g., *Hexagenia, Ephemerella, Caenis*) and caddisflies (e.g., *Helicopsyche borealis*); Kilgour et al. 2008) is likely related to the observation that *Dreissena* appear to be key structuring agents of benthic macro-invertebrate communities in freshwater habitats (Stewart et al. 1998a,b). While *Dreissena* are known to negatively impact certain taxa through competition for food and space (e.g., indigenous bivalves and amphipods (*Diporeia hoyi*)) (Howell et al. 1996, Dermott and Kerec 1997), colonization by dreissenids generally results in an increase in macro-invertebrate biomass, density and diversity of co-occuring taxa by providing habitat enhancement

and food resources (e.g., Stewart et al. 1998a,b). Shell material from live and dead mussels acts to increase the structural complexity and surface area available for colonization by periphyton and other sessile invertebrates (Stewart et al. 1998b). The interstitial spaces between the shells can also provide refuge from predators and other disturbances (Stewart et al. 1998b, Barton 2004). Moreover, organic matter, pseudofeces and other detritus that would otherwise be washed away by currents and wave action can become trapped in these interstitial spaces and become available for use within the benthos (Roditi et al. 1997).

The amphipods *Gammarus lacustris, Echinogammarus ischnus* and *Gammarus fasciatus* were reported in considerable numbers during 2005 and 2008 (Kilgour et al. 2008, D. R. Barton, Department of Biology, University of Waterloo, Waterloo, Ontario, Canada, personal communication). G*ammarus fasciatus* has recently been observed to feed directly on *Cladophora* filaments in Lake Erie (Johnson 2004) and Lake Ontario (Malkin 2007), while *G. lacustris* and *E. ischnus* are thought to graze mainly on detritus or epiphytic organisms rather than *Cladophora* (Stevens et al. 1997). However, comparable abundances of *G. fasciatus* were reported for eastern Lake Erie in the 1970s (~ 2500 to 4500 m^{-2}; Barton and Hynes 1978) when *Cladophora* readily achieved excessive biomass (e.g., Neil and Jackson 1982), suggesting that grazing by amphipods may be of little consequence.

Caddisfly and mayfly larvae (e.g., Feminella and Resh 1991, Harrison and Hildrew 2001) also graze *Cladophora* in stream and lake environments, but such activity can be species specific and vary on seasonal cycles (Feminella and Resh 1991). Larger omnivores such as crayfish (e.g., *Orconectes propinquis* and *Orconectes virilis*) have also been observed to crop *Cladophora* in stream and pond environments, even at low densities (< 10 m^{-2}) (Creed Jr. 1994, Dorn and Wojdak 2004). Currently, three species of crayfish are found in Lake Simcoe at comparable and higher densities (> 10 m^{-2}) (*O. propinquis, O. virilis*, and the invasive *Orconectes rusticus*), yet the N^{15} signatures of these crayfish indicated a predisposition to carnivory rather than omnivory (T. Ozersky, University of Waterloo, unpubl.data). The abundance of net spinning caddisflies and crayfish in the Great Lakes declined precipitously after the arrival of dreissenids, but this may be more related to the elimination of suitable refuge habitat by infilling of crushed dreissenid mussel shell material, pseudofeces and detritus (Ratti and Barton 2003). This does not appear to be the case in Lake Simcoe, but whether or not grazer abundance is sufficient to control *Cladophora* biomass remains to be tested explicitly.

6.6 Conclusion

The absence of nuisance *Cladophora* growth on areas of hard substrate in Lake Simcoe is strikingly different from the situation in the Lower Great Lakes (e.g., Higgins et al. 2005a, Malkin et al. 2008). It is possible that a number of the above mentioned factors act in synergistic manner to constrain *Cladophora* biomass in Lake Simcoe. The high availability of silica in Lake Simcoe may allow for continued epiphyte growth on *Cladophora* filaments. As a result, *Cladophora* may remain in a state of perpetual light limitation at all but the shallowest depths, resulting in reduced growth rates and biomass accrual. With a slow accumulation of *Cladophora* biomass, control via an abundant grazer community becomes more plausible, though the availability of other more palatable benthic algae is probably the preferred food source for many invertebrate grazers. The availability of silica may also influence the natural succession of the community as a whole. For example, Carrick and Lowe (2007) found that with continued enrichment of growth substrate with N, P and Si, diatoms continued to dominate the benthic algal community in Lake Michigan, effectively utilizing the additional N and P. Without the added Si, the benthic algal community progressed to one dominated by chlorophytes and blue green algae when diatom growth declined (Carrick and Lowe 2007).

In Lake Erken (Sweden), despite the establishment of dreissenid mussels in 1975, the benthic algal assemblage on hard substrate is considerably more diverse than the current mono-specific assemblage of *Cladophora* observed in the lower Great Lakes (e.g., Kahlert and Pettersson 2002). Lake Erken is also characterized by water chemistry that is remarkably similar to Lake Simcoe (Petterson 1990).

Further experimentation is clearly required to confirm the mechanism(s) responsible for the lack of excessive *Cladophora* development in Lake Simcoe. There are, however, multiple lines of evidence that the ecosystem changes induced by dreissenids are present in Lake Simcoe. There has clearly been a diversion of energy and suspended materials to the benthos as predicted by the near shore shunt hypothesis (e.g., Hecky et al. 2004). In particular, significant increases in water clarity (e.g., Eimers et al. 2005) and the dramatic increase in macrophyte cover in Cook's Bay (Chapter 7) is attributable to the filtering activity of dreissenid mussels. Increased abundance and biomass of benthic invertebrates (e.g., Kilgour et al. 2008) suggests an increase of food resources which cannot be linked to increased nutrient loading (e.g., Winter et al. 2007), but would be consistent with a diversion of energy flow to and the retention of nutrients in the benthos.

Chapter 7

Submerged Aquatic Vegetation in Cook's Bay, Lake Simcoe: Assessment of changes in response to dreissenid mussel invasion.

7.1 Overview

A high frequency echo sounding method was employed to assess the extent of macrophyte growth in Cook's Bay, Lake Simcoe during the late summer of 2006 and 2007. Results from this study are compared against historical hydroacoustic surveys in Cook's Bay conducted prior to major P loading reduction efforts (1984) and before the period of dreissenid mussel invasion (1987). While the historical studies suggest some expansion of macrophytes in response to a moderate increase in water clarity, the results of the recent surveys reveal a major increase in macrophyte cover, extending to a depth of ~ 10 m, into the middle portion of the Bay. Tissue nutrient content of the macrophytes growing in the Bay did not show major changes when compared to historical levels except in shallow waters (< 5 m) suggesting a possible relaxation of light limitation. These results suggest that macrophytes have responded to the large increase in water clarity mediated by dreissenid mussel grazing. While bio-deposition of particulate matter may be important in more nutrient poor environments, the historically enriched sediments of Cook's Bay appear to be sufficient to maintain excessive macrophyte biomass. These results are comparable to other shallow macrophyte dominated systems and indicate dreissenids as strong regulator of water clarity.

7.2 Introduction

Freshwater macrophytes are a diverse group of aquatic plants that include charophytes, bryophytes and angiosperms that comprise a major component of submerged aquatic vegetation (SAV) in aquatic ecosystems (Chambers et al. 1999). The importance of SAV to ecosystem processes is particularly evident in shallow lakes and embayments where SAV can play a significant role in structuring not only the physical and chemical environment, but also the biological components of aquatic ecosystems (Carpenter and Lodge 1988). For example, dense beds of SAV can attenuate water flow (Fonseca et al. 1982), enhancing the trapping and deposition of sediment and other particulates (Fonseca and Fisher 1986). SAV can alter the thermal structure by shading and affect dissolved oxygen levels in the water column through photosynthesis and respiration (Moore et al. 1994). SAV can provide substrate for epiphytic algae (Cyr and Downing 1988), and zooplankton and small fish can avoid predation by hiding within the plant canopy (Crowder and Cooper 1982, Timms and Moss 1984). Extensive SAV coverage in lakes therefore has the potential to affect not just biogeochemical cycling of nutrients and dissolved gases, but also the dynamics of pelagic and benthic food webs. Consequently, a change in the quantity and extent of SAV cover has the potential to affect significant change on the entire aquatic ecosystem (Carpenter and Lodge 1988).

The distribution of SAV in aquatic ecosystems is fundamentally determined by the complex interplay of numerous abiotic and biotic factors (Lacoul and Freedman 2006). These include; light quality and quantity (Chambers and Kalff 1985), nutrient availability (Barko and Smart 1998), water temperature, pH and alkalinity, sediment composition (Hutchinson 1975), disturbance by benthivorous fish (Painter et al. 1988), wind and ice scour (Crowder and Painter 1991), losses to herbivory (Søndergaard et al. 1996) and inter-specific competition for resources (Madsen et al. 1991). The quantitative role of SAV in lakes is largely coupled to their areal distribution, which is regulated by the morphometry of the lake and the maximum depth of colonization (Middelboe and Markager 1997). Previous studies have largely confirmed that the maximum depth of colonization is strongly linked to water clarity (Chambers and Kalff 1985, Hudon et al. 2000) thus changes in water clarity have the potential to expand or contract the extent of SAV cover (Sand-Jensen et al. 2008).

In lakes or embayments shallow enough to support SAV growth, nutrient enrichment generally leads to a decline in water clarity and subsequent loss of SAV (Sand-Jensen et al. 2008). In contrast, nutrient reductions can lead to improvements in water clarity (Jeppesen et al. 2005) though in some cases high levels of turbidity may remain; fueled by internal nutrient

loading or re-suspension of unstable sediments by benthivorous fish or wind and wave action (Scheffer 1990). Increased light availability in lakes is also attributed to filter feeding by the invasive dreissenid mussels (*Dreissena polymorpha* and *D. bugensis*; Karatayev, et al. 1997, Karatayev et al. 2002). Consequently, it is expected that the increased water clarity associated with dreissenid mussel invasion will lead to increased coverage of SAV in invaded lakes (Karatayev et al. 1997). Furthermore, the egestion of filtered particles and partially digested phytoplankton that remain bound in mucus can settle to the bottom, thus potentially enriching the benthos and promoting the growth of SAV or benthic algae (Vanderploeg et al. 2002, Hecky et al. 2004).

Studies in North American lakes have for the most part been unable to separate changes in water clarity related to nutrient reductions, and those attributable to dreissenid mussel filtration (but see Zhu et al. 2006) partly because of the paucity of data for the time period after P controls but prior to dreissenid invasion, and the fact that mussels invaded while nutrient reductions were still being manifested. Assessing the response of SAV in these ecosystems is further complicated by the lack of historical data on SAV distribution for the appropriate time periods (Zhu et al. 2007). Much like the Great Lakes, Lake Simcoe has been subjected to a long history of anthropogenic activity that has affected water quality, primarily through cultural eutrophication (Winter et al. 2007). Water quality problems in the lake since the 1970s have been attributed to a three fold increase in phosphorus (P) loading from pre-settlement rates (Evans et al. 1996). Recruitment failure of the native cold water fish populations and excessive growth of macrophytes and algae are among the principal concerns since water related recreational activities are of major economic importance to the region, bringing in nearly 200 million per year to the local economy (LSEMS 2003). These symptoms of eutrophication and potential economic losses prompted the development of the Lake Simcoe Environmental Management Strategy (LSEMS) in 1980 with the objective of reducing P loads to the level necessary to re-establish a naturally reproducing cold water fishery and mitigate aesthetic effects (Eimers et al. 2005).

In contrast to areas in the Great Lakes, Lake Simcoe provides a unique opportunity to compare changes in SAV cover through time periods associated with P loading reductions and the subsequent dreissenid mussel invasion. Dreissenid mussels were first observed in Lake Simcoe during 1993 but did not become widespread until 1995 (Eimers et al. 2005). Although dreissenid mussels preferentially attach to hard substrate (Karatayev et al. 1997), their ability to colonize soft substrates and macrophytes has also been documented (Haltuch et al. 2001). While early invasion studies estimated abundances of > 100,000 m^{-2} in Lake St. Clair (Griffiths et al. 1991) and European lakes (Musko and Bako 2005), estimates of dreissenid abundance on macrophytes

in Cook's Bay are closer to 2000 m^{-2} (Ozersky et al. submitted). Long term monitoring data on water chemistry and general physical limnological conditions have been routinely collected for over 20 years by the Ontario Ministry of Environment (e.g. Eimers et al. 2005), and provide context for historical changes to lake conditions during these periods. Prior hydro acoustic surveys in Cook's Bay, the first in 1984 (baseline) and second in 1987 (P reduction period, pre dreissena period) provide an estimate of SAV cover and nutrient content within the bay and can therefore serve as comparative points relative to the current distribution of SAV (2006 and 2007).

In this study, the distribution of SAV in the inner portion of Cook's Bay is assessed using a high frequency hydro-acoustic method (see Sabol et al. 2002a). These results are compared to the prior hydro-acoustic surveys in 1984 (Neil et al. 1985) and 1987 (Neil et al. 1991) to evaluate the changes in SAV cover during these three time periods. Additionally, the nutrient content of the SAV assemblage in 2006 is compared to nutrient content of the SAV assemblage in1984 and 1987 to assess the potential for dreissenid bio-deposits to enhance the nutrient content of the sediments in Cook's Bay.

7.3 Materials and Methods

7.3.1 Study Location

Cook's Bay is a shallow, soft bottom bay located at the south end of Lake Simcoe (Figure 7.1). The maximum depth of Cook's Bay approaches 15 m in the outer part toward the main basin of the lake, but much of the inner bay is characterized by depths < 6 m (Millard and Veal 1971; Figure 7.1). Most of the major rivers in the Lake Simcoe basin rise in the interlobate moraine south of Lake Simcoe and drain northward through clay plains, drumlin fields and large areas of organic soils (Johnson and Nicholls 1988). Agriculture is the dominant land use in the Lake Simcoe basin (43%; Eimers et al. 2005) consisting of mainly livestock and crop production (Winter et al. 2002). The Lake Simcoe catchment is also experiencing rapid urban growth (~ 8 km^2 per year since 1985; Winter et al. 2002). Cook's Bay receives drainage from the largest river in the Lake Simcoe basin (east and west branches of the Holland River). Treated sewage effluent from the towns of Aurora and Newmarket was diverted southward in mid 1984 via the York – Durham trunk sewer to the Duffins Waste water treatment plant on Lake Ontario, but urban runoff from these areas continues to flow northward through the east Holland River, to Cook's Bay. The largest area of organic soils along the lower Holland River was dyked and drained in the 1930s as a series of polders occupying ~ 30 km^2 (Johnson and Nichols 1988). Before the 1930s, the Holland River meandered though a large marsh but flow is now diverted to the Holland River by a series of canals (Figure 7.1). Water within the Holland River has historically been high in phosphorus (Nicholls and MacCrimmon 1975) and recent data indicate that the concentration of P in the Holland River remains well above the Provincial Water Quality of Ontario guideline of 0.03 mg L^{-1} on a regular basis (Winter et al. 2007). Consequently water quality data indicate that outer Cook's Bay remains in the mesotrophic range (seasonal average TP ~ 13 µg L^{-1}) while the lower part of Cook's bay remains nearly eutrophic, with TP often exceeding 20 µg L^{-1} (Eimers et al. 2005).

7.3.2 Acoustic Surveys and Data Processing

Acoustic surveys of Cook's Bay (Figure 7.1) were conducted on 9 August 2006 and 24 August 2007 on a 21 ft aluminum boat equipped with a BioSonics Inc. (Seattle WA, USA) DTX deck unit and two single beam transducers (430 kHz, 10.2° full beam angle, SL=213 dB re 1 µPa @ 1m and 120 kHz, 7.1° full beam angle, SL 216 dB re re 1 µPa @ 1m). Both transducers were mounted on adjustable aluminum poles attached to the side of the vessel with welded brackets.

Transducers were submerged ~ 30 cm below the surface of the water. Survey transects were aligned across the bay from east to west, with an average inter transect spacing of 150 to 170 m. The transducers were configured to ping a rate of 5 Hz, with a pulse width of 0.1 ms for the 430 kHz (standard for acoustic sensing of vegetation; Sabol et al. 2002a) and a pulse width of 0.4 ms for the 120 kHz transducer. Vessel speed was kept between 1.5 and 2.3 m sec^{-1}, separating the differentially corrected GPS reports from a JRC DGPS212 (Japan Radio Company) receiver by 3 – 5 m. Acoustic data were processed using the commercial software EcoSAV™ v1.0, after adjusting analysis parameters for proper receiver sensitivity (BioSonics Inc. 2001) and increasing the depth of maximum plant growth from 7 m to 12 m. Inspection of the echograms from Cook's Bay confirmed two common problems inherent to acoustic detection and characterization of vascular macrophytes (Sabol et al. 2002b); the first is due to areas of very dense vegetation that obscure the acoustic signal from the lake bottom. In this case, the peak of acoustic backscatter intensity falls within the plant canopy rather than at the bottom-water column interface. Because EcoSAV v1.0 functions as a bottom-up algorithm and classifier, the depth at which the peak backscatter occurs is therefore incorrectly indentified as the bottom. The second problem condition occurs when areas with very tall vegetation (i.e. vegetation growing close to or at the surface) are encountered. In this case, EcoSAV v1.0 classifies these pings as excessive noise in the water column, as the algorithm expects a minimum noise-free distance of ~ 18 cm between the transducer near field and the top of the plant canopy (Sabol et al. 2002b).

To evaluate the degree to which these conditions contaminated the acoustic data, preliminary processing was conducted using the default settings for EcoSAV v1.0. Output from the default run of EcoSAV v1.0 was then compared against the corresponding echogram file, and ping sequences where either of the above problem conditions was encountered were identified, recorded and removed from the data set. The most common form of failure was loss of the bottom signal due to dense macrophyte growth. Files where the problem conditions were identified were reprocessed using the same settings, but the trailing edge feature (B1; BioSonics 2001) was set to a lower backscatter intensity threshold (-55 dB from -50 dB). This enabled the EcoSAV v1.0 algorithm to search deeper in the echo envelope and place the bottom depth closer to the actual bottom depth, rather than placing the declared bottom within the plant canopy. Reprocessed output files were compared against the previous output files and the associated echogram. If the re-classified bottom depth was within ± 0.1 m of the observed depth for the ping sequences on the echogram and the preceding bottom depths, these pings were added back to the final data set otherwise they were deemed unrecoverable. Using this method, the number of discarded pings was reduced from 11.1% and 12.6% to 4.9% and 5.4% (2006 and 2007 respectively).

7.3.3 Geostatistical Analysis

The recent availability of high resolution data from acoustic systems has allowed exploration of various methods to interpolate between data points to provide a surface of predicted values. Guan et al. (1999) and Valley et al. (2005) have evaluated different methods and concluded that kriging provides the most robust method for regularly spaced data collected using acoustic methods. The prediction of spatial variation from point measurements over surface areas requires some realistic interpolation techniques. Deterministic and geostatistical methods are the two main groupings of interpolation techniques to produce a continuous surface from point measurements. Deterministic interpolations create surfaces from measured points using mathematical functions which are based on the extent of similarity (inverse distance weighting) or the degree of smoothing (radial basis functions). Geostatistical methods (i.e. kriging) utilize both the mathematical and statistical properties of the measured points (Isaaks and Srivastava 1989). For a detailed and in depth discussion of geostatistics and the underlying theory, the reader is referred to Journel and Huijbergts (1978) and Isaaks and Srivastava (1989). The basic assumption required for geostatistics is that the process under study is stationary, and that the observed values are simply one of many possible random realizations of the process (Webster and Oliver 2001). In addition, spatial autocorrelation must be present (i.e. one point should be able to provide some information about neighboring points).

The initial step in geostatistical analysis is the construction of the semivariogram. The semivariogram is a graphical representation of half the average squared variance between sample points as a function of separation distance *(h)* and is defined as

$$\gamma(h) = \frac{1}{2N(h)} \sum_{i=1}^{N(h)} \left[Z(x_i) - Z(x_i + h) \right]^2 \qquad (7.1)$$

where $\gamma(h)$ is the semivariance for lag *(h)*, $Z(x_i)$ is the measured value at location x_i, $Z(x_i+h)$ is the measured value at location (x_i+h) and $N(h)$ is the total number of paired samples for a given lag *(h)* (Cressie 1991). The experimental semivariogram has important characteristics that reveal the kind of spatial variation present in an area, for the variable under study. Generally, the semivariance increases as the lag distance (h) increases to a maximal value, after which the semivariance is frequently flat. This lag distance is known as the range and it represents the limit of spatial autocorrelation. By definition, $\gamma(h)=0$ when $h=0$, however any smooth curve that approximates values of γ as h approaches 0 is unlikely to pass through the origin. This value (i.e when $h=0$) is termed the nugget variance. The nugget variance is a combination of measurement error and variation at distances smaller than the shortest sample spacing which cannot be

resolved. The value of γ where γ reaches its maximum is called the sill (*C*), and represents the maximum semivariance.

To describe the spatial variation at distances other than just the lag distances, a mathematical function is fit to the experimental semivariogram data, usually using weighted least squares (Cressie 1991). Two of the three more common models were used with the acoustic data: the spherical and exponential model. These two models in terms of the semivariogram are given in equation (2; spherical model) and equation (3; exponential model);

$$\gamma(h;\theta) = \begin{Bmatrix} 0, & h = 0 \\ C_0 + C_s\ ((3/2)(\|h\|/\alpha_s) - (1/2)(\|h\|/\alpha_s)^3), & 0 < \|h\| \le \alpha_s \\ C_0 + C_s, & \|h\| \ge \alpha_s \end{Bmatrix} \quad (7.2)$$

$$\gamma(h;\theta) = \begin{pmatrix} 0, & h = 0 \\ C_0 + C_e(1 - \exp(-\|h\|/\alpha_e)), & h \neq 0 \end{pmatrix} \quad (7.3)$$

where *C* is the sill of the variogram that represents the maximal variation (C_s for the spherical model and C_e for the exponential model), α is the range of the variogram beyond which data are no longer autocorrelated (α_s and α_e as before), and C_0 is the nugget effect. A variogram model can also be nested, i.e. it can be a combination of two or more component models such as nugget and exponential. Most variograms are nested in this manner, although more complex models (i.e. a double spherical with nugget) are sometimes used. Once the semivariogram function has been defined and fit, it can be used to weight predictions in the kriging system of equations to yield the best linear unbiased estimator of the target variable. For more information on the various forms of kriging the reader is referred to Webster and Oliver (2001).

Exploratory data analysis was conducted on raw acoustic data before variogram modeling and analysis. Strong relationships between percent cover and bottom depth were observed for data collected in Cook's Bay. A non-linear, confounding effect of depth was also observed for the height variable from Cook's Bay. I therefore performed kriging with external drift for the percent cover variable with depth as a predictor, and used regression kriging for the height variable with depth as a predictor. To remove the non-linear depth trend from the height variable, I followed a similar procedure outlined in Valley et al. (2005). Briefly, a non-parametric regression smoother (generalized additive model; GAM) using the default settings in the *mgcv* package (Wood 2008) in the statistical software R (R Core Development Team 2007) was used to determine the trend in macrophyte canopy height with depth. The smoothed relationship between depth and height was a 9th order polynomial (Figure 7.2). Trend fits for depth were highly significant in both years (Chi square; p<0.0001) and explained greater than 50% of the variation in plant height (adjusted r^2,

0.599 and 0.655 in 2006 and 2007 respectively). Residuals from the macrophyte height vs depth relationships were kriged using block kriging (following the framework of Hengl et al. 2004) and the trend was added back to the interpolated residuals to provide the grid of plant height.

7.3.4 Macrophyte sampling and internal nutrient analyses

Qualitative samples of macrophytes were obtained at 26 locations in Cook's Bay during the acoustic survey on 9 August 2006 by snorkeling and with the use of a rake in deep water (Figure 7.1). Samples were placed in large garbage bags and stored in coolers until returned to the laboratory. Upon return to the lab, samples were washed to remove debris, sediment and other organisms (including attached dreissenid mussels) and sorted for identification to genus and species before drying at 65 °C for one week. Dry tissue was then ground using a ball and mill grinder prior to analysis. Homogenized sub-samples were then combusted at 450 °C for 1 hour and then autoclaved for 30 minutes in distilled water with 4% potassium persuphate solution added to a final concentration of 0.16 %. Following digestion, solubilized P was measured spectrophotometrically using the molybdate blue method (APHA 1998). Tissue C and N content was assayed using an elemental analyzer (CEC-440, Exeter Analytical, N. Chelmsford, MA)

7.3.5 Estimation of macrophyte biomass

Estimation of biomass is a commonly desired endpoint in surveys of benthic vegetation (Vis et al. 2003). Previous attempts at estimating standing crop of macrophyte biomass from echosounder data have generally followed two approaches; the first relies upon the range information (e.g., estimated height of the macrophyte canopy) to predict the standing crop of macrophyte biomass (Duarte 1987). More recent efforts have attempted to exploit characteristics of echosounder data stored in digital format, and allow for computation of standard echo integration techniques (e.g., Sabol et al. 2002a) or other measures of echo intensity (e.g., Haga et al. 2007). Yet, these newer approaches have not resulted in significant improvements, perhaps due to different acoustic reflectivity from different species of plants (e.g., Hoshauva et al. 2008), presence of epitphytic organisms (Sabol et al. 2002a) or acoustic shadowing at very high biomass (Haga et al. 2007). I therefore chose to use the method outlined by Duarte (1987), utilizing the estimates of canopy height that can be related to the growth form of the species present, and subsequently the biomass density (Duarte 1987).

The biomass density (g m^{-3}) of macrophytes can vary appreciably in mixed assemblages of freshwater macrophytes and has been demonstrated to depend on the growth form of macrophyte species (Duarte and Kalff 1987). The relationship;

$$\text{Biomass} = -343 + 37.7[\text{height}]^3 + 953[\text{growth form x height}],\ r^2=0.89 \quad (7.4)$$

developed by Duarte (1987) for temperate lakes relies on division of macrophyte species into 3 classes based on the growth form of the dominant species. Tall canopy forming species (e.g., *Myriophyllum spicatum*, *Potomogeton crispus*, *Potomogeton richardsonii*) that grow to the surface to flower have some of the lowest biomass density values and are classes as growth form 1 (Duarte 1987). Intermediate biomass density is found in species that produce relatively short understory and develop flowers that float to the surface on a short peduncle (e.g., *Utricularia* sp., *Vallisneria americana*) and these are classed as growth form 2 (Duarte 1987). The class with the highest biomass density (growth form 3), include the species with submerged flowers (e.g., *Ceratophyllum demersum*, *Chara* sp., *Elodea canadensis*) (Duarte 1987).

Two approaches were used to provide a spatially explicit estimate of macrophyte biomass. I used the growth form classification scheme suggested by Duarte (1987) for species of plants that were identified during this study (via snorkel sampling, n=6) and a second study that took place during 22-23 August 2006 where a ponar grab was used (Stantec 2006; n=121). The first approach was based on the rationale that the environmental conditions determine the growth form of the dominant species (Chambers 1987) and that echosounder tracings can estimated the growth form of the dominant species (Duarte 1987). Provided that nutrient content of the sediments is sufficient, in temperate latitudes, tall canopy producing species replace shorter understory forms as depth increases and the shorter understory forms become light limited (Chambers 1987). I set arbitrary limits on canopy heights for each growth form class; growth form 3 (most dense) was assigned to canopies < 0.5 m, growth form 2 (moderate biomass density) was assigned to canopies between 0.5 and 1.5 m in height, and class 1 (lowest biomass density) was assigned to canopies > 1.5 m in height. The equation specified by Duarte (1987) for mixed assemblages was then used to estimate the wet mass of macrophytes in each grid cell as a function of kriged canopy height and the assigned growth form. Wet mass was converted to dry mass by multiplying by a wet/dry conversion factor (0.162) empirically derived from the data in Stantec (2006).

The second approach consisted of a more complex geostatistical procedure called sequential indicator simulation. As before, the data provided in Stantec (2006) formed the bulk of the input data. For the sites within Cook's Bay sampled by Stantec (2006), the dominant growth form class was assigned to a location by determining the growth form of the species that contributed to the total biomass at each site (using the guidelines in Duarte 1987). The generation of maps depicting vegetation species or types often display non-overlapping polygons of different classes indicating the presence or absence of species (Miller and Franklin 2002). Such maps can

also be viewed as continuous distributions mapped with a given probability of occurrence if indicator transforms are used (Miller and Franklin 2002). Use of the more common geostatistical methods described above can be problematic when mapping species distributions (or in this case, growth form of the dominant species) because they assume positive autocorrelation between nearby observations to interpolate nearby values at un-sampled locations. This may be problematic for delineating vegetation because the ways in which SAV reproduces or propagates may not necessarily produce smooth surfaces. For example, although asexual or clonal reproduction via rhizomes or tubers is a common feature in some macrophytes such as *Vallisneria* sp. (Barrat-Segretain 1996) that theoretically might produce a smooth surface, the ability of many macrophytes to reproduce via fragmentation of above ground tissues, overwintering turions or seeds probably will not produce a smooth surface of species distributions as these are subjected to dispersal by water currents and biota (Lacoul and Freedman 2006).

To generate such maps, indicator kriging (IK; a non-linear kriging variant; see Goovaerts 2001) is often used. IK aims to evaluate the probability for the target variable to exceed a defined threshold (or in this case, the presence or absence of a particular growth form) at a specific location. However, IK also has a smoothing effect and the conditional cumulative distribution function (ccdf) obtained by IK can only provide a measure of local uncertainty related to a single location, while the spatial uncertainty (multi-location uncertainty) of mapping at several locations simultaneously cannot be assessed using IK (Juang et al. 2004). Sequential simulation, also called stochastic interpolation was proposed to overcome this limitation inherent in IK (Deutsch and Journel 1998). The simulation methods are based on probabilistic models; systematically adding a stochastic noise component into the kriging model (Juang et al. 2004). Unlike kriging, where the focus is on minimizing the error variance, simulation focuses on reproduction of statistics such as the sample semivariogram and the honoring of original data values (Goovaerts 2001). Consequently, realizations generated by sequential simulation look more realistic and these are an effective way of describing the variability in spatial fields (Juang et al. 2004). Sequential simulation yields not one but *n* numbers of realizations, each of which is an equally likely outcome.

The sequential simulation method involved the following steps. The first step involves coding each growth form observation into a vector of indicator values by indicator transforms as follows:

$$I(x;z_c)=\begin{cases}1, & z(x)=z_c \\ 0, & otherwise\end{cases} \quad c=1,2,3 \tag{7.5}$$

Where z_c is a desired classification. In this study the classification was simply the presence or absence of the particular growth form in question (1, 2 or 3). For each growth form, the experimental indicator semivariogram was computed as above and a valid semivariogram model (e.g., spherical or exponential) fit and the parameters of the fitted model determined – the nugget, the sill and the range. Next, the prior distribution estimation is done by defining a random path to unsampled locations and visit each location to simulated only once. At each unsampled location, the indicator variogram is used to estimate the probability of the presence of each growth form.

$$F[x, z_c \mid n] = \Pr ob_{IK}[z(x) = z_c \mid n] = E[I(x, z_c \mid n)] \quad (7.6)$$

where $F(x,z_c|n)$ is the ccdf of $Z(x)=z_c$ and $E[I(x,z_c|n)]$ is the expected value of $I(x,z_c)$ which is obtained via indicator kriging. The prior distribution is then built with calculated probability of growth form presence. All original data and values that are simulated previously within a local neighborhood are included in the simulation. Multiple realizations are produced, each following a random path representing equiprobable spatial distribution of growth form presence. Therefore numerous realizations can be used to evaluate the variation and uncertainty of the presence/absence of each growth form following:

$$\Pr ob_{SIS}[z(x) = z_c] = \frac{n[z(x)]}{m} \quad (7.7)$$

where the sequential indicator simulation was carried out m times and $n[z(x)]$ is the number of realizations where each growth form was simulated to be present. For the generation of indicator growth form maps, 500 sequential indicator simulations were conducted using a local neighborhood determined by the range of the indicator semivariogram. Each simulation was then compiled and converted to a single map representing the probability of occurrence for each growth form in each grid cell. A composite growth form map was then created by assigning the growth form with the highest probability of occurrence to the grid cell in question. Sequential indicator simulation was performed using the *gstat* package (Pebesma 2004) in the statistical software 'R' (R Core Development Team, 2007). Biomass was then subsequently computed using the Duarte (1987) equation as above.

.

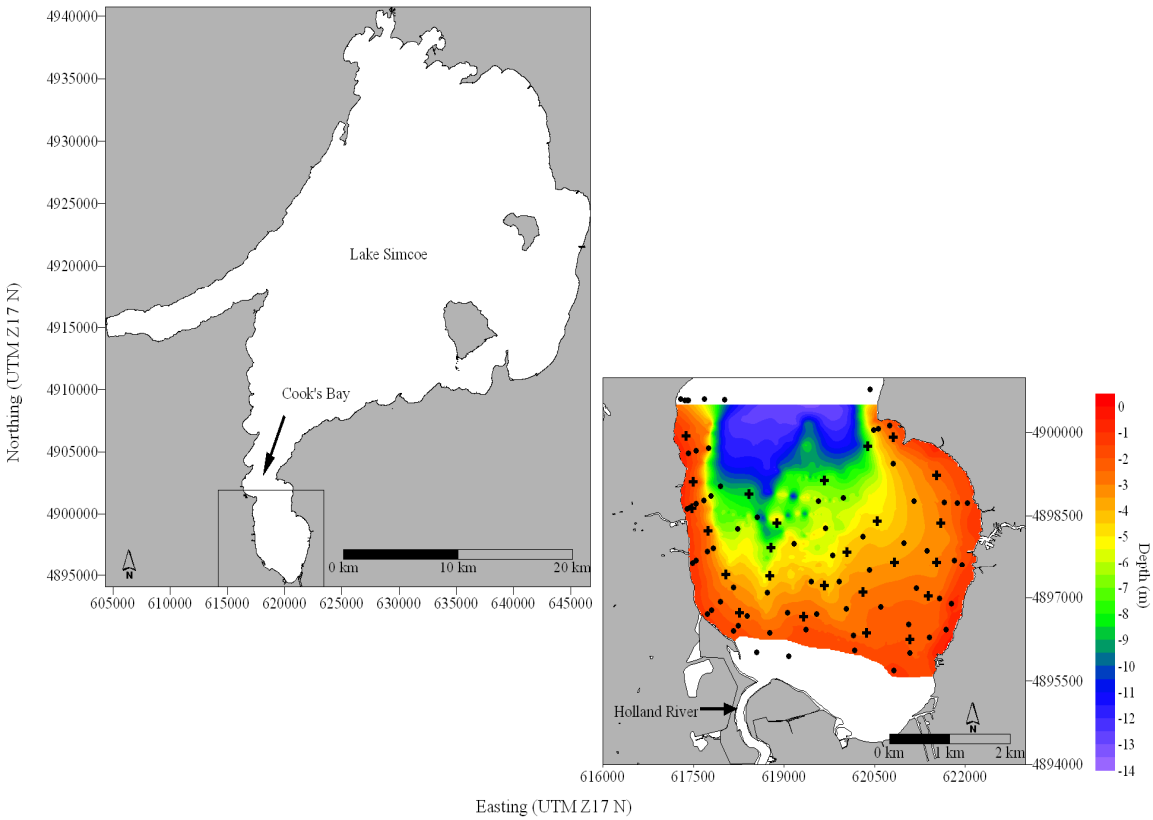

Figure 7.1. Map showing the location of Cook's Bay in Lake Simcoe. Zoomed rectangle indicates the approximate location of the acoustic surveys. Bathymetry of Cook's Bay was generated using universal kriging with northing as the covariate and is shown in the zoomed portion**.** Note that the inner portion of the bay (blank) is too shallow for vessel passage and is characterized by heavy growths of emergent vegetation.(✚) denotes the locations of rake based macrophtye sampling from this study and (●) denotes the locations of ponar samples taken by Stantec (2006).

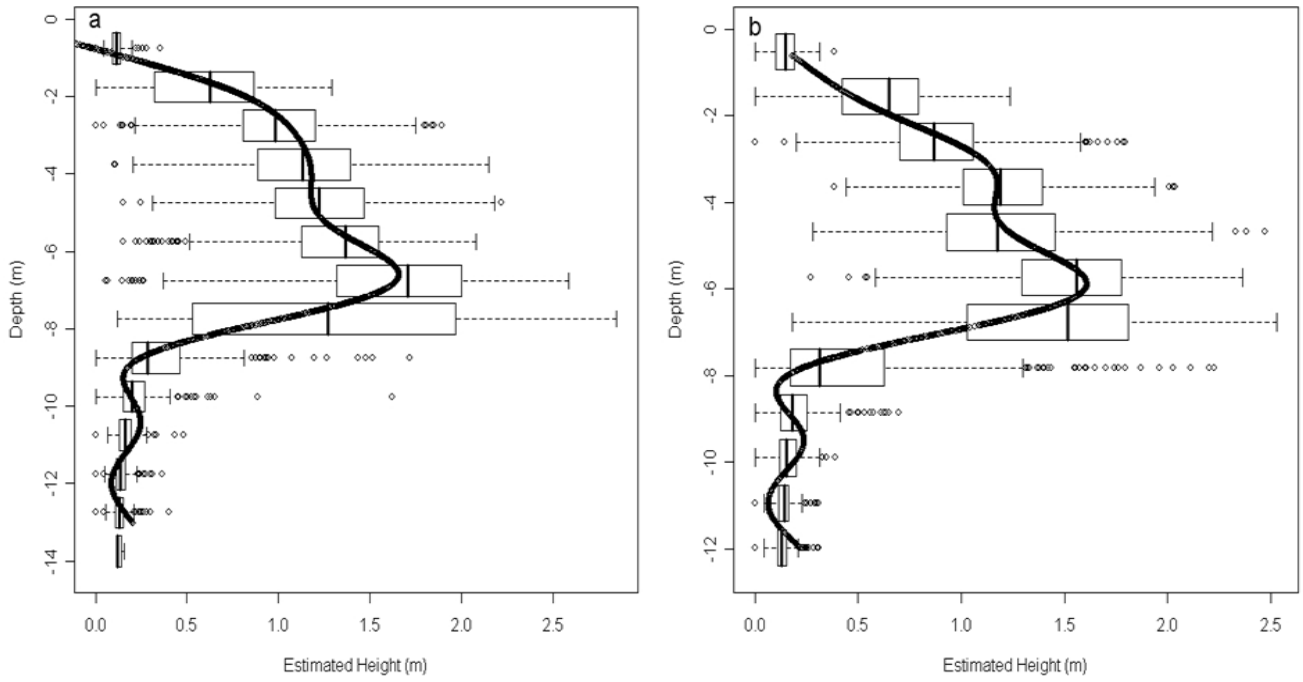

Figure 7.2. Boxplots of acoustically estimated plant height (binned into 1 m depth intervals) in Cook Bay in 2006 (a) and 2007 (b). Black lines are the fitted GAM models for each year.

7.4 Results

7.4.1 Acoustic Surveys – Patterns of macrophyte growth and biomass in Cook's Bay

Empirical semivariograms for percent cover and stand height residuals and indicator semivariograms for the three different growth form classifications are shown in Figure 7.3 a-g and summarized in Table 7.1. Anisotropy was not detected when directional semivariograms were computed, therefore the omnidirectional semivariograms were used for kriging. Much of the spatial dependency ($1 - C_0 / C_0 + C$) in the residuals for percent cover and stand height was accounted for by the semivariogram models chosen (Table 7.1). Sill and range parameters for percent cover and canopy heights in both years were comparable (Table 7.1) and indicate that the pattern of macrophyte cover and canopy height was relatively consistent between 2006 and 2007.

In Cook's Bay, macrophyte growth covered nearly 100% of the bottom out to a depth of 8 m (Figure 7.4a and b). Some areas near the shoreline near the southeast end of the bay had negligible macrophyte cover, however these areas are close to a heavily developed shoreline that experiences excessive boat traffic (personal observation). In general, taller (e.g., > 1.5 m), canopy forming species occupied depths between 4 and 8 m, with shorter, understory species colonizing shallow depths (Figure 7.4c and d). The maximum depth where I observed a plant-like acoustic signature was 10 m, and while underwater video indeed confirmed macrophytes at these depths, I cannot confirm whether the plants were rooted here or simply transient material that had been uprooted and drifted to these locations.

The majority of the locations sampled by Stantec (2006) (74 %) were dominated by species of class 3 (e.g., highest biomass density), even in relatively deep water. Samples dominated by class 1 species were considerably less (14 %), and samples dominated by species of class 2 comprised a mere 6 %. Indicator semivariograms for macrophyte growth forms (Figure 7.3 e -g) displayed ranges of autocorrelation on the range of ~ 500 m (Table 7.1) and, at least for growth form 1 and growth form 3 displayed comparable nugget and sill values. The low spatial dependence observed for these indicator semivariograms is suggestive of a relatively connected pattern of autocorrelation (Figure 7.4 e-g). The absence of a nugget value for growth form 2 likely reflects the low frequency of this growth form as a dominant component in the data set.

Estimates of standing crop as dry biomass using the first method (using acoustically estimated canopy height to classify the dominant growth form) resulted in a total dry biomass of 3706 T for the area surveyed (data not shown). Expressed on a per m^2 basis, this is equivalent to 186 g m^{-2}. Estimated standing crop from the indicator simulation maps of species growth form

yielded a total of 6028 T for the same area (Figure 7.4h). This is equivalent to 303 g m^{-2} on an average areal basis.

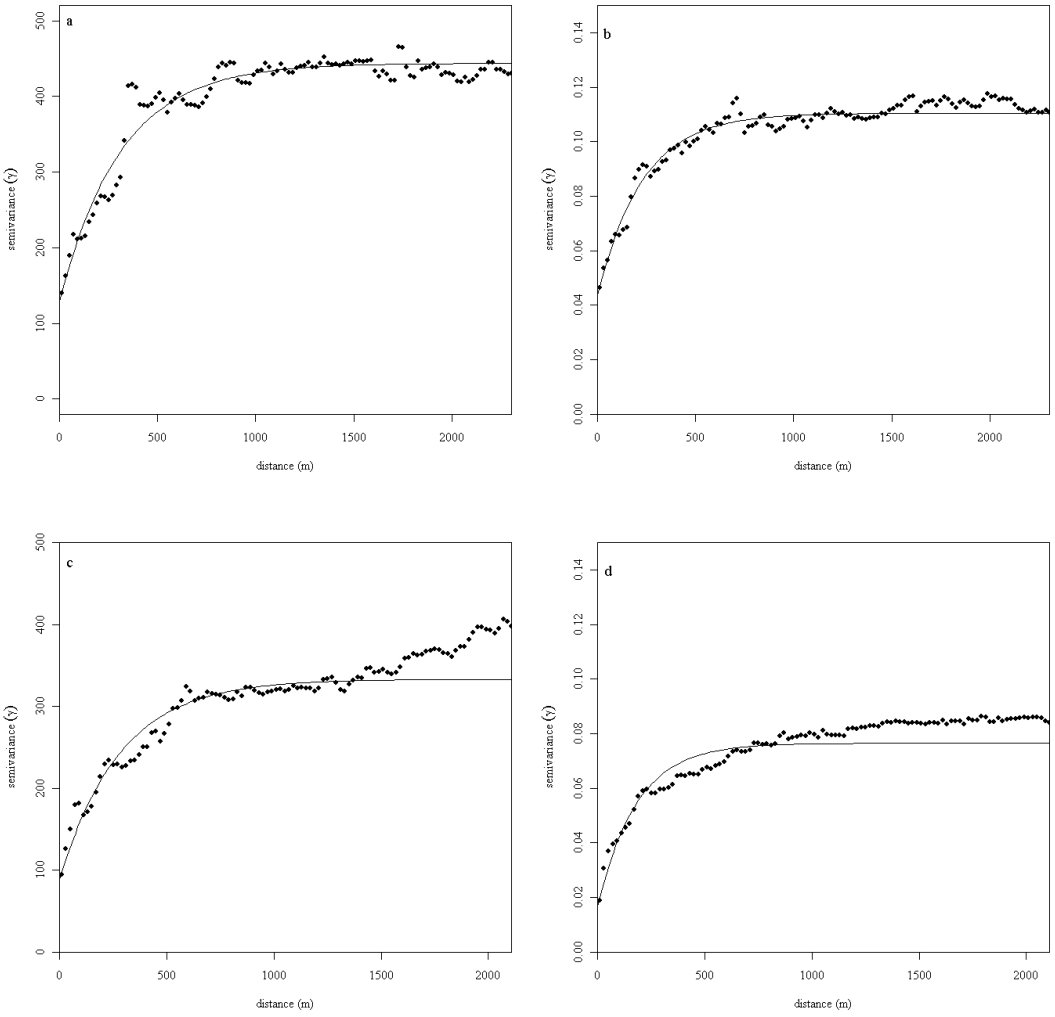

Figure 7.3. Semivariograms and fitted models for percent cover residuals in Cook's Bay in 2006 (a) and 2007 (b) and for height residuals in 2006 (c) and 2007 (d)

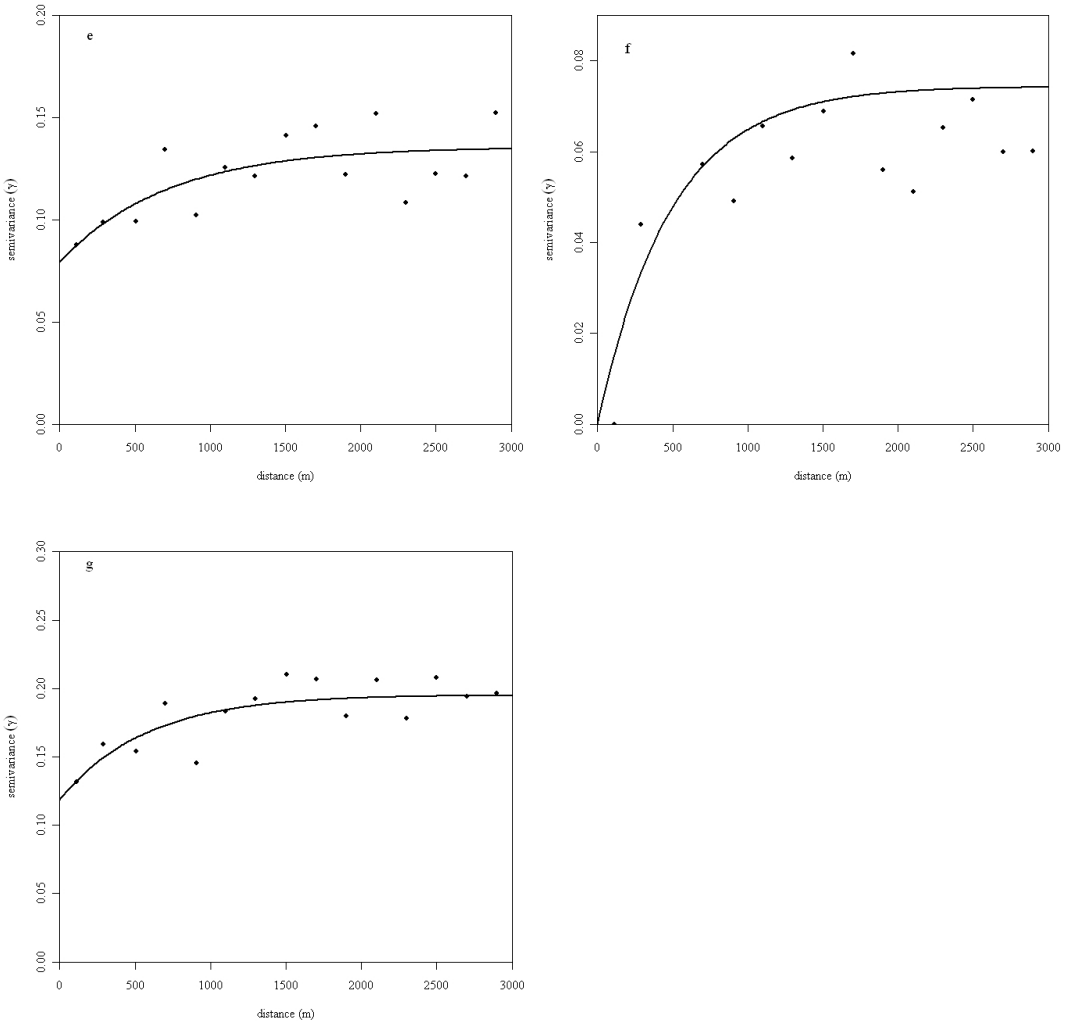

Figure 7.3. cont.. indicator semivariograms and fitted models for growth form 1 (e); growth form 2 (f); and growth form 3 (g) in Cook's Bay.

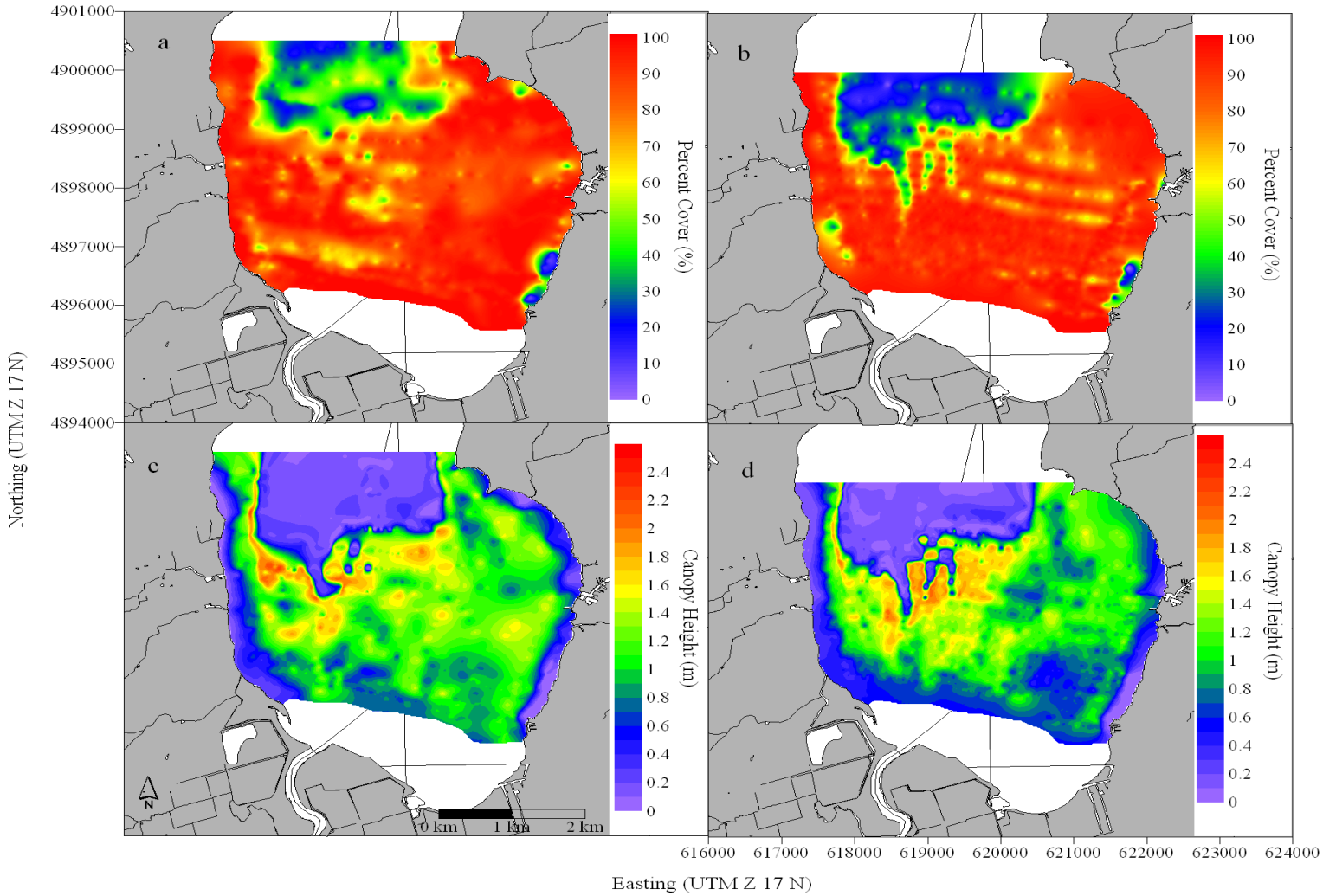

Figure 7.4. Kriged maps of percent cover August 9 2006 (a) and August 24 2007 (b) and stand height August 9 2006 (c) and August 24 2007 (d) for acoustic surveys in Cook's Bay.

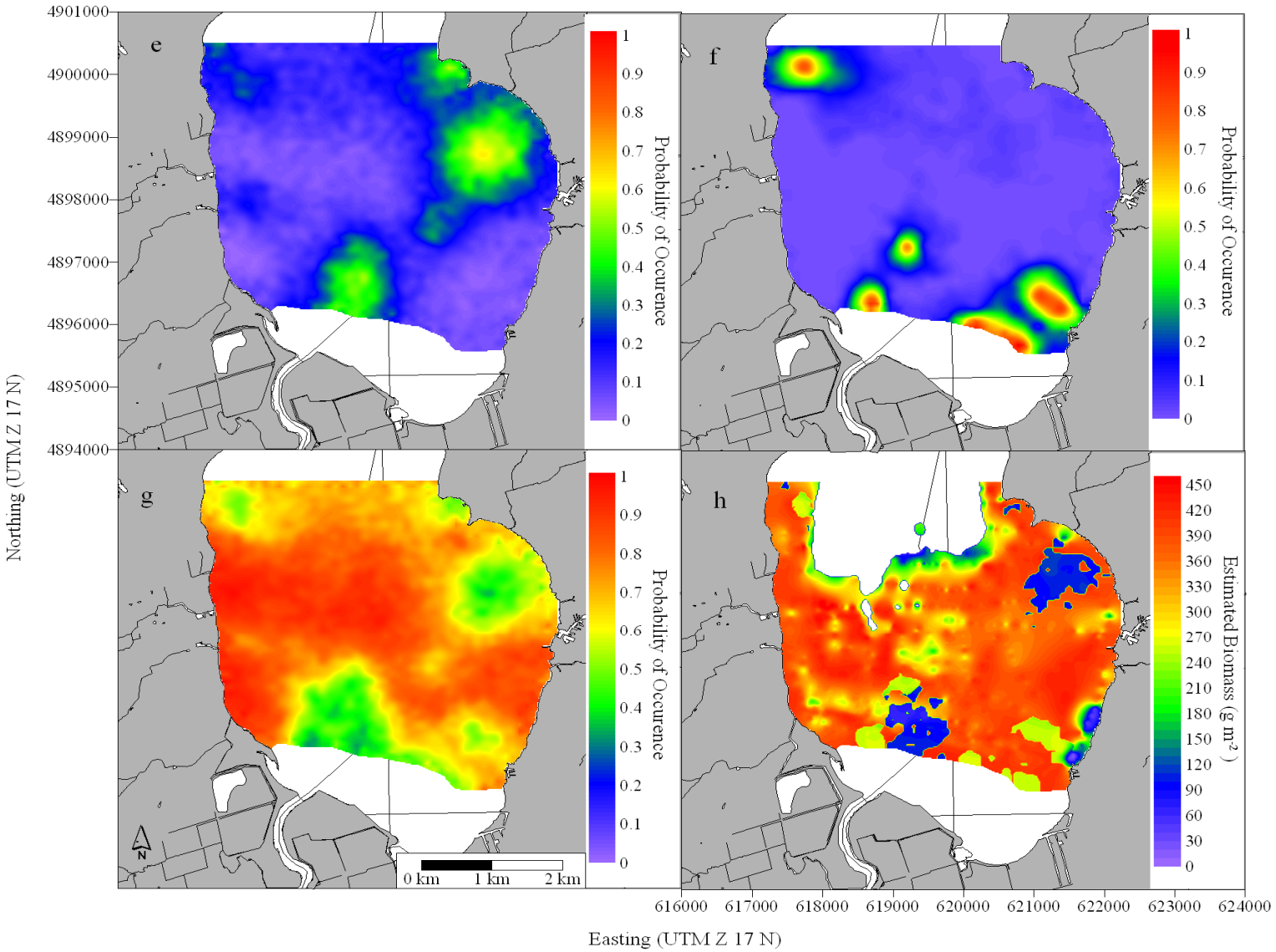

Figure 7.4 continued e) probability of occurrence for growth form 1, f) probability of occurrence for growth form 2, g) probability of occurrence for growth form 3, and h) estimated biomass from the growth form composite map.

7.4.2 Comparison of current macrophyte distribution to historical macrophyte distribution

The historical surveys conducted in 1984 and 1987 employed an analog echosounder and data was recorded on chart paper rather than stored digitally on a computer as ours was. Comparison to the historical data is therefore limited by interpretation of chart paper recordings. In the previous surveys, the authors categorized macrophyte cover as "continuous" or "discontinuous". Based on inspection and interpretation of these chart recordings and the digital echograms and subsequent classifications for these surveys, I approximated the "continuous" cover tracings to be equivalent to > 80 % cover as determined by EcoSAV v1.0, and "discontinous" to be < 80% cover as determined by EcoSAV v1.0.

From 1984 to 1987, the increase in "continuous cover" was modest (~ 16 %) and comparable to the increase in "discontinuous" cover (~ 24 %) observed between the two years (Table 2). In total, the estimated increase in colonized area was ~ 20 % (Table 7.2). From 1987 to the years 2006 and 2007, "continuous cover" (e.g., >80% cover) increased dramatically (mean 107 %) while "discontinuous cover" (e.g., < 80% cover) increased only by 21 %. Combined, the total area covered by SAV in Cook's Bay has increased ~ 65 % since 1987 (Table 7.2).

7.4.3 Macrophtye assemblage and tissue nutrients

Rake and snorkel sampling identified ten different species in Cook's Bay. The ten species were; coontail (*Ceratophyllum demersum),* Eurasian milfoil (*Myriophyllum spicatum*), wild celery (*Vallisneria americana*), common waterweed (*Elodea canadensis*), flat stemmed pondweed (*Potamogeton zosteriformis*), clasped leaf pondweed (*Potamogeton richarsonii*), big leaf pondweed (*Potamogeton ampifolus*), common bladderwort (*Utricularia vulgaris)*, the macroalgae (*Chara* sp. and *Cladophora* sp.), and one unidentifiable (*Potamogeton* spp). The most commonly observed species from sampling was *Ceratophyllum demersum*, appearing in 50 % of the samples across a range of depths. *Myriophyllum spicatum* was the second most commonly observed species, (46 %) followed by *Elodea canadensis* and *Vallisneria americana* at 25 % each. Other species generally had less than 10 % occurrence in the rake samples.

P and N concentrations in macrophyte tissue displayed positive correlations with depth (Pearson correlation coefficient, r = 0.56 and 0.62 for P and N respectively in 2006; Figure 7.5), perhaps indicating that macrophytes growing in shallow waters may no longer be light limited, but light limitation in deeper water (e.g., > 5m depth) may persist. Although a negative correlation did exist between depth and % N and % P for samples from 1984, the samples taken from a depth of 1 m in 1984 were sampled directly at the mouth of the Holland River, and tissue

nutrient content is probably biased high as a result of the high nutrient loading and turbid light regime. Eliminating these samples removes the negative correlation associated with depth, but significant positive correlations with depth after are still lacking. %P (as AFDW) was significantly lower in 2006 than in 1984 (t-test, t=-2.84, p<0.005), but %N (as AFDW) was equivalent (t-test, t=0.59, p<0.6). The N:P ratios for 2006 samples are in the same range as those observed in 1984, but were significantly higher than those observed in 1984 (t-test, t=-2.95, p <0.005). N:P in 2006 were generally above the limit suggested by Duarte (1992) to indicate P limitation for freshwater macrophytes (Figure 7.6).

Table 7.1. Summary of semivariogram model parameters for the nugget (C_0), sill (C), and range (α) and model denotes the form of semivariogram model fitted to the residuals where "Exp" is exponential form.

	Location	***Variable***	***C_0***	***C***	***α***	***%Sp***	*Model*
9 August 2006	Cook's Bay	% Cover	130.00	313.81	313.43	71 %	Exp
		Height	0.043	0.067	228.83	61 %	Exp
	Cook's Bay	Form 1	0.079	0.056	711.59	41 %	Exp
		Form 2	0	0.074	485.27	100 %	Exp
		Form 3	0.118	0.076	564.95	39 %	Exp
24 August 2007	Cook's Bay	%Cover	89.06	244.20	281.52	73 %	Exp
		Height	0.016	0.060	180.62	79 %	Exp

Table 7.2 Summary of the area covered by macrophytes in Cook Bay as estimated by hydroacoustic surveys during 1984, 1987 and 2006 and 2007. Discontinuous cover is defined as cover < 80%, while continuous cover is defined as > 80%. Mean tissue P and N are averages for all samples taken within the Bay.

Year	**Discontinous Area (km^2)**	**Continuous Area (km^2)**	**Total Area (km^2)**	**P (% AFDW)**	**N (% AFDW)**
1984	4.46	5.07	9.53	0.36	2.87
1987	5.51	5.88	11.39	0.21	2.20
2006	6.86	12.79	19.65	0.29	2.85
2007	6.42	11.49	17.91	ND	ND

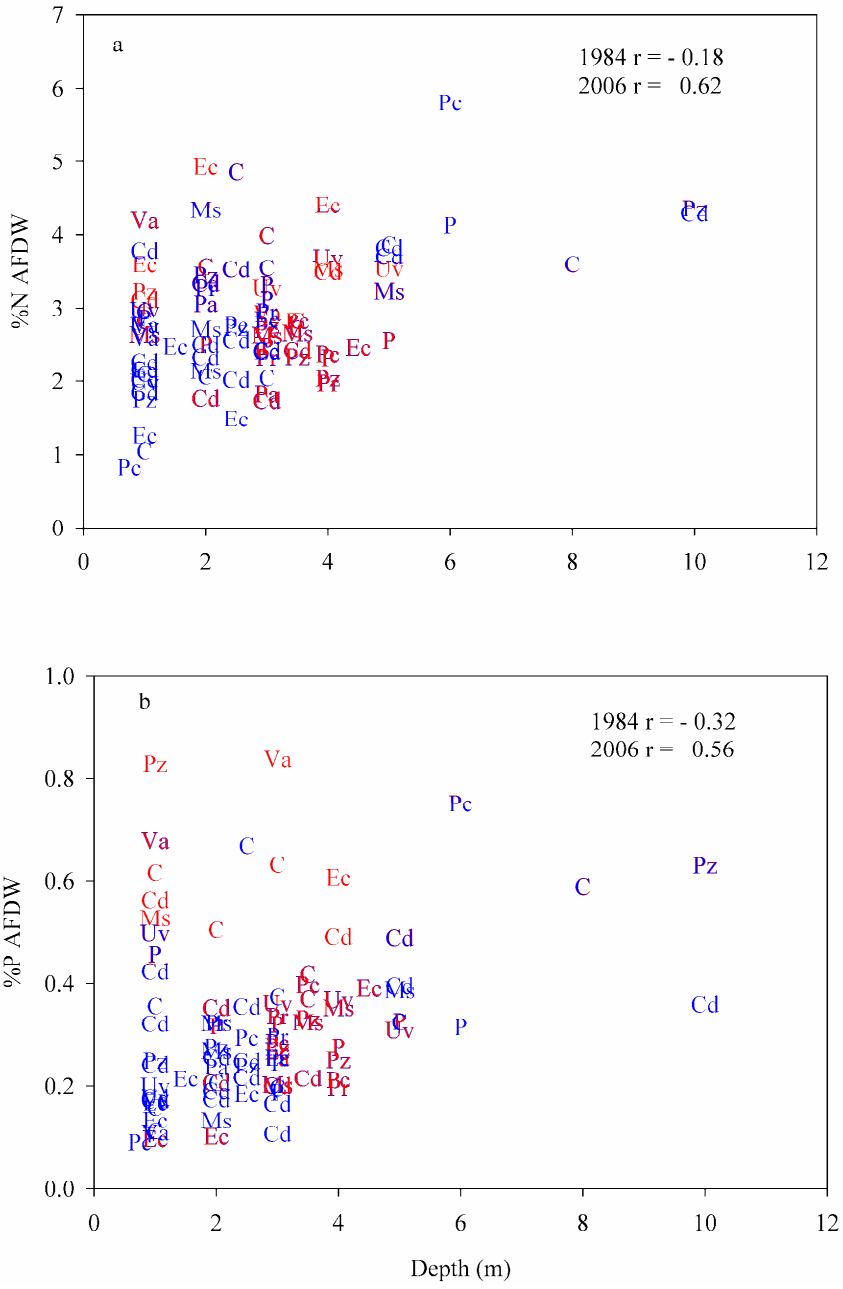

Figure 7.5. a) %N vs depth and b) %P vs depth for macrophytes collected in 1984 (red) and 2006 (blue) in Cook Bay. Pearson correlation coefficents are given for relationships in each year. Species names as in Figure 7.6.

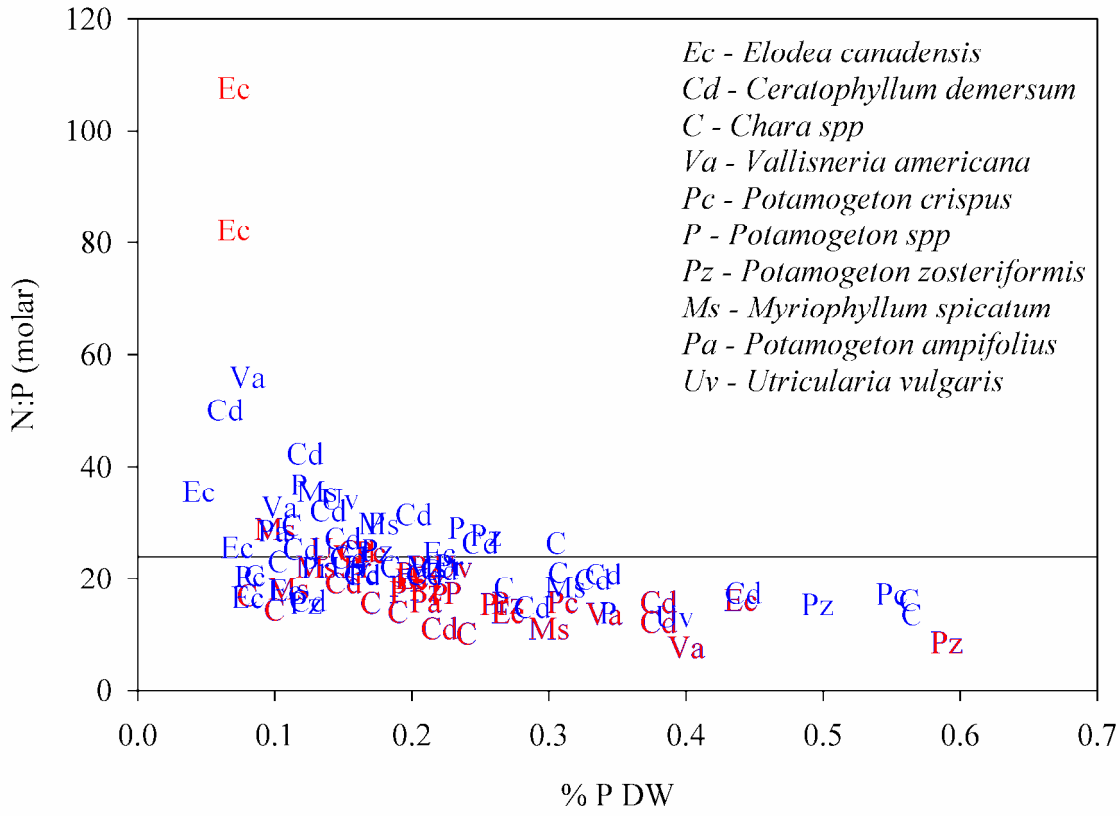

Figure 7.6 N:P molar ratio as a function of % tissue P (AFDW) for macrophyte samples collected in 1984 (red) and 2006 (blue). Solid line is N:P of 24, suggested by Duarte (1992) to indicated P limitation.

Table 7.3 Summary of studies on lake or embayments containing macrophytes that were colonized by dreissenid mussels. Change in parameters (e.g., change in TP, light penetration and macrophyte cover) refers to the percent change in mean parameter values from the time period post P control but prior to dreissena invasion to post dreissena invasion.

System	*Change in TP*	*Change in light penetration*	*Change in macrophyte cover*	*Reference*
Oneida Lake, NY	-43 %	+35 %	+ 23 %	Zhu et al. 2006
Bay of Quinte, ONT	-25 %	+60 %	+260 %	Sefried 2002
Chaumont Bay, NY	ND	ND	+35 %	Zhu et al. 2007
Sodus Bay, NY	ND	ND	+198 %	Zhu et al. 2007
Saginaw Bay, MI	ND	No change to + 60 %[b]	+15 %	Skubbina et al. 1995
Cook's Bay, ONT	[d]No change to -35%	[c]+30 to + 60 %	+65 %	This study

[a]ND implies no data for the time period, [b]based on changes over a number of different transects, [c]Nicholls 1998, [d]Eimers et al. 2005.

7.5 Disscussion

Information on the areal distribution and biomass of SAV are essential for the monitoring, management and understanding of shallow aquatic ecosystems (Vis et al. 2003). Large scale synoptic assessments are becoming increasingly common in the literature, and are helpful for assessing and reconciling the spatial and temporal heterogeneity inherent in SAV communities (Vis et al. 2003, Zhu et al. 2007). Vis et al. (2003) review a number of these methods, and I therefore refrain from discussing the benefits and drawbacks of different approaches, but rather focus on the interpretation of this data. In this study, I used a combination of echo sounder surveys and geostatistical methods to assess the degree of SAV cover and to estimate the standing crop of SAV in Cook's Bay, Lake Simcoe.

Acoustics have been used to assess SAV distribution both in other systems (e.g., Fortin et al. 1993, Sabol et al 2002a, Winfield et al. 2007, Zhu et al. 2006, 2007, Istanovics et al. 2008) and in Lake Simcoe (e.g., Neil et al. 1985,1991), yet few studies have examined the wealth of information collected in a geostatistical framework to create accurate maps that can be used to make informed decisions regarding the management and monitoring of SAV (but see Guan et al. 1999, Valley et al. 2005). One of the drawbacks of the acoustic method is that it cannot adequately sample transition areas where the water depth is too shallow for either vessel navigation or the water column is in the near field of the echosounder (Vis et al. 2003). In this study, depths < 1.5 m were systematically under-sampled due to this restriction. However, the use of geo-statistical methods allows for and estimation and extrapolation into these un-sampled areas. Further limitations are imposed by the method of processing the acoustic data. SAV that grows to the surface is by default excluded by the EcoSAV processing algorithm, and very dense SAV may obscure the reflection of the substrate, making accurate determination of the plant canopy difficult. I was unable to eliminate the the problem with canopies that were classified as "too-tall" and thus excessive noise, but these comprised a small percentage of the input data (see Materials and Methods). Furthermore, I was able to develop a work around to the problem of excessively dense SAV obscuring the bottom depth by relaxing the trailing edge feature in the EcoSAV algorithm. Therefore, I believe that the interpolations of SAV cover and canopy height are a reliable representation of the current SAV distribution in Cook's Bay.

The methods chosen to estimate the standing crop of SAV in the area surveyed is modeled after the work of Duarte (1987) who showed that use of macrophyte growth forms could improve the estimation of biomass determined from echosounder tracings (Duarte 1987). Other methods to estimate SAV biomass from acoustic data have either provided estimates that are

poorly unconstrained due to variability in scattering strength (e.g., Sabol et al. 2002a), or have suffered from acoustic shadowing at high biomass (Haga et al. 2007). Although I lacked growth form data at the same spatial resolution in this study, determination of growth form from echosounder tracings is advocated by Duarte (1987). The first method was based on observations that taller canopy forming plants tended to occupy intermediate depth ranges (e.g., > 4 m), and shorter understory forms occupied shallower waters (e.g., < 4m). This is not inconsistent with observed distributions of these growth forms in temperate lakes (e.g., Chambers and Kalff 1985, Chambers 1987). This method of estimating standing crop (as dry weight) produced a bay wide estimate of 3.71 x 10^3 kg of total SAV mass, equivalent to 186 g m^{-2}.

The second approach relied on conditional simulation to reproduce 500 simulations of species growth form distribution based on the data of Stantec (2006). This approach relies on honoring the input data and modeling the distribution of growth forms in a probabilistic environment. Using this method, the SAV standing crop was estimated to be 6.03 x 10^3 kg, equivalent to 303 g m^{-2}. The overwhelming preponderance of growth form 3 in the data set compared to growth forms 1 and 2 suggests that perhaps the ponar grab does not adequately sample tall canopy forming species particularly well. This would inflate the estimated biomass because it assigns a high biomass density value (from growth form class 3) to an area with a tall canopy. However, the 2006 study which I culled the dominant macrophyte growth form data from Stantec (2006) provided an average dry biomass of 233 g m^{-2}, which is close to the estimates for both approaches if the standard error for the Duarte (1987) equation (± 68 g m^{-2} expressed as dry weight) is considered, suggesting the estimates of biomass may not be unreasonable. However, further and more intensive calibration and evaluation is recommended before such approaches can be confirmed as robust methods for estimating SAV biomass.

This study demonstrates an unequivocal increase in SAV cover and in the maximum depth of SAV colonization in Cook's Bay since the last survey in 1987, prior to the invasion of dreissenid mussels. Luxuriant growth of SAV has been a seasonal occurrence in Cook's Bay for several decades; Millard and Veal (1971) conducted the first SAV survey in Cook's Bay and found extensive heavy growth in the lower portion of the bay (e.g., > 80% cover) where water depth was < 4 m. In subsequent years, hydro-acoustic surveys in 1984 (Neil et al. 1985) and 1987 (Neil et al. 1991) found that SAV growth extended to depths of 6 m. Currently, SAV in Cook's Bay grows continuously to a depth of ~ 9 m, and I observed SAV on echograms and underwater video at depths of 10 m, though I cannot confirm that plants were actually rooted at these depths. I estimated that "continuous cover" (e.g., > 80%) has increased substantially since 1987, while "discontinuous cover" has increased by a smaller percentage (Table 7.1).

Underwater irradiance has been identified as the primary factor controlling the distribution of SAV (Spence 1982, Chambers and Kalff 1985). Long term (20 + years) monitoring of Lake Simcoe by the Ontario Ministry of Environment has documented changes in water clarity since the early 1980s when nutrient loading reduction programs were implemented (Eimers et al. 2005). The 1984 and 1987 surveys were designed to assess the response of SAV to a reduction in P loading that occurred with diversion of ~ 6 T yr^{-1} of sewage effluent from Aurora and Newmarket out of the Lake Simcoe watershed in 1984 (Evans et al. 1996). Water quality in the lower Holland River was expected to improve after the diversion of sewage effluent in 1984, and there is some evidence of immediate reductions in SRP and TP concentrations at monitoring stations in the River (Nicholls 1998). Accordingly, the total area of Cook's Bay covered by SAV growth in 1987 (post effluent diversion) was estimated to have increased ~ 20 % from 1984 (pre effluent diversion), a change that was attributed to a modest improvement in water clarity (mean secchi depth increased from 1.7 to 2.1 m; Neil et al. 1991). Nicholls (1998) attributed the modest change in water clarity in Cook's Bay after 1984 to "legacy P" that is stored in the sediments in the Holland River. During the summer months, the lower reaches of the Holland River become stagnant, and considerable P in the form of PO_4 is released back into the water column, fueling phytoplankton growth (Nicholls 1998). This increase in phytoplankton biomass subsequently affects the water clarity in the receiving waters of the Bay (Nicholls 1998). Further declines in TP concentration and calculated P loads were estimated to continue for the main tributaries draining into |Cooks Bay (Holland River and upper Schomberg River) well into the early 1990s (Winter et al. 2007) which is after the 1987 hydro acoustic survey. However, water clarity both in Cooks Bay and elsewhere in Lake Simcoe did not change significantly (Eimers et al. 2005). Water clarity dramatically increased in 1996, approximately one year after the establishment of a lake wide population of dreissenids. Changes in phytoplankton bio-volume and TP concentration were also consistent with this, declining at all stations in the lake (Eimers et al. 2005).

The observed temporal changes in SAV cover in Cook's Bay observed from 1984 to this study are largely consistent with the temporal changes in water clarity for observed in Lake Simcoe (Eimers et al. 2005). Similar sequences of change have been noted in other systems where data is of sufficient temporal resolution. For example, in Oneida Lake, NY Zhu et al. (2006) clearly document that the largest changes in water clarity during times of nutrient reductions were associated with the arrival of dreissenid mussels. In the Bay of Quinte, a mild increase in water clarity (k_{PAR} declined from 0.67 to 0.61 m^{-1}, c.f. Millard et al. 2003) was observed between 1972 and 1977 after point source P controls were implemented (Millard et al. 2003). However, the resultant increase in SAV cover in the shallow upper bay was modest, and

increases into the deeper, outer bay did not occur (Bristow et al. 1977, Crowder and Bristow 1986). Following invasion of Lake Ontario and the Bay of Quinte by mussels in the late 1980s – early 1990s, water clarity increased and expansion of SAV into the deeper outer bay occurred invasion (Seifried 2002). Similar changes in SAV cover and depth of colonization have been inferred from historical collections of aerial photographs for other bays in Lake Ontario (e.g., Sodus Bay, and Chaumont Bay; Zhu et al. 2007) during the same time period.

These results are consistent with these previous studies that have recorded an increase in areal coverage and depth distribution of SAV in systems that have been invaded by dreissenid mussels after or during a period of nutrient reduction (Table 7.3), and confirms that a common theme among these studies implicates the increased water clarity (and by extension, the quantity of light reaching the bottom) as the causative factor governing the distribution of SAV in these systems. Consequently, I argue that mussel filtration has had a stronger effect on water clarity in Cook's Bay than reductions in nutrient loading.

While water clarity appears to exert a primary control governing the distribution of SAV in Cook's Bay, the nutrient content of the sediment likely sets the upper limit on the biomass yield. Because rooted macrophytes generally acquire nutrients such as N and P from the sediment (Barko and Smart 1981, Carignan and Kalff 1980), any additional input of nutrients to the sediment may act to increase SAV cover and biomass. Dreissenids may therefore augment the nutrient content of the sediment by depositing undigested algae and other particulate matter in the benthos (Vanderploeg et al. 2002). Pseudofecal aggregations (e.g., Stanczykowska and Lewandowski 1993) are generally produced at food concentrations above 200 µg C L^{-1}, and production increases with increasing food concentration (Walz 1978). The amount of deposited material is likely to be a function of dreissenid density, temperature, seston concentration and degree of exposure to re-suspension (Klerks et al. 1996). For example, (Madenjian 1995) estimated that the mussel population in western Lake Erie consumed 5 million T of phytoplankton and deposited 1.4 million T on the bottom in the form of feces and pseudofecal matter. In Cook's Bay, dreissenids are found largely attached to macrophyte stems and near the base of the plants, but dreissenid densities are relatively low (~2000 m^{-2}; Ozersky et al. submitted) compared to areas of hard substrate (Ozersky et al. submitted). The elemental composition of the feces and pseudofeces can be altered due to different assimilation efficiencies (Sterner and Elser 2002). For example, in oligotrophic Lake Constance, dreissenids excrete fecal matter that is depleted in P relative to the seston (Gergs et al. 2009). For a shallow eutrophic system such as Cook's Bay, production of pseudofecal material is likely to be significant, and

dreissenid mussels have the potential to augment the sediment nutrient content, and thereby affect the growth of SAV (Vanderploeg et al. 2002, Hecky et al. 2004).

The tissue N and P concentrations reported here, however, do not indicate that major changes have occurred that would support the hypothesis that dreissenids are enriching the sediment to the benefit of SAV in Cook's Bay. While many of the samples I collected in 2006 exceeded the 0.13 % P (DW) critical value suggested by Gerloff and Krombholz (1966) for maximum yield limitation of freshwater macrophytes, these often fall below the species specific growth rate threshold (Colman et al. 1987). The interplay of many abiotic (e.g., light availability, sediment type, pH) and plant related factors (e.g., taxonomy, presence of epiphytes) render generic statements about the occurrence or lack thereof of nutrient limitation at a given site uncertain in the absence of laborious and time consuming sediment fertilization experiments (Moeller et al. 1998), but there is no support for the hypothesis that macrophyte growth has increased due to increased nutrient supply from dreissenid bio-deposits in Cook's Bay. Factorial experiments with macrophytes and manipulated sediment P levels designed to test this hypothesis in mesocosms (Zhu et al. 2008) concluded that increased biomass is primarily in response to changes in light climate rather than sediment nutrient content (Zhu et al. 2008).

The excessive biomass of SAV in Cook's Bay is likely a result of decades of nutrient loading from the watershed that created a soft sediment bottom rich in nutrients. Sediment TP in Cook Bay in 2005 ranged from 0.7 to 1 mg g^{-1} dry sediment (Kilgour et al. 2008) and more recent spatially explicit estimates are consistent with these values (V. Hiriart-Baer, Environment Canada, pers. comm.). These values of sediment TP are near the upper end of the range for other temperate meso-eutrophic systems (0.3 to 1.2 mg g^{-1} dry sediment; Carignan and Kalff 1980, Rooney et al. 2003). Cook's Bay receives nutrient input from ~ 25 % of the Lake Simcoe watershed (Nicholls 2001). Prior to European settlement, P loading to the sediment of Cook's Bay was estimated to be approximately 1.5 T yr^{-1} (Johnson and Nicholls 1989). This represented ~ 5 % of the P retained in the lake sediments each year (Johnson and Nicholls 1989). In the 1930s, the marshes at the end of the Holland River were channelized and removed, leading to dramatic increases in P sedimentation in Lake Simcoe, particularly in Cook's Bay (Johnson and Nicholls 1989). P loading to the sediment of Cook Bay in the 1980s was estimated to be approximately 20 T yr^{-1} (~ 26 % of the total load to the lake sediments; Johnson and Nicholls 1989). Assuming that the retention of P has not dramatically changed since 1982 (~ 48 % in 1982; Johnson and Nicholls 1989), based on recent loading estimates to Cook's Bay (27 T yr^{-1} for 1990-98; Nicholls 2001) this equates to a sediment P load of nearly 13 T yr^{-1}. For comparative purposes, dreissenid mussels at similar densities to those in Cook's Bay were estimated to

generate ~ 783 T of fecal and pseudofecal matter over a 6 month period in shallow eutrophic Lake Mikoljaske (Poland) (Stanczykowska and Lewandowski 1993). Assuming a constant P content of the fecal matter (0.1 %; Stanczykowska et al. 1975) this is equivalent to 0.78 T yr^{-1} of P directed to the sediments, or about 6 % of the P load derived form the catchment each year. Although the estimate of P diverted by mussels is likely conservative, since they were derived from a 6 month period of active feeding in a Polish lake, filtration and pseudofecal production is not likely to continue during the winter months, as mussels attached to macrophytes will likely be transported elsewhere with scenescent macrophyte material, or fall to the bottom and perhaps be covered by decaying SAV. Furthermore, the increase in SAV cover and biomass that is apparent since the late 1980s has likely further enhanced P retention mechanisms by reductions in hydraulic flow in the inner portion of the bay and reducing re-suspension of sediment (e.g., Barko and James 1998).

7.6 Conclusions

The expanded distribution of macrophytes is an expected outcome in systems where light penetration has increased significantly (Sand-Jensen et al. 2008). The increase in macrophyte cover and biomass in Cook Bay since 1987 is likely due to the arrival and colonization of Lake Simcoe by dreissenid mussels and portends a similar response in other areas of Lake Simcoe where macrophytes are known to grow. In particular, expansion of macrophyte growth into areas formerly unsuitable for rooted plants may occur as shell material and soft substrate comprised of re-suspended sediments and mussel fecal and pseudofecal matter accumulate. Although nutritional subsidies via bio-deposition of dreissend fecal and pseudo-fecal matter are unlikely to be of importance to macrophytes in Cook's Bay, their importance cannot be discounted in other more nutrient poor areas. For example, some of the rocky areas in the lake where insufficient sediment accumulation formerly inhibited macrophyte growth now is characterized by high mussel abundance (e.g., Ozersky et al. submitted) and in some areas heavy cover of macrophytes (Chapter 6, personal observation). The expansion of macrophytes associated with dreissenids into areas formerly unsuitable for macrophyte growth may be partly facilitated by insufficient wave energy that appears to be unable to pulverize empty dreissenid shell material into fine fragments (D.R. Barton, Biology Dept. University of Waterloo, personal communication). This accumulating shell material creates a complex three dimensional structure that allows for fecal and pseudofecal matter to accumulate in interstitial spaces, and provide a potential rooting medium for macrophytes.

Because much of the nutrients sequestered by macrophytes are unavailable for much of the growing season, macrophytes represent a potential, although poorly characterized mechanism for nutrient storage and mobilization (Barko and Smart 1981). For example, using the bay wide biomass estimates from 2006 and the average tissue nutrient content, the macrophyte community in Cook's Bay is estimated to contain between 7.0 and 11.4 T of P and 68.6 and 111.7 T of N (assuming a DW to AFDW conversion of 0.65; D. Depew, unpubl. data). Considering the target loading budget for the lake of 75 T yr^{-1} (c.f. Winter et al. 2007), the extensive SAV growth present in Cook's Bay and likely elsewhere in the lake represents a significant albeit poorly characterized nutrient reservoir. Since SAV beds are generally considered to be a long term sink for both sediment and P (e.g., Rooney et al. 2003), the importance of macrophytes to nutrient dynamics in Lake Simcoe is likely to increase. Furthermore, given the relatively shallow nature of Lake Simcoe, the potential impact of an increased SAV community on nutrient and oxygen dynamics merits further study.

Chapter 8

Summary of Conclusions

Throughout the littoral areas of much of the lower Great Lakes, the filamentous alga *Cladophora* accumulates to nuisance proportions. The depth of colonization for *Cladophora* appears to have increased in recent years, largely due to the establishment of dreissenid mussels which can clarify the water column, provide expanded substrate for algal attachment and potentially provide a nutrient subsidy to benthic algae (Hecky et al. 2004). Previous work on *Cladophora* in the Great Lakes has relied primarily on labor intensive quadrat sampling to derive estimates of algal biomass (e.g., Higgins et al. 2005). These labor intensive methods may be accurate on a point by point scale, but are largely insufficient for characterizing the spatial extent of nuisance algal growth over larger scales. In Chapter 2, the utility of high frequency echosounder to detect and characterize nuisance algal growth was explored. Ground truthing at two different locations in Lake Ontario revealed that for algal stands that exceeded the minimum detection threshold, detection and characterization was largely successful. While it must be acknowledged that algal stands below the height threshold will not be detected either because the classification algorithm excludes them completely, or they are not distinguishable from bottom reverberation, the presence of algal stands below this height threshold are not likely to be the most problematic from a shoreline resident or lake manager viewpoint. With higher frequencies and further experiementation, it may be possible to reduce to minimum detectable stand height. However, such attempts must balance the need or desire to gain additional information on areas with low biomass against the inevitable increase in energy absorption that comes with using higher frequencies or the increased signal to noise ratio that comes with shorter pulse lengths. Both these problems will limit the effective survey depth, but it may be worth exploring if a moderate increase in acoustic frequency is beneficial.

In Chapter 3, the hydroacoustic methodology was applied to map the spatial distribution of *Cladophora* along selected shorelines in the Great Lakes. These shorelines were selected to encompass varying land use types, dreissenid mussel abundances and ambient water quality conditions. In addition to the shorelines, two offshore shoals were surveyed to provide conditions that more closely resemble open lake nutrient conditions. The results of this study showed clearly that nuisance *Cladophora* grew quite well in Lakes Erie and Ontario, but failed to achieve comparable levels in Lake Huron. Nuisance

Cladophora biomass appeared to be unrelated to land use types and near shore nutrient concentrations, but did show a significant relationship with dreissenid mussel abundance. These results are consistent with the shunt hypothesis (e.g., Hecky et al. 2004) and the presence of significant nuisance *Cladophora* growth at offshore shoals in Lake Eire and Ontario suggests that even in the absence of adjacent catchment loading, nuisance *Cladophora* growth can occur given suitable substrate and light conditions. This is perhaps the strongest evidence that dreissenids are a key link in the return of nuisance Cladophora growth to the lower Great Lakes.

To further build on the evidence from Chapter 3, in Chapter 4, a modified survey approach with the hydroacoustic surveys was undertaken at two heavily urbanized shorelines in Lake Ontario. The rationale for this study was principally to determine whether patterns of nuisance *Cladophora* growth displayed any spatial association with shoreline sources of nutrients such as storm sewers and tributaries, or from municipal sewage treatment plant outfalls. The working hypothesis was that if these potential nutrient sources were responsible for the resurgence of nuisance *Cladophora* growth, then excessive biomass should manifest itself in patterns that indicate the proximal importance of a nutrient source, as it did in Lake Huron in the 1970s (e.g., Auer et al. 1982). However, this hypothesis is predicated on the assumption that nutrient conditions in the near shore had not returned to historical levels, when concentrations were high enough to support widespread growth on much of the available substrate (Wernezak and Lyzenga 1975). It was apparent during this study that some symptoms of near shore enrichment were present (e.g., Cl^- and turbidity) but that the same patterns did not extend to P concentrations. Yet, at both study sites, the fall months (September and October) presented extremely high concentrations of P that are characteristic of nearshore enrichment. The lack this pattern during the May – August period may reflect P sequestration though biological activity, and this complicates determination of whether or not catchment sources are increasing their nutrient loads. Nuisance *Cladophora* growth was widespread at both study sites, but appeared to be substrate limited at Pickering. Relationships between nuisance *Cladophora* biomass did not display strong spatial relationships with the municipal sewage treatment plant outfalls or tributaries at Oakville, but did show significant associations with proximity to storm sewers.However, these relationships are confounded by complimentary relationships with low bathymetric slope, which may act to reduce *Cladophora* biomass loss, or perhaps enhance sloughed biomass deposition. At Pickering, no significant relationships were observed between nuisance *Cladophora* biomass and storm sewers or the Duffins Creek sewage treatment plant outfall, and significant relationships with proximity to tributaries were largely explained by excessive macrophyte/*Cladophora* growth in outer Frenchman's Bay. Further research at a site specific level with

finer temporal sampling is required to fully confirm the impact such features would have on *Cladophora* growth, but this study provides the identification of where such studies might be performed.

Studies in estuaries and other semi enclosed systems have indicated that benthic algae and phytoplankton may interact in complex ways, potentially competing for resources, despite the obvious disadvantages that encumber benthic algae at the lake bottom. In Chapter 5, two contrasting time periods were examined at high spatial resolution during night time surveys of the Oakville site in Lake Ontario, to look for spatial patterns and potential influences. The first survey took place during the post-slough period when much of the *Cladophora* biomass had detached from the bottom. Downwelling appeared to dominate the hydrodynamic regime, and patterns of water temperature, pCO_2, and phytoplankton photosynthetic efficiency (F_v/F_m) were characterized by little spatial variation, and indicated thorough mixing in the horizontal plane. Nutrient concentrations at this time were high, and the near optimal photosynthetic efficiency of the phytoplankton measured at this time is not inconsistent with this. In contrast, during the period of near maximal *Cladophora* growth, upwelling dominated the hydrodynamic regime, and tributary influence was evident as warmer water trapped at the surface of the recently upwelled lake water. Spatial variability was far greater during this time due to the interaction of tributary discharge and cooler upwelled water, and patterns of water temperature, conductivity, phytoplankton taxonomy, photosynthetic efficiency (F_v/F_m) all displayed significant spatial variation that was primarily oriented in an along shore pattern. Nutrient conditions during this time were moderate and consistent with other seasonal data from this location (Malkin 2007, Chapter 4). Further support for the dominance of long shore flow was provide by patterns of super-saturated O_2 and under-saturated pCO_2 in shallow waters that are consistent with the influence of benthic algal metabolism in the shallow depths, but are smeared by water movement along shore. Although no direct association between benthic algae and phytoplankton photosynthetic efficiency was found in this study, this does provide a framework and basis for future research. Given the dynamic nature of the near shore environment, high resolution studies are likely to further enhance the knowledge of these complex systems.

In Chapter 6, hydroacoustic surveys were undertaken in Lake Simcoe. This study focused on two areas where hard susbtrate dominated, along with dreissenid mussels (Ozersky et al. submitted). The rationale for this work was to see if nuisance *Cladophora* would manifest itself given comparable nutrient chemistry, light climate and dreissenid mussel abundances to the Great Lakes. Suprisingly, nuisance growth of *Cladophora* was not a seasonal occurrence in Lake Simcoe. While the exact cause for the lack of such nuisance algal growth is not known, there are several distinguishing characteristics that separate

Lake Simcoe from the near shore areas of the Great Lakes. First, many areas of the near shore of Lake Simcoe may not experience sufficient turbulence to support nuisance *Cladophora* accumulation in the absence of exceedingly high nutrient concentrations. This was cited as a plausible cause for the lack of *Cladophora* growth beyond the splash zone in many of the other areas of Lake Simcoe in the 1980s (Jackson 1982). Currently, Lake Simcoe has comparable P concentrations to near shore areas of the Great Lakes, and insufficient turbulence may limit the growth of *Cladophora* in many shoreline sites, but limited measures of current speeds near the study sites did not appear to differ greatly from current speeds in the Great Lakes, suggesting that other factors may be important in controlling nuisance *Cladophora* accumulation in Lake Simcoe. *Cladophora* collected from the survey sites appeared to be heavily encrusted with epiphytic diatoms, and is not inconsistent with the greater availability of silica in Lake Simcoe as compared to Lakes Erie and Ontario. This higher availability of silica may allow for continued growth of epiphytes, such that *Cladophora* cannot outgrow its epiphyte coating as it appears to do in Lake Ontario (Malkin et al. 2009). This effectively leaves *Cladophora* in a state of perpetual light limitation except at the shallowest of depths, where physical disturbance may prevent significant accumulation of biomass. Additional control of *Cladophora* biomass accumulation may arise from the abundant invertebrate grazer community that currently exists in Lake Simcoe (Kilgour et al. 2008, Ozersky et al. unpubl.data), which has increased significantly coinciding with the dreissenid invasion. Further research is needed to verify the proximal cause(s) of why *Cladophora* does not accumulate to nuisance biomass in Lake Simcoe, for example, by using grazer exclusion experiments or with the use of artificial substrates to alter nutrient regimes.

In the last chapter, acoustic surveys were conducted in Cook's Bay, Lake Simcoe. Here, the objective was to assess the current distribution of submerged aquatic vegetation (SAV) and infer changes in distribution as a result of the invasion of dreissenids. Historical acoustic surveys were performed in Cooks Bay during the 1980s to assess the response of the SAV community to reductions in nutrient loading that occurred when treated sewage effluent was diverted out of the Lake Simcoe watershed. These surveys were conducted prior to the invasion of dreissena, thus the current distribution of SAV in Cook's Bay can be appreciated against the historical changes due to nutrient loading reductions. In this study, SAV was demonstrated to have dramatically increased in areal cover, and expanded into waters 9 to 10 m deep. Long term monitoring conducted by the MOE (Eimers et al. 2005) clearly show that the largest changes in water clarity, TP concentrations, and phytoplankton biovolume occurred in the years immediately following invasion by dreissena. Taken together, these unequivocally implicate dreissenids

as the principal factor governing the penetration of light to the benthos, and thus determine the distribution of SAV in Lake Simcoe.

In summary, these chapters bring together new and evolving technologies and through the application of spatial data analysis techniques, provide a framework to answer ecological questions in environments that are complex and dynamic. The research in this thesis provides support for the hypothesis that the resurgence of nuisance algae in the Great Lakes is closely linked to dreissenid mussels. Furthermore, the research from Lake Simcoe supports that idea that mussels are effective ecosystem engineers (Zhu et al. 2006) and have fundamentally altered the dynamics of aquatic ecosystems as predicted by the near shore shunt (Hecky et al. 2004) and the benthification hypotheses (Zhu et al. 2006).

References

American Public Health Association (APHA). 1998. *Standard methods for the examination of water and wastewater*, 20th ed. United Book Press.

Arnott, D.L., and Vanni, M.J. 1996. Nitrogen and phosphorus recycling by the zebra mussel (*Dreissena polymorpha*) in the western basin of Lake Erie. Can. J. Fish. Aquat. Sci. **53**: 646-659.

Auer, M.T., and Canale, R.P. 1982a. Ecological and mathematical modelling of *Cladophora* in Lake Huron: 3. The dependance of growth rates in internal phosphorus pool size. J. Great Lakes Res. **8**: 93-99.

Auer, M.T., and Canale, R.P. 1982b. Ecological and mathematical modelling of *Cladophora* in Lake Huron: 2. Phosphorus uptake kinetics. J. Great Lakes Res. **8**: 84-92.

Auer, M.T., Canale, R.P., Grundler, H.C., and Matsuoka, Y. 1982. Ecological studies and mathematical modelling of *Cladophora* in lake Huron:1. Program description and field monitoring of growth dynamics. J. Great Lakes Res. **8**: 73-83.

Arrhenius, F., Benneheij, B.J.A.M., Rudstam, L.G., and Boisclair, D. 2000. Can stationary bottom split-beam hydroacoustics be used to measure fish swimming speed in situ? Fish. Res. **45**: 31–41.

Aquafor Beech 2006. Aquafor Beech Limited, *Final report: Conservation Halton LOSAAC water quality study*, Aquafor Beech Limited, Brampton, Ontario (2006).

Baird, W.F. 2006. Lake Simcoe hydrodynamic and water quality model. Report # 10940, W.F. Baird and Associates, Oakville, Ontario.

Bannerman, R.T., Owens, D.W., Dodds, R.B. and Hornewer, N.J. 1993. Sources of pollutants in Wisconsin stormwater. Wat. Sci. Tech. **28**: 241-259.

Barbiero, R.P., Balcer, M., Rockwell, D.C., and Tuchman, M.L. 2009. Recent shifts in the crustacean zooplankton community of Lake Huron. Can. J. Fish. Aquat. Sci. **66**: 816-828.

Barko, J.W., and Smart, R.M. 1981. Sediment-based nutrition of submersed macrophytes. Aquat. Bot. **10**: 339-352.

Barko, J.W., and James, W.F. 1988. Effects of submerged aquatic macrophytes on nutrient dynamics, sedimentation, and resuspension. *In* The structuring role of submerged macrophytes in lakes. *Edited by* E. Jeppesen, M. Sondergaard, M. Sondergaard and K. Christoffersen. Springer-Verlag, New York. pp. 197-214.

Barton, D.R., Johnson, R.A., Campbell, L.M., Petruniak, J., and Patterson, M.W.R. 2005. Effects of round gobies (*Neogobius melanostomus*) on dreissenid mussels and other invertebrates in eastern Lake Erie, 2002-2004. J. Great Lakes Res. **31**: 252-261.

Barton, D.R., and Hynes, H.B.N. 1978. Wave-zone macrobenthos of the exposed Canadian shores of the St. Lawrence Great Lakes. J. Great Lakes Res. **4**: 27-45.

Barrat-Segretain, M.H. 1996. Stategies of reproduction, dispersion and competition in river plants: A review. Vegetatio **123**. 13-37.

Beardall, J., Berman, T., Heraud, P., Kadiri, M.O., Light, B.R., Patterson, G., Roberts, S., Sulzberger, B., Sahan, E., Uehlinger, U., and Wood, B. 2001. A comparison of methods for detection of phosphate limitation in microalgae. Aquat. Sci. **63**: 107-121.

Berges, J.A., Charlebois, D.O., Mauzerall, D.C., and Falkowski, P.G. 1996. Differential effects of nitrogen limitation on photosynthetic efficiency of photosystems I and II in microalgae. Plant Physiol. **110**: 689-696.

Bergey, E.A., Boettiger, C.A., and Resh, V.H. 1995. Effects of water velocity on the arcitechture and epiphytes of *Cladophora glomerata* (Chlorophyta). J. Phycol. **31**: 264-271.

Beutler, M., Wiltshire, K.H., Meyer, B., Moldaenke, C., Luring, C., Meyerhofer, M., Hansen, U., and Dau, H. 2002. A fluorometric method for the differentiation of algal populations *in vivo* and *in situ*. Photosyn. Res. **72**: 39-53.

Bibby, T.S., Gorbunov, M.Y., Wyman, K.W., and Falkowski, P.G. 2008. Photosynthetic community responses to upwelling in mesoscale eddies in the subtropical North Atlantic and Pacific oceans. Deep Sea Res. II. **55**: 1310-1320.

Biggs, B.F.J. 1996. Patterns of benthic algae of streams. *In* Algal ecology: Freshwater benthic ecosystems. *Edited by* R.J. Stevenson, M.L. Bothwell and R.L. Lowe. Academic Press, pp. 31-51.

Binding, C. E., Jerome, J.H., Bukata, R.P., and Booty, W.G. 2007. Trends in water clarity of the lower Great Lakes from remotely sensed aquatic color. J. Great Lakes Res. **33**:828-841.

BioSonics Inc. 2001. EcoSAV^{TM}: Submerged aquatic vegetation detection and analysis users manual. BioSonics, Inc. Seattle, WA, USA.

BioSonics Inc. 2004a. EcoSAV^{TM} v2.0. Users guide. BioSonics Inc., Seattle, WA., USA.

BioSonics Inc. 2004b. DT4 file format specification. BS&E-2004-07-0009-1.3., BioSonics Inc., Seattle, WA., USA.

Bishop, T.F.A., and McBratney, A.B. 2001. A comparison of prediction methods for the creation of field extent soil property maps. Geoderma. **103**: 149-160.

Blanc, S., Benitez, C.E., De Milou, M.I.E., Mosto, P., Lascelea, G., and Juarez, R.E. 2000. Acoustical behaviour of phytoplanktonic algae. Acoust. Lett. **23**: 175-182.

Bocaniov, S. 2007. Plankton metabolic balance and its controlling factors in the coastal zone of the Laurentian Great Lakes. PhD Thesis, University of Waterloo, Waterloo, Ontario, Canada.

Bootsma, H.A., Young, E.B., and Berges, J.A. 2005. Temporal and spatial patterns of *Cladophora* biomass and nutreint stochiometry in Lake Michigan. *In* Cladophora *Research and Management in the Great Lakes* (*Workshop Proceedings*). GLWI Special Report No. 2005-01. Great Lakes Water Institute, University of Wisconsin - Milwaukee, pp.81-8.

Brazner, J.C., and Beals, E.W. 1997. Patterns in fish assemblages from coastal wetland and beach habitats in Green Bay, Lake Michigan: A multivariate analysis of abiotic and biotic forcing factors. Can. J. Fish. Aquat. Sci. **54**: 1743-1761.

Bristow, J.M., Crowder, A.A., King, M.R., and van der Kloet, S. 1977. The growth of macrophytes in the Bay of Quinte prior to sewage removal. Nat. Can. **104**: 465-473.

Budd, J. W., Drummer, T.D., Nalepa, T.F., and Fahnenstiel, G.L. 2001. Remote sensing of biotic effects: Zebra mussel (*Dreissena polymorpha*) influence on water clarity in Saginaw Bay, Lake Huron. Limnol. Oceanogr. **46**: 213-223.

Bulit, C., Diaz-Avalos, C., Signoret, M., and Montagnes, D.J.S. 2003. Spatial structure of planktonic ciliate patches in a tropical coastal lagoon: An application of geostatistical methods. Aquat. Microb. Ecol. **30**: 185-196.

Byron, E.R., and Goldman, C.R. 1989. Land-use and water quality in tributary streams of Lake Tahoe, California-Nevada. J. Environ. Qual. **18**: 84-88.

Campbell, D.A., Hurry, V., Clarke, A.K., Gustafsson, P., and Oquist, G. 1998. Chlorophyll fluorescence analysis of cyanobacterial photosynthesis and acclimation. Micrbiol. Mol. Biol. Rev. **62**: 667-683.

Canale, R.P., and Auer, M.T. 1982. Ecological studies and mathematicall modelling of *Cladophora* in lake Huron: 7. model verification and system response. J. Great Lakes Res. **8**: 134-143.

Carbó, R., M, and ero, A.C. 1997. Scattering strength of a gelidium biomass bottom. Appl. Acoust. **51:** 343-351.

Carignan, R., and Kalff, J. 1980. Phophorus sources for aquatic weeds: Water or sediments? Science. **207**: 987-989.

Carpenter, S.R., Elser, M.M., and Elser, J.J. 1986. Chlorophyll production, degradation, and sedimentation: Implications for paleolimnology. Limnol. Oceanogr. **31**: 112-124.

Carpenter, S.R., and Lodge, D.M. 1988. Effects of submersed macrophytes on ecosystem processes. Aquat. Bot. **26**: 341-370.

Carrick, H.J., and Lowe, R.L. 2007. Nutrient limitation of benthic algae in Lake Michigan: The role of silica. J. Phycol. **43**: 228-234.

Chambers, P.A. 1987. Light and nutrients in the control of aquatic plant community structure. II. In situ observations. J. Ecol. **75**:621-8.

Chambers, P.A., and Kalff, J. 1985. Depth distribution and biomass of submersed aquatic macrophyte communities in relation to secchi depth. Can. J. Fish. Aquat. Sci. **42**: 701-709.

Chambers, P.A., DeWreede, R.E., Irlandi, E.A., and Vandermeulen, H. 1999. Management issues in aquatic macrophyte ecology: A Canadian perspective. Can. J. Bot. **77**: 471-487.

Checkley, D.M. 2000. Effects of langmuir circulations on the plankton.Scripps Institute of Oceanography, La Jolla, California.

Chivers, R.C., Emerson, N. and Burns, D.R. 1990. New acoustic processing for underway surveying. Hydrogr. Journ. **56**: 1–17.

Choo, K.s., Snoeijs, P., and Pedersen, M. 2002. Uptake of inorganic carbon by *Cladophora glomerata* (Chlorophyta) from the Baltic Sea. J. Phycol. **38**: 493-502.

Cleveland, J.S., and Perry, M.J. 1987. Quantum yield, relative specific absorption and fluorescence in nitrogen-limited *Chaetoceros gracilis*. Mar. Biol. **94**: 489-497.

Cochran, W.W. 1977. Sampling techniques. John Wiley and Sons, New York.

Colman, J.A., Sorsa, K., Smith, C.S., and Andrews, J.H. 1987. Yield-derived and photosynthesis-derived critical concentrations of tissue phosphorus and their significance for growth of Eurasian water milfoil, *Myriophyllum-spicatum* L. Aquat. Bot. **29**: 111-122.

Conroy, J.D., Edwards, W.J., Pontius, R.A., Kane, D.D., Zhang, H., Shea, J.F., Richey, J.N., and Culver, D.A. 2005. Soluble nitrogen and phosphorus excretion of exotic freshwater mussels (*Dreissena spp*.): Potential impacts for nutrient re-mineralisation in western Lake Erie. Freshwat. Biol. **50**: 1146-1162.

Creed Jr., R.P. 1994. Direct and indirect effects of crayfish grazing in a stream community. Ecology **75**: 2091-2103.

Cressie, N. 1991. Statistics for Spatial Data. John Wiley and Sons, New York, NY, USA. 920pp.

Cressie, N., and Hawkins, D.M. 1980. Robust estimation of the variogram. Math. Geol. **12**: 115-125.

Cressie, N. 1986. Kriging nonstationary data. J. Am. Stat. Assoc. **81**: 625-634.

Crowder, A. and Bristow, M. 1986. Aquatic macrophytes in the bay of Quinte, 1972–82. Can. Spec. Publ. Fish. Aquat. Sci. **86**: 114-127.

Crowder, A. and Painter, D.S. 1991. Submerged macrophytes in Lake Ontario: Current Knowledge, Importance, Threats to Stability and Needed Studies. Can. J. Fish. Aquat. Sci. **48**: 1539-1545.

Crowder, L.B., and Cooper, W.E. 1982. Habitat structural complexityand the interaction between bluegills and their prey. Ecology **63**: 1802-1813.

Csanady, G.T. 1970. Dispersal of effluents in the Great Lakes. Wat. Res. **4**: 79-114.

Cullen, J.J., and Davis, R.F. 2003. The blank can make a big difference in oceanographic measurements. Limnol. Oceanogr. Methods. **12**: 29-34.

Cyr, H., and Downing, J.A. 1988. Empirical relationships of phytomacrofaunal abundance to plant biomass and macrophyte bed characteristics. Can. J. Fish. Aquat. Sci. **45**: 976-984.

Danz, N.P., Niemi, G.J., Regal, R.R., Hollenhorst, T., Johnson, L.B., Hanowski, J.M., Axler, R.P., Ciborowski, J.J.H., Hrabik, T., Brady, V.J., Kelly, J.R., Morrice, J.A., Brazner, J.C., Howe, R.W., Johnston, C.A., Host, G.E. 2007. Integrated Measures of Anthropogenic Stress in the U.S. Great Lakes Basin. Env. Man. **39**:631–647.

Davies, J.M., and Hecky, R.E. 2005. Initial measurements of benthic photosynthesis and respiration in Lake Erie. J. Great Lakes Res. **31**: 195-207.

DeJong, D.2000. The growth and distribution of the green alga *Cladophora* at Presqu'ile provincial park : Implications for management. MSc Thesis, Wilfrid Laurier University, Waterloo, Ontario.

Depew, D.C. 2003. Production and respiration of phytoplankton communities in eastern Lake Erie. M.Sc. Thesis, University of Waterloo, Waterloo, Ontario, Canada.

Depew, D.C., Guildford, S.J., and Smith, R.E.H. 2006. Nearshore-offshore comparison of chlorophyll a and phytoplankton production in the dreissenid colonized eastern basin of Lake Erie. Can. J. Fish. Aquat. Sci. **63**: 1115-1129.

Dermott, R. and Kerec, D. 1997. Changes to the deepwater benthos of eastern Lake Erie since the invasion of Dreissena: 1979-1993. Can. J. Fish. Aquat. Sci. **54**: 922-930.

Dermott, R., Witt, J., Um, Y.M., and Gonzalez, M. 1998. Distribution of the Ponto-Caspian amphipod *Echinogammarus ischnus* in the Great Lakes and replacement of native *Gammarus fasciatus*. J. Great Lakes Res. **24**: 442-452.

Devilla, R.A., Brown, M.T., Donkin, M., and Readman, J.W. 2005. The effects of a PSII inhibitor on phytoplankton community structure as assessed by HPLC pigment analyses, microscopy, and flow cytometry. Aquat. Tox. **71**: 25-38.

Deutsch, J.P. and Journel, A.G. 1998. GSLIB. Geostatstical Software Library and User's Guide. Oxford University Press, New York.

Dillon, P.J., and Kirchner, W.B. 1975. The effects of geology and land use on the export of phosphorus from watersheds. Wat. Res. **9**: 135-148.

Dodds, W.K. 1991. Community interactions between the filamentous algae *Cladophora glomerata* (L.) Kuetzing, its epiphytes, and epiphyte grazers. Oecologia. **85**: 572-580.

Dodds, W.K., and Gudder, D.A. 1992. The ecology of *Cladophora*. J. Phycol. **28**: 415-427.

Dolan and McGunagle 2005

Dommise, M., Urban, D., Finney, B., and Hills, S. 2005. Potential depth biasing using the biosonics VBT seabed classification software. Mar. Technol. Soc: 90-93.

Dorn, N.J., and Wojdak, J.M. 2004. The role of omnivorous crayfish in littoral communities. Oecologia. **140**: 150-159.

Duarte, C.M. 1987. Use of echosounder tracings to estimate the aboveground biomass of submerged plants in lakes. Can. J. Fish. Aquat. Sci. **44**: 732-735.

Duarte, C.M. 1992. Nutrient concentrations of aquatic plants: Patterns across species. Limnol. Oceanogr. **37**: 882-889.

Duarte, C.M. and Kalff, J. 1987. Weight-density relationships in submerged macrophytes: The importance of light and plant geometry. Oceologia. **72**:612-117.

Duthie, H., and Jones, D.K. 1990. Epilithic algal productivity on the submerged Niagara escarpment, Georgian Bay, Canada. Verh. Internat. Verein. Limnol. **24**: 411-415.

Edsall, T.A. Charlton, M.N. 1997. Nearshore waters of the Great Lakes. State of the Lakes Ecosystem Conference 1996. Available from http://www.epa.gov/solec/solec_1996.

Eimers, M.C., Winter, J.G., Scheider, W.A., Watmough, S.A., and Nicholls, K.H. 2005. Recent changes and patterns in the water chemistry of Lake Simcoe. J. Great Lakes Res. **31**: 322-332.

Emery, X. and Ortiz, J. M. 2007. Weighted sample variograms as a tool to better assess the spatial variability of soil properties, Geoderma **140**: 81-89

Evans, D.O., Nicholls, K.H., Allen, Y.C., and McMurtry, M.J. 1996. Historical land use, phosphorus loading, and loss of fish habitat in Lake Simcoe, Canada. Can. J. Fish. Aquat. Sci. **53**: 194-218.

Falkowski, P.G. 1992. Molecular ecology of phytoplankton photosynthesis. primary productivity and biogeochemical cycles in the sea. *In* Primary productivity and biogeochemical cycles in the sea. *Edited by* P.G. Falkowski and A.D. Woodhead. Plenum Press, New York, USA. pp. 47-67.

Falkowski, P.G., and Raven, J.A. 1997. Aquatic photosynthesis. Blackwell Science, Malden, Mass.

Feminella, J.W., and Resh, V.H. 1991. Herbivorous caddisflies, macroalgae, and epilithic microalgae: Dynamic interactions in a stream grazing system. Oecologia. **87**: 247-256.

Finlay, J.C., Sterner, R.W., and Kumar, S. 2007. Isotopic evidence for in-lake production of accumulating nitrate in Lake Superior. Ecol. Appl. **17**: 2323-2332.

Fitzgerald, D.G., Zhu, B., Hoskins, S.B., Haddad, D.E., Green, K.N., Rudstam, L.G., and Mills, E.L. 2006. Quantifying submerged aquatic vegetation using aerial photograph interpretation: Application in studies assessing fish habitat in freshwater ecosystems. Fisheries. **31**: 61-73.

Fong, D.A., and Geyer, W.R. 2001. Response of a river plume during an upwelling favorable wind event. J. Geophys. Res. **106**: 1067-1084.

Fonseca, M.S., and Fisher, J.S. 1986. A comparison of canopy friction and sediment movement between four species of seagrass with reference to their ecology and restoration. Mar. Ecol. Prog. Ser. **29**: 15-22.

Fonseca, M.S., Fisher, J.S., Zieman, J.C., and Thayer, G.W. 1982. Influence of the seagrass *Zostera marina* on current flow. Est. Coast. Shelf Sci. **15**: 351-364.

Fraterrigo, J.M., and Downing, J.A. 2008. The influence of land use on lake nutrients varies with watershed transport capacity. Ecosystems. **11**: 1021-1034.

Fuchs, E., Zimmerman, R.C., and Jaffe, J.S. 2002. The effect of elevated levels of phaeophytin in natural water on variable fluorescence measured from phytoplankton. J. Plankt. Res. **24**: 1221-1229.

Gal, G., Rudstam, L.G., and Greene, C.H. 1999. Acoustic characterization of *Mysis relicta*. Limnol. Oceanogr. **44**: 371-381.

Garwood, P.E. 1982. Ecological interactions among *Bangia*, *Cladophora* and *Ulothrix* along the Lake Erie shoreline. J. Great Lakes Res. **8**: 54-60.

Geider, R.J., Greene, R.M., Kolber, Z., MacIntyre, H., and Falkowski, P.G. 1993. Fluorescence based assessment of the maximum quantum efficiency of photosynthesis in the western North Atlantic. Deep Sea Res. **40**: 1205-1224.

Gergs, R., Rinke, K., and Rothhaupt, K. 2009. Zebra mussels mediate benthic–pelagic coupling by biodeposition and changing detrital stoichiometry. Freshwat. Biol. **54**: 1379-1391.

Gerloff, G.C., and Fitzgerald, G.P. 1976. The nutrition of great lakes *Cladophora*. EPA 60013-76-044, United States Environmental Protection Agency.

Gerloff, G.C., and Krombholz, P.H. 1966. Tissue analysis as a measure of nutrient availability for the growth of angiosperm aquatic plants. Limnol. Oceanogr. **11**: 529-537.

Ghadouani, A., and Smith, R.E.H. 2005. Phytoplankton distribution in Lake Erie as assessed by a new in situ spectrofluorometric technique. J. Great Lakes Res. **31**: 154-167.

Glooschenko, W.A., Moore, J.E., and Vollenweider, R.A. 1972. The seasonal cycle of pheo-pigments in lake ontario with particular emphasis on the role of zooplankton grazing. Limnol. Oceanogr. **17**: 597-605.

Glooshenko, W.A., Moore, J.E., Munawar, M., and Vollwenweider, R.A. 1974. Primary production in lakes Ontario and Erie: A comparative study. J. Fish. Res. Bd. Can. **31**: 253-263.

Goovaerts, P. 1999. Using elevation to aid the geostatistical mapping of rainfall erosivity. Catena. **34**: 227-242.

Goovaerts, P. 2001. Geostatistical modeling of uncertainty in soil science. Geoderma **103**. 3-26.

Goslee, S.C., and Urban, D.L. 2007. The ecodist package for dissimilarity-based analysis of ecological data. J. Stat. Soft. **22**: 1-19.

Gotway, C.A., and Stroup, W.W. 1997. A generalized linear model approach to spatial data analysis and prediction. J.Agr.Biol.Env.Stat. **2**: 157-178.

Gotway-Crawford, C.A. and Young, L.J. 2005. Change of support: An interdisciplinary challenge.p. 1-13. In: Geostatistics for Environmental Applications. Proceedings of the 5th Euroopean Conference of Geostatistics in Environmental Applications. Springer, The Netherlands.

Gouvea, S.P., Melendez, C., Carberry, M.J., Bullerjahn, G.S., Wilhelm, S.W., Langen, T.A., and Twiss, M.R. 2006. Assessment of phosphorus - microbe interactions in lake Ontario by multiple techniques. J. Great Lakes. Res. **32**: 455-470.

Graham, L.E. 1982. Cytology, ultrastructure, taxonomy and phylogenetic relationships of Great Lakes filamentous algae. J. Great Lakes Res. **8**: 3-9.

Graham, J.M., Auer, M.T., Canale, R.P., and Hoffmann, J.P. 1982. Ecological studies and mathematical modeling of *Cladophora* in lake Huron: 4. photosynthesis and respiration as functions of light and temperature. J. Great Lakes Res. **8**: 100-111.

Graham, J.M., Kranzfelder, J.A., and Auer, M.T. 1985. Light and Temperature as factors regulating seasonal growth and distribution of *Ulothrix zonata* (Ulvophyceae). J. Phycol. **21**: 228-234.

Graham, J.M., Lembi, C.A., Adrian, H.L., and Spencer, D.F. 1995. Physiological responses to temperature and irradiance in *Spirogyra* (Zygnematales, Charophyceae). J. Phycol. **31**: 531-540.

Greene, R.M., Kolber, Z.S., Swift, D., Tindale, N.W., and Falkowski, P.G. 1994. Physiological limitation of phytoplankton photosynthesis in the eastern equatorial Pacific determined from variability in the quantum yeild of fluorescence. Limnol. Oceanogr. **39**: 1061-1074.

Greene, R.M., Geider, R.J., and Falkowski, P.G. 1991. Effect of iron limitation on photosynthesis in a marine diatom. Limnol. Oceanogr. **36**: 1772-1782.

Gregor, D.J., and Rast, W. 1982. Simple trophic state classification of the Canadian nearshore waters of the Great Lakes. Wat. Res. Bull. **18**: 565-573.

Griffiths, R.W., Schloesser, D.W., Leech, J.H., and Kvalak, W.P. 1991. Distribution and dispersal of the zebra mussel (*Dreissena polymorpha*) in the Great Lakes region. Can J. Fish. Aquat. Sci. **48**: 1381-1388.

Griffiths, M. 1990. *Canadian Great Lakes Basin Intake - Outfall Atlas, Volume 7, Lake Ontario***.** Kleinfeldt Consultants Ltd., Toronto, Ontario. Prepared for Ontario Water Resources Branch. 333 maps; 28 x 44 centimetres.

Guan, W., Chamberlain, R., Sabol, B.M., and Doering, P. 1999. Mapping submerged aquatic vegetation with GIS in the Caloosahatchee estuary: Evaluation of different interpolation methods. Mar. Geod. **22**: 69-91.

Guildford, S.J., and Hecky, R.E. 2000. Total nitrogen, total phosphorus and nutrient limitation in lakes and oceans: Is there a common relationship? Limnol. Oceanogr. **45**: 1213-1223.

Guildford, S.J., Depew, D.C., Hecky, R.E., Houben, A., and Ozersky, T. Seasonal and spatial trends in TP and chlorophyll in Lake Simcoe: Impact of dreissenids? submitted to J. Great Lakes Res.

Haffner, G.D., Griffiths, M., and Hebert, P.D.N. 1984a. Phytoplankton community structure and distribution in the nearshore zone of lake Ontario. Hydrobiol. **114**: 51-66.

Haffner, G.D., Yallop, M.L., Hebert, P.D.N., and Griffiths, M. 1984b. Ecological significance of upwelling events in lake Ontario. J. Great Lakes Res. **10**: 28-37.

Haga, H., Ohtsuka, T., Matsuda, M., and Ashiya, M. 2007. Echosunding observations of coverage, height, PVI and biomass of submerged macrophytes in the southern basin of lake Biwa, Japan. Limnol. **8**: 95-102.

Hall, S.R., Pauliukonis, N.K., Mills, E.L., Rudstam, L.G., Schneider, C.P., Lary, S.J., and Arrhenius, F.J. 2003. A comparison of total phosphorus, chlorophyll a, and zooplankton in embayment, nearshore, and offshore habitats of lake Ontario. J. Great Lakes Res. **29**: 54-69.

Haltuch, M.A., Berkman, P.A., and Garton, D.W. 2000. Geographic information system (GIS) analysis of ecosystem invasion: Exotic mussels in Lake Erie. Limnol. Oceanogr. **45**: 1778-1787.

Hamilton, L. J. (Aeronautical and Maritime Research Laboratoy, Fishermans Bend, Victoria, Australia). 2001 Nov. Acoustic seabed classification systems. DSTO Aeronautical and Maritime Research Laboratory. Report nr DSTO-TN-0401. Available from: http://www.dsto.defence.gov.au/corporate/reports/DSTO-TN-0401.pdf.

Harremoes, P. 1988. Stochastic models for estimation of extreme pollution from urban runoff. Wat. Res. **22**: 1017-1026.

Harrison, S.S.C., and Hildrew, A.G. 2001. Epilithic communities and habitat heterogeneity in a lake littoral. J. Animal Ecol. **70**: 692-707.

Haynes, J.M., Tisch, N.A., Mayer, C.M., and Rhyne, R.S. 2005. Benthic macroinvertebrate communities in southwestern Lake Ontario following invasion of *dreissena* and *echinogammarus*: 1983 to 2000. J. N. Am. Benthol. Soc. **24**: 148-167.

Hecky, R.E., Smith, R.E.H., Barton, D.R., Guildford, S.J., Taylor, W.D., Charlton, M.N., and Howell, T. 2004. The nearshore phosphorus shunt: A consequence of ecosystem engineering by dreissenids in the Laurentian Great Lakes. Can. J. Fish. Aquat. Sci. **61**: 1285-1293.

Hengl, T., Heuvelink, G.B.M., and Rossiter, D.G. 2007. About regression kriging: From equations to case studies. Comp. Geosci. **33**: 1301-1315.

Hengl, T., Heuvelink, G.B.M., and Stein, A. 2004. A generic framework for spatial prediction of soil variables based on regression kriging. Geoderma. **120**: 75-93.

Herbst, R.P. 1969. Ecological factors and the distribution of *Cladophora glomerata* in the Great Lakes. Am. Midl. Nat. **82**: 90-98.

Hermand, J.P. 2006. Continuous monitoring of physiological and environmental processes in seagrass prairies with focus on photosynthesis. *In* Acoustic sensing techniques for the shallow water environment. *Edited by* A. Caiti, N.R. Chapman, J.P. Hermand and S.M. Jesus. pp. 183-196.

Heuvelink, G.B.M. 2002. Analysing uncertainty propagation in GIS: Why is it not that simple? *In* Uncertainty in remote sensing and GIS. *Edited by* G.M. Foody and P.M. Atkinson. Wiley, Chichester. pp. 155-165.

Hewitt, J.E., Thrush, S.F., Legendre, P.F.,G.A., Ellis, J., and Morrison, M. 2004. Mapping of marine soft-sediment communities: Integrated sampling for ecological interpretation. Ecol. Appl. **14**: 1203-1216.

Higgins, S.N. 2005. Modeling the growth dynamics of *Cladophora* in eastern Lake Erie. Ph.D. Thesis, University of Waterloo, Waterloo, Ontario, Canada.

Higgins, S.N., Hecky, R.E., and Guildford, S.J. 2008. The collapse of benthic macroalgal blooms in response to shelf-shading. Freshwat. Biol. **53**: 2557-2572.

Higgins, S.N., Hecky, R.E., and Guildford, S.J. 2005a. Modeling the growth, biomass, and tissue phosphorus concentration of *Cladophora glomerata* in eastern Lake Erie: Model description and field testing. J. Great Lakes Res. **31**: 439-455.

Higgins, S.N., Howell, E.T., Hecky, R.E., Guildford, S.J., and Smith, R.E.H. 2005b. The wall of green: The status of *Cladophora glomerata* on the northern shores of Lake Erie's Eastern basin, 1995-2002. J. Great Lakes Res. **31**: 547-563.

Higgins, S.N., Malkin, S.Y., Howell, E.T., Guildford, S.J., Campbell, L., Hiriart-Baer, V., and Hecky, R.E. 2008. An ecological review of *Cladophora glomerata* (Chlorophyta) in the Laurentian Great Lakes. J. Phycol. **44**: 839-854. doi: 10.1111/j.1529-8817.2008.00538.x.

Hillebrand, H., and Sommer, U. 1999. The nutrient stochiometry of benthic microalgal growth: Redfield proportions are optimal. Limnol. Oceanogr. **44**: 440-446.

Hillebrand, H. 2002. Top-down versus bottom-up control of autotrophic biomass—a meta-analysis on experiments with periphyton. J. N. Am. Benth. Soc. **21**: 349-369.

Hiriart-Baer, V.P., Diep, N., and Smith, R.E.H. 2008. Dissolved organic matter in the great lakes: Role and nature of allochthonous material. J. Great Lakes Res. **34**: 383-394.

Hiriart-Baer, V.P., Arciszewski, T.J., Malkin, S.Y., Guildford, S.J., and Hecky, R.E. 2009. Use of pulse amplitude modulated fluorescence to assess the physiolgical status of *cladophora* sp. along a water quality gradient. J. Phycol. **44**: 1604-1613.

Hoffmann, J.P., and Graham, L.E. 1984. Effects of selected physicochemical factors on growth and zoosporogenesis of *Cladophora glomerata* (Chlorphyta). J. Phycol. **20**: 1-7.

Hohausova, E., Kubecka, J., Frouzova, J., Husak, S., and Balk, H. 2008. Experimental biomass assessment of three species of freshwater aquatic plants by horizontal acoustics. J. Aquat. Plant Man. **46**: 82-88.

Holliday, D.V., and Pieper, R.E. 1995. Bioacoustical oceanography at high frequencies. ICES J. Mar. Sci. **52**: 279-296.

Holmes, R.M., Aminot, A., Kerouel, R., Hooker, B.A., and Peterson, B.J. 1999. A simple and precise method for measureing ammonuim in marine and freshwater ecosystems. Can. J. Fish. Aquat. Sci. **56**: 1801-1808.

Hopkins, W.G. 1999. Introduction to Plant Phyiology. 2nd Ed. John Wiley and Sons.New York.

Houben, A.J. 2007. Organic tissue stoichiometry of *Cladophora glomerata* and its relation to coastal land use in the Laurentian Great Lakes. M.Sc. Thesis, University of Waterloo, Waterloo, Ontario.

Howarth, R.W., Billen, G., Swaney, D., Townsend, A., Jaworski, N., Lajtha, K., Downing, J.A., Elmgren, R., Caraco, N.F., Jordan, T., Berendse, F., Freney, J., Kudeyarov, V., Murdoch, P., and Zhu, Z.L. 1996. Regional nitrogen budgets and riverine N & P fluxes for the drainages to the North Atlantic ocean: Natural and human influences. Biogeochemistry. **35**: 75-139.

Howell, E.T. 2004. Occurence of nuisance benthic algae on the southwestern shores of Lake Huron, 2003.

Howell, E.T., Marvin, C.H., Bilyea, R.W., Kauss, P.B., and Somers, K. 1996. Changes in environmental conditions during *dreissena* colonization of a monitoring station in eastern Lake Erie. J. Great Lakes Res. **22**: 744-756.

Hudon, C., Lalonde, S. and Gagnon, P. 2000. Ranking the effects of site exposure, plant growth form, water depth, and transparency on aquatic plant biomass. Can. J. Fish. Aquat. Sci. **57**: 31-42.

Hutchinson, G.E. 1975. A treatise on Limnology. John Wiley and Sons, New York.

Hwang, S.J., Havens, K.E., and Steinman, A.D. 1998. Phosphorus kinetics of planktonic and benthic assemblages in a shallow subtropical lake. Freshwat. Biol. **40**: 729-745.

International Joint Commission. 1980. Phosphorus management for the Great Lakes. Final report of the Phosphorus Management Strategies Task Force to the International Joint Commission's Great Lakes Water Quality Board and Great Lakes Science Advisory Board. Windsor, Ontario, Canada.

International Lake Ontario - St Lawrence River Water Pollution Board. 1969. Pollution of Lake Ontario and the international section of the St. Lawrence River. Volume 3, International Joint Commission, Windsor, Ontario.

Isaaks, E.H., and Srivastava, R.M. 1989. Applied geostatistics. Oxford University Press, New York.

Istvanovics, V., Honti, M., Kovacs, A., and Osztoics, A. 2008. Distribution of submerged macrophytes along environmental gradients in large, shallow lake Balaton (Hungary). Aquat. Bot. **88**: 317-330.

Jackson, M.B. 1985. The red alga *Bangia* in Lake Simcoe. J. Great Lakes Res. **11**: 179-181.

Jackson, M.B. 1982. *Cladophora* in Lake Simcoe, 1976 and 1980. Ontario Ministry of Environment.

Jackson, D.A., and Somers, K.M. 1989. "Are probability estimates from the permutation model of mantel's test stable?". Can. J. Zool. **67**: 766-769.

Jackson, M.B. 1988. The dominant attached filamentous algae of Georgian Bay, the north channel and eastern Lake Huron: Field ecology and biomonitoring potential during 1980. Hydrobiol. **163**: 149-171.

Jackson, M.B., Nakamoto, L.K., and Lueck-Wong, S. 1985. The nearshore water quality of southeastern lake Huron. Ontario Ministry of Environment, Toronto, Ontario.

Jensen, O.P., and Miller, T.J. 2005. Geostatistical analysis of the abundance and winter distribution patterns of the blue crab *Callinectes sapidus* in Chesapeake Bay. Trans. Amer.Fish.Soc. **134**: 1582-1598.

Jeppesen, E., Sondergaard, M., Jensen, J.P., Havens, K.E., Anneville, O., Carvalho, L., Coveney, M.F., Deneke, R., Dokulil, M.T., Foy, B., Gerdeaux, D., Hampton, S.E., Hilt, S., Kangur, K., Kohler, J., Lammens, E.H.H.R., Lauridsen, T.L., Manca, M., Miracle, M.R., Moss, B., Noges, P., Persson, G., Phillips, G., Portielje, R., Romo, S., Schelske, C.L., Straile, D., Tatrai, I., Willen, E., and Winder, M. 2005. Lake responses to reduced nutrient loading - an analysis of contemporary long-term data from 35 case studies. Freshwat. Biol. **50**: 1747-1771.

Johnson, M.G. and Nicholls, K.H. 1988. Temporal and spatial trends in metal loads to sediments of Lake Simcoe, Ontario. Wat. Air Soil Poll. **39**:337-354.

Johnson, M.G., and Nicholls, K.H. 1989. Temporal and spatial variability in sediment and phosphorus loads to Lake Simcoe, Ontario. J. Great Lakes Res. **15**: 265-282.

Johnson, R.A. 2004. The benthic food web on nearshore hard substrates at Peacock Point, eastern Lake Erie. M.Sc. Thesis, University of Waterloo, Waterloo, Ontario, Canada.

Jones, K.B., Neale, A.C., Nash, M.S., Van Remortel, R.D., Wickham, J.D., Ritters, K.H., and O'Neill, R.V. 2001. Predicting nutrient and sediment loadings to streams from landscape metrics: A multiple watershed study from the United States mid Atlantic region. Landsc. Ecol. **16**: 301-312.

Journel, A.G., and Huijbergts, C.J. 1978. Mining geostatistics. Academic Press, London.

Juang, K.W., Chen, Y.S., and Lee, D.Y. 2004. Using sequential indicator simulation to assess the uncertainty of delineating heavy metal contaminated soils. Environ. Pollut. **127**. 229-238.

Kahlert, M. 1998. C:N:P ratios of freshwater benthic algae. Arch. Hydrobiol. Spec. Issue Adv. Limnol. **51**: 105-114.

Kahlert, M., and Pettersson, K. 2002. The impact of substrate and lake trophy on the biomass and nutrient status of benthic algae. Hydrobiol. **489**: 161-169.

Karatayev, A.Y., Burlakova, L.E., and Padilla, D.K. 2002. Impacts of zebra mussels on aquatic communities and their role as ecosystem engineers. *In* Invasive aquatic species of europe. *Edited by* E. Leppakoski, S. Olenin and S. Gollasch. Kluwer Academic Publishers, Netherlands. pp. 433-447.

Karatayev, A.Y., Burlakova, L.E., and Padilla, D.K. 1997. The effects of *Dreissena polymorpha* (pallas) invasion on aquatic communities in eastern Europe. J. Shellfish Res. **16**: 187-203.

Kelly, J.R. 2009. Chapter 5.1. Nutrients and the Great Lakes nearshore, circa 2002-2007. SOLEC 2008 Meeting, Niagara Falls, ON, Canada, October 22-23, 2008, Section in: Report on Nearshore Areas of the Great Lakes 2009, pp.49-56.

Kendrick, G.A., Holmes, K.W., and Van Neil, K.P. 2008. Multi-scale spatial patterns of three seagrass species with different growth dynamics. Ecography. **31**: 191-200.

Kilgour, B., Clarkin, C., Morton, W., and Baldwin, R. 2008. Influence of nutrients in water and sediments on spatial distributions of benthos in Lake Simcoe. J. Great Lakes Res. **34**: 365-377.

Kirk, J.T.O. 1994. Light and photosynthesis in aquatic ecosystems. Oxford University Press, Cambridge, England.

Klerks, P.L., Fraleigh, P.C., and Lawniczak, J.E. 1996. Effects of zebra mussels (*Dreissena polymorpha*) on seston levels and sediment deposition in western Lake Erie. Can. J. Fish. Aquat. Sci. **53**: 2284-2291.

Koblizek, M., Kaftan, D., and Nedbal, L. 2001. On the relationship between the non-photochemical quenching of the chlorophyll fluorescence and the photosystem II light harvesting efficiency. A repetitive flash fluorescence induction study. Photosyn. Res. **68**: 141-152.

Kolber, Z., Wyman, K.D., and Falkowski, P.G. 1990. Natural variability in photosynthetic energy conversion efficiency: A field study in the gulf of Maine. Limnol. Oceanogr. **35**: 72-79.

Kolber, Z., and Falkowski, P.G. 1993. Use of active fluorescence to estimate phytoplankton photosynthesis in situ. Limnol. Oceanogr. **38**: 1646-1665.

Kolber, Z., Prasil, O., and Falkowski, P.G. 1998. Measurements of variable chlorophyll fluorescence using fast repetition rate techniques: Defining methodology and experimental protocols. Biochim. Biophys. Acta. **1367**: 88-106.

Kolber, Z.S., Zehr, J., and Falkowski, P.G. 1988. Effects of growth irradiance and nitrogen limitation on photosynthetic energy conversion in photosystem II. Plant Physiol. **88**: 923-929.

Kruskopf, M., and Flynn, K.J. 2006. Chlorophyll content and fluorescence responses cannot be used to guage reliably phytoplankton biomass, nutrient status or growth rate. New Phytol. **169**: 525-536.

Kubecka, J. 1996. Use of horizontal dual-beam sonar for fish surveys in shallow waters. *In* Stock assessment in inland fisheries . *Edited by* I.G. Cows. Blackwell, Oxford. pp. 165-175.

Kubecka, J., Frouzová, J., Cech, M., Peterka, J., Ketelaars, H.A.M., Wagenwoort, A.J., and Papácek, M. 2000. Hydroacoustic assessment of pelagic stages of freshwater insects. Aquat. Liv.Res. **13**: 361-366.

Lacoul, P., and Freedman, B. 2006. Environmental influences on aquatic plants in freshwater ecosystems. Environ. Rev. **14**: 89-136.

LaLonde, R.T., Morris, C.D., Wong, C.F., Gardner, L.C., Eckert, D.J., King, D.R., and Zimmerman, R.H. 1979. Response of *Aedes triseriatus* larvae to fatty acids of *Cladophora*. J. Chemi.Ecol. **5**: 371-381.

Lake Simcoe Region Conservation Authority, 2009. Report on the phosphorus loads to Lake Simcoe 2004-2007. Lake Simcoe Region Conservation Authority, Newmarket Ontario.

Laney, S.R. 2003. Assessing the error in photosynthetic properties determined by fast repetition rate fluorometry. Limnol. Oceanogr. **48**: 2234-2242.

Lean, D.R.S., Neilson, M.A., Stevens, J.J., and Mazumder, A. 1990. Response of Lake Ontario to reduced phosphorus loading. Verh. Internat. Verein. Limnol. **24**: 420-425.

Lee, H., Bakowsky, W., Riley, J.L., Bowles, J., Puddister, M., Uhlig, P., and McMurray, M. 1998. Ecological land classification for southern ontario: First approximation and its applications.Ontario Ministry of Natural Resources.

Legendre, P. 2000. Comparison of permutation methods for the partial correlation and partial mantel tests. J. Stat. Comp. Sim. **67**: 37-73.

Legendre, P., and Trousselier, M. 1989. Aquatic heterotrophic bacteria: Modelling in the presence of spatial autocorrelation. Limnol. Oceanogr. **33**: 1055-1067.

Lepisto, A., Granlund, K., Kortelainen, P., and Raike, A. 2006. Nitrogen in river basins: Sources, retention in the surface waters and peatlands, and fluxes to estuaries in Finland. Sci. Tot. Env. **365**: 238-259.

Ley, A.C., and Mauzerall, D.C. 1982. Absolute absorption cross-sections for photosystem II and the minimum quantum requirement for photosynthesis in *Chlorella vulgaris*. Biochim. Biophys. Acta. **680**: 95-106.

Lippemeier, S., Hartig, P., and Colijn, F. 1999. Direct impact of silicate on the photosynthetic performance of the diatom *thalassiosira weissflogii* assessed by on and off-line PAM fluorescence measurements. J. Plankt. Res. **21**: 269-283.

Lorenz, R.C., Monaco, M.E., and Herdendorf, C.E. 1991. Minimum light requirements of substrate colonization by *Cladophora glomerata*. J. Great Lakes Res. **17**: 536-542.

Lorenzen, C. 1966. A method for the continuous measurement of in vivo chlorophyll concentration. Deep Sea Res. I. **13**: 223-227.

Mackey, S.D., and Goforth, R.R. 2005. Special issue on great lakes nearshore and coastal habitats. J. Great Lakes Res. **31**.

Mackey, S.D. and Leibenthal, D.L. 2005. Mapping changes in Great Lakes near shore substrate distributions. J. Great Lakes Res. **31**: 75-89.

Madenjian, C.P. 1995. Removal of algae by the zebra mussel (*Dreissena polymorpha*) population in western Lake Erie: A bioenergetics approach. Can. J. Fish. Aquat. Sci. **52**: 381-390.

Madsen, J.D., Hartleb, C.F. and Boylen, C.W. 1991. Photosynthetic characteristics of *Myriophyllum spicatum* and six submersed aquatic macrophyte species native to Lake George, New York. Freshwat. Biol. **26**: 233-240.

Makarewicz, J.C., and Dilcher, R.C. 1988. Occurence of macrophytes in nearshore Lake Ontario. J. Great Lakes Res. **14**: 405-410.

Malkin, S.Y. 2007. The ecology of the nuisance macroalga, *Cladophora glomerata*, and its resurgence in lake Ontario. PhD Thesis, University of Waterloo, Waterloo, Ontario.

Malkin, S.Y., Guildford, S.J., and Hecky, R.E. 2008. Modeling the growth response of *Cladophora* in a Laurentian Great Lake to the exotic invader dreissena and to lake warming. Limnol. Oceanogr. **53**: 1111-1124.

Malkin, S.Y., Sorichetti, R.J., Wiklund, J.A., and Hecky, R.E. 2009. Seasonal abundance, community composition, and silica content of diatoms epiphytic on *Cladophora glomerata*. J. Great Lakes Res. **35**: 199-205.

Maravelias, C.D., Reid, D.G., Simmonds, E.J., and Haralabous, J. 1996. Spatial analysis and mapping of acoustic survey data in the presence of high local variability: Geostatistical application to north sea herring (*Clupea harengus*). Can. J. Fish. Aquat. Sci. **53**: 1497-1505.

Marsalek, J., and Rochfort, Q. 2004. Urban wet-weather flows: Sources of fecal contamination impacting on recreational waters and threatening drinking-water sources. J. Tox. Env. Health, Part A. **67**: 1765-1777.

Martini, I.P., and Kwong, J.K.P. 1985. Nearshore sediments of lake Ontario with special reference to the Presqu'ile - Wellington Bay area. 5557, Ontario Geological Survey. Ottawa, Ontario, Canada.

Marwood, C.A., Smith, R.E., Solomon, K.R., Charlton, M.N., and Greenberg, B.M. 1999. Intact and photomodified polycyclic aromatic hydrocarbons inhibit photosynthesis in natural assemblages of lake Erie phytoplankton exposed to solar radiation. Ecotoxicol. Environ. Saf. **44**: 322-327.

Masse, A.K., and Murthy, C.R. 1992. Analysis of the Niagara river plume dynamics. J. Geophys. Res. **97**: 2403-2420.

Matheron, G. 1963. Principles of geostatistics. Econ. Geol. **58**: 1246-1266.

McCarthy, E.M. 1997. Acoustic characterization of submerged aquatic vegetation.Proceedings of the High Frequency Acoustics in Shallow Waters Conference, NATO SACLANT Undersea Research Centre, Lerici, Italy.

McGlathery, K.J., Krause-Jensen, D., Rysgaard, S., and Christensen, P.B. 1997. Patterns of ammonium uptake within dense mats of the filamentous macroalga *Chaetomorpha linum*. Aquat. Bot. **59**: 99-115.

McGlathery, K.J., and Pedersen, M. 1999. The effect of growth irradiance on the coupling of carbon and nitrogen metabolism in *Chaetomorpha linum* (Chlorophyta). J. Phycol. **35**: 721-731.

McNaught, D.C., and Hasler, A.D. 1966. Photoenvironments of planktonic crustacea in Lake Michigan. Verh. Int. Ver. Limnol. **16**: 194-203.

Medeiros, A.S., and Molot, L.A. 2006. Trends in iron and phosphorus loading to Lake Ontario from waste water treatment plants in Hamilton and Toronto. J. Great Lakes Res. **32**: 788-798.

Medwin, H., and Clay, C.,S. 1998. Fundamentals of acoustical oceanography. Academic Press, San Diego, CA.

Megard, R.O., Kuns, M.M., Whiteside, M.C., and Downing, J.A. 1997. Spatial distribution of zooplankton during coastal upwelling in western Lake Superior. Limnol. Oceanogr. **42**: 827-840.

Mello, L.G.S., and Rose, G.A. 2005. Using geostatistics to quantify seasonal distribution and aggregation patterns of fishes: An example of Atlantic cod (*Gadus morhua*). Can. J. Fish. Aquat. Sci. **62**: 659. doi: 10.1139/f04-227.

Menge, B.A., Daley, B.A., Wheeler, P.A., Dahlhoff, E., Sanford, E., and Strub, P.T. 1997. Benthic-pelagic links and rocky intertidal communities: Bottom up effects on top down control? Proc. Natl. Acad. Sci. **94**: 14530-14535.

Middelbøe, A.L., and Markager, S. 1997. Depth limits and minimum light requirements of freshwater macrophytes. Freshwat. Biol. **37**: 553-568.

Millard, E.S., and Veal, D.M. 1971. Aquatic weed growth in Lake Simcoe. Ontario Water Resources Commission, Toronto, ON.29 pp.

Millard, E.S., Johannsson, O.E., Neilson, M.A., and El-Shaarawi, A.H. 2003. Long term, seasonal and spatial trends in nutreints, chlorophyll a and light attenuation in Lake Ontario. *In* State of Lake Ontario: Past, present and future. *Edited by* M. Munawar. Aquatic Ecosystem Health and Management Society, Burlington, ON.

Miller, J. and Franklin, J. 2002. Modeling the distribution of four vegetation alliances using generalized linear models and classification trees with spatial dependence. Ecol. Mod. **157**: 227-247.

Millner, G.C., Sweeney, R.A., and Frederick, V.R. 1982. Biomass and distribution of *Cladophora glomerata* in relation to some physical-chemical variables at two sites in Lake Erie. J. Great Lakes Res. **8**: 27-29.

Mills, E.L., Casselman, J.M., Dermott, R., Fitzsimons, J.D., Gal, G., Holeck, K.T., Hoyle, J.A., Johannsson, O.E., Lantry, B.F., Makarewicz, J.C., Millard, E.S., Munawar, I.F., Munawar, M., O'Gorman, R., Owens, R.W., Rudstam, L.G., Schaner, T., and Stewart, T.J. 2003. Lake Ontario: Food web dynamics in a changing ecosystem. Can. J. Fish. Aquat. Sci. **60**: 471-490.

Minasay, B., and McBratney, A.B. 2007. Spatial prediction of soil properties using EBLUP with the matern covariance function. Geoderma. **140**: 324-336.

Ministry of Environment. 1980. Lake Ontario nearshore water quality atlas. Water Resources Branch, Great Lakes Unit, Toronto, Ontario.

Ministry of Natural Resources. 2002. Southern ontario land resource information system. Peterborough, ON.

Mitson, R.B. 1983. Acoustic detection and estimation of fish near the seabed and surface. 300, FAO Fisheries Technical Reports.

Moeller, R.A., Wetzel, R.G., and Osenberg, C.W. 1998. Concordance of phosphorus limitation in lakes: Bacterioplantkon, phytoplankton, epiphyte-snail consumers, and rooted macrophytes. *In* The structuring role of submerged macrophytes in lakes. *Edited by* E. Jeppesen, M. Sondergaard and M.C. Sondergaard K. Springer-Verlag, New York. pp. 318-325.

Molot, L.A., and Dillon, P.J. 1993. Nitrogen mass balances and denitrification rates in central Ontario lakes. Biogeochemistry. **20**: 195-212.

Moore, B.C., Funk, W.H., and Anderson, E. 1994. Water quality, fishery, and biologic characteristics in a shallow, eutrophic lake with dense macrophyte populations. Lake Res. Manage. **8**: 175-188.

Moore, C.M., Sugget, D., Hickman, A.E., Kim, Y.N., Tweddle, J.F., Sharples, J., Geider, R.J., and Holligan, P. 2006. Phytoplankton photoacclimation and photoadaptation in response to environmental gradients in a shelf sea. Limnol. Oceanogr. **51**: 936-949.

Moore, C.M., Suggett, D.J., Holligam, P.M., Sharples, J., Abraham, E.R., Lucas, M.I., Rippeth, T.M., Fisher, N.R., Simpson, J.H., and Hydes, D.J. 2003. Physical controls on phytoplankton physiology and production at a shelf sea front: A fast repetition rate fluorometer based field study. Mar. Ecol. Prog. Ser. **259**: 29-45.

Moore, M.C., Lucas, M.I., Sanders, R., and Davidson, R. 2005. Basin scale variability of phytoplankton bio-optical characteristics in relation to bloom state adn community structure in the northeast Atlantic. Deep-Sea Res. I. **52**: 401-419.

Mortimer, C.H. 1988. Discoveries and testable hypotheses arising from coastal zone color scanner imagery of southern Lake Michigan. Limnol. Oceanogr. **33**: 203-226.

Munawar, M., Munawar, I.F., McCarthy, L., Page, W., and Gilron, G. 1993. Asessing the impact of sewage effluent on the ecosystem health of the Toronto waterfront (Ashbridges bay), Lake Ontario. J. Aquat. Ecosyst. Health. **2**: 287-315.

Murthy, C.R., and Csanady, G.T. 1971. Outfall simulation experiment in Lake Ontario. Wat. Res. **5**: 813-822.

Musko, L.B. and Bako, B. 2005. The density and biomass of *Dreissena polymorpha* living on submerged macrophytes in Lake Balaton (Hungary). Arch. Hydrobiol. **162**: 229-251.

Nalepa, T.F., Fanslow, D.L., Pothoven, S.A., Foley, A.J., and Lang, G.A. 2007. Long-term trends in benthic macroinvertebrate populations in lake Huron over the past four decades. J. Great Lakes Res. **33**: 421-436.

Neil, J.H. 1974. *Cladophora* in the Great Lakes. International Joint Commission, Windsor, Ontario, Canada.

Neil, J.H., Graham, J., and Warren, J. 1991. Aquatic plants of Cook Bay, Lake Simcoe 1987. Imp. B14, Lake Simcoe Region Conservation Authority, Newmarket, Ontario.

Neil, J.H., Kamaitis, G.A., and Robinson, G.W. 1985. Aquatic plant assessment in Cook Bay, Lake Simcoe. Imp. B4, Lake Simcoe Region Conservation Authority, Newmarket, Ontario.

Neil, J.H., and Jackson, M.B. 1982. Monitoring *Cladophora* growth conditions and the effect of phosphorus additions at a shoreline site in northeastern Lake Erie. J. Great Lakes Res. **8**: 30-34.

Neil, J.H. and Owen, G.E. 1964. Distribution, environmental requirements, and significance of *Cladophora* in the Great Lakes. *In*: Proceedings of the 7th Conference on Great Lakes Research. Publ. 11. Great Lakes Research Division, University of Michigan, Ann Arbor, pp 113-121.

Neilson, M., L'Italien, S., Glumac, V., Williams, D., and Bertram, P. 1995. 1994 state of the lakes ecosystem conference background paper. Nutrients: Trends and system response. EPA 905-R-95-015.

Neilson, M.A., Painter, D.S., Warren, G., Hites, R.A., Basu, I., Weseloh, D.V., Whittle, D.M., Christie, G., Barbeiro, R.P., Tuchman, M.L., Johansson, O.E., Nalepa, T.F., Edsall, T.A., Fleischer, G., Bronte, C.,

Smith, S.B., and Baumann, P.C. 2003. Ecological monitoring for assessing the state of the nearshore and open waters of the Great Lakes. Env. Mon. Assess. **88**: 103-117.

Nicholls, K.H., and Tudorancea, C. 2001. Species-level and community-level data analyses reveal spatial differences and temporal change in the crustacean zooplankton of a large Canadian lake (Lake Simcoe, Ontario). J. Limnol. **60**: 155-177.

Nicholls, K.H. and MacCrimmon, H.R. 1975. Nutrient loading to Cook bay of Lake Simcoe from the Holland river watershed. Int. Rev. Hydrobiol. **60**: 159-193.

Nicholls, K.H. 2001. The relative effects of major sources of phosphorus loading on phosphorus concentration in Cook's Bay of Lake Simcoe. Lake Simcoe Region Conservation Authority, Newmarket, ON.

Nicholls, K.H. 1998. Lake Simcoe water quality update, with emphasis on phosphorus trends. Imp. B18, Lake Simcoe Region Conservation Authority, Newmarket, ON.

Nicholls, K.H., and Hopkins, G.J. 1993. Recent changes in Lake Erie (north shore) phytoplankton: Cumulative impacts of phosphorus loading reductions and the zebra mussel introduction. J. Great Lakes Res. **19**: 637-647.

Nicholls, K.H., Hopkins, G.J., and Standke, S.J. 1999. Reduced chlorophyll to phosphorus ratios in nearshore Great Lakes waters coincide with the establishment of dreissenid mussels. Can. J. Fish. Aquat. Sci. **56**: 153-161.

Nicholls, K.H., Hopkins, G.J., Standke, S.J., and Nakamoto, L. 2001. Trends in total phosphorus in Canadian near-shore waters of the Laurentian Great lakes: 1976-1999. J. Great Lakes Res. **27**: 402-422.

Niemi, G.J., Kelly, J.R., and Danz, N.P. 2007. Environmental indicators for the coastal region of the North American Great Lakes: Introduction and prospectus. J. Great Lakes Res. **33**: 1-12.

North, R.L. 2008. Phytoplankton dynamics in nearshore and offshore regions of great lakes Erie, Malawi, Tanganyika, and Victoria. PhD Thesis, University of Waterloo, Waterloo, Ontario, Canada.

Nowell, A.R.M., and Jumars, P.A. 1984. Flow environments of aquatic benthos. Ann. Rev. Ecol. Syst. **15**: 303-328.

Odeh, L., McBratney, A.B., and Chittleborough, D. 1995. Further results on prediction of soil properties from terrain attributes: Heterotopic cokriging and regression kriging. Geoderma. **67**: 215-226.

Olaizola, M., La Roche, J., Kolber, Z., and Falkowski, P.G. 1994. Non-photochemical fluorescence quenching and the diadinoxanthin cycle in a marine diatom. Photosyn. Res. **41**: 357-370.

Olaizola, M., Geider, R.J., Harrison, W.G., Graziano, L.M., Ferrari, G.M., and Schlittenhardt, P.M. 1996. Synoptic study of variations in the fluorescence-based maximum quantum efficiency of photosynthesis across the North Atlantic ocean. Linol. Oceanogr. **41**: 755-765.

Olapade, O.A., Depas, M.M., Jensen, E.T., and McLellan, S.L. 2006. Microbial communities and fecal indicator bacteria associated with cladophora mats on beach sites along Lake Michigan shores. Appl. Environ. Microbiol. **72**: 1932-1938. doi: 72/3/1932 [pii]; 10.1128/AEM.72.3.1932-1938.2006 [doi].

Ona, E., and Mitson, R.B. 1996. Acoustic sampling and signal processing near the seabed: The deadzone revisted. ICES J. Mar. Sci. **53**: 677-690.

Ontario Ministry of Environment. 1975. Great Lakes Water Quality Data, 1972 .Water Resources Branch, Ontario Ministry of Environment, Toronto, Ontario.

Ontario Ministry of Environment 1980. Lake Ontario Nearshore Water Quality Atlas, 1976 - 1979. Water Resources Branch, Ministry of Environment, Great Lakes Unit. Toronto, Ontario.

Ontario Ministry of the Environment. 1982. Observations on *Cladophora* growth in some nearshore areas of lake Huron and southern Georgian Bay : Field work, 1981. Ministry of the Environment, Toronto.

Ontario Ministry of Environment. 1999. Surface water monitoring and assessment: 1997 Lake Ontario report featuring a summary of tributary and nearshore conditions and trends for the Lake Ontario basin.Ontario Ministry of Environment, Toronto, Ontario.

Ostrovsky, I. 2003. Methane bubbles in lake Kinneret: Quantification and temporal and spatial heterogeneity. Limnol. Oceanogr. **48**: 1030-1036.

Ozersky, T., Malkin, S.Y., Barton, D.R., and Hecky, R.E. 2009. Dreissenid phosphorus excretion can sustain *C. glomerata* growth along a portion of lake Ontario shoreline. J. Gt. Lakes Res. doi: 10.1016/j.jglr2009.05.001.

Ozersky, T., Barton, DR., Depew, D.C., Hecky, R.E. and Guildford, S.J. Disturbance and habitat availability shape dreissenid mussel distribution and biomass in Lake Simcoe, Ontario.submitted to J. Great Lakes Res.

Paalme, T., Kukk, H., Kotta, J., and Orav, H. 2002. "In vitro" and "in situ" decomposition of nuisance macroalgal *Cladophora glomerata* and *Pilayella littoralis*. Hydrobiol. **475**: 469-476.

Painter, D.S., and Kamaitis, G. 1987. Reduction of *Cladophora* biomass and tissue phosphorus in Lake Ontario 1972-83. Can. J. Fish. Aquat. Sci. **44**: 2212-2215.

Parker, J.E., and Maberly, S.C. 2000. Biological response to lake remediation by phosphate stripping: Control of *Cladophora*. Freshwat. Biol. **44**: 303-309.

Parkhill, J.P., Maillet, G., and Cullen, J.J. 2001. Fluorescence-based maximal quantum yield for PSII as a diagnostic of nutreint stress. J. Phycol. **37**: 517-529.

Patterson, M.W., Ciborowski, J.J., and Barton, D.R. 2005. The distribution and abundance of *Dreissena* species (dreissenidae) in Lake Erie, 2002. J. Great Lakes Res. **31**: 223-237.

Pawlowicz, R. 2002. Observations and linear analysis of estuarine flow and sill-generated internal tides in Haro strait. J. Geophys. Res. **107**: 3056.

Pebesma, E.J. 2004. Multivariable geostatistics in S: The gstat package. Comp. Geosci. **30**: 683-691.

Pemberton, K.L., Smith, R.E.H., Silsbe, G.M., Howell, E.T., and Watson, S.B. 2007. Controls on phytoplankton physiology in Lake Ontario during the late summer "taste and odour" period: Evidence from new fluorescence methods. Can. J. Fish. Aquat. Sci. **64**: 58-73.

Peterson, G.S., Sierzen, M.E., Yurista, P.M., and Kelly, J.R. 2007. Stable nitrogen isotopes of plankton and benthos reflect a landscape level influence on Great Lakes coastal ecosystems. J. Gt. Lakes Res. **33**: 27-41.

Peterson, J.O., and Peterson, W.T. 2008. Influence of the Columbia River plume (USA) on the vertical and horizontal distribution of mesozooplankton over the Washington and Oregon shelf. ICES J. Mar. Sci. **65**: 477-483.

Pinel-Alloul, B., and Ghadouani, A. 2007. Spatial heterogeneity of planktonic microoraganisms in aquatic systems: Mutiscale patterns and processes. *In* The spatial distribution of microbes in the environment. *Edited by* R. Franklin and A. Mills. Springer, New York. pp. 203-307.

Pothoven, S.A., and Nalepa, T.F. 2006. Feeding ecology of lake whitefish in lake Huron. J. Great Lakes Res. **32**: 489-501.

R Core Development Team. 2007. R: A language and environment for statistical computing. Vienna, Austria.

Raateoja, M., Seppälä, J., and Kuosa, H. 2004. Bio-optical modelling of primary production in the SW Finnish coastal zone, Baltic sea: Fast repetition rate fluorometry in case 2 waters. Mar. Ecol. Prog. Ser. **267**: 9-26.

Randall, R.G., and Minns, C.K. 2002. Comparison of a habitat productivity index and an index of biotic integrity for measuring the productive capacity of fish habitat in nearshore areas of the Great Lakes. J. Great Lakes Res. **28**: 240-255.

Rao, Y.R., Skafel, M.G., Howell, E.T., and Murthy, C.R. 2003. Physical processes controlling taste and odour episodes in Lake Ontario drinking water. J. Great Lakes Res. **29**: 70-78.

Rao, Y.R., and Schwab, D.J. 2007. Transport and mixing between the coastal and offshore waters of the Great lakes: A review. J. Great Lakes Res. **33**: 202-218.

Rao, Y.R., and Murthy, C.R. 2001. Coastal boundary layer characteristics during summer stratification in Lake Ontario. J. Phys. Oceanogr. **31**: 1088-1104.

Rao, Y.R., Skafel, M.G., and Charlton, M.N. 2004. Circulation and turbulent exchange characteristics during thermal bar in Lake Ontario. Limnol. Oceanogr. **49**: 2190-2200.

Rao, Y.R., Murthy, R.C., Chiocchio, F., Skafel, M.G., and Charlton, M.N. 2003. Impact of proposed burlington and hamilton sewage discharges in western Lake Ontario. Water Qual. Res. J. Canada. **38**: 627-645.

Ratti, C., and Barton, D.R. 2003. Decline in the diversity of benthic invertebrates in the wave-zone of eastern lake Erie, 1974–2001. J. Great Lakes Res. **29**: 608-615.

Rawson, D.F. 1930. The bottom fauna of Lake Simcoe and its role in the ecology of the lake. PhD. Thesis, University of Toronto, Toronto, Ontario.

Riber, H.H. and Wetzel, R.G. 1987. Boundary-layer and internal diffusion effects on phsophorus fluxes in lake periphyton. Limnol. Oceanogr. **32**: 1181-1194.

Ricciardi, A., Whoriskey, F.G., and Rassmussen, J.B. 1997. The role of the zebra mussel (*Dreissena polymorpha*) in structuring macroinvertebrate communities on hard substrata. Can. J. Fish. Aquat. Sci. **54**: 2596-2608.

Ricciardi, A., and MacIsaac, H.J. 2000. Recent mass invasion of the North American Great Lakes by Ponto-Caspian species. Trends Ecol. Evol. **15**: 62-66.

Riegl, B.M., Moyer, R.P., Morris, L.J., Virnstein, R.W., and Purkis, S.J. 2005. Distribution and seasonal biomass of drift macroalgae in the Indian River lagoon (Florida, USA) estimated with acoustic seafloor classification (QTCView, echoplus). J. Exp. Mar. Biol. Ecol. **326**: 89-104.

Rivoirard, J. 2002. On the structural link between variables in kriging with external drift. Math. Geol. **34**: 31-47.

Roditi, H.A., Strayer, D.L., and Findlay, S.E.G. 1997. Characteristics of zebra mussel (*Dreissena polymorpha*) biodeposits in a tidal freshwater estuary. Arch. Hydrobiol. **140**: 207-219.

Rooney, N., Kalff, J., and Habel, C. 2003. The role of submerged macrophyte beds in phosphorus and sediment accumulation in Lake Memphremagog, Quebec, Canada. Limnol. Oceanogr. **48**: 1927-1937.

Rosemarin, A.S. 1982. Phosphorus nutrition of two potentially competing filamentous algae, *Cladophora glomerata* (L.) Kütz. and *Stigeoclonium tenue* (Agardh) Kütz. from Lake Ontario. J. Great Lakes Res. **8**: 66-72.

Ross, D.I., and Chatterjee, R.M. 1977. Water quality assessment of some Ontario embayments on lake Huron, including Goderich, Port Elgin, Southampton, Tobermory, Owen Sound, Collingwood, and Parry Sound. D-27, Ontario Ministry of the Environment, Toronto, Ontario.

Ross, S.J. 2006. Molecular phylogeography and species discrimination of freshwater Cladophora (Cladophorales, Chlorophyta) in North America. M.Sc. Thesis, University of Waterloo, Waterloo, Ontario, Canada.

Rudstam, L.G., Parker, S.L., Einhouse, D.W., Witzel, L.D., Warmer, D.M., Stritzel, J.L., Parrish, D.L., and Sullivan, P.J. 2003. Application of in situ target strenght estimations in lakes: Examples from rainbow smelt surveys in lakes Erie and Champlain. ICES J. Mar. Sci. **60**: 500-507.

Rufino, M.M., Maynou, F., Abello, P., Gil de Sola, L., and Yule, A.B. 2005. The effect of methodological options on geostatistical modelling of animal distribution: A case study with *Lidocarcinus depurator* (crustacea: Brachyura) trawl survey data. Fish. Res. **76**: 252-265.

Rukavina, N. 1976. Nearshore sediments of lakes Ontario and Erie. Geosci. Canada. **3**: 185-190.

Rukavina, N. 1970. Lake Ontario nearshore sediments, Whitby to Wellington, Ontario. Proceedings of the 13th Conference on Great Lakes Research, pp. 266-272.

Sabol, B.M., and Burczynski, J. 1998. Digital echosounder systems for characterizing vegetation in shallow water environments. Proceedings of the 4th European Conference on Underwater Acoustics, Rome, pp. 165-171.

Sabol, B.M., Burczynski, J., and Hoffman, J. 2002a. Advanced digital processing of echosounder signals for characterization of very dense submerged aquatic vegetation. ERDC/EL TR-02-30, U.S. Army Engineers Research and Development Center, Vicksburg.

Sabol, B.M., Melton, R.E.J., Chamberlain, R., Doering, P., and Haunert, K. 2002b. Evaluation of a digital echosounder system for detection of submersed aquatic vegetation. Estuaries. **25**: 133-141.

Sahely, H.R., Dudding, S., and Kennedy, C.A. 2003. Estimating the urban metabolism of Canadian cities: Greater Toronto area case study. Can. J. Civ. Eng. **30**: 468-483.

Sand-Jensen, K. 1977. Effect of epiphytes on eelgrass photosynthesis. Aquat. Bot. **3**: 55-63.

Sand-Jensen, K. and Søndergaard, M. 1981. Phytoplankton and epiphyte development and their shading effect on submerged macrophytes in lakes of different nutrient status. Int. Rev. Ges. Hydrobiol. **66**: 529-552.

Sand-Jensen, K., Pedersen, N.L., Thorsgaard, I., Moeslund, B., Borum, J., and Brodersen, K.P. 2008. 100 years of vegetation decline and recovery in lake Fure, Denmark. J. Ecol. **96**: 260-271.

Sarnelle, O., Hratz, K.W., and Cooper, S.D. 1993. Effects of an invertebrate grazer on the spatial arrangement of a benthic microhabitat. Oecologia. **96**: 208-218.

Schelske, C.L., Stoermer, E.F., Fahnensteil, G.F., and and Haibach, M. 1986. Phosphorus enrichment, silica utilization, and biogeochemical silica depletion in the Great Lakes. Can. J. Fish. Aquat. Sci. **43**: 407-415.

Schindler, D.W. 2006. Recent advances in the understanding and management of eutrophication. Limnol. Oceanogr. **51**: 356-363.

Seifried, K.E. 2002. Submerged macrophytes in the Bay of Quinte: 1972 to 2000. M.Sc. Thesis, University of Toronto, Toronto, Ontario, Canada.

Sharpley, A. and Rekolainen, S. 1997. Phosphorus in agriculture and its environmental implications. p. 1-54. *In*: H. Tunney, O.T. Carton, P.C. Brookes and A.E. Johnston (eds) Phosphorus loss from sail to water. CAB Int. Press, Cambridge, UK.

Sharlpey, A., Meisinger, J.J., Breeuwsma, A., Sims, J.T., Daniel, T.C., and Schepers, J.S. 1998. Impacts of animal manure management on ground and surface water quality. p.173-242. *In*: J.L. Hatfield and B.A. Stewart (ed) Animal waste utilization: Effectie use of manure as a soil resource. Sleeping Bear Press, Boca Raton FL.

Sharpley, A., Foy. B. and Withers, P. 2000. Practical and innovative measures for the control of Agricultural phosphorus losses to water: An Overview. J. Env. Qual. **29**: 1-9.

Shear, H., and Konasewich, D.E. 1975. *Cladophora* in the Great Lakes. Great Lakes Research Advisory Board, Windsor, Ontario, Canada.

Sheath, R.G., Hambrook, J.A., and Nerone, C.A. 1988. The benthic macro-algae of Georgian Bay, the north channel and their drainage basin. Hydrobiol. **163**: 141-148.

Simmonds, E.,J., and MacLennan, D.,N. 2005. Fisheries acoustics. Blackwell Publishing, Oxford.

Simons, T.J., and Schertzer, W.M. 1987. Stratification, currents and upwelling in Lake Ontario, summer 1982. Can. J. Fish. Aquat. Sci. **44**: 2047-2058.

Smith, R.E.H., Furgal, J.A., Charlton, M.N., Greenberg, B.M., Hiriart, V., and Marwood, C. 1999. The attenuation of ultraviolet radiation in a large lake with low dissolved organic matter concentrations. Can. J. Fish. Aquat. Sci. **56**: 1351-1361.

Smouse, P.E., Long, J.C., and Sokal, R.R. 1986. Multiple regression and correlation extensions of the mantel test of matrix correspondence. Syst. Zool. **35**: 627-632.

Sonzogni, W.C., Chapra, S.C., Armstrong, D.E., and Logan, T.J. 1982. Bioavailability of phosphorus inputs to lakes. J. Environ. Qual. **11**: 555-563.

Sorrano, P.A., Hubler, S.L., Carpenter, S.R., and Lathrop, R.C. 1996. Phosphorus loads to surface waters: A simple model to account for spatial pattern of land use. Ecol. Appl.**6**: 865-878.

Spence, D.H.N. 1982. The zonation of plants in freshwater lakes. Adv. Ecol. Res. **12**: 37-125.

Stadelmann, P., Moore, J.E., and Pickett, E. 1974. Primary production in relation to temperature structure, biomass concentration, and light conditions at an inshore and offshore station in Lake Ontario. J. Fish. Res. Bd. Can. **31**: 1215-1232.

Stainton, M.P., Capel, M.J., and Armstrong, F.A.J. 1977. The chemical analysis of freshwater.

Stanczykowska, A., Lawacz, W., and Mattice, J. 1975. Use of field measurements of consumption and assimilation in evaluation of the role of *Dreissena polymorpha* pall. in a lake ecosystem. Pol. Arch. Hydrobiol. **22**: 509-520.

Stanczykowska, A., and Lewandowski, K. 1993. Effect of filtering activity of *Dreissena polymorpha* (pall.) on the nutrient budget of the littoral of lake Mikolajskie. Hydrobiol. **251**: 73-79.

Stantec 2006. Aquatic macrophyte survey of Cook's Bay, Lake Simcoe, August 2006. Report: 160940049.Stantec Consulting Ltd.

Statistics Canada. 2001. A geographical profile of manure production in Canada. 16F0025X1B.

Stein, A., and Ettema, C. 2003. An overview of spatial sampling procedures and experimental design of spatial studies for ecosystem comparisons. Agr. Ecosys. Environ. **94**: 31-47.

Sterner, R.W., and Elser, J.J. 2002. Ecological stoichiometry: The biology of elements from molecules to the biosphere. Princeton University Press, Princeton, New Jersey, USA.

Stevens, A.W., Lacy, J.,R., Finlayson, D.,P., and Gelfenbaum, G. 2008. Evaluation of single beam sonar system to map seagrass at two sites in northern Puget Sound, Washington. 2008-5009, U.S. Geological Survey.

Stevens, L.E., Shannon, J.P., and Blinn, D.W. 1997. Colorado River benthic ecology in the Grand Canyon, Arizona, USA: Dam, tributary and geomorphological influences. Reg. Rivers: Res. Mgmt.. **13**: 129-149.

Stevens, R.J.J., and Neilson, M.A. 1987. Response of Lake Ontario to reductions in phosphorus load, 1967-82. Can. J. Fish. Aquat. Sci. **44**: 2059-2067.

Stevens, R.J.J., Neilson, M.A., and Warry, N.D. 1985. Water quality of the Lake Huron - Georgian Bay system. Scientific Series 143, Inland Waters Directorate, Ontario Region, Burlington, Ontario.

Stevenson, R.J., and Stoermer, E.F. 1982. Seasonal abundance patterns of diatoms on *Cladophora* in Lake Huron. J. Great Lakes Res. **8**: 169-183.

Stewart, T.W., Miner, J.G., and Lowe, R.L. 1998a. Quantifying mechanisms for zebra mussel effects on benthic macroinvertebrates: Organic matter production and shell generated habitat. J. N. Am. Benth. Soc. **17**: 81-94.

Stewart, T.W., Miner, J.G. and Lowe, R.L. 1998b. Macroinvertebrate communities on hard substrates in western Lake Erie: Structuring effects of Dreissena. J. Great Lakes Res. **24**: 868-879.

Stone, M., and English, M.C. 1993. Geochemical composition, phosphorus speciation and mass transport of fine-grained sediment in two lake Erie tributaries. Hydrobiol. **253**: 17-29.

Suggett, D.J., Maberly, S.C., and Geider, R.J. 2006. Gross photosynthesis and lake community metabolism during the spring phytoplankton bloom. Limnol. Oceanogr. **51**: 2064-2076.

Suggett, D.J., Moore, C.M., Hicknman, A.E., and Geider, R.J. 2009. Interpretation of fast repetition rate (FRRF) fluorescence: Signatures of phytoplankton community structure versus physiological state. Mar. Ecol. Progr. Ser. **376**: 1-19.

Suggett, D.J., MacIntyre, H.L., and Geider, R.J. 2004. Evaluation of biophysical and optical determinations of light absorption by photosystem II in phytoplankton. Limnol. Oceanogr. Methods. **2**: 316-332.

Sullivan, P.J. 1991. Stock abundance estimation using depth-dependant trends and spatially correlated variation. Can. J. Fish. Aquat. Sci. **48**: 1691-1703.

Sylvan, J.B., Quigg, A., Tozzi, S., and Ammerman, A.W. 2007. Eutrophication-inducedphosphorus limitation in the Mississippi river plume: Evidence from fast repetition rate fluorometry. Limnol. Oceanogr. **52**: 2679-2685.

Taft, C.E., and Kishler, W.J. 1973. *Cladophora* as related to pollution and eutrophication in Western Lake Erie. Report # 332, Ohio State University.

Taylor, J.T. 1938. The spectrum of turbulence. Proc. Royal Soc. A.(164).

Tennekes, H., and Lumley, J. 1999. A first course in turbulence. MIT Press, Cambridge, MA.

Thomas, R.L., Kemp, A.L., and Lewis, C.F.M. 1973. The surficial sediments of Lake Huron. Can. J. Earth Sci. **10**: 226-271.

Thomas, G.L., Theisfield, S.L., Bonar, S.A., Crittenden, R.N., and Pauly, G.B. 1990. Estimation of submergent plant bed biovolume using acoustic range information. Can. J. Fish. Aquat. Sci. **47**: 805-812.

Timms, R.M., and Moss, B. 1984. Prevention of growth of potentially dense phytoplankton populations by zooplankton grazing in the presence of zooplanktivorous fish in a shallow wetland ecosystem. Limnol. Oceanogr. **29**: 427-486.

Turner, M.A., Robinson, G.G.C., Townsend, B.E., Hann, B.J., and Amaral, J.A. 1995. Ecological effects of blooms of filamentous green algae in the littoral zone of an acid lake. Can. J. Fish. Aquat. Sci. **52**: 2264-2275.

Valley, R.D., Drake, M.T. and Anderson, C.S. 2005. Evaluation of alternative interpolation techniques for the mapping of remotely sensed vegetation. Aquat. Bot. **81:** 13-25**.**

Valley, R.D., and Drake, M.T. 2006. Accuracy and precision of hydroacoustic estimates of aquatic vegetation and the repeatability of whole-lake surveys: Field tests with a commercial echosounder.

Valley, R.D. and Drake, M.T. 2007. What does resilience of a clear-water state in lakes mean for the spatial heterogeneity of submersed macrophyte biovolume?. Aquat. Bot. **87**:307-319.

Vanderploeg, H.A., Nalepa, T.F., Jude, D.J., Mills, E.L., Holeck, K.T., Liebig, J.R., Grigorovich, I.A., and Ojaveer, H. 2002. Dispersal and emerging ecological impacts of ponto-caspian species in the Laurentian Great Lakes. Can. J. Fish. Aquat. Sci. **59**: 1209-1228.

Vis, C., Hudon, C., and Carignan, R. 2003. An evaluation of approaches used to determine the distribution and biomass of emergent and submerged aquatic macrophytes over large spatial scales. Aquat. Bot. **77**: 187-201.

Vogel, S. 1994. Life in moving fluids: The physical biology of flow. Princeton University Press, New Jersey, NJ.

Walz, N. 1978. The production and significance of the *Dreissena* population in the nutrient cycle in lake Constance. Arch. Fur Hydrobiol. **82**: 482-499.

Warren, J.D., and Peterson, B.J. 2007. Use of a 600-kHz acoustic doppler current profiler to measure estuarine bottom type, relative abundance of submerged aquatic vegetation, and eelgrass canopy height. Est. Coast. Shelf Sci. **72**: 53-62.

Webster, R., and Oliver, M. 2001. Geostatistics for environmental scientists. John Wiley and Sons, New York.

West, L.J.A., Li, K., Greenberg, B.M., Mierle, G., and Smith, R.E.H. 2003. Combined effects of copper and ultraviolet radiation on a microscopic green alga in natural soft lake waters of varying dissolved organic carbon content. Aquat. Tox. **64**: 39-52.

Wetzel, R.G. 2001. Limnology : Lake and river ecosystems. Academic Press, San Diego, California.

Wezernak, C.T., and Lyzenga, D.R. 1975. Analysis of *Cladophora* distribution in Lake Ontario using remote sensing. Remote Sens. Environ. **4**: 37-48.

Whitton, B.A. 1970. Biology of *Cladophora* in freshwaters. Wat. Res. **4**: 457-476.

Wiebe, P.H., Greene, C.H., Stanton, T.K., and Burczynski, J. 1990. Sound scattering by live zooplankton and micronekton: Empirical studies with a dual beam acoustical system. J. Acoust. Soc. Amer. **88**: 2346-2360.

Wilson, K.A., Howell, E.T., and Jackson, D.A. 2006. Replacement of zebra mussels by quagga mussels in the Canadian nearshore of lake Ontario: The importance of substrate, round goby abundance, and upwelling frequency. J. Great Lakes Res. **32**: 11-28.

Winfield, I.J., Onoufriou, C., O'Connell, M.J., Godlewska, M., Ward, R.M., Brown, A.F., and Yallop, M.L. 2007. Assessment in two shallow lakes of a hydroacoustic system for surveying aquatic macrophytes. Hydrobiol. **584**: 111-119.

Winter, J.G., Dillon, P.J., Futter, M.N., Nicholls, K.H., Scheider, W.A., and Scott, L.D. 2002. Total phosphorus budgets, and nitrogen loads: Lake Simcoe, Ontario (1990 to 1998). J. Great Lakes Res. **28**: 301-314.

Winter, J.G., Eimers, M.C., Dillon, P.J., Scott, L.D., Scheider, W.A., and Willox, C.C. 2007. Phosphorus inputs to Lake Simcoe from 1990 to 2003: Declines in tributary loads and observations on water quality. J. Great Lakes Res. **33**: 381-397.

Wolter, P.T., Johnston, C.A., and Niemi, G.J. 2006. Land use land cover change in the U.S. great lakes basin 1992 to 2001. J. Great Lakes Res. **32**: 607-628.

Wood, S.N. 2008. Fast stable direct fitting and smoothness selection for generalized additive models. J. Royal Stat. Soc.(B). **70**: 495-518.

Woodson, C.B., Webster, D.R., Weissburg, M.J., and Yen, J. 2005. Response of copepods to physical gradients associated with structure in the ocean. Limnol. Oceanogr. **50**: 1552-1564.

Yemefack, M., Rossiter, D.G., and Njomgang, R. 2005. Multi-scale characterization of soil variability within an agricultural landscape mosaic system in southern Cameroon. Geoderma. **125**: 117-143.

Zhu, B., Mayer, C.M., Rudstam, L.G., Mills, E.L., and Ritchie, M.E. 2008. A comparison of irradiance and phosphorus effects on the growth of three submerged macrophytes. Aquat. Bot. **88**: 358-362.

Zhu, B., Fitzgerald, D.G., Mayer, C.M., Rudstam, L.G., and Mills, E.L. 2006. Alteration of ecosystem function by zebra mussels in oneida lake: Impacts on submerged macrophytes. Ecosystems. **9**: 1017-1028.

Zhu, B., Fitzgerald, D.G., Hoskins, S.B., Rudstam, L.G., Mayer, C.M., and Mills, E.L. 2007. Quantification of historical changes of submerged aquatic vegetation cover in two bays of lake ontario with three complementary methods. J. Great Lakes Res. **33**: 122-135.